Integrated Assessment of Gully Erosion Processes, Using Multispectral Remote Sensing, Stochastic Modelling, and GIS-based Morphotectonic Analysis; A Case Study in the Southwest of Iran

Dissertation

der Mathematisch-Naturwissenschaftlichen Fakultät
der Eberhard Karls Universität Tübingen
zur Erlangung des Grades eines
Doktors der Naturwissenschaften
(Dr. rer. nat.)

vorgelegt von
Reza Zakerinejad
aus (Andimeshk) Iran

Tübingen
2015

Tag der mündlichen Qualifikation:	**14.12.2015**
Dekan:	**Prof. Dr. Wolfgang Rosenstiel**
1. Berichterstatter:	**Prof. Dr. Volker Hochschild**
2. Berichterstatter:	**Dr. habil. Michael Märker**

Dedication:

This thesis is dedicated to my parent for all love, help, moral support, confidence and understanding in me, during the overall period of my study.

Content

Abstract

Water erosion and especially gully erosion is one of the most effective phenomena that leads to decreasing soil productivity and pollution of water resources in many part of the world. Gully erosion as one of the most intensive land degradation processes especially in large parts of Iran, is the main threat for agriculture and range land. According to previous research lithology, vegetation density, topography as well as land use and land cover changes are effective drivers for soil loss in general and gully erosion in particular. In the first part of this thesis the susceptibility of the Mazayjan basin (MZJ) in the Southwest of Iran, where gully erosion is the main environmental threat, has been assessed. Therefore, a detailed terrain analysis and a stochastic modeling approach using mechanical statistics have been used. Among the terrain indices utilized in the prediction, the most important ones are: convergence index, plan curvature and slope. Gully erosion is the predominant type of water erosion and contributes to the sediment dynamics in a significant way in this catchment. Hence, in the second part of this thesis, GIS and satellite image analysis techniques were applied to derive input information for the numeric models to estimate the rate of soil erosion and deposition in the MZJ basin. Since the different types of water erosion such as rill, sheet and gully erosion are quite common in the MZJ basin, the Unit Stream Power-based Erosion Deposition (USPED) Model was integrated with a combined Stream Power Index (SPI) and Flow Accumulation (FA) approach. According to the integrated final map of erosion and deposition processes modeled with USPED including the gully erosion processes derived by SPI, round about 17.5 % of area is stable or characterized by very low erosion or deposition classes. Very high erosion values cover 28.2 % of the area, whereas 19.2 % of the area is related to deposition processes.

Tectonic activities in this study area that is part of the Zagros Mountains (ZM) significantly contributed to the formation of the existing drainage systems and hence, to landscape evolution. Neo-tectonics (Upper Quaternary) in form of earthquakes and associated uplifting, fracturing and faulting are still active in large parts of this area. In the third part of this study, we focused especially on the assessment of the vulnerability of the geologic formations to gullying and the effects of neo-tectonic processes inducing gully erosion using different data sources (ASTER GDEM., topography map information and aerial photographs) and resolutions (30 m, 10 m and 5 m) of digital elevation models (DEMs). An investigation on the location of gully features like headcuts and stream profile knickpoints reveals that the areas highly sensitive to gullying are related to stream sections showing uplifting and faulting. The

TecDEM software was used to identify knickpoints showing that abrupt changes in the river profiles are located in the central part (colluvial/alluvial deposits) of the catchment. Hence, the location of knickpoints indicates tectonic activity in turn changing the drainage network along the longitudinal profile. The results illustrate that severe gully erosion is related to these tectonic processes, especially in the Southwest of the MZJ basin.

In the last part of this thesis, the spatial distribution of gully susceptibilities was modeled with a GIS-based statistical mechanics approach. Therefore, we used bands ratios from ASTER multispectral images taking into account the lithologic characteristics of the study area most likely influencing the spatial distribution of gully erosion. The results show that the multispectral analysis of the ASTER data yield valuable results in terms of mineral differentiation in the ZM area and hence, can be utilized as a useful tool for lithological mapping. In this study we used a statistical mechanics approach to assess the relation between existing gully locations and the combinations of predictor variables consisting in topographic indices and ASTER band rations. The spatial prediction shows that gullies have a high probability in areas with high amounts of salt, gypsum and silty deposits especially in the plain part of the study area. The proposed methodology allows conducting a proper gully erosion assessment in order to identify the priority areas for soil conservation and land use management in the Southwestern parts of Iran.

Zusammenfassung

Bodenerosion und besonders Gully-Erosion sind zwei der hauptverantwortlichen Erscheinungen auf der Erde, die zu einer Abnahme der Produktivität von Böden und zur Verunreinigung von Wasserressourcen führen. Gully-Erosion gehört zu den intensivsten Prozessen der Land-Degradation, besonders in großen Teilen Irans, die ackerbauliche Nutzung und Weideland bedrohen. Vorangegangenen Studien zufolge zählen das anstehende Gestein, die Vegetationsdichte, die Topographie und die Landnutzung und ihre Veränderung zu den Hauptursachen für Bodenerosion und Gully-Erosion im Speziellen.

Im ersten Teil der Arbeit wird die Anfälligkeit des Mazayjan-Beckens (MZJ) im Südwesten Irans hinsichtlich der Gully-Erosion ermittelt. Hierfür wurden eine detaillierte digitale Geländeanalyse sowie eine stochastische Modellierung basierend auf den Prinzipien der mechanischen Statistik durchgeführt. Zu den Geländeparametern mit dem größten Einfluss zählen der Konvergenz Index, die Horizontalwölbung sowie die Hangneigung. Gully-Erosion ist die einflussreichste Form der Wasser-Erosion und trägt signifikant zur Sedimentdynamik im Einzugsgebiet bei.

Aus diesem Grund wurden im zweiten Teil dieser Arbeit Geographische Informationssysteme und Fernerkundungsdaten eingesetzt, um Eingabedaten für die numerischen Modelle zu generieren, welche Erosions- und Ablagerungsraten im MJZ-Becken ermitteln. Da verschiedene Mechanismen wie Graben-, Sheet- und Gully-Erosion im Untersuchungsgebiet vorkommen, wurde das Unit Stream Power-based Erosion Deposition-Modell (USPED) in Kombination mit dem Stream Power Index (SPI) und der Flow Accumulation (FA) ausgewählt. Den Berechnungen zufolge, bei welchen die USPED angewandt und Gully-Erosion durch den SPI ermittelt wurde, sind rund 17,5 % der Flächen im Untersuchungsgebiet stabil oder von sehr geringen Erosions- und Ablagerungsraten betroffen. 28,2 % hingegen unterliegen sehr hoher Erosion und 19,2 % sind von Ablagerungsprozessen betroffen.

Tektonische Aktivität im Untersuchungsgebiet, welches Teil der Zargos-Berge (ZM) ist, trug in der Vergangenheit signifikant zur Ausbildung der Abflussbedingungen bei und dadurch zur Entwicklung der Landschaft. Jüngere tektonische Prozesse (Oberes Quartär) in Form von Erdbeben und damit verbundenen Hebungsprozessen, Brüchen und Verwerfungen sind in großen Teilen des Untersuchungsgebiets noch aktiv.

Im dritten Teil dieser Arbeit liegt der Schwerpunkt auf der Ermittlung der Anfälligkeit geologischer Formationen hinsichtlich der Gully-Erosion, welche auch durch die jüngeren tektonischen Aktivitäten verursacht wurden. Dies erfolgte anhand von Digitalen

Oberflächenmodellen (DEMs) unterschiedlicher Herkunft (ASTER-Daten, Topographische Karten und Luftbilder) und räumlicher Auflösung (30 m, 10 m und 5 m). Weitere Untersuchungen zum Vorkommen von Gullysystemen und tektonischen Aktivitäten, wie beispielsweise die Analyse von Flußeinzugsgebietsmorphologien sowie der Analyse der Longitudinalprofile der Vorfluter, zeigen dass die Gebiete, welche besonders anfällig gegenüber Gully-Erosion sind, durch Hebungen und Verwerfungen geprägt sind. Die Software TecDEM wurde verwendet, um abrupte Veränderungen im Flussprofil im mittleren Bereich des Einzugsgebiets (alluviale Ablagerungen) zu ermitteln. Folglich deutet das Vorhandensein von "Knickpoints" tektonische Aktivitäten an, welche wiederum die Erosionsprozesse entlang des Flussprofils verändern. Die Ergebnisse zeigen, dass starke Gully-Erosion in Zusammenhang mit diesen tektonischen Aktivitäten steht, insbesondere im Südwesten des MZJ-Beckens.

Im letzten Teil dieser Arbeit wurde die Anfälligkeit für Gully-Erosion in einem GIS-basierten stochastischen Modell, dem "Maximum Entropy Modell" regionalisiert. Dies erfolgte unter der Verwendung von multispektralen ASTER-Daten, aus welchen die geologischen Faktoren, welche hauptverantwortlich für die räumliche Verteilung von Gully-Erosion sind, durch Band-Ratios abgeleitet wurden. Eine multispektrale Analyse von ASTER-Daten liefert wertvolle Ergebnisse über die mineralische Ausdifferenzierung im ZM-Gebiet, welche räumlich höher aufgelöste Informationen liefert als die herkömmlichen geologischen Karten des Gebiets.

In dieser Studie wurde das Verhältnis zwischen vorhandener Gully-Erosion und der Kombination von Predictor-Variablen, bestehend aus topographischen Indizes und ASTER-Band-Ratios, untersucht. Die räumliche Vorhersage zeigt, dass Gully-Erosion überwiegend in colluvialen/ alluvionalen Gebieten mit hohen Anteilen von Salz, Gips und/ oder schluffiger Textur auftritt und besonders in den Ebenen im südlichen Untersuchungsgebiet vorkommen. Die vorgestellte Methode ermöglicht eine wirkungsvolle Abschätzung der Gully-Erosion, welchen den Bodenschutz und das Land-Management im Südwesten Irans unterstützen kann.

List of Abbreviations

AUC	Area Under Curve
Cs -137	Caesium-137
EC	Electric Conductivity
DEM	Digital Elevation Model
FA	Flow Accumulation
FAO	Food and Agriculture Organization
GIS	Geographic Information System
GPS	Global Positioning System
GE	Google Earth
LULC	Land Use/ Land Cover
MZJ	Mazayjan
MEM	Maximum entropy Model
NPO	National Petroleum Organization
RS	Remote Sensing
SPI	Stream Power Index
SAR	Sodium Absorption Ratio
SWIR	Short wave infrared
VNIR	Visible and near infrared
TIR	Thermal infrared
TA	Terrain Analysis
ZB	Zagros Belt
ZM	Zagros Mountain

List of figures

List of tables

List of Papers

This cumulative doctoral thesis is based on the following papers. Next to each paper, the author's contribution is highlighted;

- Paper A

Zakerinejad R and Märker M (2014) Prediction of Gully erosion susceptibilities using detailed terrain analysis and maximum entropy modeling: a case study in the Mazayjan Plain, Southwest Iran. Geogr Fis Din Quat 37 (1): 67–76.

Author contribution: Conception and design, data collection and preparation, data analysis, figures and writing the paper.

- Paper B

Zakerinejad R and Märker M (2015) An integrated assessment of soil erosion dynamics with special emphasis on gully erosion in the Mazayjan basin, southwestern Iran. Natural Hazards, 79 (1): 25-50

Author contribution: Conception and design, data collection and preparation, data Analysis and interpretation, figures and writing the article.

- Paper C

Zakerinejad R., Hochschild V., Rahimi M., Märker M (2015) Morphotectonic analysis of the Zagros Mountains using high resolution DEM to assess gully erosion processes: A case study in the Fars province, Southwest of Iran. International Geoinformatics Research and Development Journal (IGRDJ), accepted for publication.

Author contribution: Conception and design, data collection and preparation, data analysis, figures and writing the article.

- Paper D

Zakerinejad R., Omran A., Hochschild V., Märker M (2015) Assessment of gully erosion using multispectral remote sensing, GIS and stochastic modelling in the Southwest of the Zagros Mountains- Iran. Natural Hazards, in review.

Author contribution: Conception and design, data collection and preparation, data analysis, figures and writing the article.

Acknowledgement

First of all, I would like to express my sincere gratitude to my advisor Dr. habil. Michael Märker who has done his best to motivate me during my study. I learnt a lot through his comments and his office door was always open to me. I would like to thank Professor Volker Hochschild for the continuous support of my Ph.D study and for his patience, motivation, enthusiasm.

It is my pleasure to extent my sincere gratitude to Dr. Jan Kropacek, who as a good friend, was always willing to help and give his best suggestions throughout my study at the University of Tübingen. During these four years of research I collaborated with different friends, researchers and colleagues that I would like to express my sincere gratitude to all of them.

Furthermore I would like to thank the Dr. Hans-Joachim Rosner, Dr. Saman Heydari-Guran, Richard Szydlak, Adel Omran, Geraldine Quénéhervé, Gebhard Warth, Christian Bick, Andreas Braun, Mansour Mahamane, Elio Flores, Singh Prabhjeet, Silvia Duttle, Sonia Silva, for their guidance and encouragement during the time I was at the University of Tübingen.

I would like to acknowledge the Ministry of Science, Research and Technology of Iran to finance my research abroad and Hasbkarji Company for providing the data (aerial photos and climate data).

I would like to thank the Natural Resource Organization in Fars province, Natural Resource Brench in Zarindasht city for their cooperation for my field work in 2012 and 2013.

Last but not the least, I am extremely grateful to my parents, they were always supporting me and encouraging me with their best wishes. Also I express my thanks to my sister, brothers and grandmother for their support and valuable prayers.

1 Introduction

Soil erosion processes are the main cause of land degradation especially in arid and semi-arid areas. It is the most severe limitation for a sustainable development in many part of the world (Brunner et al., 2002; Valentin et al., 2005; Wang et al., 2013; Nasri et al., 2013). Moreover, soil loss effects greatly the hydrological soil behavior and therefore runoff dynamics in river catchments. Soil erosion consists of the process of detachment, transportation and deposition of soil materials by wind or water through the erosive forces of raindrops and surface flow (Foster et al., 1972; Ventura et al., 2002; La 2003; Shi et al., 2012). Soil erosion is often more severe in developing countries and the most severe limitation for a sustainable development in many parts of the world, especially in areas with arid and semi-arid climate due to a lack of financial resources to cope with and mitigate the effects of soil erosion (Tamene & Vlek 2008). In fact the loss of soil productivity is closely related to the reduction of soil fertility (Masoudi & Zakerinejad 2011; Kairis et al., 2013; Mahamane 2015; Ionita et al., 2015) particularly in the south and southwest of Iran.

Soil erosion causes the decreasing of soil quality, reducing soil nutrients especially in the top soil and is a major restriction in producing enough food to feed the world′s growing population (Lal 1998; La 2003; Pimentel 2006). In the last decades human activities in large parts of the world modified the ecosystem with changing land use/land cover (LULC), hence causing decreases of soil biodiversity and productivity. Over use of the natural resources such as deforestation, overgrazing and other practices have speeded up the intensity of soil erosion and deposition in many areas of the world (Starkel 2005; Dotterweich et al., 2012). The impact of soil erosion and related sediments decrease dramatically water quality and reservoir capacity (Tangestani 2006; Kefi et al., 2011). Therefore, the assessment of soil loss is urgently needed especially in areas affected by intensive water erosion processes and fragile, susceptible ecosystems. In fact monitoring of soil erosion can be a useful tool to estimate the severity of soil erosion and consequently helps land use planner to evaluate the life expectancy of dams and reservoirs. Gully erosion is the most intensive type of water erosion and hence, it is an important sediment source (see Poesen et al., 1996; Sidorchuk et al., 2003; Valentin et al. 2005). Thus, it is a major threat also for agricultural areas. Therefore, the assessment of soil loss considering gully erosion processes in their temporal and spatial distribution is one of the major objectives for water managers, farmers, and landuse planner (Karaburun 2010; Ehiorobo & Audu 2011). Hence, a research focus lies in the development and implementation of strategies to reduce the effect of soil erosion in different environmental conditions (Colombo et al., 2005).

1.1 Main factors of soil erosion

Although many factors effect soil conditions and in consequence soil erosion processes, the most important factors which defining the rate and magnitude of soil erosion by water are: i) rainfall intensity and runoff, ii) percentage and type of vegetation cover, iii) lithology, iv) terrain morphology, v) soil type, vii) organic matter, viii) tectonic activity, and ix) socio-economics (Egboka & Nwankwor 1985; Egboka et al., 1990; Boardman et al., 2003; Karaburun 2010; Bosco et al., 2015; Florecs et al., 2015). Especially runoff flowing on prone soils with low vegetation cover causes shear stress to the soil surface which, if this force exceeds a critical threshold, causes the detachment of soil particles (Loch & Silburn 1997; Merritt et al., 2003).

Human pressure can increase the rate of soil erosion, due to over use of agriculture and range land (overgrazing) especially in the regions with susceptible conditions like in arid and semi-arid areas. Actually, soils with low amounts of organic matter and high amounts of silty sandy textures are more prone to raindrop impacts. In other words, soils with high organic matter and well improved structure have a higher resistance against soil erosion activities. The role of vegetation is crucial for soil erosion processes in reducing runoff speed and adding root strength and organic matter to the soil. Instead bare soils or soils with very poor vegetation are more susceptible to erosion. For example, in arid and semi-arid areas a low density of vegetation cover and organic matter allow a detachment and down slope transport of fertile top soil particles. The terrain conditions such as slope gradient and slope length (LS-factor) for instance were used in many empirical modelling approaches for evaluating the potential of water erosion (Nazari et al., 2009; Masoudi et al., 2010; Zakerinejad & Masoudi 2014; Mahamane 2015; Bosco et al., 2015). Moreover, neo-tectonic activities are also seriously influencing the rate and intensity of water erosion (Montgomery & Brandon 2002; Blanckenburg et al., 2004). Soil loss by water increases normally with slope length or upslope catchment area due to the accumulation of runoff. Therefore, areas with a complex topography and high slope–length gradients show higher rates of soil erosion.

1.2 Soil erosion under an Iranian perspective

Iran is located in the Northern hemisphere, between 25° to 40° N and 44° to 63° E, in the Middle East, bordered by Armenia, Azerbaijan and Turkmenistan, as well as the Caspian Sea to the north, Turkey and Iraq to the west, the Persian Gulf and the Gulf of Oman to the south and Pakistan and Afghanistan to the east (Fig. 1). Iran covers an area of 1.648.000 km² and is the second largest country in the Middle East after Saudi Arabia. Iran has two major mountain ranges;

i) The Zagros Mountains (ZM) are part of an alpine orogenic system and extend into north-western Iran, towards the Turkish border and towards the Persian Gulf, south of Iran (Heydari-Guran 2015). The Iranian Zagros belt is part of the larger Alpine-Himalayan system and occupies an irregular central position within two important tectonic features resulting from the closure of the Tibetan plateau and the Mediterranean Sea (Khadivi 2010);

ii) The northern part of the Iranian Plateau covers the Alborz and Talesh Mountains. These massive ranges cover at least 900 km, forming an arc south of the Caspian Sea. This arc begins at the border with Armenia in the west and ends at the border with Turkmenistan in the east (Heydari-Guran 2014).

The most deserted areas of Iran extend across the plateau from the north-west, close to Tehran and Qom provinces. Approximately one-sixth of the total surface of Iran is barren desert or with very poor vegetation because of complex terrain and arid and semi-arid conditions. Around 75% of Iran is dominated by an arid and semi-arid climate with annual precipitation varying from 350 mm to less than 50 mm (Kehl 2009). Iran has a variable climate from north to south and west to east, varying considerably from region to region. For example in the northwest, winters are cold and heavy snowfall occurs while spring and fall are relatively mild and summers are dry and hot. In the south and southwest of Iran such as in the Fars province, winters are mild and the summers are very hot. Due to lacking precipitation in most parts of the arid and semi-arid areas of Iran, irrigation agriculture prevails. In general, Iran has an arid climate with most of the annual rainfall falling during spring and winter seasons while the two other seasons receive only little or no rainfall. Because of several drought events in the last decades and overuse of ground water particularly in south and southwest of Iran, many agriculture areas were abandoned and become barren land. In fact the climate together with the socio-economic conditions increased the velocity and intensity of desertification in many parts of the country.

The deserts of Iran are mainly located on the central and eastern half of the Iranian Plateau, for example the Yazd and Kerman are two most affected provinces from wind erosion and sand dune movement. In general, the two major deserts in Iran are i) the Dasht-e-Kavir, which is located in central Iran towards the East and ii) the Kavir-e-Lut, which locates in the Southeast of Iran.

Because of the very low precipitation in these areas land cover is almost bare soil with very sparse vegetation. Large parts of central Iran have been affected by wind erosion. In this part of the country during the recent decades high population growth and drought condition increased the demand for water and agricultural products enormously. Especially, in the last decade many parts in south and south west of Iran are strongly affected by droughts and shortages of rainfall. Demand for fuel wood for cooking and heating in rural area also increased during the past droughts. Over grazing is also a serious problem leading to land degradation and desertification.

Soil erosion and especially water erosion is a serious problem that affects many countries in the world. In Iran aquatic erosion processes are the most important cause of land degradation (Ahmadi 1995; Masoudi et al., 2010; Nazari 2009; Zakerinejad & Masoudi 2010).

More than 60% of Iran's land surface is located in arid and semi-arid regions, with about 100 million ha at high risk of desertification (Ahmadi 2007; Masoudi 2010; Noormohammadi et al., 2014). Especially large parts of the Southern Farce province are affected seriously by soil erosion and degradation processes. The latter are related to population growth, overgrazing, expanding agricultural land and deforestation.

As already has been mentioned, in this thesis the physiographical settings of Iran within the arid and semi-arid climatic belt leads to accelerated land degradation progress. The average rate of soil erosion in Iran is about 33 t ha $^{-1}$ year $^{-1}$ that is the highest rate in the word (Ahmadi 1995; Hosseini & Gorbani 2005; Omidvar 2010; Asrari & Masoudi 2011) and many people are affected from this type of land degradation. The main type of water erosion especially in large parts of Iran consists of rill, sheet, gully and bank erosion. Compared to other countries in the Middle East, the present status of desertification in Iran is highly alarming since about 94% of arable land and rangeland are estimated to be in the process of degradation (Food and Agriculture Organization; FAO, 1994). This includes large proportions of the arable land (45%), which has already been affected by different degrees of water erosion (Masoudi et al., 2010). More than 85% of Iran is covered by arid and semi-arid areas, with desert land accounting for 34 million ha (FRW; Forest, Range, and Watershed Management Organization 2004). However, a lack of reliable data in large parts of the arid and semi –arid areas of Iran makes it difficult to apply conceptual modelling approaches for a proper water erosion assessment. In the past decades low rainfall, high temperatures and evaporation rates lead to high water requests for irrigation purposes and dramatic drops in ground water levels in many parts of Fars province in the southwest of Iran. LULC changes in vast parts of Iran covered by sensitive geological formations and poor vegetation cover are some of the main factors responsible for millions of tons of sediment available for erosion and transport (Soufi 2004; Nazari et al., 2009).

Gully erosion is an important form of soil erosion in arid and semi-arid areas of Iran (Soufi 2004; Shahrivar & Christopher 2012; Masoudi & Zakerinejad 2010). It is the dominant sediment source in the semi-dry areas delivering sediments into the stream network and consequently, affects water quality and quantity (Poesen et al., 1996; Sidorchuk et al., 2003). Gully erosion constitute about 45–90% of the total sediment production of agricultural lands in many arid and semi-arid areas (Ogbonna & Ijioma 2010). Gully erosion as one of the most intensive land degradation processes especially in large parts of Iran is the main threat to agriculture and range land cultivations. Gully erosion causes degradation in arable land by reducing the ground water table and depleting the available water reserves in susceptible areas (Poesen et al., 1996; Poesen et al., 2006).

There are many factors influencing on gully erosion processes like the characteristics of the catchment, soil type, climate condition, vegetation, tectonic and landuse type (Vandekerckhove et al., 2001; Kheir et al., 2007; Nazari et al., 2009; Zakerinejad & Märker 2015). The importance of threshold conditions is different in various climates with different LULC conditions and soil types (Nazari et al., 2009). However, often gullying depends also on human activities such as improper landuse, overgrazing, deforestation or road constructions. In the recent decades the negative impact and extent of gully erosion on human welfare and agricultural land in Iran especially in the south and southwest increased (Soufi 2004). The effect and severity of gully erosion is considered in many desertification assessment models as the most intensive level of water erosion (Soufi 2004; Amadi 2007; Masoudi & Zakerinejad 2010). Therefore, the assessment of gully erosion in arid and semi-arid areas in Iran using numerical or stochastic modelling approaches is very important especially, for areas with low data quality and quantity.

1.5 Modelling of water erosion

The assessment of erosion processes of a catchment is an essential prerequisite of integrated watershed management (May & Place 2005; Singh et al., 2008). For assessing the rate of soil erosion, different approaches can be applied. A distinction can be made between expert-based and model-based approaches (Van der Knijff et al., 2000). The assessment of water erosion with a qualitative model (expert basis) like the IMDPA model (Amadi 2007; Masoudi & Zakerinejad 2010) or the modified MEDALUS (Sepehr et al., 2007) was suggested for the different climate conditions in Iran. A limitation of these qualitative models is that they often rely on expert knowledge and subjective decisions in the scoring procedure (Yassoglou et al., 1998; Zakerinejad & Märker 2015). Many of these qualitative models used to assess desertification and water erosion neglect gully erosion processes. In the recent decades of soil erosion research, quantitative models were developed to assess and evaluated soil loss and to manage the environment. In the last decades computing and processing power increased allowing a rapid development in the identification and quantification of catchment water erosion processes (Merritt et al., 2003; May & Place 2005). The application of different soil erosion models and soil conservation methods are differing in their context, purpose, and degree of detail and therefore, the most suitable model depend on the proposed use, and the characteristics of the basin being considered (Rose 2001; Rose et al., 2003; May & Place 2005). The numerical models for the assessment of water erosion consist of physically based models, stochastic models and empirical models (Fig 1). According to the different models, users have to select specifically the relevant input data and processing techniques, depending on their expertise, local conditions and data availability (Conoscenti et al., 2008; Karydas 2013). Generally, the input data for each of these models are the limiting factor, especially, in the areas with low coverage and/ or availability or difficulty to access the data.

Physically-based (mechanistic or process-based) models which simulate the physical erosion processes differ from empirically-based models in terms of their degree of complexity (May & Place 2005; Bras et al., 2003; Conoscenti et al., 2008; Bosco et al., 2015). Physically-based models, such as the WEPP (Water Erosion Prediction Project; Flanagan & Nearing 1995) model were applied to represent the main processes that control soil loss, such as interrill and rill erosion (Sharma et al., 1995). Actually physical based models are limited due to the requested input data. The data required are often related to a cost intensive, time consuming acquisition and often the needed detail and scale is not available. Consequently, empirical models can be a useful tool to resolve this problem (Jetten et al., 1999; May & Place 2005).

However, these physical based models differ considerably in the processes they represent, their data requests and complexity (Merritt et al., 2003; Bosco et al., 2015). The Universal Soil Loss Equation (USLE; Wischmeier & Smith 1978) and the RUSLE (Revised USLE; Renard et al., 1997) are the most used empirical models for the assessment of rill and sheet erosion, but one of the limitations of these models are, that the most important erosion process namely gullying is not considered and also sediment deposition processes are not taken into account (May & Place 2005; Kakembo et al., 2009; Kinnell 2010). The USLE is detachment limited whereas, e.g. the Unit Stream Power Erosion Deposition Model (USPED, Mitasova et al., 1996), which is considering transport and deposition processes, is a transport capacity limited model. This model is based on the assumption that soil erosion depends on the detachment capacity and the sediment transport capacity of surface runoff (Mitasova et al., 1996). In may recent studies the USLE and RUSLE have been used for evaluation water erosion in many different climates. The USPED model just recently becomes more and more utilized to estimate erosion and deposition (Warren et al., 2005; Alimohammadi et al., 2006; Leh et al., 2011). However, also the USPED models do not consider the sediment yield from gullies, stream banks, and stream bed erosion (Grove & Rackham 2001; Zakerinejad & Märker 2015).

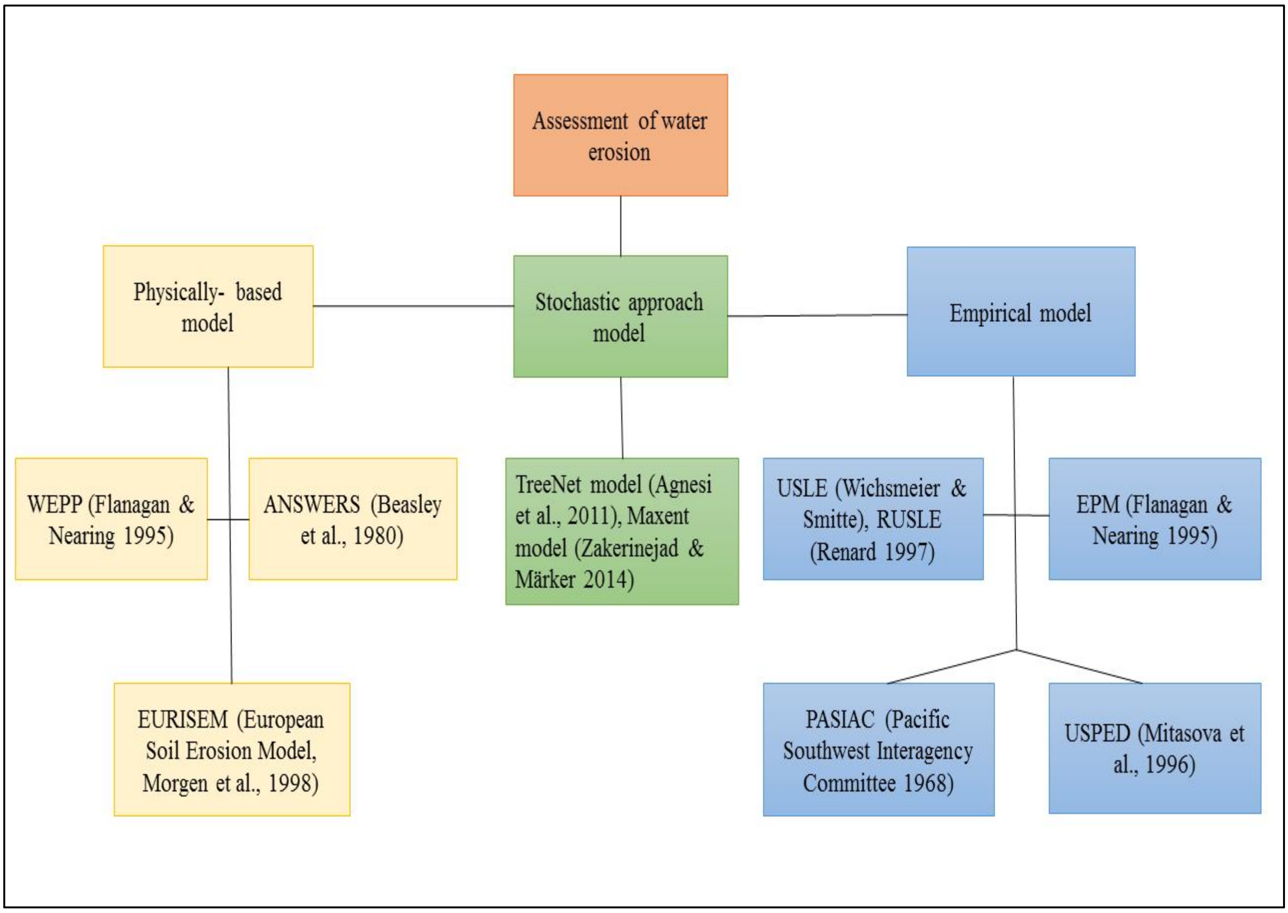

Fig. 1 Flowchart of water erosion modelling.

2 Aims and Objectives

2.1 General problem description, research deficit and research framework

Gully erosion as one of the most important types of soil erosion and hence, land degradation is of significant importance in many parts of the world due to its impacts on the ecosystem and effects on socio- economic aspects of the respective areas. In many parts of Iran rangeland and arable areas are highly degraded showing high rates of soil loss (Ahmadi 2007; Sepehr et al., 2007; Solaimani et al., 2009; Masoudi & Zakerinejad 2010; Falehgari et al., 2011; Imani et al., 2014). Among different erosion processes or different types of water erosion gully erosion is the most intensive one. Due to the complexity and scales of gully erosion processes it is also difficult to assess. Thus, most of the studies focus on rill interrill erosion processes (sheet erosion) because they are easier to assess and need less data input and quality. Only recently the interest in gully erosion processes in southern Iran increased due to the fact that water erosion and especially gully erosion destroy agriculture areas and/or reduce soil productivity in many catchments especially in the South and Southwest of Iran. Hence, there is a specific need to assess and evaluate gullying processes and to understand the important driving forces such as geology, LULC, topography, or neo-tectonic activity. In fact because of many frequent droughts and high rates of soil loss in Iran, the water and soil resources are in a critical stage concerning their economic, social and environmental implications.

There are many factors that influence soil erosion in general and gully process in particular such as; climate condition (amount frequency, duration, and intensity), LULC change, terrain parameters, organic matter, lithology and soils properties (Morgan 1986; Hallsworth 1987; Kheir et al., 2007; Sepehr et al., 2007; Nazari 2009; Zakerinejad & Märker 2015).

The quantitative estimation of soil erosion by water is an important key of land use management plans which are designed to protect and recover soils (Bonilla et al., 2010). Additionally, the severity and spatial distribution of soil erosion are important factors to soil conservation planning and watershed management (Popp et al., 2000; Kumar et al., 2006). Among different types of water erosion, gully erosion is one of the most predominant processes and hence, also main sources of sediment in catchments, although gully channels often occupy less than 5 % of the area of a catchment (Ionita et al., 2015), especially in the south and southwest of Iran. Although there are many models available to evaluate water erosion processes, only a few studies consider the role of gullying in water erosion assessment. However, soil erosion assessment in Iran, is mainly based on empirical prediction models and hence, more research is required to understand the important dynamics and spatial distribution of gully erosion (Kompani et al., 2011; Soufi 2002; Ahmadi 2007; Nazari et al., 2009). In contrast to several studies using PASIAC, MPASIC, EPM and IMDPA etc. in Iran only very little research was done on gully erosion, its dynamics and driving factors.

Although there is no documentation of reliable soil erosion rates at a national level, at least for some reservoir watersheds soil erosion rates were measured using 137Cs and suspended sediment gauging stations. For these catchments water erosion varies from 7.6 to 32 ton $ha^{-1}y^{-1}$ (Nazari et al., 2009). However, these catchments are mainly affected by rill and sheet erosion. Nevertheless some research was carried out on gully processes and stages of gully development as well as on thresholds for gully initiation (Soufi 2002; Kompani et al., 2011; Nasri et al., 2013). Anyway, there is no study conducted to examine the environmental characteristics to predict the susceptible areas for gully erosion. The assessment of neotectonic activity on gully erosion dynamics is not studies at all in the ZM. A common assessment of the probability of the occurrence of soil erosion processes in a specific area can be evaluated using the susceptibility concept (see Märker 2001; Agnesi et al., 2011; Conoscenti et al., 2013a; Conoscenti et al., 2013b). For the assessment of the important variables driving gully erosion process stochastic modelling approaches can be utilized since they are an efficient method to cover large areas in terms of costs and time expenses. According to that point statistic relationships between the spatial distribution of gully locations and the environmental parameters, which are assumed to represent the controlling factors of the gully erosion process are a key tool to predict the susceptible areas for gullying. Recently, some models using stochastic approaches to assess water erosion (gully & landslide erosion) were tested (Carrara & Guzzetti 1995; Agnesi et al., 2011; Conoscenti et al., 2013a; Zakerinejad & Märker 2014; Mahamane 2015). Apart of the stochastic models yielding information of the susceptible areas and empirical models considering gully erosion processes especially in the Southwest of Iran are very important to evaluate water erosion and soil loss. In other words, prediction of the areas with higher susceptibility to gully erosion is crucial and a key information for land use management. Using practical techniques to control gully erosion is difficult and expensive especially in developing countries. Therefore, the prediction of the susceptible areas and the understanding of the important environmental factors driving the processes of gully erosion are the main focus of this research. Especially the role of geologic formations and the effects of neo-tectonic processes have not been studied yet in the ZM and hence, are a mayor objective of this thesis. Tectonic activities cause disturbances on the ground surface that propagate through the hydrological system triggering also gullying. To the knowledge of the authors especially the mechanics of stream networks and erosional process related to neo-tectonics are still poorly studied in the ZM. As already mentioned the lithological character of the surface substrates is one of the most important variables for soil erosion processes. Accurate lithological maps with a proper resolution are thus, a prerequisite for soil erosion and gullying processes assessments. Using multispectral satellite images one can produce accurate litho-geological maps of the study area. Particularly in the southwest of Iran in the remote and steep mountain areas fieldwork is difficult due to limited access. Hence, the use of modern satellite images such as Landsat, ASTER or other images provided by satellite images (e.g. Quickbird or Rapideye) might be very efficient to evaluate soil loss and create lithological maps of the area. In fact the existing available lithology maps were generated by the Iranian National Petroleum Organization (NPO) with a scale of 1:100.000 (Nazari et al., 2009). These maps do not provide the accuracy needed for gully erosion assessment. Consequently, a proper and detailed lithology map for large parts of Iran is not available.

2.2 Main goals of the thesis

The main aims and objectives of this thesis are the quantification and evaluation of soil loss with particular emphasis on gully erosion processes and features in the Mazayjan catchment (MZJ) in the southwest of Iran. Especially, the spatial distribution of soil loss due to rill-interrill and gully erosion is a prerequisite for a proper land management. The general objectives of this study are mentioned in detail below:

i) Investigating the distribution of gully erosion with a quantitative method based on terrain analysis, lithological information and a mechanical statistics;
ii) Assessing soil erosion dynamics with special emphasis on gully erosion applying an integrated modelling approach;
iii) Studying the effects of lithology and morpho-tectonics on the gully erosion processes and features of the study area.

The distribution of gully erosion is closely connected to topography parameters, soil types, lithology, tectonic, climate variability, etc. However, since long-term meteorological measurements and also other environmental input data for applying physically based models are not existing or do not have the proper quality we will apply and test empirical modelling approaches based on simple and available datasets. Hence, in order to achieve the above mentioned general objectives of the study, the following specific objectives are proposed:

i) to predict the spatial distribution of gully susceptibility using stochastic modeling (Maxent model);

ii) to evaluate functional relationships between topographic indices and mapped gully locations;

iii) to identify the spatial distribution and intensity of the major erosion process dynamics including gully erosion;

iv) to estimate quantitatively the average rate of water erosion using an integrated empirical modelling approach combining the USPED model with an SPI based index.

v) to investigate the role of active tectonics on soil erosion and the distribution of gully erosion features taking into account i) the role of tectonics on drainage systems and ii) assessing different DEM resolutions (30 m, 10 m and 5 m) utilized for the stream network and geomorphotectonic analysis;

vi) to evaluate the application of remote sensing data to map the lithology;

vii) to predict the susceptible area of gully erosion considering multispectral parameters.

3 Structure of the thesis

This thesis consists of four peer-reviewed papers addressing the different objectives mentioned above. After the introduction highlighting i) the role of soil erosion as an important type of land degradation, ii) the factors driving water erosion and also iii) the quantitative assessment of water erosion processes in the following chapters we will discuss the general problems related to soil erosion and gullying in the study area and reveal the importance of gully erosion.

The following chapter provides an overview of the study area including geology, lithology, soils, vegetation and tectonic activity.

In chapter 5 we provide for each paper a short summary containing the specific motivation of the research, the applied methodology and the main results.

The major results of the single studies are discussed in depth in chapter 6. Moreover we sum up the mayor findings of the stochastic and empirical modelling as well as of the GIS and RS analysis.

The last chapter presents an outlook to future research in the study area and gives a prospective for the regional and national implications of this work (chapter 5).

4 Study Area

The Mazayjan study area is located in the ZM in the south-west of Fars province around 32 km southwest of Zarindasht city in the Fars Province, SW Iran (54° 34' to 54° 44' E and 27° 59' to 28° 5' N) (Fig 2). The study area covers 900 km^2 consisting of mountains and hills in the south and north of the study area and a plain area in the central part extending from west to east. The area is mostly arid, having a mean annual rainfall of 240 mm and mean monthly maximum and minimum temperatures of 31 °C and 18 °C, respectively. This area is located in the ZM, and is characterized by northwest to southwest striking folds. The ZB convergence movement between Arabia and Eurasia is about 2- 3cm/yr in a N-S direction and is assumed to be unchanged since10 Ma (Khadivi 2010). The study area represents the environmental diversity of south and south west of Iran in terms of geology, soil, morphotectonics, land cover and climate. Moreover, it is affected by severe water erosion processes and features. Gully erosion is the most intensive soil erosion process in this area.

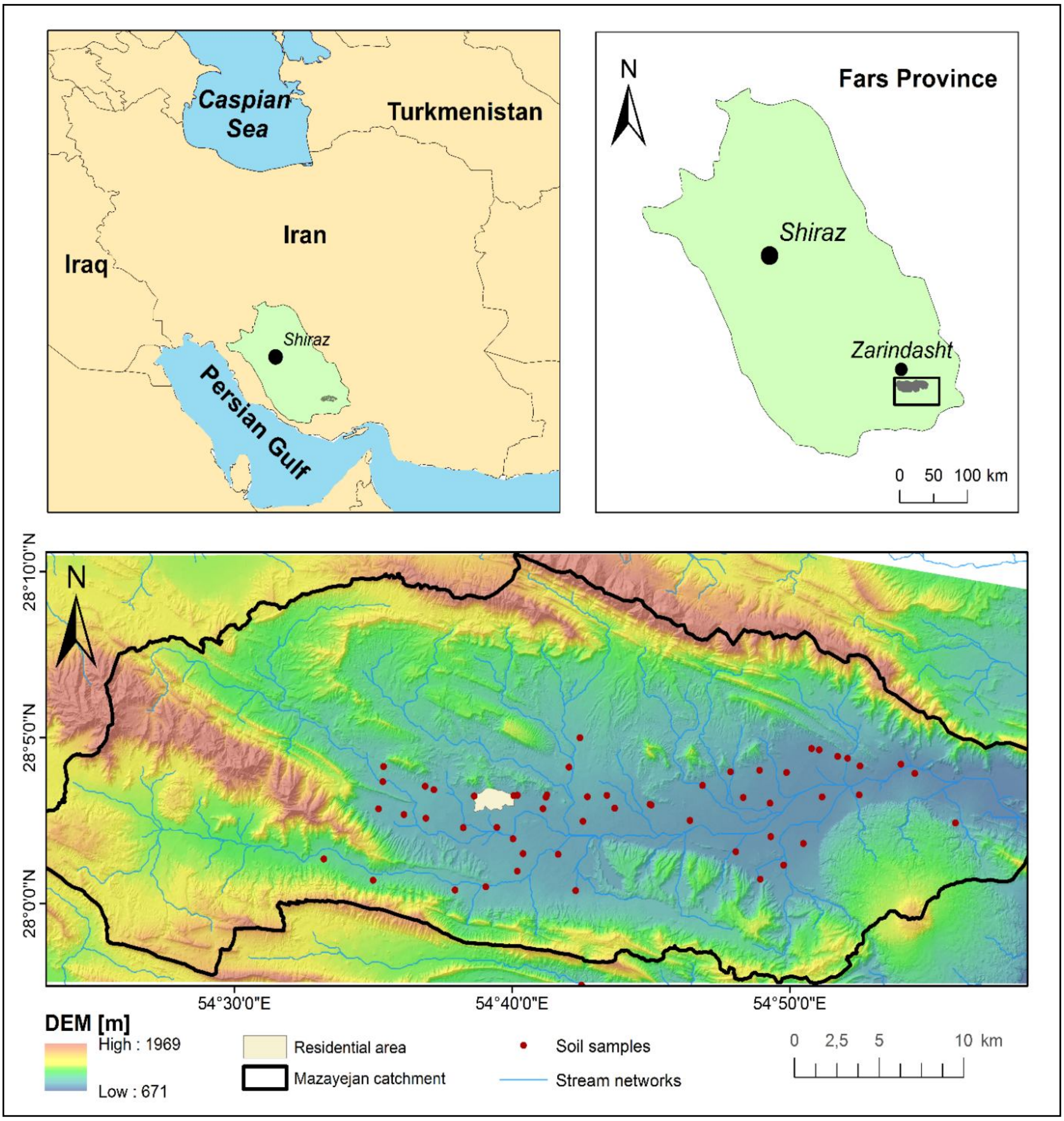

Fig. 2 Study area: Mazayjan catchment in the Southeast of Iran.

4.1 Rill- Interrill erosion and gully erosion in the Mazayjan basin

Rill-interrill and sheet erosion and gully erosion processes are the most predominant types of water erosion in the MZJ basin in recent years (Masoudi & Zakerinejad 2010; Masoudi & Zakerinejad 2011; Zakerinejad & Märker 2014). Actually sheet erosion processes are more common in the steep areas in the north and south of the study area while gully features are more frequent in the low sloping parts in the centre of the catchment. Gully erosion is a major threat for the agriculture and arable land in the southwest of Iran and this type of water erosion is the main source of the sediments delivered into the rivers systems. According to many extensive field surveys, water erosion and especially gully erosion are the predominant type of land degradation in the MZJ basin. This type of soil loss effected especially large parts in south and southwest of the catchment. In the agriculture areas gully erosion is the main reason for the reduction of soil fertility in the recent years. Due to drought conditions in the last decades, over exploitation of ground water, over grazing and the general low amount of organic matter soil productivity is significantly reduced.

The agriculture land is the most important resource of the inhabitants of this area. Hence, the main income of the inhabitant is related to agriculture production. According to two filed survey in 2012 and 2013 and aerial photos the gully features are mainly located in the southwest and south of the pediment parts (flat area) of the MZJ catchment with low slopes (less 10 %)(Fig. 3). Figure 4 shows a sample of the gully erosion feature in the southwest of the MZJ basin based on SPOT images from 2009 available via GE (Google Earth) . The low vegetation cover in the area makes it easy to identify the different types of water erosion showing that the area is seriously affected by water and especially by gully erosion. The gully areas in the MZJ catchment mostly consist in Quaternary deposits (alluvial material) that are more susceptible to water and gully erosion (Faiznia 2003). In the following part of this thesis we will describe shortly the most important characteristics of the catchment including soils, geology, tectonic processes, topography, climate and vegetation.

Fig. 3 Gully erosion shown in the centre of the study area.

Fig. 4 Identified and mapped gully features from Satellite images.

4.2 Soil types in the Mazayjan basin

Soil properties affect the risk of water and wind erosion, because each specific soil has its own natural erodibility characteristics. Soils with low organic matter are more susceptible to water erosion. Moreover, silty soils are more susceptible to erosion than coarse sandy or clay textures. Therefore, the understanding of the soil texture distribution is a prerequisite to help land use manager to evaluate the soil loss. According to the climate and moisture records of the area the soil moisture regime is aridic and also the temperature regime is hyper thermic, the average soil temperature is above 22 ° C (Masoudi & Zakerinejad 2010).

The most dominant physiographic units of the study area consist in mountainous relief, huge alluvial fans and pediment plains as well as low land areas. Alluvial fans and piedmont plains are developed on the Quaternary alluvial deposits characterized by more erodible soils (Faiznia 2007). In this area, the soil types are mostly shallow sandy-clays covering the mountains and hilly areas. According to field surveys and aerial photos the alluvial fan deposits are generally found in the south and northeast of the area. The soil originated from these materials is coarse-grained and usually contains some carbonates and gypsum. In this research we have collected 52 soil samples from different land units based on a combination of lithology, land use and slope. Each sample was randomly selected and represents the topsoil up to 25cm depth (Fig. 2). According to the soil taxonomy classification, most of the soil samples in this area are Entisols and Aridisols. The soil characteristics such as soil texture, organic matter, EC were analyzed in the laboratory. Then soil texture was determined by separating the relative proportions of sand, clay and silt by the pipette method (see Gee & Bauder 1986). The soil erodibility was estimated according to the soil textures for the whole study area (Table 1).

Table 1 K- factor based on soil texture of the MZJ basin

Soil type	K factor (ton.ha)(ha.hr/MJ.mm)
Sandy Loam	0.112-0.281
Silty loam	0.2902-0.332
Loam	0.194- 0.292
Sandy Clay loam	0.190-0.210
Silty Clay loam	0.312-0.325

Soil texture analyses show that the soils in the flat areas are mainly consisting of silty soil textures. Comparing the spatial soil texture distribution to the lithology map we find more susceptible soils with high silt contents located in the Quaternary deposits.

Fig. 5 Field work in 2012 to collecting soil samples.

4.3 Geology of the Mazayjan basin

The lithologic formations are one of the most important parameters influencing soil erosion due to the nature of the respective weathering products (Noormohammadi et al., 2014).

According to structure, sedimentary, metamorphism and also deformation, the Iranian plateau was subdivided into eight continental areas following Stoecklin (1968) (i.e,. Zagros belt (ZB), Urumieh-Dokhtar, Central part of Iran, Albourz mountain, Kopeh-Dagh, Lut, Sanadaj-Syrjan and Makran.

In south-west Iran, that is part of the ZM, Oligocene–Miocene marine sedimentary deposits are well represented (Zabihi et al., 2013). The MZJ basin is located in the ZM showing high intensive thrust, fault and folding processes. Fault and fold systems in this area cause the uplift of salt formations, called Hormoz formation, especially in some parts in southwest and southeast of the study area. These salt domes affect the sedimentation processes and the ground water quality. The salt plugs are covered by weathered minerals such as clay minerals and gypsum and halite at the distal part of the dome features. The MZJ basin is located in the synclinal gap between four anticlines including; Bondasht in the north, MZJ anticline in the northwest, Koheghach in the west and Kohpahn in the southeast of the study area.

The lithologic formation of each area plays an important role for the amount and type of sedimentation. Therefore, the assessment of the lithology of this area is a prerequisite to evaluate water driven erosion processes. Furthermore, the geology in the MZJ basin affects the quality and quantity of the ground water. The plain areas in the catchment are mostly covered with Quaternary sediments. According to the seismic data record more than 40 earthquakes from 1961-2011 with magnitudes of 6.2 to 8.5 (Richter scale) were registered (Iranian of Natural Resources Center; 2006). Therefore, the tectonic activity in this part of Zagros can be considered very intensive.

The MZJ basin Formation contains a distinctive assemblage of lime-marl, limestone, shale, marl, sandstone and conglomerates (Fig. 6).

The lithology of this catchment according to the geology map (1:25000) is subdivided into two main rocks units. The first unit consists in Precambrian rocks which are covered by the salt plugs and extends to an area of about 109 km^2. The second rock unit is represented by the Phanerozoic rocks which are mainly sedimentary rocks that are formed during Cretaceous to Quaternary age, covering a total area of 1279 km^2. The main lithological formations of Phanerozoic sediments are presented in Tab 2 and can be defined as follows:

i) Alluvial deposits of Quaternary age – 470 km^2: Alluvial deposition consisting of rounded gravels, sand, silt, and clay are responsible for the infilling of the basins and valleys in many parts of Iran;

ii) Aghajari Formation - Upper Miocene to Pliocene rock) – 219 km^2: Aghajari Formation consists ca. 3000 m of alternating layers of brown to gray calcareous sandstones and red marls with gypsum interlayers and red siltstones (Bahrami 2009b). The Aghajari Formation is present throughout the ZM (Fig 7), but because of its gradual subsidence during deposition, it is best developed in the Dezful Embayment (about 3000 m) in the north of the Khozestan province;

iii) Asmari - Oligocene to Lower Miocene – 196 km^2: The Asmari Formation is the youngest and most important lithologic formation of the ZM in the south-west of Iran (Roozbahani 2011). This formation is present throughout the Zagros basin but it is prevalently developed in the Dezful Embayment in Khoestan province in the southwest of Iran (Bahrami 2009a). This Formation is divided into three units: the Lower Asmari with an Oligocene age, the Middle Asmari with an Aquitanian age, and the Upper Asmari with a Burdigalian age. The Asmari Formation has a good porosity and permeability and hence is forming a hydrocarbon reservoir containing a major portion of the oil reserves (Bordenave et al., 1990). It is also known as Upper Fars Group and consists of 2966 m fluctuating layers of brown to gray calcareous sandstones and red marls with gypsum interlayers and red siltstones (Bahrami 2009b). This type of formation is more predominate in the north and northwest of the study area. The Aghajari formation is generally more susceptibility to water erosion.

iv) Bakhtyari Formation (Upper Pliocene to Pleistocene) is the main formation in the southwest of the study area. This formation was studied and named as Bakhtyari series by G. E. Pilgrim (1908) and now formally adopted as Bakhtyari Formation in the nomenclature of the ZM. It is especially found in south and southwest of Iran. The thickness of this Formation is up to 500 m (Khaksar & Khaksar 2012). The sediments of the Bakhtyari Formation in this part of basin consist of conglomerates that resulted from sedimentation on the alluvial fan environment and tectonic activities.

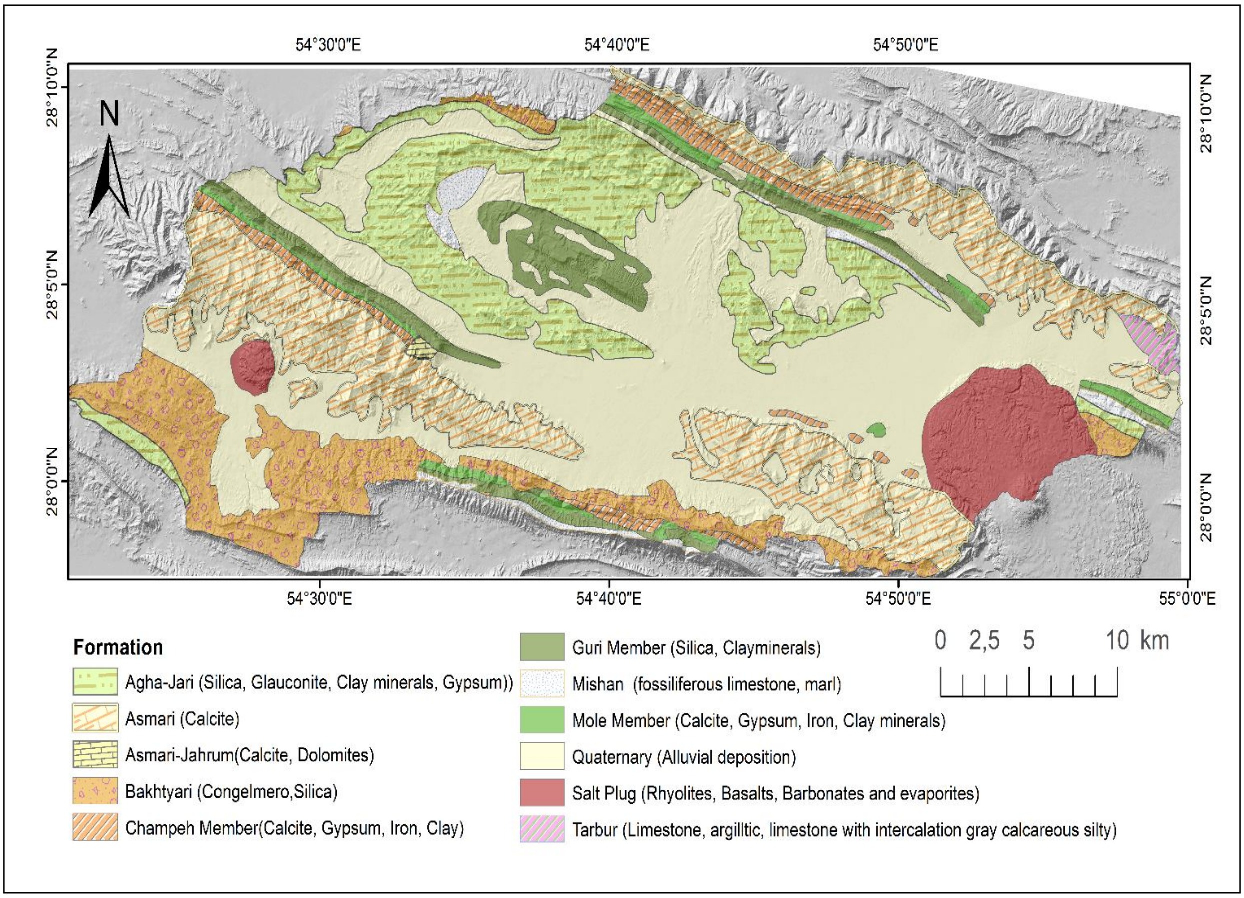

Fig. 6 Lithological map of study area (1:25000).

The degree of susceptibility of the ZM formations to water erosion in Iran, are ranked according to Tab 3 (Faiznia 2003). In consequence the Quaternary sediments are the most susceptible formations to water erosion, while the Asmari-Jahrom Formations are less prone. Meanwhile Aghajari, Mishan and Gachsaran formations (deposition of the evaporitic and detritial sediments) known as Fars group are also highly sensitive to water erosion (Bahroudi & Koyi 2003). Gachsaran Formation (lower Miocene) consists mainly of evaporites, it also contains marls, limestones and shales (James & Wynd 1965). According to many studies conducted in Iran the highest amount of sediments which are produced by gully erosion were observed especially in the Quaternary formations (Sadeghi et al., 2008; Noormohammadi et al., 2014).

Table 2 Lithological map of study area in the ZM

Age	Formation	Lithology	Minerals
Quaternary		Alluvia are composed of poorly sorted and poorly-rounded fragments to pebbles of purple gray siltstones. They are cemented in places, mostly by gypsum. incl. pebbles to cobbles of marl, mudstone or shale.	Silica,Clay mineras (Kaolinite.), Calcite
(Upper Pliocene to Pleistocene)	**Bakhtyri**	Pebble to boulder conglomerate with subordinate cross-bedded sandstones and sandy siltstones. Conglomerates are cemented by pedogenic carbonate cement of the caliche (calcrete).	Silica, Calcite
(Upper Miocene to Pliocene)	**Agha Jari**	Alternation of sandstones, mudstones to shales, sandy siltstones. Fine clastics locally show light green color and contain even abundant glauconite. It is composed of siltstones, silty marls, interbedded with sandstones and gypsum.	Silica,Glauconite , Clayminerals (Kaolinite), Gypsum
(Lower to Middle Miocene)	**Mishan**	A sequence of bedded limestone, often chalky (lower part)– Guri member (Grm) and (the upper part) The dominant part of the member consists mostly of green marls, in places slightly gypsiferous, with intercalations of coquinoid packstones to grainstones in the lower two-thirds, and with silty sandstone, sandy mudstone and organodetrital sandstone.	Silica,Clay minerals
(Lower Miocene)	**Gachsaran**	Is composed of chalky-gypsiferous limestones to dolostones with horizons of marls and nodular to crystalline gypsum, sequence of reddish to multicolored gypsiferous marls interbedded with thin layers of gypsiferous limestones and gypsum.	Calcite, Gypsum Iron, Gypsum, clay, Calcite
(Oligocene to Lower Miocene)	**Asmari**	Thick nummulitic grainstonesto packstones and fine-grained packstones and grainstones witha distinct cross-bedding. (Lime stone).	Calcite

Table 3 Suscptibilty of lithological formations in the ZM to water erosion (Faiznia 2003)

Formation	water erosion susceptibility scores
Hormoz(Salt Dom) Formation	**7**
Tarbour Formation	**2**
Sachon Formation	**4**
Asemari-Jahrom Formation	**1**
Asemari Formation	**3**
Gachsaran Formation	**5**
Champe-part	**4**
Moel-part	**2**
Geory-part	**2**
Mishan Formation	**6**
Agajari Formation	**3**
Bakhtiari Formation	**3**
Quaternary sediments	**9**

Fig. 7 Sedimentary structures in Aghajari formation (sandstones) of the MZJ.

4.4 Vegetation types of the Mazayjan basin

Vegetation cover influences water erosion processes by intercepting raindrops, increasing infiltration, providing additional surface roughness and adding organic materials and root strength to the soil (e.g., Viles 1990; Morgan 1995; Gyssels et al., 2005). In fact vegetation cover is one of the most important factors in soil erosion and especially for gullying in many arid and semi-arid areas (Igwe 2012). There are several types of shrubs, grass and trees in the study area that are restricted by soil moisture, EC, salinity and texture of soil. According to field surveys in 2012 and 2013, main parts of the catchment have no or very poor vegetation covers. Especially the areas affected by gully erosion features in the southwest of the MZJ catchment are scarcely vegetated. In fact the shortage of rainfall and the high temperature during the summer and autumn are the reasons for poor to very poor vegetation cover especially during the dry seasons (from June until October). In the recent years, due to overgrazing and over exploitation of the ground water, many parts of the area were abandoned. In fact the deterioration of vegetation cover is one of the most important factors for gully initiation in southwest of Iran (Soufi 2002). According to field surveys and satellite data analysis the vegetation cover is very poor especially in the pediment areas in the flat parts of the catchment (Masoudi & Zakerinejad 2010; Zakerinejad & Märker 2015). The main land use in this area consists in rangeland, agriculture, abandonment areas and wet lands. Agriculture production and animal husbandry are the main incomes. The dominant agricultural products of the area are wheat, cotton and barely. There are different types of shrub species like, Salsola sp, Stipa sp. especially found in the plain part of the catchment. The predominated tree type is Tamarix with a scarce distribution in the west and the east part of the catchment. Table 4 shows the predominant vegetation types in the study area.

Table 4 the predominant type of vegetation in the MZJ area

Vegetation type	Area(ha)
Salsola arbuscula – Salsola orientalis- Stipa capensis	10322.5
Salsola lanata- Salsola lachnanth	2922.4
Salsola brachiate	2455.2
Convolvulus sp.- Stipa capensis	147.9

Fig. 8 Poor vegetation with sheet erosion in the east of the study area.

Fig. 9 Agricultural area in the MZJ basin.

4.5 Climate in the Mazayjan basin

The climatic conditions and their hydrological consequences may result in significant modifications of soil conditions (Várallyay 2010). As already mentioned, Iran's climate varies from arid and semi-arid to sub-tropical. The study area, as a part of Fars province in the south-west of Iran shows heavy and aggressive rain fall events. The nature of the rainfall with high intensities causes significant soil erosion events. The normal annual average of precipitation in this study area is almost 250 mm showing a high diversity in amount and intensity. The

Intensity-Duration-Frequency curve (IDF) illustrated in Fig. 10 shows high intensities for the area. The 30-min precipitation intensity for a 2 year return period amounts to 23.5 mm h^{-1} and the 25 years return period yield about 56.1 mm h^{-1}. The majority of the rainfall takes place during winter, especially in the mountain areas with high elevations. The Larstan station is sited close to the study area and provides the longest time series (Tab 5). The average temperature at this station varies between 13.1° C in winter and 34.9° C in summer and with 24.1°C annual average. The lowest monthly temperature for this station is 8.9 °C in January and the highest monthly temperature is 41.8° C in August. Evaporation in the southwest of Iran in general and in the study area in particular is very high, especially in summer, but variable within different months. Average evaporation rate is about 1758.5 mm/y (averaged over 32 years, unpublished data, Iranian Water Organization, 2006).

Generally, the amount of precipitation increases from the flat area in the central part to the mountain areas in the north and south of the catchment. Precipitation falls mainly in winter and spring seasons arriving from westerly Mediterranean directions. In this study 9 climate stations nearby the study area have been chosen to calculate the monthly and daily precipitation (Table 5).

Table 5 Meteorological stations in the southwest of Fars Province used for this study

Station	Longitude [Decimal Degree]	Latitude [Decimal Degree]	Elevation [m]	Mean annual evaporation(mm)	Mean annual rainfall (mm)
Darb ghale	54,23	28,55	1430	2696.8	344.0
Ghozan	54,27	28,49	1300	3129.78	347.6
Hajiabad	54,25	28,22	1060	2788.98	248.3
Brak	53,09	28,39	870	2519.18	354.0
Farag	55,12	28,22	890	2696.8	213.5
Khasoe	54,23	28,33	1070	2547.58	241.5
Layzgan	54,58	28,41	2000	No data	492.9
Larstan	54,19	27,38	860	2670.7	270.3
Avaz	54,00	27,46	860	2060.2	236.1

According to the Ombrothermic curve (Fig 11) only from December till mid of April there is a humid climate related to the coldest month of year.

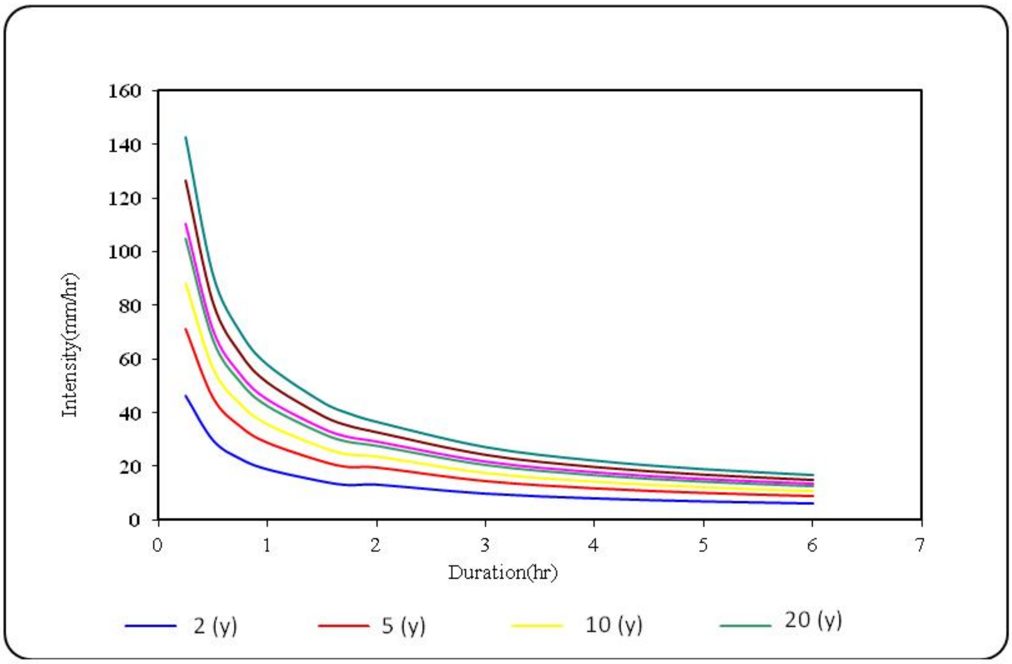

Fig. 10 Intensity-Duration-Frequency curve (IDF) for the study area.

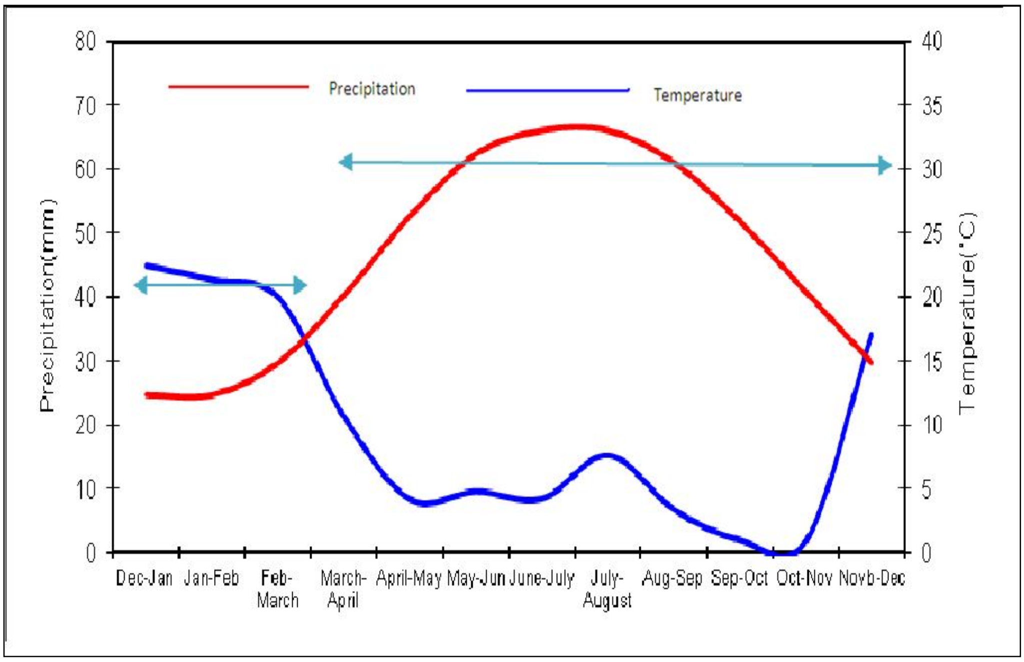

Fig. 11 Ombrotermic curve of the studied sites- monthly precipitation and temperature.

Figure 11 shows the Ombrothermic curve (monthly precipitation and temperature) for the study area with a high inter-annual variability and very dry summer months (June to October). According to this graph a dry period persists during most of the spring time and the summer month.

4.6 Climate change scenarios for the study area

The climate change effects might be one of the most important challenges that many parts of the world, with significant impact on the hydrologic and geomorphologic (Imeson & Emmer, 1992; Wei et al., 2009) especially areas with high susceptibility to erosion processes will be facing. In many researches the relationships between climate and soil erosion have been investigated (Kirkby and Cox, 1995; Imeson & Lavee 1998; Märker et al., 2007; Mahamane 2015). About 75 % of the total land surface of Iran is dominated by arid and semi-arid climate condition with annual precipitation rates of 350 mm to less than 50 mm (Kehl 2009). The soil erosion intensity actually arises both from human effects on ecosystems and also from climate conditions. On the other hand, the character of climate change effects such as the increase of precipitation amount and/ or intensity or drought conditions might affect also soil stability and vulnerability in different climate zones. It was shown by Dastorani & Poormohammadi (2012) that mostly the northern and southern coast's are the regions that will have the highest increase in precipitation using the IPCC scenarios A2 and B2 in 2010-2039. Increasing precipitation results generally in an increased flooding and soil erosion risk. Prediction of climate change effects might help the landuse planners to consider more effective management strategies and hence protection of soil resources in future. In the current study the Long Ashton Research Station Weather Generator (LARS-WG) was utilized as weather generator (Qian et al., 2005; Karimi et al., 2015) and was applied to downscale daily precipitation and daily maximum (T_{max}) and minimum (T_{min}) temperatures in Larestan (near to our study area) in the Fars province. The data is used to predict future changes of precipitation and temperature. According to the result for this station precipitation will decrease in the period February to May and October to December while temperature will increase during the entire period (2010-2039) under both A2 and B2 scenarios (Fig 12).

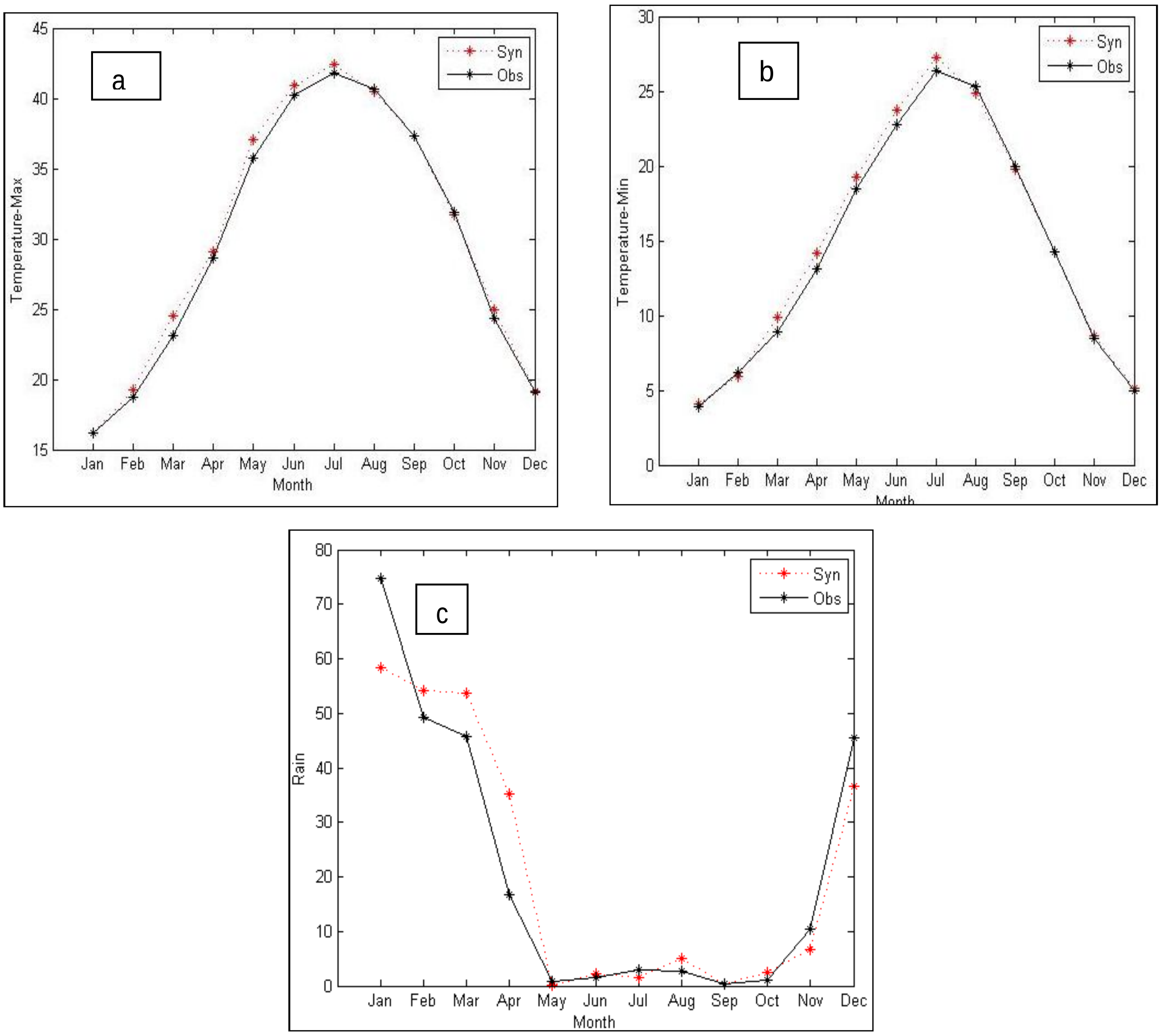

Fig. 12 Tmin (a) Tmax (b) Precipitation (c) using LARS-WG model from 1980-2005.

4.7 Tectonic activity in the Mazayjan basin

In the Pliocene and Quaternary periods the orogeny has altered the Iranian platform morphology and developed the Alborz, Zagros, Makran and Kope-dagh mountain ranges (Khaksar & Khaksar 2012). The width of the orogeny is controlled by the balance between erosion flux and accretion flux (Khadivi 2010). Tectonic is a highly important factor controlling landform development and evolution in the study area. Moreover, tectonic considerably affects fluvial systems in the central of the ZM (Dehbozorgi et al., 2010). The Zagros fold structure is over thrust along and interrupted by the Zandan thrust about 75 km east of the Bandar Abbas province in the south of Iran. It exhibits a variety of active depositional environments (Bosák et al., 1998; Zabihi et al., 2013). Active tectonic in the area involves the formation of landforms and drainage networks. Actually, the tectonic activity in this area has an important role on the evolution and intensity of soil erosion.

These aspects may be highlighted by the evaluation of knickpoints along the drainage network and hence, gives information about uplift processes and in consequence also on the occurrence of gully features.

4.8 The topography of the Mazayjan basin

Topography has an important role on the soil evolution in different climates. The topography of our study area is undulating, with a variation of mountainous, pediment and plain landscapes. The flat area or pediment area with lower slopes less than 5 % are mainly covered by alluvial deposits. This part of the catchment shows more gully features and most of the agriculture activity is located in this part of the area. The elevation in the study area varieties between 604 m to 1989 m. The highest elevations can be found in the north and south of the study area. In the west and southeast of the catchment there are two Precambrian salt Doms that are the main source of salt accumulations in the flat areas. Due to the complex topography of the study area the access for soil sampling and ground control is often very difficult. The central pediment parts reflect a syncline structure filled with Quaternary alluvial deposits. The ephemeral MZJ river that is flowing from the west to east of the study area is the main drainage of the catchment.

5 Research Summaries

5.1 Prediction of gully erosion susceptibilities using detailed terrain analysis and Maximum Entropy modeling: A case study in the Mazayjan plain, southwest Iran

Motivation: Soil erosion is a serious environmental problem in the recent decades in many parts of the world and especially in Iran, reducing soil productivity and as a consequence leads to land degradation and desertification. Gully erosion as a process of soil loss often has been neglected in many modelling approaches of water erosion over the past decades. Gully erosion is spatially and temporally very heterogeneous and hence it is difficult to measure and monitor the processes quantitatively, especially in remote areas (Vázquez & Zinck 1994; Poesen et al., 1996; Märker et al., 2001; Sidorchuk et al., 2003). Consequently, the prediction of gully development using numerical models is difficult, time consuming and expensive since the different input parameters involved in the prediction are not so easy to determine (Jacob et al., 2012). Even though several studies have already been carried out on the morpho-genesis of gully erosion in Iran (Soufi 2004; Nazari et al., 2009; Shahrivar et al., 2012) only a few studies exist that assess the spatial distribution of gully erosion on larger areas considering the relevant environmental driving factors. However, there are many causes for gullying such as; climate conditions, topography, lithology, soils and LULC etc. (Poesen et al., 2003; Ahmadi 2007; Zakerinejad & Märker 2015). The susceptibility to gully erosion is mainly a function of erodibility of outcropping materials, vegetation coverage, rainfall characteristics and topographic information (Conscenti et al. 2008a; Frankl et al., 2013). Therefore, this study is concentrating on the MZJ plain of Southern Iran and aims at investigating the distribution of gully erosion with a quantitative method based on terrain analysis and mechanical statistics. Moreover, we want to identify the most important environmental indices triggering gully erosion in the study area and finally we derive a map of the spatial distribution of gully erosion susceptibilities.

Method: In this research terrain analysis (TA) and data mining techniques were applied to predict the susceptible areas to gully erosion. Field surveys in 2012/13, Satellite images (2012) and aerial photographs (scale1:20000) taken in 2006 helped us to identify gully features in order to map the gully areas in the MZJ basin. Since soil erosion processes are mainly triggered by topography we used some specific topography indices such as; wetness index, stream power (SPI), slope, LS-factor, profile curvature, plan curvature, catchment area, curvature, convergence index, channel network, channel network base level, altitude above channel network and aspect.

The topographic indices were extracted from a digital elevation model (DEM) with 10 m resolution based on a topographic map (1:25000) using the counter lines and elevation points and the topo to raster module in ARCMap 10.2. In this research the topographic indices were utilized as independent variables. As dependent variable the extent of the mapped gully systems transformed in point data were used. We applied a stochastic classification method, namely the Maximum entropy distribution model (Maxent) (Phillips et al., 2006) (Fig 13). The Maxent model was trained using 90% of the mapped point type gully extent data as target or dependent variable and the raster type topographic indices describing the environmental characteristics of the area as independent variables. The resulting model was subsequently validated using randomly selected 10% of the mapped gully data.

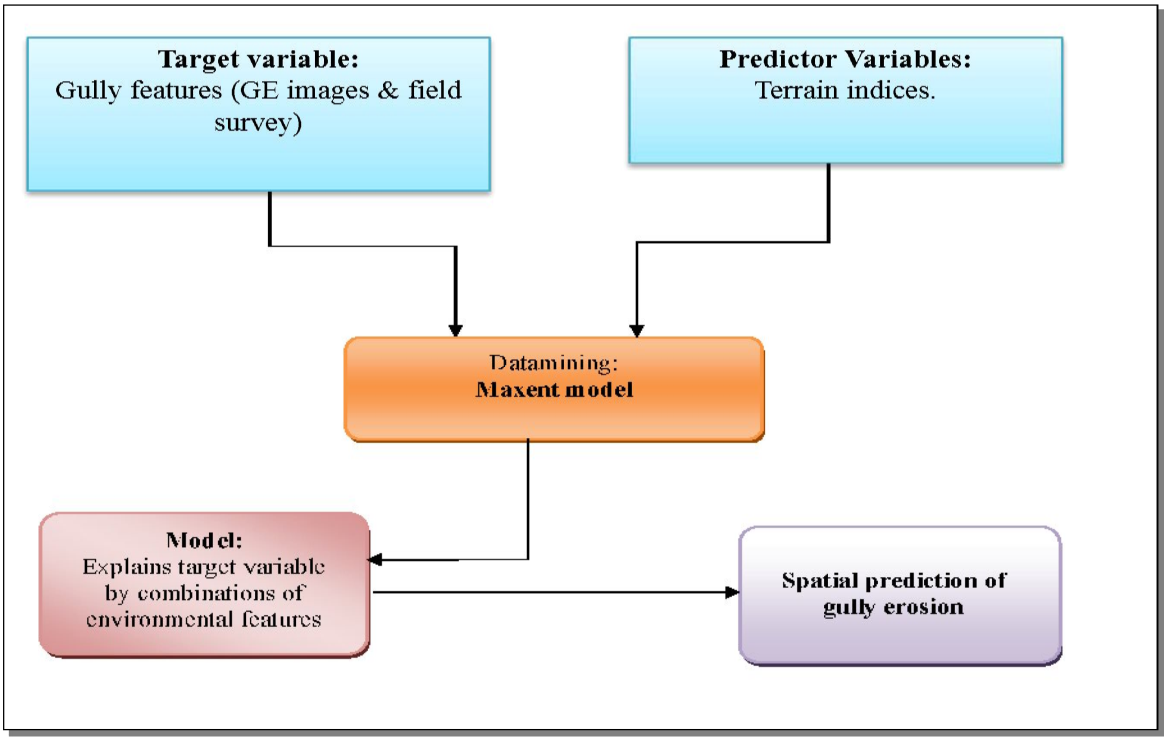

Fig. 13 Stochastic Modelling Approach in the study area.

Result & Conclusions: The result of the applied model shows that the susceptible areas are mostly located in the south and south west of the catchment. The internal validation via the AUC graph for the training and testing data with values of 0.95, 0.94 respectively indicates outstanding results in terms of model performance. The most important variable is the convergence index calculated following Köthe & Lehmeir (1993) with 38.7%. This index is a proxy for the accumulation or distribution of water. The second most important index is plan curvature with 36.4 % contribution. This index indicates the accumulation or distribution of surface runoff. It was calculated using the algorithm of Zevenbergen & Thorn (1987). Slope and aspect with 7% and 4.6% respectively were less important. The model was subsequently applied to the whole data set in order to predict the gully susceptibility for the entire study area. In fact the mountain areas with no or very low soil depth, rock outcrops and steep slopes show very low susceptibilities while the more susceptible areas are found in the pediment or alluvial flat parts of the catchment. If we only relate to the susceptible areas 79.95%, 17.74% and 2.8% respectively are in the slight, moderate and high gully erosion susceptibility classes. Fig 14 shows severe, intensive gully erosion in the plain area in the south west of the MZJ basin with very low vegetation cover. The integration of GIS with statistical analyses yields valuable information on areas susceptible to gully erosion. However, the source data must be prepared carefully to avoid any artifacts or errors in the digital elevation model and should reflect the spatial scale of the investigated features. If so, the approach is a valuable tool for landuse manager.

Fig. 14 Severe gully erosion in Southwest of the MZJ basin.

5.2 **An integrated assessment of soil erosion dynamics with special emphasis on gully erosion in the Mazayjan basin, southwestern Iran**

Motivation: Water erosion is a serious problem threading the sustainability of arable land and water resources especially in the Southwest of Iran. A large part of Iran (1.6 million km^2) is prone to both wind and water driven soil erosion processes. Gullies, rill-interrill and sheet erosion features are the predominate types of water erosion. In the last decades several models were applied to assess soil erosion phenomena in Iran in a quantitative and qualitative way concentrating on rill and sheet erosion (Tangestani & Moore 2001; Meamarian & Esmaeilzadeh 2003 Masoudi et al., 2006; Tangestani 2006). However, the quantitative and qualitative assessment of gully features has been widely neglected and thus, the estimation of erosion and quantification of sediment production is always limited (Kumar et al., 2013). This study is aimed at identifying and quantifying the main erosion process dynamics including gully erosion in southwest of Iran as a part of ZM.

Method: In this research GIS and satellite image analysis techniques were used to derive input information for the numeric models. For sheet and rill erosion the Unit Stream Power-based Erosion Deposition Model (USPED; Mitasova et al., 1996) was utilized. The spatial distribution of gully erosion was assessed using a statistical approach, based on three variables (stream power index, slope, and flow accumulation) to predict the spatial distribution of gullies in the study area. The eroded gully volumes were estimated for a 7-year period by fieldwork and GE high-resolution images. Figure 15 shows the methodology and input layers data for the USPED and SPI index to evaluate the severity of soil loss in the MZJ basin.

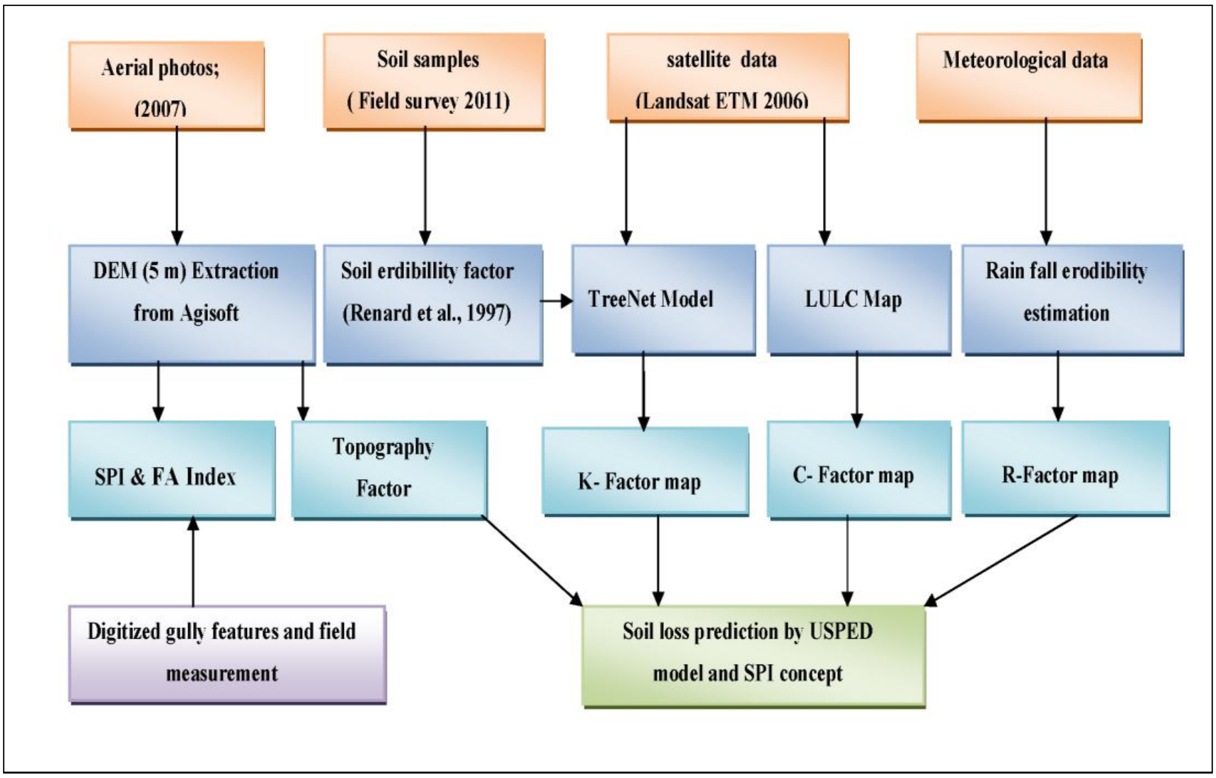

Fig. 15 Flow chart of methodology of soil erosion modeling using USPED & SPI index.

Result & Conclusions: According to the USPED model algorithm the input data (R, K, C, P and topographic factor) were multiplied with the raster calculator in ArcGIS 10.0 to get the erosion/deposition rates in t ha^{-1} yr^{-1} for each grid cell. According to the combined final map of erosion deposition processes modeled with USPED and including the gully erosion processes derived by SPI about 17.5 % of area is stable or characterized by very low erosion or deposition classes. Very high erosion values cover 28.2 % of the area, whereas 19.2 % of the area is related to deposition processes. The integrated USPED/SPI approach shows that more than 43 % of the area is affected by soil erosion with more than 10 t ha^{-1} $year^{-1}$. Moreover, the average value of erosion with 37.6 t ha^{-1} year is higher than the annual average of soil erosion (33 t ha^{-1} $year^{-1}$) for Iran (Hosseini & Gorbani, 2005; Omidvar 2010). Furthermore, the average predicted soil loss rate for the study area is four times higher than the mean global soil loss (Omidvar, 2010). The simplicity of the methodology, the availability of low cost and easy access data as well as concentrated filed work activities, made this model relatively applicable for areas that are affected by rill-interrill and gully erosion, especially in southwestern Iran.

5.3 Morphotectonic analysis of the Zagros Mountains using high resolution DEM to assess gully erosion processes: A case study in the Fars province, Southwest of Iran

Motivation: Soil erosion is a serious type of land degradation in many parts of Iran, particularly in the south and south west of Iran. Gully erosion as one type of soil loss is among the most hazardous natural disasters (Boardman et al. 2003; Poesen et al. 2006; Marzolff et al., 2011). In the ZM the main factors influencing soil erosion processes include geology, tectonics, climate, topography and land cover. In this part of Iran especially the role of active tectonics is crucial for the evolution of landforms and stream networks. In other words the tectonic activity in the ZM seems to have an important effect on the evolution and intensity of soil erosion processes. Therefore, the main objective of this study is to understand the role of tectonic activity on gully erosion processes and stream network evolution. The specific objectives of this study are threefold:
i) Assessment of tectonic effects on the drainage systems in the study area ii) Comparing different DEM resolutions and their effects (30 m, 10 m, and 5 m) on the morphotectonic analysis iii) Understanding the relationship between the faults, gully processes and knickpoints in the study area.

Method: In this study three DEMs namely; the ASTER GDEM (30 m), a DEM based on topographic maps 1:25.000 with 10 m resolution (Iranian Cartographic Centre, 1994), and a DEM with 5 m resolution based on stereo aerial photos were used to analysis neotectonics and gully features. To generate the DEM with the 5 m resolution stereo aerial photographs at 1:20.000 scale (Iranian National Survey Mapping 2006) having 60 % overlap were used. In this research the Agisoft PhotoScan software (http://www.agisoft.com) was utilized to generate the 5 m DEM. Subsequently basin asymmetry and Hypsometric Integral (HI), the morphology of the stream longitudinal profiles and knickpoints analyses were carried out using the TecDEM software (Shahzad & Gloaguen, 2011) (Fig. 16).

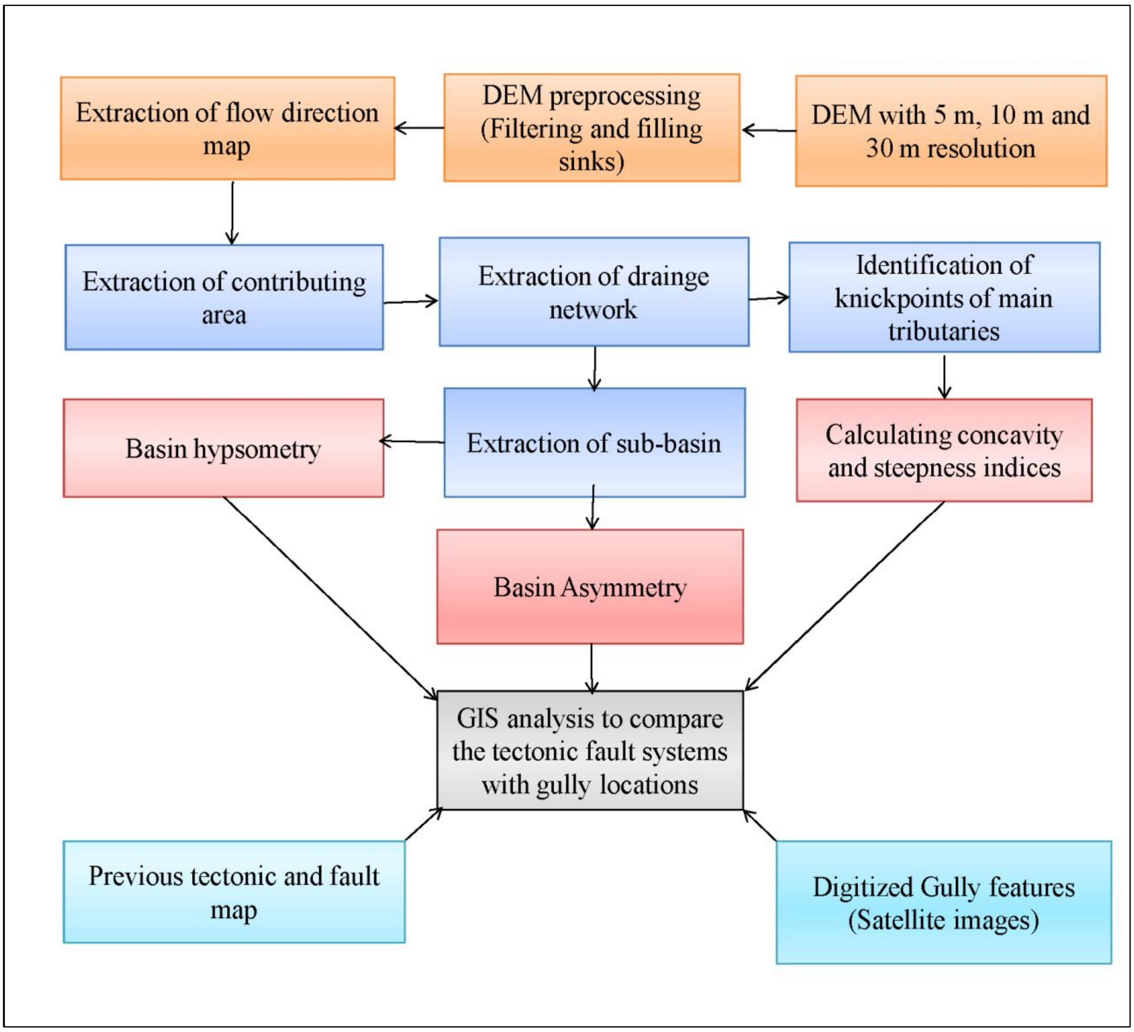

Fig. 16 Flow chart showing the applied analysis steps to assess the relation between tectonic and gully erosion processes.

Result & Conclusions: The basin asymmetry for the eight 4th order sub-catchments and one 5th order catchments were calculated. Strong tectonic activity can be supposed especially in the southern and western parts of the catchment with high asymmetry values. The basin asymmetries also yield information about the prevailing direction of tilting. In this study the tilting directions point towards the south in the western, central and southern parts and into northern directions in the east and central western parts of the of the study area. This is in line with the geological surveys conducted in the area and reported in the geological maps. The HI for the south and south western parts of the catchment is almost 0.60 indicating an active phase of soil erosion while in the North the values are lower than 0.30 pointing to a monadnock phase in landscape evolution.

For the south and south western parts of the catchment a HI value of almost 0.60 indicates an active phase of soil erosion while in the north the values are lower than 0.30 pointing to a monadnock phase in landscape evolution. Longitudinal profiles of the 7 tributaries of the MZJ catchment were extracted with concavity and steepness indices. However, the analysis showed that the DEM with 10 m resolution derived from the topography map (1:25000) and the 30 m ASTER GDEM do not have a proper quality due to artifacts and errors and hence, tectonic processes cannot be assessed adequately. Comparing the fault lines and gully locations in the catchment it was shown that more knickpoints are approximately near to fault lines in the southwest and north-east of the catchment. Since the climatic conditions do not changed much and also the geology of the valley bottom areas is quite homogeneous it seems that the tectonic processes control the watershed dynamic in terms of knickpoint development and migration. The results indicate that the erosion processes may also be amplified by the tectonic activity of the study area.

5.4 Assessment of gully erosion using multispectral remote sensing, GIS and stochastic modeling in the Southwest of the Zagros Mountains- Iran

Motivation: The process of gully erosion as important type of water erosion is among others also highly depending on the lithology of area. Actually the recognition and analysis of the factors leading to gully erosion is crucial for the assessment of soil loss and gully erosion process (Ogbonna 2012). However, areas with susceptible lithology are more prone to sheet wash and gully processes while formations with components of resistant material generally show lower susceptibilities to erosion processes. Access to geologic information with an accurate resolution can be quite difficult in many parts of the world. Therefore, remotely sensed data with respective spectral, spatial and temporal resolution might be a useful way to get proper geological information for large areas. The overall object of this research was to generate a lithology map from multispectral ASTER data and to improve the understanding of the links between geology, substrates and gully extension in the MZJ basin in southwest of Iran as a part of the ZM. Therefore, the purpose of this study in particular is:

i) The assessment of band ratios of ASTER multispectral data to differentiate specific sedimentary rock units or lithologies according to their spectral reflectance, and hence, to improve the existing geological map of the study area.

ii) The analysis of potential areas for gully erosion in relation to the lithology.

Method: In this study, we used data collected by field survey, aerial photos, and ASTER (advanced space borne thermal emission and reflection radiometer) multispectral images. Moreover, we assessed the information with a GIS-based model and a machine learning algorithm based on a stochastic modeling (MaxEnt model) approach, to examining factors most likely influencing the spatial distribution of gully erosion in this arid catchment area. In this research a band ratio stacking using the band ratios 4/9; 4/6; and 9/8 is assessed to differentiate between different lithological units in the study area (Fig 17).

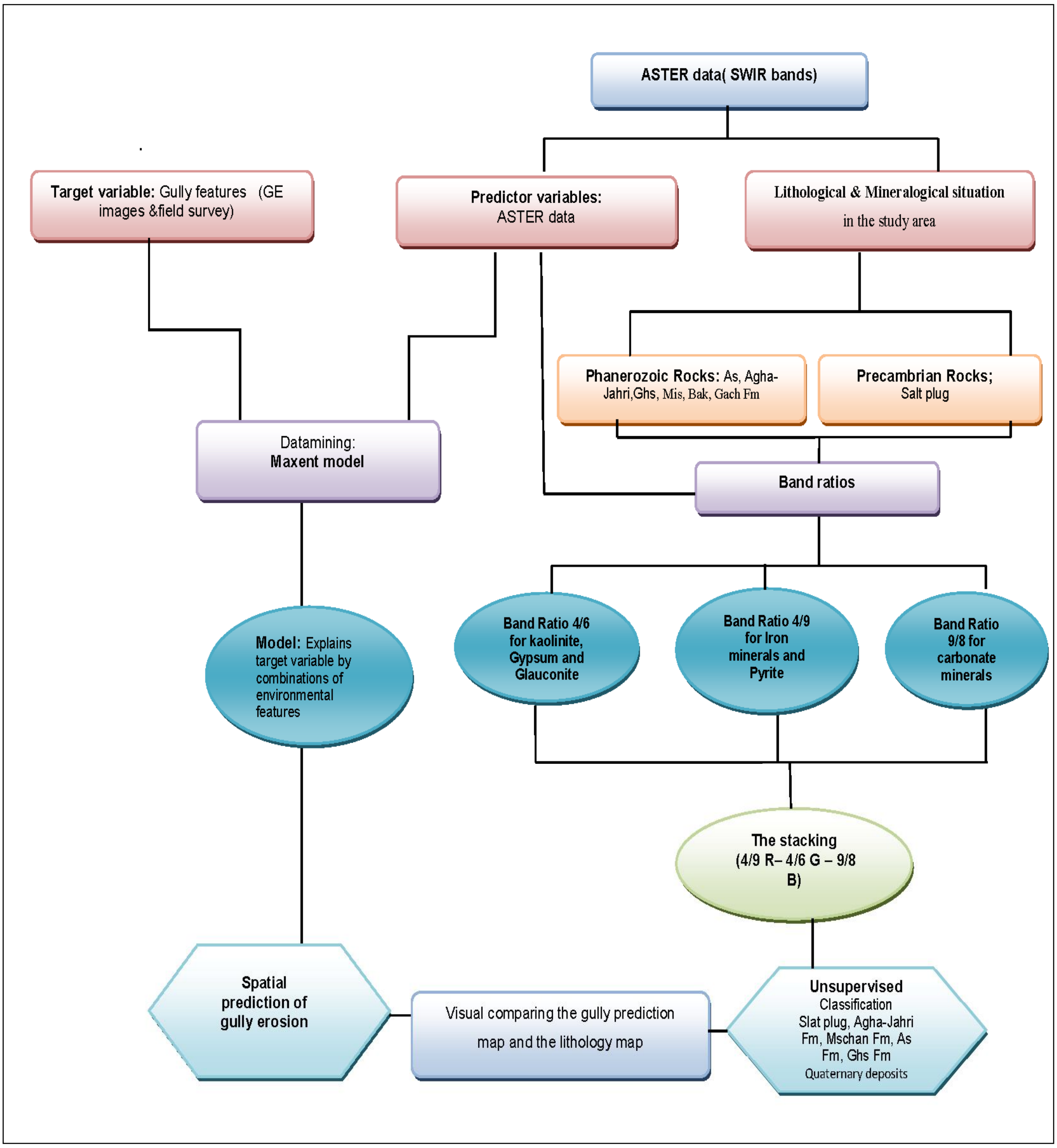

Fig.17 The flow chart for the applied methodology in the MZJ basin.

Result & Conclusions: The result of the unsupervised classification of the lithological units was attributed to different sedimentary rocks in the first step and validated with the field data. Based on the geological map, the following band ratios were attributed to specific lithological units. The first ratio of bands 4/6 describes best the Agha-Jahri formation appearing in dark

color due to high concentration of Glauconite mineral whereas the presence of Gypsum and Kaolinite minerals in the Mischan formation produces a grey to light grey color. Gypsum deposits at the distal part of the Salt plug zone are also discriminated. Band ratio 4/9 characterizes especially Precambrian rocks because of their high contents in pyrite and iron minerals. Band ratio 9/8 identifies carbonatic rocks with brighter color than other rock types. The rocks units (Asmari and Gachsaran formations) are shown with white to light grey color in the scene, indicating their high carbonate content whereas weathered minerals like Gypsum and kaolinite occur with dark grey to black color especially in alluvial deposits (Black color). For the stochastic modelling approach we used as dependent variables the gully features and as independent variables the bands ratios of the ASTER data. We validated the performance of the Maxent model using AUC diagrams. The results show AUC values of 0.98 and 0.90 respectively for learning and testing data and hence an outstanding model performance.
Based on the MEM, the susceptible areas to gully erosion have been predicted in the entire of the study area. It was shown that most of the gully features are concentrating on the alluvial deposits characterized by highly erodible, non cemented sediments and high EC and salt contents especially in the west and east of the catchment.

6 Discussion and conclusions

In this thesis different approaches have been applied to assess and predict gully erosion features in the MZJ catchment in the ZM in southwest of Iran. Particularly, in the related publications the use of satellite data, GIS applications and stochastic modelling approaches were highlighted that increase the amount and accuracy of the input data. Although the applied methodology have many advantages and easily might be adapted and applied in other regions with different environmental conditions, still there are some limitations that are discussed in this part of the thesis.

GIS and data mining techniques like the Maxent model were applied in this study to predict the spatial distribution of probabilities for gully erosion related to terrain and geological parameters. The first part of this research was aimed at the analysis of the functional relationships between a set of terrain parameters (topographic indices) and gully erosion processes using the Maxent model and subsequently to predict the susceptible areas of the study basin. In fact, the information about the spatial distribution of susceptible areas to gullying processes is useful and an effective way to recognize the prone areas. However, since gully erosion may occur in different evolution stages and dominated by different controlling factors, it can be considered as the most complicated linear erosion process (Sidorchuk 2005). Therefore, the evaluation of this type of soil erosion and of its main driving factors are crucial for a better understanding and hence, assessment of the processes. In many studies of gully erosion around the world, but especially in Iran, the applied models focused especially on the analysis of the gully morphologies and the stages of gully development while no research focused on the modelling of the spatial susceptibility distribution using e.g. data mining. Moreover, also the role of neo-tectonic as a driving factor for gullying was completely neglected. As already mentioned we firstly focused on the topographic indices because these layers reproduce the geographic variability of the main factors potentially controlling the spatial distribution of gullying (Vandekerckhove et al., 2001; Koco 2006; Kheir et al., 2007; Nazari et al., 2010).

The applied model showed an accurate prediction of the susceptible areas to gully process in the entire area of the MZJ catchment. Using the present gully locations as the dependent variable is one of the advantages of the MEM model that, to the knowledge of the author, was applied for the first time in Iran for soil erosion assessment modelling. Most of the models used in soil erosion or mass movement assessments need also absence data like the no-gully or no-landslide data (e.g. Sidorchuk et al., 2003; Märker et al., 2011; Safaei et al., 2012; Agnesi et al., 2011). Sometimes this absence data is difficult to obtain or one just not know if an area that today has no sign of gullying may not be affected in future. Moreover, generally high densities of vegetation make it difficult to recognize gully areas or landslides especially if satellite images or aerial photos are utilized.

As already mentioned the MEM model is able to identify the importance of the single variables contributing to the entire model of gully susceptibility. The predictor variable extracted from a DEM with 10 m resolution based on a topographic map (1:25000) was evaluated to understand the important factors that determine the susceptible areas prone to gully erosion processes. The most effective parameters in this study were aspect, plan curvature, slope and convergence index. According to the indices curvature and catchment area especially concave morphologies and medium sized contributing areas were depicted. The latter ones cause enough runoff that concentrates (concave curvatures) and at a certain flow length becomes turbulent and start eroding the substrates. Based on these results a suitable management of the prone areas is feasible since the model shows the spatial distribution of the susceptible areas to gullying processes. For example, the prediction showed highly susceptible areas particular in the south and southwest of the MZJ catchment. Actually, the mountain areas show only low values of probability because of their steep slopes and very shallow soils. The gully probability prediction map enables landuse managers for gully prevention and control in the MZJ basin. Moreover, the validation of the model shows outstanding overall model performances for the prediction of the susceptible areas given by high AUC values. Although this model is very effective to predict the susceptible areas, however, the accuracy of the DEM as primary source for the extraction of terrain attributes is crucial. In other words, the model is very sensitive to errors or artifacts in the digital elevation model. In our study we used filter methods to avoid terrace effects due to interpolation of contour lines especially in the flat areas.

In order to implement a sustainable management of the fragile areas like the MZJ basin in southwest of Iran, the rate and severity of soil loss should be known. Therefore, GIS techniques were utilized. In the second part of this study we focussed on the integration of rill-interrill erosion and deep linear erosion processes like gullying. For the rill-interrill assessment we applied the USPED model and for the gullying we used an SPI based approach. In many previous studies in Iran qualitative models were used for the assessment of water erosion (Ahmadi 2007; Masoudi et al. 2006; Masoudi & Zakerinejad 2010; Amiri 2010; Amini et al., 2010; Yousefi et at., 2014) but gully erosion was completely neglected.

The USPED model (R, K, C, P and topographic factor) was applied to get the erosion and deposition rates in t ha^{-1} yr^{-1} for each grid cell. As mentioned one of the main problems in many empirical modelling approaches is the negligence of gully erosion process. However, gullying is the main source of sediments in many catchments in arid and semi-arid areas in Iran. Therefore, the USPED model was used to evaluate the area with sheet and rill erosion. In fact, comparing the results of the model with the gully feature map we show that the model is not able to identify the potential areas of gully erosion. According to the results of the USPED model, the lower erosion and deposition classes are located in the areas with high gully features especially in the low sloping areas in the south and southwestern parts of the MZJ catchment. Hence, the SPI has been applied to identify gully erosion as the main source of sediment in our study area.

The Soil erodibility (K-factor) that was generated using a boosted regression tree approach, the TreenNet model, showing a variation between 0.11 t ha MJ^{-1} mm^{-1} in the northern and northeastern part of the study area with more sandy loam and sandy clay soils, to 0.32 t ha MJ^{-1} mm^{-1} in the southwestern and southeastern part of the area with silty loam soils that are more prone to water erosion. Comparing the different rock types of the area using the ASTER multispectral data in the last part of this thesis we have figured out that the most sensitive areas are located within the Quaternary formations and alluvial deposits. The Crop and management factor (C) was generated using the Landsat ETM, 2007 data and field survey to identify the different vegetation types. The respective identified land use classes where then attributed with C factor values derived from the literature. The maximum C-values coincide with the barren areas in the ridge positions in the north and southwest of the watershed, while the lowest values are related to the areas with better vegetation cover condition in the east of the catchment. The high value of rainfall erodibility is related to the mountain areas with high elevations in the north and south west of the study area. The areas with low elevations are located in the plain parts in the center of the MZJ basin. The obtained values range from 212.6 to 424.6 MJ mm/ ha y. The average values for the MZJ watershed amount to 265.2 MJ mm/ha year^{-1}. The final map of the soil loss combining the USPED (for rill and sheet) and the SPI approaches (for gully erosion) for the entire study area shows high soil loss classes specially in the flat areas due to gully erosion. According to these results the potential areas for gully erosion process were integrated using the SPI index in the model. The high deposition areas are mainly located in the central part and along the drainage networks because of lower transport capacities when water flow is low. The location of the low soil loss classes are mainly related to the area with low soil erodibilty and denser vegetation cover while the barren land areas are very sensitive to soil loss, especially in the west and southwest where abandoned land prevails. According to the filed survey these areas were overexploited for agricultural activity while after some years soil productivity decreases and gullying may take place.

These abandoned, barren land areas are more prone to soil loss process induced by wind and water. Therefore, in the affected areas priority should be given to increase the vegetation cover in order to decrease runoff velocities and protect soils from wind and water detachment. However, many uncertainties in empirical soil erosion modelling approaches are due to the quality and accuracy of the input data and especially the DEM resolution. The proposed model considering rill, sheet and gully erosion is very simple and needs only a few requirements as input for the model. Therefore, it can be applied also at larger scales like all the entire ZM or at the national scale. The results of this methodology could be useful for land use planner to get a better understanding of the soil loss and in consequence to develop an appropriate land use planning and management strategy in these areas.

Many studies investigated the interactions between erosion, morphometry and tectonic activity (Tibaldi & Leon, 2000; Montgomery & Brandon 2002; Blanckenburg et al., 2004;

Norton et al., 2008; Andermann & Gloaguen 2009) but still there is a research gap concerning the assessment of the role of tectonics on the spatial distribution of the gully erosion, especially in the ZM in southwest of Iran with intensive tectonic activities.

In fact the mechanics of gully erosion and their relation to tectonic processes are still poorly studied in the ZM. In this study we used a high resolution DEM (5m) based on aerial photos (1:20.000) to conduct a morphotectonic analysis with emphasis on the plain areas with predominant gully processes.

As already illustrated, we recognized the susceptible areas for gully formation in the area with low slopes in the central part of the MZJ catchment. An investigation of the location of gully features like headcuts and stream profile knickpoints shows that the sensitive areas to gullying are related to areas with up-lifting and faulting. Moreover the result from the basin hypsometry and asymmetry analysis indicates an active phase of soil erosion especially in the south and south-western parts of the catchment. Although we have applied three different sources of DEMs (ASTER GDEM, topographic map, and aerial photos) only the highest resolution allowed a detailed assessment of the stream longitudinal profiles in the plain areas, while the other sources of DEMs had too much noise and/or artifacts. According to the findings of the morphotectonic analysis, active tectonics is an important factor for gully evolution. Knickpoint analysis is a useful tool to interpret the uplift processes changing the longitudinal stream profiles. In fact knickpoints are clearly related to areas with high gully density. The analysis indicates strong effects of tectonic activity on gully erosion processes especially in the west and southwest of the study area.

In the last part of this study the mineral differentiation analysis using ASTER multispectral data yield a useful map to derive a first detailed overview of the lithology of the MZJ catchment in southwest of Iran. The results reveal the potential of multispectral satellite data analysis to get detailed lithological data particular in remote areas with difficult accessibility for field survey. In this study the results obtained from different band ratios displayed a good relation between the predicted susceptible gully areas and the mineral differentiation map. According to these finding, the band ratio 9/8, with the value range between 0.80 and 1.10, is less important for the gully prediction model while the values higher and less than this range are the most important once for the prediction of the prone areas. Band 8 is also a very strong predictor variable especially if values of more than 160 are reached.

The general results obtained from the terrain analysis, the multispectral lithology assessment and the tectonic analysis allowed a detailed investigation and evaluation of gully erosion processes in the MZJ basin. We identified the important environmental factors triggering gully erosion processes. The general findings of this study indicate simple ways to identify the degree of gully erosion susceptibility according to main variables describing the terrain, the lithology and the tectonic activity. The use of remote sensing data such as ASTER and Landsat ETM data can provide valuable input information required for soil erosion modelling with GIS. Furthermore, the predicted map of water erosion based on the integrated USPED/ SPI model allows a detailed assessment of the prone areas for an appropriate prevention of land degradation. In this study we applied stochastic models to generate detailed maps for K-factor (TreeNet) or susceptible areas for gully erosion (MaxEnt). The application of data mining methods in this research is a key tool to evaluate the vulnerability of soils to water erosion on catchment scale. Gully features in particular, wherever they occur are environmental disasters that are related to enormous losses of arable lands, infrastructures and private properties. The investigation may also lead to some specific actions such as: i) rising public awareness concerning the rate of soil loss and land degradation in the study area, ii) proper farming techniques regarding the types of crop and irrigation systems adapted to the shortage of water, iii) the use of the available material to prevent gully headcut retreat, iv) encouraging the inhabitants to improve the agroforestry system with cultivation of native tree or shrubs or planting deep-rooted perennial pastures, trees, or v) an appropriate mixture of both that tolerate also drought conditions. Although in the recent years the local organizations in this area helped the local population to use native shrubs and trees species to combat desertification (Fig. 18) still more attention and financial contribution is needed from the government to speed up the implementation of these plans. Improved land use, forest, soil and conservation practices should be adopted by the local population and related organizations.

7 Outlook

The presented methodology may be also useful for a proper LULC management and landuse planning in different desertification prone areas to evaluate gully erosion process. Prevention measures like the impediment of the processes or mechanisms that result into or advance to gully erosion should be considered by all stakeholders in environmental management and planning especially in susceptible areas such as the MZJ catchment in the southwest of Iran.

Although the government of Iran tries to combat soil erosion with different strategies many LULC changes in recent years and additionally climate change effects, increase the susceptible areas that need more attention and priority. Gully erosion processes destroy arable land and reduce soil productivity and thus, are a serious threat especially in agriculture based countries like Iran (Zakerinejad & Märker 2014; Imani et al. 2014). Moreover, soil loss and its effects on the water quality and dam reservoirs require an appropriate management and landuse taking into account different socio-economic and climate change scenarios in the susceptible areas.

Although ASTER GDEM (30 m) and DEMs extracted from the topography map (10 m) have a higher resolution than e.g. SRTM 90m, they are not suitable for these analyses. However, the results of this thesis indicate that higher quality DEMs derived from aerial photos or high resolution satellite images are needed in order to improve the results of soil erosion modelling.

Even though this study emphasizes on gully erosion processes, in future, research should also include different other types of water and wind erosion. The conditions and rates of land degradation and soil erosion are one of the most common questions that land use planner are facing in future. Therefore, applying different LULC and climate change scenarios might be a useful way to estimate the rate and condition of soil loss in future. In fact recognized trends of LULC changes can be studied in detail by proper scenarios of future LULC and climate change and thus, is an important way to an appropriate soil erosion conservation planning. Finally, considering other socio-economic effects like over grazing, or subsidies etc., that might accelerate the progress of gully and soil erosion are also very important drivers that could be considered in further research.

Fig. 18 Cultivation of shrubs by the natural resources cooperation and local residents.

Reference:

Ahmadi H (1995) Applied geomorphology. Tehran University Publication, Iran, p 613.

Ahmadi H., Mohammadi A.A., Ghodousi J., Salajegheh A (2007) Testing the four models for prediction of gully head advancement (case study: Hableh Rood basin - Iran). Biaban 12: 61-68.

Agnesi V., Angileri S., Cappadonia C., Conoscenti C., Rotigliano E (2011) Multi-parametric GIS analysis to assess gully erosion susceptibility: a test in southern Sicily, Italy. Landform Analysis, 17: 15–20.

Alimohammadi A., Sheshangosht S., Soltani M.J (2006) Evaluation of relations between DEM-Based USPED Model Output and Satellite-based spectral indices. Conference Proceedings of Map India 2006. http://www.gisdevelopment.net/proceedings/mapindia/2 006/index.htm.

Amini S., Rafiei B., Khodabakhsh S., Heydari M (2010) Estimation of erosion and sediment yield of Ekbatan Dam drainage basin with EPM, using GIS. Iranian Journal of Earth Sciences, 2:173-180.

Amiri F (2010) Estimate of Erosion and Sedimentation in Semi-arid Basin using Empirical Models of Erosion Potential within a Geographic Information System. Soil and Water Research, 3: 37–44.

Andermann C., Gloaguen R (2009) Estimation of erosion in tectonically active orogenies, Example from the Bhotekoshi catchment, Himalaya (Nepal). International Journal of Remote Sensing, 30 (12): 3075-3096.

Asrari E., Masoudi M (2011) Development of a new model of risk analysis for water erosion by using GIS. Journal of Applied technology in Environmental Sanitation, 1: 5 3 - 67.

Bahrami M (2009a) Stratigraphy, microfacies and sedimentary environments of Asmari Formation at Tang-e-Bolhayat, north of Kazerun, Fars Province, Iran. Geophysical Research Abstracts, EGU General Assembly, 11.

Bahrami M (2009b) Lithofacies and Sedimentary Environments of Aghajari Formation in Dehsheikh Mountain, West of Shiraz, Iran. World Applied Sciences Journal 6 (4): 464-473.

Bahroudi A., Koyi H. A (2003) Tectono-sedimentary framework of the Gachsaran Formation in the Zagros foreland basin. Marine and Petroleum Geology 21: 1295–1310.

Blanckenburg F., Hewawasam T., W. Kubik P (2004) Cosmogenic nuclide evidence for low weathering and denudation in the wet, tropical highlands of Sri Lanka. *J.* Geophys. Res., 109, F03008, DOI:10.1029/2003JF000049.

Bras R. L., Tucker G. E., Teles V (2003) Six Myths About Mathematical Modeling in Geomorphology, in Prediction in Geomorphology. edited by: Wilcock, P. R. and Iverson, R. M., American Geophysical Union, Washington, D. C, 63–79.

Boardman J., Parson AJ., Holland R., Holmes PJ., Washington R (2003) Development of badlands and gullies in the Sneeuberg, Great Karoo, South Africa. Catena 50 (2–4): 165–184.

Boardman J., Poesen J., Evans R (2003) Socio-economic factors in soil erosion and conservation. Environmental Science & Policy 6:1-6.

Bosák P., Jaroš J., SpudiL J., Sulovský S., Václavek V (1998) Salt Plugs in the Eastern Zagros, Iran: Results of Regional Geological Reconnaissance. GeoLines (Praha).

Bosco C., Rigo. D. de, Dewitte O., Poesen J., Panagos P (2015) Modelling soil erosion at European scale: towards harmonization and reproducibility. Nat. Hazards Earth Syst. Sci., 15: 225–245.

Bonilla CA., Reyes JL., Magri A (2010) Water erosion prediction using the revised universal soil loss equation (RUSLE) in a GIS framework, Central Chile. Chil J Agric Res 70 (1):159–169

Bordenave M.L., Burwood R (1990) Source rock distribution and maturation in the Zagros Orogenic Belt: Provenance of the Asmari and Bangestan reservoir oil accumulations. Org. Geochem. 16: 369-387.

Brunner A. C., Ruecker, G. R., Park S. J., Vlek P. L. G (2002) Modelling approach to identify sustainable land management techniques on erosion affected slopes. In: Nkonya, E.; Sserunkuuma, D. and Pender. J. (eds.) Policies for improved land management in Uganda: Second National Workshop. EPTD Workshop.

Carrara A., Guzzetti F (eds) (1995) Geographical information systems in assessing natural hazards. Kluwer Academic Publishers, Dordrecht.

Colombo S., Hanley N., Calatrava J (2005) Designing policy for reducing the off-farm effect of soil erosion using choice experiments. Journal of Agricultural Economics, 56: 81–95.

Conoscenti C., Maggio C. D., Rotigliano E (2008) Soil erosion susceptibility assessment and validation using a geostatistical multivariate approach: a test in Southern Sicily. Natural Hazards, 46(3): 287-305.

Conoscenti C., Angileri S., Cappadonia C., Rotigliano E., Agnesi V., Märker M (2013a) Gully erosion susceptibility assessment by means of GIS-based logistic regression: a case of Sicily (Italy). Geomorphology. In Press. DOI:10.1016/j.geomorph.2013.08.021.

Conoscenti C., Agnesi V.,Angileri S., Cappadonia C ., Rotigliano E., Märker M (2013b) A GIS-based approach for gully erosion susceptibility modelling: A test in Sicily, Italy. Environ Earth Sci 70: 1179–1195.

Dastorani M.T., Poormohammadi S (2012) Evaluation of the Effects of Climate Change on Temperature, Precipitation and Evapotranspiration in Iran. International Conference on Applied Life Sciences (ICALS2012), Turkey.

Dehbozorgi M., Pourkermani M., Arian M., Matkan A.A., Motamedi H., Hosseinias A (2010) Quantitative analysis of relative tectonic activity in the Sarvestan area, central Zagros, Iran. Geomorphology, 121(3–4):329–341.

Dotterweich M., Rodzik J., Zgłobicki W., Schmitt A., Schmidtchen G., Bork H-R (2012) High resolution gully erosion and sedimentation processes, and land use changes since the Bronze Age and future trajectories in the Kazimierz Dolny area (Nałe˛czo´w Plateau, SE-Poland). Catena 95: 50–62.

Egboka B. C., Nwankwor G. I (1985) Hydrogeological and geotechnical parameters as agents for gully-type erosion in the Rain-Forest Belt of Nigeria. J. African Earth Sci. 3: 417-25.

Egboka B. C. E., Nwankwor G. I., Orajaka I. P (1990) Implications of palæo- and neotectonics in gully erosion-prone areas of southeastern Nigeria. Natural Hazards, 3 (3): 219-231.

Ehiorobo J.O., Audu H.A.P (2011) Monitoring of Gully Erosion in an Urban Area Using Geoinformation Technology. Journal of Emerging Trends in Engineering and Applied Sciences (JETEAS) 3 (2): 270-275.

Falehgari M., Talebi A., Dastorani M., Rangavar A (2011) Application Rangeland Hydrology and Erosion Model (RHEM) in Dry regions (case study: Sangane watershed- khorasan razavy). 5th conference soil conservation, Kerman, Iran (in Persian).

FAO (1994) Land degradation in South Asia: its severity causes and effects upon the people. FAO, UNDP and UNEP report, Rome.

Flanagan D.C., Nearing M.A (1995) USDA-Water Erosion Prediction project: Hillslope profile and watershed model documentation. Report No. 10, National Soil Erosion Research Laboratory, West Lafayette, IN 47097-1196.

Faiznia S (2003) Rock resistance against water erosion in different climates in Iran. Nat Resour J, 47: 95–116 Iran (in Persian).

Flores-Prieto E., Quénéhervé G., Bachofer F., Shahzad F., Maerker M (2015) Morphotectonic Interpretation of the Makuyuni Catchment in Northern Tanzania using DEM and SAR data. Geomorphology, 248:427–439.

Foster G.R., Meyer L.D (1972) A Closed-form soil erosion Equation for upland areas in sedimentation. Symposium in Honor Porf. H.A. Einstein; Sten, Colorado State University: Ft. Collins, CO, USA, pp. 12.1–12.19.

Igwe C.A (2012) Gully Erosion in South-Eastern Nigeria: Role of Soil Properties and Environmental Factors. Intech-Open Access Company. DOI: 10.5772 51020, Chapter 8.

Iranian of Natural Resources Center (2006) The report of physiography of Mazayjan plain in Fars province. Department of Natural Resources of Fars Province, Iran.

Grove AT., Rackham O (2001) The nature of Mediterranean Europe: an ecological history. Yale University Press, New Haven.

Gyssels G., Poesen J., Bochet E., Li Y (2005) Impact of plant roots on the resistance of soils to erosion by water: a review. Progress in Physical Geography 29 (2): 189–217.

Gee G.W., Bauder J.W (1986) Particle-size analysis. In R. Burt (ed), Soil survey field and laboratory methods manual. report no 51 p 53-54, U.S Depart. of agriculture, Lincoln, Nebraska.

Hallsworth E.G (1987) Anatomy, Physiology and Psychology of Erosion. Wiley, Chichester, UK, 176 pp.

Heydari-Guran S (2015) Tracking Upper Pleistocene human dispersals into the Iranian Plateau: a geoarchaeological model. (ed) Nuria Sanz. In: Human Origin Sites and the World Heritage Convention in Eurasia. HEADS 4, Vol. I. DOI: 10.13140/RG.2.1.5094.9604

Heydari-Guran S (2014) Palaeolithic Landscapes of Iran. BAR International Series, Vol. 2568.

Imani R., Ghasemieh H., Mirzavand M (2014) Determining and Mapping Soil Erodibility Factor (Case Study: Yamchi Watershed in Northwest of Iran), Open Journal of Soil Science, 4: 168-173.

Imeson A.C., Lavee H (1998) Soil erosion and climate change: the transect approach and the influence of scale, Geomorphology 23: 219–227.

Imeson A.C., Emmer I.M (1992) Implications of climatic change on land degradation in the Mediterranean. In: Jeftick, L., Millman, J.D., Sestini, G. (Eds.), Climatic Change in the Mediterranean. Edward Arnold, London, pp. 175–232.

Ionita I., Fullen M. A., Zgłobicki W., Poesen J (2015) Gully erosion as a natural and human-induced hazard. Natural Hazards, 79 (1): 1-5.

Hengl T., David G., Rossiter, T (2003). Supervised landform classifi- cation to enhance and replace photo-interpretation in semi-detailed soil survey. Soil Sci Soc Am J, 67: 1810–182.

Hosseini S., Gorbani M (2005) Economics of soil erosion. Ferdowsi University of Mashhad Press, 126 pp (in Persian).

Jaynes E.T (1957) Information theory and statistical mechanics. Phys. Rev. 106: 620–630.

Jetten V., De Roo A., Favis-Mortlock D (1999) Evaluation of field scale and catchment-scale soil erosion models. Catena 37: 521-541.

James G. A., Wynd J. G (1965) Stratigraphic nomenclature of Iranian oil consortium agreement area. American Association of Petroleum Geologists Bulletin, 49: 2182–2245.

Kakembo V., Xanga WW., Rowntree K (2009) Topographic thresholds in gully development on the hill slopes of communal areas in Ngqushwa Local Municipality, Eastern Cape, South Africa. Geomorphology 110 (3–4): 188–194.

Karaburun A (2010) Estimation of C factor for soil erosion modeling using NDVI in Buyukcekmece watershed. Ozean Journal of Applied Sciences 3 (1).

Karydas C., Petriolis M., Manakos I (2013) Evaluating Alternative Methods of Soil Erodibility Mapping in the Mediterranean Island of Crete, Agriculture, *3*: 362-380.

Kairis O., Karavitis C., Kounalaki A., Salvati L., Kosmas C (2013) The effect of land management practices on soil erosion and land desertification in an olive grove. Soil Use and Management, 29: 597–606.

Karimi S., Karimi S., Yavari A.R., Niksokhan M.H (2015) Prediction of Temperature and Precipitation in Damavand Catchment in Iran by Using LARS –WG in Future. Earth Sciences; 4 (3): 95-100.

Kehl M (2009) Quaternary climate change in Iran – the state of knowledge. Erdkunde, 63 (1): 1 – 17.

Kefi M., Yoshino K., Setiawan Y., Zayani K.,Boufaroua M (2011) Assessment of the effects of vegetation on soil erosion risk by water: a case of study of the Batta watershed in Tunisia. Environmental Earth Sciences, 64(3), 707-719. DOI: 10.1007/s12665-010-0891.

Kinnell PI (2010) Event soil loss, runoff and the Universal Soil Loss Equation family of models: A review. Journal of Hydrology 385: 384–397.

Kirkby M.J., Cox N.J (1995) A climatic index for soil erosion potential. Catena 25: 333–352.

Kheir R., Wilson J., Deng Y (2007) Use of terrain variables for mapping gully erosion susceptibility in Lebanon. Earth Surf Process Land 32: 1770–1782.

Khaksar K., Khaksar K (2012) Correlation between Quaternary stratigraphy units in different geological zones of Iran. International Research Journal of Geology and Mining (IRJGM) (2276-6618), 2 (6): 141-147.

Khadivi S.h (2010) Tectonic evolution and growth of the Zagros Mountain Belt (Fars, Iran): constraints from magnetostratigraphy, sedimentology and low- temperature thermochronometry. Earth Sciences. Universit´e Pierre et Marie Curie – Paris.

Kompani-Zare M, Soufi M, Hamzehzarghani H, Dehghani M (2011) The effect of some watershed, soil characteristics and morphometric factors on the relationship between the gully volume and length in Fars Province, Iran. Catena, 86 (3): 150–159.

Kumar S. G., Higaki D., Bhattarai T. P (2013) Estimation of Soil Erosion Rates and Eroded Sediment in a Degraded Catchment of the Siwalik Hills, Nepal. Land Journal, 2: 370-391.

Köthe R., Lehmeier F (1993) - SAGA - Ein Programmsystem zur Automatischen Relief-Analyse. Zeitschrift für Angewandte Geographie, 4/1993: 11-21.

Loch R.J., Silburn D.M (1997) Soil erosion. In: Clarke, A.L., Wylie, P.B. (Eds.), Sustainable Crop Production in the Sub-Tropics: An Australian Perspective. Information Series QI97035, QDPI Monograph. Queensland Department of Primary Industries, Brisbane, 27–41.

Lal R (1998) Soil erosion impact on agronomic productivity and environment quality: Critical Review. Plant Science, 17: 319 – 464.

Lal R (2003) Soil erosion and the global carbon budget. Environment International 29: 437 – 450.

Le Roux JJ., Morgenthal TL., Malherbe J., Pretorius DJ., Sumner PD (2008) Water erosion prediction at a national scale for South Africa. Water SA 34, http://www.wrc.org.za (last view 30.01.2015).

Leh M., Bajwa S., Chaubey I (2011) Impact of land use change on erosion risk: An integrated remote sensing, geographic information system and modeling methodology. Land Degrad. Develop. DOI: 10.1002/ldr.1137.

May L., Place C (2005) A GIS-based model of soil erosion and transport. Freshwater Forum 23: 48–61.

Noormohammadi F., Soufi M., Sadeghi S. H., Mirrezaie S., et al (2014) Storm-Wise Sediment Production of Gully Erosion in the West of Iran. Ecopersia, 2 (2): 539-556.

Märker M (2001) Assessment of gully erosion process dynamics for water resources management in a semiarid catchment of Swaziland (Southern Africa). Erosion Prédiction in Ungauged Basins: Integrating Methods and Techniques (Proceedings of symposium HS01 held during IUGG2003 al Sapporo, July 2003), AHS Publ. no. 279.

Märker M., Angeli L., Bottai L., Costantini R (2007) Assessment of land degradation susceptibility by scenario analysis: A case study in Southern Tuscany, Italy. Geomorphology 93: 120–129.

Märker M., Pelacani S., Schröder B (2011) A functional entity approach to predict soil erosion processes in a small Plio-Pleistocene Mediterranean catchment in Northern Chianti, Italy, Geomorphology 125: 530–540.

Masoudi M., Patwardhan AM., Gore SD., et al (2006) Risk assessment of water erosion for the Qareh Aghaj subbasin, southern Iran. Stoch Env Res Risk Assess 21: 15–24.

Masoudi M., Zakerinejad R (2010) Hazard assessment of desertification using MEDALUS model in Mazayjan plain, Fars province, Iran. Ecology, Environment and Conservation Journal, 16 (3): 425-430.

Masoudi M., Zakerinejad R (2011) A new model for assessment of erosion using desertification model of IMDPA in Mazayjan plain, Fars province, Iran. Ecol Environ Conserv 17 (3): 489–594.

Mahamane M (2015) Assessing soil erosion risk in the Tillabery landscape, Niger, 9 (3): 176-191.

Merritt W.S., Letcher R.A., Jakeman A.J (2003) A review of erosion and sediment transport models. Environmental Modelling & Software 18: 761–799.

Meamarian H., Esmaeilzadeh H (2003) The Sediment yield potential estimation of Kashmar watershed (Iran) using MPSIAC model in the GIS framework. http://www.gisdevelopment.net/application/2003. (last view 30.01.2015).

Mitasova H., Hofierka J., Zlocha M., Iverson LR (1996) Modelling topographic potential for erosion and deposition using GIS. Int J Geogr Inf Syst 10: 629–641.

Miliaresis G (2001) Extraction of Bajadas from digital elevation models and satellite imagery. Comput. Geosci, 27: 1157-1167.

Montgomery D.R., Brandon M.T (2002) Topographic controls on erosion rates in tectonically active mountain ranges. Earth and Planetary Science Letters 201: 481-489.

Morgan R.P.C (1986) Soil Erosion and Conservation. Longman Press, Harlow, UK, 298 pp.

Morgan RPC (1995) Soil erosion and conservation. 2nd edn. Longman, London, 198 pp.

Marzolff I., Poesen J., Ries JB (2011) Short to medium-term gully development: human activity and gully erosion variability in selected Spanish gully catchments. Landf Anal 17:111–116.

Nasri M., Gholami A., Najafi A., Modarres R (2006) The Estimation of soil erosion and sediment yield using GIS and statistical multivariate techniques, proceedings of 5th symposium Agro-inviron, Ghent university, Ghent, Belgium.

Nasri M., Feiznia S., Jafari M., Ahmadi H (2013) Application of Gully and Rill Erosion Indicators for Estimating Soil Loss Using GIS Techniques (Case Study: Menderjan Watershed, Iran). DESERT 17: 119-128.

Nazari samani A., Ahmadi H., Jafari M., Boggs G (2009) Geomorphic threshold conditions for gully erosion in Southwestern Iran (Boushehr-Samal watershed). Earth Sciences, 35: 180-189.

Norton KP., von Blanckenburg F., Schlunegger F., Schwab M., Kubik PW (2008) Cosmogenic nuclide-based investigation of spatial erosion and hill slope channel coupling in the transient foreland of the Swiss Alps. Geomorphology 5: 474–486. DOI: 10.1016/j. geomorph.2007.07.013.

Noormohammadi F., Soufi M., Sadeghi S., Mirrezaie S et al (2014) Storm-Wise Sediment Production of Gully Erosion in the West of Iran. ECOPERSIA, 2 (2): 539-556.

Ogbonna J.U., Ijioma M.A (2010) Mapping gully erosion susceptibility in Old Imo State, Nigeria using probability and statistics model. American Journal of Geographic Information Systems.1: 45 – 50.

Ogbonna J. U (2012) Examining the vulnerability of gully erosion in the Old Imo State using logistic regression models and GIS. American Journal of Geographic Information Systems, 2: 35 – 42.

Omidvar K (2010) Introduction to soil conservation and watershed, 2nd edn. Yazd University Press, Yazd (in Persian).

Pimentel D (2006) Soil Erosion: A Food and Environmental Threat. Environment, Development and Sustainability 8: 119–137.

Phillips S.J., Anderson R.P., Schapire R.E (2006) Maximum entropy modeling of species geographic distributions. Ecological Modelling, 190: 231-259.

Poesen J., Nachtergaele J., Verstraeten G., Valentin C (2003) Gully erosion and environmental change: importance and research needs. Catena 50 (2–4): 91–133.

Poesen J., Vandaele K., van Wesemael B (1996) Contribution of gully erosion to sediment production on cultivated lands and rangelands. In Erosion and Sediment Yield: Global and Regional Perspectives, Walling DE, Webb BW (eds). IAHS Publication No. 236. IAHS Press: Wallingford: 251–266.

Poesen J., Vanwalleghem T., de Vente J., Knapen A., Verstraeten G., Martinez-Casasnovas JA (2006) Gully erosion in Europe. In: Boardman J, Poesen J (eds) Soil erosion in Europe. Wiley, Chichester, 515–536.

Popp JH., Hyatt DE., Hoag D (2000) Modeling environmental condition with indices: a case study of sustainability and soil resources. Ecol Model 130 (1–3): 131–143.

Qian B., Hayhoe H., Gameda Sa (2005) Evaluation of the stochastic weather generators LARS-WG and AAFC- WG for climate change impact studies, Climate Research Clim Res, 29: 3–21.

Renard KG., Foster G.R., Weesies GA., McCool DK., Yoder DC (1997) Prediction soil erosion by water: aguide to conservation planning with the revised universal soil loss equation. Agricultural Handbook 703. US Department of Agriculture p. 404.

Rose C.W (2001) Soil Erosion Models and Implications for Conservation of Sloping Tropical Lands. Conservation Organization Meeting held May 24-29, 1999 at Purdue University and the USDA-ARS National Soil Erosion Research Laboratory: 852-859.

Roozbahani P (2011) Lithostratigraphy and biostratigraphy Of Oligocene Miocene Deposits (Asmari Formation) in South-West Iran (Zagros Basin, Northern Khorramabad), Geo.Alp, 8: 46–55.

Sadeghi S.H.R., Nourmohammadi F., Soufi M., Yasrebi B (2008) Estimating of storm-wise sediment yield from gully erosion using important rainfall components. J. Agri. Sci. Natur. Resour. 15 (1): 172-180 (in Persian).

Safaei M., Omar H., Yousof Z. B. M., Motevalli A (2012) Application of a physically based Model for Terrain Stability Mapping in North of Iran. Global Journal of Researches in Engineering General Engineering, 13 (2).

Salarian T., Zare M., Jouri M., Miarrostami S., Mahmoudi M (2014) Evaluation of shallow landslides hazard using artificial neural network of Multi-Layer Perceptron method in Subalpine Grassland (Case study: Glandrood watershed - Mazandaran). Intl J Agri Crop Sci. 7 (11): 795-804.

Sidorchuk A., Maerker M., Moretti S., Rodolfi G (2003) Gully erosion modelling and landscape response in the Mbuluzi River catchment of Swaziland. Catena 50: 507–525.

Sidorchuk A (2005) Stochastic components in the gully erosion modeling. Catena 63: 299–317.

Singh PK., Bhunya PK., Mishra SK., Chaube UC (2008) A sediment graph model based on SCS-CN method. J Hydrol 349: 244-255.

Sepehr A., Hassanli A.M., Ekhtesasi M.R., Jamali J.B (2007) Erosion probability maps: Quantitative assessment of desertification in south of Iran using MEDALUS method. Journal of Environmental Monitoring and Assessment, 134 (1-3): 243-254.

Sharma P.P., Gupta S.C., Foster G.R (1995) Raindrop-induced soil detachment and sediment transport from interrill areas. Soil Science Society of America Journal, 59: 727-734.

Shahrivar A., Tehbconsung C., Jusop S., Abdul Rahim A., Soufi M (2012) Roles of SAR and EC in Gully Erosion Development (A Case Study of Kohgiloye va Boyerahmad Province, Iran). Journal of Research in Agricultural Science, 8 (1): 1-12.

Shahrivar A., Christopher T.B.S. (2012) The effects of soil physical characteristics on gully erosion development in Kohgiloyeh & Boyer Ahmad Province, Iran. Advances in Environmental Biology, 6 (1): 367-405.

Shi Z.H., Fang N.F., Wu F.Z., Wanga L., Yue B.J., Wu G.L (2012) Soil erosion processes and sediment sorting associated with transport mechanisms on steep slopes. Journal of Hydrology 454-455: 123-130.

Shahzad F., Gloaguen R. (2011a) TecDEM: A MATLAB based toolbox for tectonic geomorphology, Part 1: Drainage network pre-processing and stream profile analysis. Computers & Geosciences, 37 (2): 250-260.

Shahzad F., Gloaguen R. (2011b) TecDEM: A MATLAB based toolbox for tectonic geomorphology, Part 2: Surface dynamics and basin analysis. Computers & Geosciences, 37 (2): 261-271.

Solaimani K., Modallaldoust S., Lotfi S (2009) Soil Erosion Prediction Based on Land Use Changes (A Case in Neka Watershed). American Journal of Agricultural and Biological Sciences 4 (2): 97-104.

Soufi M (2002) Characteristics and Causes of Gully Erosion in Iran. 12th ISCO Conference, Beijing 2002.

Soufi M (2004) A Survey of the Morpho-climatic Characteristics of Gullies in Fars province. Final report of research plan, Ministry of Jihad-e-Agriculture, Agricultural Research and Education Organization, Fars Research Center for Agriculture and Natural Resources, S/N 83/1153, 130 pp.

Starkel S (2005) Role of climatic and anthropogenic factors accelerating soil erosion and fluvial activity in central Europe. Studia Quaternaria, 22: 27–33.

Stoecklin J (1968) Structural history and tectonics of Iran. A review, Bull. amer. Assoc. Petroleum Geol. 52/7. 1229-1258.

Tangestani MH., Moore F (2001) Comparison of three principal component analysis techniques to porphyry copper alteration mapping, A case study, Meiduk area, Kerman, Iran. Can J Remote Sens 27 (2): 176–182.

Tangestani M (2006) Comparison of EPM and PSIAC models in GIS for erosion and sediment yield assessment in a semi-arid environment: Afzar Catchment, Fars Province, Iran. J Asian Earth Sci27: 585–597.

Tamene L., Vlek PLG (2008) Soil erosion studies in northern Ethiopia. In Land Use and Soil Resources, Braimoh AK, Vlek PLG (eds). Springer: Stockholm, 73–100.

Tibaldi A., Leon J. R (2000) Morphometry of late Pleistocene-Holocene faulting and volcano-tectonic relationship in the southern Andes of Colombia. Tectonics, 19(2): 358–377. DOI: 10.1029/1999TC900063.

Valentin C., Poesen J., Li Y (2005) Gully erosion: Impacts, factors and controls. Catena 63: 132–153.

Van der Knijff J. M., Jones R.J.A., Montanarella L (2000) Soil erosion risk assessment in Europe. European Commission Directorate General JRC Joint Research Centre Space Applications Institute.

Várallyay G (2010) The impact of climate change on soils and on their water management. Agronomy Research 8 (II): 385–396.

Vázquez Selem l., Zinck J.A (1994) Modelling gully distribution on volcanic terrains in the Huasca area, Central Mexico. ITC Journal, 3: 238-251.

Vandekerckhove L., Muys B., Poesen J., De Weerdt B., Coppe´ N (2001) A method for dendrochronological assessment of medium-term gully erosion rates. Catena 45: 123–161.

Ventura E., Nearing MA., Amore E., Norton LD (2002) The study of detachment and deposition on a hillslope using a magnetic tracer. Catena 48: 149-161.

Viles H.A (1990) The agency of organic beings: a selective review of recent work in biogeomorphology. In Thornes, J.B., editor, Vegetation and erosion: processes and environments, Chichester: Wiley, 5–25.

Yassoglou N., Montanarella L., Govers G., Van Lynden G., Jones R.J.A., et al. (1998) Soil Erosion in Europe. European Soil Bureau.

Yousefi S., Moradi N., Ramezani B., Rasoolzadeh N., Naderi N., Mirzaee S (2014) An Estimation of Sediment by Using Erosion Potential Method and Geographic Information Systems in Chamgardalan Watershed: A Case Study of Ilam Province, Iran. Geodynamics Research International Bulletin, 2 (2).

Wang B., Zheng F., Römkens M., Darboux F (2013) Soil erodibility for water erosion: A perspective and Chinese experiences. Geomorphology 187: 1–10.

Warren S.D., Mitasova H., Hohmann M.G., Landsberger S., et al (2009)Validation of a 3-D enhancement of the Universal Soil Loss Equation for prediction of soil erosion and sediment deposition. Catena 64: 281 – 296.

Wei W., Chen L., Fu B (2009) Effects of rainfall change on water erosion processes in terrestrial ecosystems: a review. Prog Phys Geogr 33: 307–318.

Wischmeier WH., Smith SS (1978) Predicting rainfall-erosion losses: a guide to conservation planning.Agriculture Handbook No. 537. US Department of Agriculture, Washington, DC.

Zabihi F., Vahidinia M., Mahboubi A., BAakhtiar H.A (2013) Facies analysis and sequence stratigraphy of the Asmari Formation in the northern area of Dezful Embayment, south-west Iran. Studia UBB Geologia, 58 (1): 45 – 56.

Zgłobicki W., Baran-Zgłobicka B (2012) Impact of loess relief on land use mosaic in SE Poland. Catena 96: 76–82.

Zakerinejad R., Märker M (2014) Prediction of Gully erosion susceptibilities using detailed terrain analysis and maximum entropy modeling: a case study in the Mazayejan Plain, Southwest Iran. Geogr Fis Din Quat 37 (1): 67–76.

Zakerinejad R., Märker M (2015) An integrated assessment of soil erosion dynamics with special emphasis on gully erosion in the Mazayjan basin, southwestern Iran. Natural Hazards, 79(1): 25-50.

Zevenbergen L.W., Thorne C.R (1987) Quantitative Analysis of Land Surface Topography. Earth Surface Processes and Landforms, 12: 47-56.

Paper A

Prediction of Gully erosion susceptibilities using detailed terrain analysis and maximum entropy modeling: a case study in the Mazayjan Plain, Southwest Iran

Current status: published, Geogr Fis Din Quat 37(1): 67–76.

Geogr. Fis. Dinam. Quat.
37 (2014), ..., 6 figg., 3 tabb.

DOI 10.4461/GFDQ.2014.37.0

REZA ZAKERINEJAD (*,***) & MICHAEL MARKER (**,***)

PREDICTION OF GULLY EROSION SUSCEPTIBILITIES USING DETAILED TERRAIN ANALYSIS AND MAXIMUM ENTROPY MODELING: A CASE STUDY IN THE MAZAYEJAN PLAIN, SOUTHWEST IRAN

ABSTRACT: ZAKERINEJAD R. & MÄRKER M., *Prediction of gully erosion susceptibilities using detailed terrain analysis and maximum entropy modeling: a case study in the Mazayejan plain, southwest Iran*. (IT ISSN 0391-9838, 2014).

Gully erosion is one of the most severe environmental problems in large areas of Iran. Land degradation and accelerated desertification are the consequence in susceptible areas. Gully erosion normally takes place when surface runoff is concentrated and thus, detach and transfer soil particles down the slopes into the drainage network. In traditional soil erosion studies these processes often have been neglected. In this study we investigate the spatial distribution of gully erosion processes with a quantitative method since in many national assessment approaches just qualitative models were applied. For this study we utilized a detailed terrain analysis and a stochastic modeling approach using mechanical statistics. Moreover we predict the potential spatial distribution of gullies in the Mazayejan plain of Fars province in southwestern Iran where gully erosion is the main environmental threat. Our methodological approach consists in the following steps: i) mapping of gully erosion phenomena in a test area based on Google Earth images; ii) development of a digital elevation model (DEM) with 10 meter resolution, iii) detailed terrain analysis deriving more than 20 terrain indices, iv) application of the Maxent model for the test area using the gully erosion forms as dependent variable and topographic indices as predictor variable and finally v) prediction of the spatial distribution of gully erosion potential for the entire study area. Model performance was evaluated by the Receiver Operating Characteristic (ROC). The results obtained show that the Maxent model perform very well and thus, it is suitable for the prediction of the gully erosion potential in the area. Among the terrain indices utilized in the prediction the most important ones are: convergence index, plan curvature, and slope. The proposed methodology allows conducting a proper gully erosion assessment in order to identify the priority areas for soil conservation and land use management.

KEY WORDS: Gully Erosion, Maxent Model, Terrain Analysis, Iran, Fars, Mazayejan Plain.

(*) *Faculty of Desert Studies, Semnan University, Semnan, Iran.*
(**) *Dipartimento Scienze della Terra, Università di Firenze, Piazzale delle Cascine 4, 50144 Firenze, Italia.*
(***) *Institute for Geography, Eberhard-Karls-University of Tübingen, Rümelinstraβe 19-23, 72070 Tübingen, Germany.*
Corresponding Author: Michael Maerker, mmaerker@unifi.it

پیشگویی فرسایش خندقی با استفاده آنالیز منطقه ی ومدل MAXENT:
منطقه مورد مطالعه : دشت مزایجان, جنوب غرب ایران

چکیده

فرسایش خندقی یکی از عوامل شدید تخریب محیطی در سطح وسیعی از اراضی ایران می باشد. تخریب اراضی و بیابان زایی از عوامل شدید تهدید کننده در این نواحی حساس محسوب می گردند. فرسایش خندقی زمانی که رواناب به صورت متمرکز موجب کنده شدن ذرات خاک و انتقال آنها به رودخانه می شود. در مطالعات صورت گرفته این نوع فرسایش کمتر مورد مطالعه قرار می گرفت. در این تحقیق به ارزیابی توزیع مکانی فرسایش خندقی با استفاده از مدل های کمی می پردازیم زیرا که در بسیاری از تحقیقات صورت گرفته تنها از مدل های کیفی بهر جسته شده است. در این مطالعه با استفاده از آنالیز منطقه ای و مدل های آماری به پیشگویی پتانسیل فرسایش خندقی در منطقه مزایجان شهرستان زرین دشت در استان فارس می پردازیم. اهداف این تحقیق شامل: 1- ترسیم نقشه ی مناطق فرسایش خندقی با استفاده از تصاویر گوگل ارث 2- تهیه نقشه رستری ارتفاع با دقت 2 متر 3-آنالیز منطقه ای با 20 شاخص توپوگرافی مستخرج از نقشه ی رستری ارتفاع 4-استفاده از مدل مکسنت که نقاط فرسایش خندقی به عنوان پارامتر مستقل و شاخص های توپوگرافی به عنوان عوامل پارامترهای وابسته جهت پیشگویی مناطق دارای پتانسیل خندقی استفاده گردید. ارزیابی مدل با استفاده از اندکس منحنی مشخصه عملکرد سیستم (ROC) صورت گرفت. نتایج این پژوهش نشان داد که مدل مکسنت به خوبی مناطق دارای پتانسیل خندقی را پیشگویی می نماید. از میان پارامترهای توپوگرافی به عنوان پارامترهای مستقل شاخص های اندکس همگرایی، شاخص انحنا و شیب می باشند. با استفاده از نتایج این تحقیق می توان اقدامات مدیریتی مناسب جهت جلوگیری از فرسایش خاک را در مناطق دارای حساسیت بالا انجام داد.

کلمات کلیدی:فرسایش خندقی، مدل مکسنت، آنالیز منطقه ای،دشت مزایجان.

INTRODUCTION

Gully erosion has been defined as a steep-side channel caused by erosion due to the intermittent flow of water and often recurs in narrow channels and removes the soil from this narrow area to considerable depths (Poesen, 1996; Poesen & *alii*, 2003). It is a serious problem in many parts of the world because of specific climatic, lithologic, soil, land use and land cover conditions that favor gully erosion processes (Torkashvand, 2008). Gully erosion take place when excessive surface run off flows with high velocity and thus, detach and transfer soil particles down slope

(Ehiorobo & Audu, 2012). Hence, gullying is an important type of water driven erosion processes that cause land degradation and instabilities in natural and agricultural landscapes (Nekooeimehr & Emami, 2007). Moreover, gully erosion has also a great impact on the drainage dynamics of soils and, hence, influence soil moisture conditions and ground water dynamics, especially in arid and semi arid regions (Avni, 2005; Nyssen & *alii*, 2004). Several studies on gully erosion in Southern Iran show that this phenomenon and the related processes are leading to accelerated desertification in the susceptible areas (Isaie & Soufi, 2007; Soufi, 2008; Sadeghi & Noormohamadi, 2011; Shahrivar & *alii*, 2012).

This study was carried out in the Fars province in Southwestern Iran (fig. 1). Gully erosion is very frequent and is threatening large areas and seriously damage agricultural land. However due to onsite damages such as soil loss, decreasing soil fertility and water holding capacity and off site damages like siltation of reservoirs, gully erosion has attracted more and more attention in the recent years in Iran (Soliemanpour & *alii*, 2010).

Gully erosion is generally considered as an indicator for desertification (Shruthi & *alii*, 2011), therefore this phenomena is often used by different qualitative desertification assessment methodologies as indicator for water erosion (FAO-UNEP,1984; Nikegbal & Farajzadeh, 2007; Sepehr & *alii*, 2007; Khosravi, 2005; Fozoni, 2007). Approaches like the Iranian Model of Desertification Potential Assessment (IMDPA) (Ahmadi, 2004) have been applied in many studies in the Southern parts of Iran. IMDPA considers nine criteria to assess desertification, namely: climate, geology, geomorphology, soil, vegetation cover, agriculture, water, erosion (including wind and water erosion), socio-economics, and technology of urban development. Proxies for these criteria are normally used to identify areas with a higher degree of degradation susceptibility or hazard and thus of a certain desertification status that is described relatively e.g. in four classes: slight, moderate, severe, and very severe. However, these qualitative models often rely on expert knowledge and subjective decisions in the scoring procedure. Moreover the qualitative assessment methods are only rarely based on detailed spatially distributed information.

This is the reason why gully erosion phenomena often have been neglected because of the spatial and temporal heterogeneity of the related processes and the difficulties to measure and monitor the processes quantitatively, especially in remote areas (Gomez & *alii*, 2003; Sidorchuk & *alii*, 2003; Poesen & *alii*, 1996; Märker, 2001; Vázquez Selem & Zinck 1994). Consequently, the prediction of gully development using numerical models is difficult, time consuming and expensive since the different input parameters involved in the prediction are not so easy to determine (Ehiorobo & Audu, 2012). However, soil erosion assessment in Iran is mainly based on empirical prediction models and hence, more research is required to understand the role and spatio-temporal distribution of gully erosion in Iran (Nazari Samani & *alii*, 2010; Bayramün & *alii*, 2003).

Even though recently several studies have already been carried out on the morpho-genesis of gully erosion (Shahrivar & *alii*, 2012; Soliemanpour & *alii*, 2010**;** Soufi, 2004; Nazari Samani & *alii*, 2009) few studies exist that assess the spatial distribution of gully erosion on larger areas considering the relevant environmental driving factors. Albeit, digital elevation models and terrain analysis were already applied in Erosion Risk Assessments (see Pallaris, 2009, Suriyaprasit, 2008) there are only very few studies combining stochastic models and terrain analysis (e.g. Kheir & *alii*, 2007; Angileri, 2012; Hughes & Prosser, 2012, Conforti & *alii*, 2010, Gutiérrez & *alii*, 2009a, 2009b).

Therefore, this study in the Mazayejan plain of Southern Iran aims at investigating the distribution of gully erosion with a quantitative method based on terrain analysis and mechanical statistics. Moreover, we want to identify the most important environmental indices triggering gully erosion in the study area and finally derive a map of the spatial distribution of gully erosion susceptibility.

STUDY AREA

The study area is located in the Fars province, southwest of Iran, (54° 34' to 54° 44' E and 27° 59' to 28° 5' N) (fig. 1). The area covers ca. 20.000 ha and is drained by the Mazayejan river. According to the national topography map (1:25.000; Iranian Cartographic Center,1994) the elevation is ranging from 693 m a.s.l. to a maximum altitude of 1.371 m a.s.l.. The annual average rainfall is around 243 mm with a high inter-annual variability characterized by very dry summer months (June to September) followed by short period of heavy rainfall from December till March which often provokes severe erosion and flooding events. The 30-min precipitation intensity for a 2 year re-turn period amounts to 23.5 mm h^{-1}. The 25 years return period is about 56.1 mm h^{-1}. Particularly gully erosion processes and forms are very common in the area. In this arid environment, the hottest month is August and the coldest is February, with mean monthly maximum and minimum temperatures of 31 °C and 18 °C, respectively. The above cited climate data was calculated using the following meteorological stations (tab. 1). The precipitation data was spatialized using an elevation based co-kriging (Rossiter, 2012)

TABLE 1 - Calculated R factor values of selected meteorological stations

Station	Longitude	Latitude	Elevation	Meanannual rainfall (mm)
Darb ghale	54 23	28 55	1430	344
Ghozan	54 27	28 49	1300	347.6
Hajiabad	54 25	28 22	1060	248.3
Brak	53 09	28 39	870	354
Farag	55 12	28 22	890	213.5
Khasoe	54 23	28 33	1070	241.5
Layzgan	54 58	28 41	2000	492.9

Fig. 1 - Study area: Mazayejan Plain in Fars province Southwestern Iran.

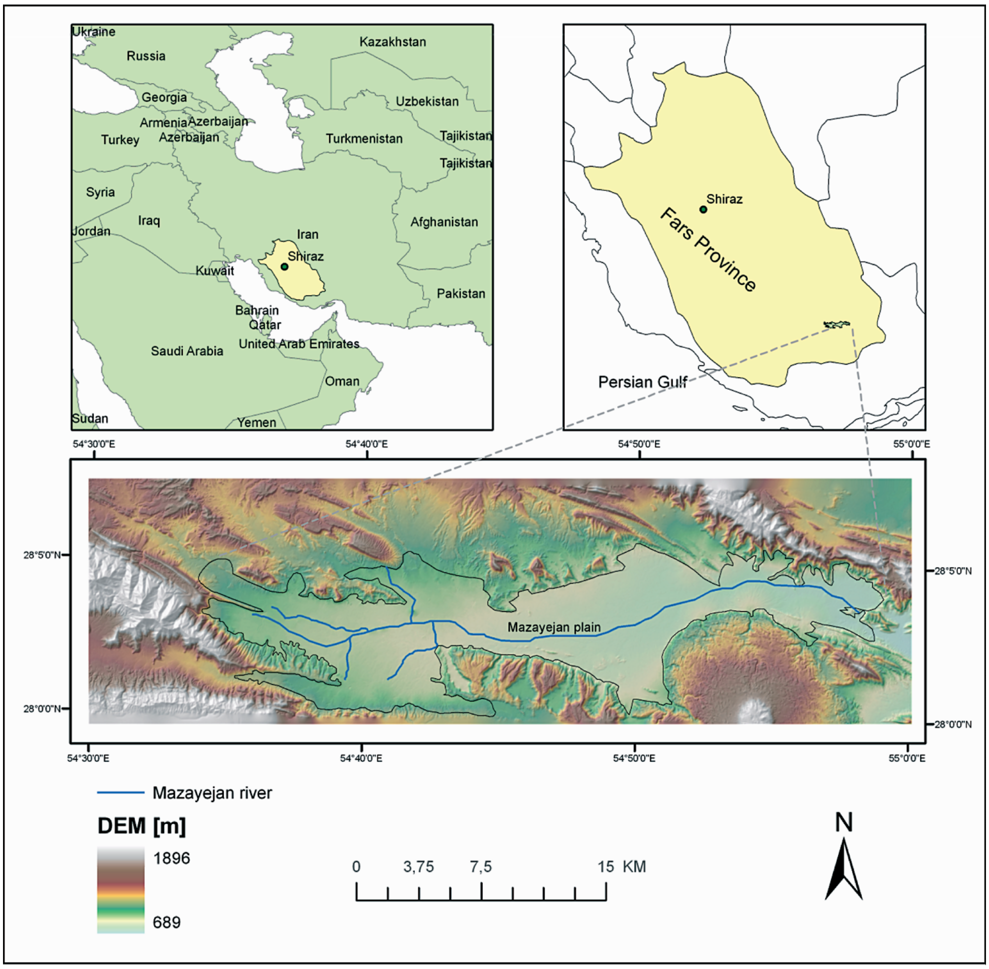

The Mazayejan plain has a variety of different landscapes due to its diversity in morphology, soils, geology and vegetation characteristics. The substrates and sediments are of quaternary origin and underwent climatic changes. The area is dominated by pediments and field observations showed gullies that are especially located in areas with fluvio-aeolian Quaternary deposits. Approximately 5% of the study area has slopes exceeding 20% and 60% of the area has slopes with less that 2% inclination. The average elevation of the area is 733 m a.s.l..

The Mazayejan alluvial plain is characterized by Aghajari marls, Bakhtiyari conglomerates, Mishan carbonates, siliciclastic facies deposited in a carbonatic rimmed shelf and Gachsaran Anhydrite, Marl, and Salt formations (Lasemi & *alii*, 2001; Hasbekarji, 2006). The chemical properties in these deposits are very sensitive to water erosion and are also affecting the quality of ground water. Generally, the groundwater is of bad quality with high chloride and sodium contents. The area is drained by the Mazayejan River which is an ephemeral drainage system flowing towards the East. According to Soil Taxonomy the soils of the study area are mainly Aridisols and Entisols. Due to water shortage and arid climate the main land use is pasture, rain fed cultivations and irrigated agriculture. Main crops produced are winter wheat, cotton and barley. Animal husbandry often leads to overgrazing and consequently, to the destruction of the vegetation cover favoring rill-interrill and gully erosion phenomena. Large part of the population is working in the agricultural sector.

MATERIAL AND METHODS

Gully erosion involves a complex set of factors, causing a variety of damages to the environment and destroys the soil cover. It is closely related to many environmental factors but especially to topographic characteristics and features especially when substrates and climate are very homogeneous. We extracted these topographic characteristics from a digital elevation model (DEM) with 10 m resolution. This DEM is based on an interpolation of contour lines of a 1:25000 topographic map (Iranian Cartographic Center, 1994) using a thin plate spline algorithm proposed by Hutchinson (1991). The DEM was preprocessed with low pass filtering to extract artefacts and errors like local noise and terraces (Märker & Hedary Guran 2009; Vorpahl & *alii*, 2012) using ARCGIS 9.3 (ESRI, 2010). Subsequently, the DEM was hydrologically corrected eliminating sinks using the algorithm proposed by Planchon and Darboux (2001).

Digital terrain analysis is a process to quantitatively describe the terrain using a DEM. We can differentiate between morphometric parameter describing i) the morphology of the surface, ii) hydrological parameters to describe runoff generation and potential flow pattern, iii) transport and deposition of sediments and iv) climatic parameters (Hengl & *alii*, 2003). A DEM consists of a spatially registered set of elevation points that collectively describe a topographic surface (Montgomery & Dietrich, 1994). This in turn has an important role for the runoff and the concentration of water on the soil surface. We performed a detailed Terrain Analysis on the DEM using SAGA2.0.3 (System for Automated Geo-scientific Analyses, Conrad, 2006). For the further stochastic analysis we selected especially those topographic indices that describe the erosive power of runoff, flow velocity and transport capacity and thus, have an important effect on erosion and especially on gully erosion.

STOCHASTIC MODELING OF GULLY EROSION

In this study we applied the Maximum entropy distribution or Maxent Model (Phillips & *alii*, 2006). Maxent is a type of machine based learning algorithm based on mechanical statistics. Here we use version 3.3.3k (http://www.cs.princeton.edu/~schapire/maxent/) to assess the environmental relations responsible for the spatial distribution of gully erosion features. The model requires presence only data and a set of environmental variables that are spatially continuously distributed. In this case the probability distribution of gullies is estimated using the presence of gully features and environmental predictor variables (continuous or categorical) that are delineated form the DEM (Kumar & Stohlgren, 2009). The advantage of the use of presence-only information lays in the fact that the absence of a feature or species at a certain location is difficult to proof or may not be evident (Phillips & *alii*, 2004; Elith & *alii*, 2006; Phillips & *alii*, 2006; Howard, 2012). In this study we used mapped gullies to train the model and to decipher susceptible areas for gully erosion. The model assigns an a priori probability in absence of problem specific information (Phillips & *alii*, 2006). Maxent calculates the spatial distribution of probabilities for a specific process, in this case gullies. Probabilities are ranging between 0 which means no susceptibility or probability for gullying and 1 standing for a very high susceptibility or probability for the occurrence of a gully. The model was trained and tested using a sample of 65.536 points showing gully erosion phenomena. Here we use 90% (N_{train} = 58982) of the data to train the model and 10% of the data to test the model (N_{test} = 6554).

MAPPING SPATIAL DISTRIBUTION OF GULLY FEATURES

In order to train the Maxent model we mapped the gully systems in our study area. In the past gullies have been mapped through conventional field surveying, which is expensive for large areas and time consuming (Johansen & *alii*, 2012). For this study we utilized a satellite image from Google Earth (GE). GE provides free access to very high resolution satellite images (Potere, 2008; Angileri, 2012). In this case the GE images available for the Mazayejan plain are based on Spot images with a 2.5 meter resolution. The availability of very high resolution satellite imagery is providing new solutions for a quick appraisal of gully networks over large areas (McInnes & *alii*, 2011). Shruthi & *alii* (2011) showed that object-oriented image analysis based gully mapping is quicker and more objective than traditional methods. Thus, satellite image with high resolution are required to cover vast areas for the assessment of gully erosion. Due to the fact that the study area is characterized by an arid climate with poor vegetation cover it is unproblematic to distinguish and map gully features and forms based on GE satellite images with high accuracy. In contrast, McInnes & *alii* (2011) describe the limits of the methodology especially in forested catchments in combination with small gully systems.

Based on our knowledge of the study area and using the images provided by GE we identified and mapped gullies as polygons which are later on transformed into points. Although it is sometimes difficult to distinguish gullies from streams due to the common ephemeral character of the drainage system we followed the general definition of gullies that are related to streams or drainage lines of third or greater order (McInnes, 2011; Peasley & Taylor, 2009). With regard to this definition of gullies we utilized a stream network layer of the basin to facilitate the identification and mapping of gullies and to distinguish between gullies and streams. We mapped several areas distributed randomly over the whole basin to cover the entire heterogeneity of environmental situations present within the basin. In the next step we converted this layer from GE-KML format to a shape file format (see fig. 2).

ENVIRONMENT LAYERS

For this study we derived a set of topographic indices (tab. 2) that included: elevation, slope, aspect, analytical hill

TABLE 2 - Topographic Indices used as environmental predictors in the Maxent model

Topographic indices	Method
Watershed sub bins	Olaya & Conrad, 2008
Wetness index	Olaya & Conrad, 2008
Stream power	Olaya &Conrad, 2008
Slope	Zevenbergen & Thorn,1987
LS-factor	Olaya & Conrad, 2008
Profile curvature	Olaya & Conrad, 2008
Plan curvature	Zevenbergen & Thorn,1987
Catchment area	Olaya & Conrad, 2008
Curvature classification	Dikau,1988
Curvature	Zevenbergen & Thorn,1987
Convergence index	Köthe & Lehmeir, 1993
Channel network base level	Olaya & Conrad, 2008
Channel network	Olaya & Conrad, 2008
Aspect	Zevenbergen & Thorn,1987
Altitude above channel network	Olaya & Conrad, 2008
Elevation	Preprocessed in ArcGIS9.2

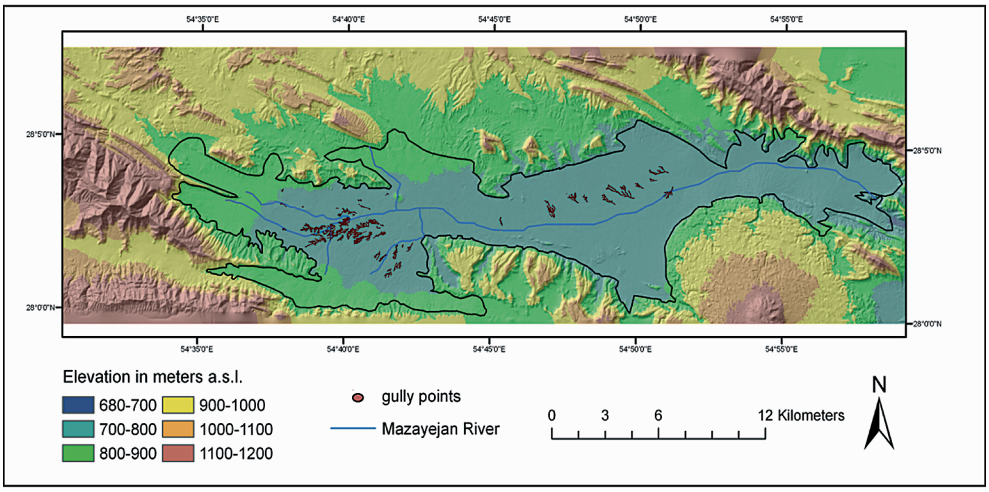

FIG. 2 - Mapped gully locations of Mazayejan plain using Google Earth images.

shading, plan- and profile curvature, curvature classification, convergence index, altitude above channel network, catchment area, stream power index, length-slope factor (LS-factor), topographic wetness index. These indices were used to predict gully erosion by means of the Maxent method. Tab. 2 shows these indices and the respective method applied for their delineation from the DEM. We used SAGA 2.0.3 software to derive the topographic indices at a 10 m resolution. The layers were post-processed and transformed into ascii raster data with the same spatial reference (WGS84, Zone 40) and resolution (10 m). Tab. 3 reports the statistics of the single environmental layers.

MODEL VALIDATION

To evaluate the performance of the model and its predictions we divided the data randomly into a training- and a test subset, thus creating quasi-independent data for model testing (Fielding & Bell, 1997). In this study the Maxent model was applied to a 10% random test dataset (N_{test} = 6554) selected from the entire data set of gully points (N_{tot} = 65.536). Model results were evaluated using the receiver operating characteristic (ROC) curve for training and test data. In an ROC curve the true positive rate (sensitivity) is plotted over the false positive rate (1-specificity) for all possible cut-off points (Sweets, 1988). Each point on the ROC plot represents a sensitivity/ specificity pair corresponding to a particular decision threshold. A perfect discrimination between positives and negatives has an ROC plot that passes through the upper left corner (100% sensitivity, 100% specificity), so that the area under curve, AUC, is 1 (cf. Märker & *alii*, 2012). Therefore, the closer the ROC plot to the upper left corner, the higher the overall accuracy of the test. According to Hosmer and Lemeshow (2000), AUC values exceeding 0.7/0.8/0.9 indicate acceptable/excellent/outstanding predictions.

RESULTS

Spatial distribution of mapped gullies

According to the digitized gully distribution mapped using GE and own field observations the gullies normally form in rangeland and agriculture areas, with U shaped cross sections and a digitate form. The average gully depth at 50% of its length is 1,5 m and the top width is 9,6 m. The medium heights of the head cuts are around 0.80 m (Soufi, 2004). Moreover the clay content in top soil (up to 20 cm) is higher than in the sub-subsoil layer in the gullied area indicating high surface run off potential and thus intense erosion processes (Soufi; 2004).

As illustrated in fig. 2 the gully density is generally higher in the southwest of the study area because of the very low vegetation cover and silty loam to loamy soil surface texture.

The EC and SAR of this area is very high indicating high Sodium contents that amplifies gully erosion and the degradation of rangeland (Shahrivar & *alii*, 2012; Masoudi & Zakerinejad 2010, Faulkner & *alii*, 2003). Moreover, there are several problems related to socioeconomic impacts such as i) overgrazing, ii) land use changes from rangeland to dry land, and iii) overexploitation of ground water for irrigation that promote and favor gully formation.

MODEL PERFORMANCE

The Maxent model was trained using 90% of the mapped point type gully data (N_{train} = 58982) as target or dependent variable and the raster type environmental layers derived from the DEM as independent variable. The resulting model is then validated using the randomly selected 10% of mapped gully data (N_{test} = 6554). Figure 3 shows the ROC graph and integral (area under curve, AUC) for training data with AUC values of 0.95. The validation test data yield AUC values of 0.941. According to Hosmer & Lemeshow (2000) these values indicate an out-

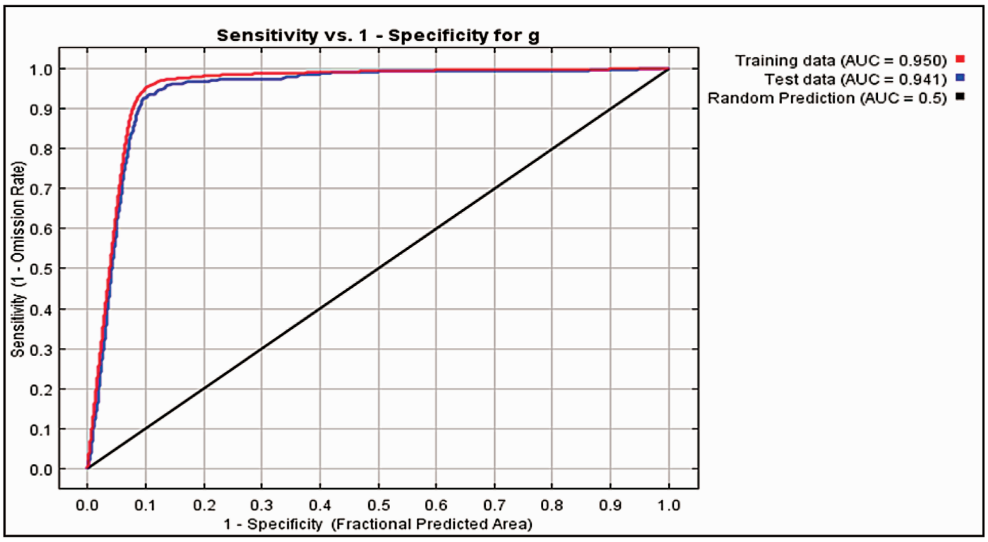

FIG. 3 - The Receiver-Operating Characteristic (ROC) Curve and related AUC values (red = training data set; blue = test data set).

standing performance for both train and test dataset. Hence, the models can be considered as highly robust in terms of sensitivity and specificity.

VARIABLE IMPORTANCE

According to the model performance we can point out the relevance of the topography for the modeled gully susceptibility. Stochastic approaches like statistical mechanics provide a powerful tool to study the relations between gully location and environmental characteristics that in this case consist exclusively of topographic indices.

As shown by various authors (see Vandekerckhove *et a,* 2001; Nazari Samani & *alii*, 2010; Kheir & *alii*, 2007; Flügel & *alii*, 2003; Märker & *alii*, 2012) in areas with comparatively homogeneous substrates, soils and land use, the spatial distribution of gully areas is mainly depending on topographic constraints expressed here as topographic indices. Among these topographic indices especially curvatures, slope and catchment area show a high variable importance. The entire distribution of variable importance is reported in fig. 4.

Relative values are scaled to the most important one. These variables have specific value ranges illustrated in tab. 3. The most important index is the convergence index calculated following Köthe & Lehmeir (1993) with 38.7%. The convergence index is a proxy for the accumulation or distribution of water, thus, for concentrated and turbulent runoff and hence for erosion and sediment transport (Vigiak & *alii*, 2009). The second important index is plan curvature with 36.4% contribution. It was calculated using the algorithm of Zevenbergen & Thorn (1987). Especially in plain type landforms with low slope gradients the plan curvature, like the convergence index, indicates the accumulation or distribution of surface runoff (e.g. Angileri, 2012; Capra & Scicolone, 2002). Finally, slope and aspect with 7% and 4.6% respectively were the most important indices after convergence and plan curvature index. Generally slope determines the velocity of runoff and thus is directly linked to soil erosion. The aspect gives important information on microclimate and on evaporation and soil

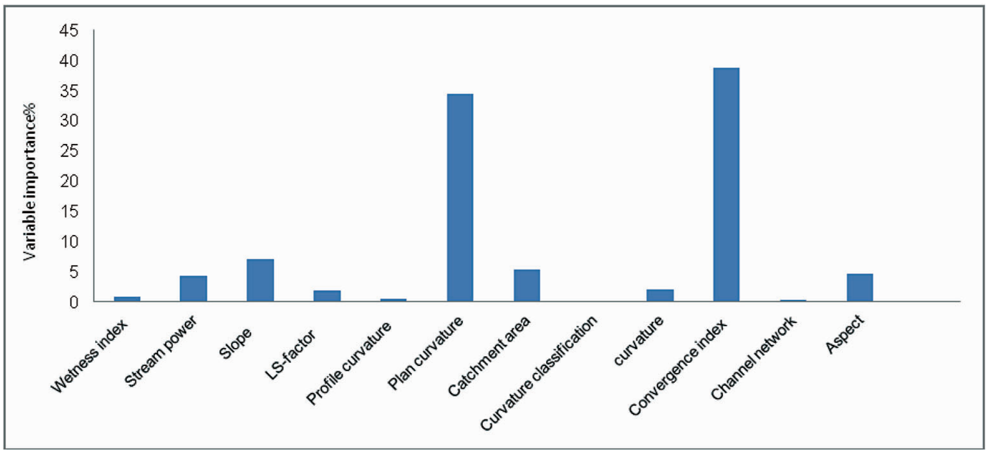

FIG. 4 - Variable importance for the environment layers.

TABLE 3 - value range and standard deviation for topographic indices in the study area

Topographic indices	Interval	Std. dev.
Watershed sub bins	1/8039	2269.40
Wetness index	5.44/14.68	2.57
Stream power	0.1/132255.12	64965.53
Slope	0/31.42	4.2
LS-factor	0/79.84	29.16
Profile curvature	-0.0068/0.0063	0
Plan curvature	-0.00621/0.00681	0.001
Catchment area	100/19699814	9691480
Curvature classification	0/8	
Curvature	-0.0105/0.0105	0.01
Convergence index	-27.29/27.277	13.44
Channel network base level	689.98/118.94	144.65
Channel network	-1/694	322.19
Aspect	0/360	102.38
Altitude above channel network	0/91.65	31.21

moisture (Wilson & Gallant, 2000). Also very important is the catchment area (5.4%) characterizing the discharge volumes (Hengl & Reuter, 2009).

SPATIAL PREDICTION

Figure 5 illustrates the spatial distribution of gully susceptibility. During a field stage in March 2012 the map was validated in the field showing very high correspondence between observed and modeled gully areas (fig. 6). The model was subsequently applied to the whole data set in order to predict the gully locations for the entire study area. We classified the resulting map of gully erosion probabilities in four susceptibility classes: i) no gully erosion (0-10% probability); ii) slight gully erosion (10-15% probability), iii) moderate gully erosion (15-30% probability) and iv) high gully erosion probability (30-100%). If we relate the susceptibilities only to the gullied areas we have 79.95% with slight gully susceptibility, 17.74% with moderate gully susceptibility, and 2.8% of the gullied area is belonging to the high gully susceptibility class. As the map of predicted gully erosion susceptibilities shows (fig. 5) the south and south west of the Mazayejan plain is gen-erally more sensitive to gully erosion. This area is charac-terized by less vegetation cover and thus more or higher run off than in the other areas.

DISCUSSION & CONCLUSIONS

Gully erosion is an important sediment source (Poesen & *alii*, 1996) and is causing serious land degradation (Valentin & *alii*, 2005). Thus, gully erosion is a major hazard especially for agricultural areas in the South of Farce province. Consequently, the knowledge of the spatial distribution of gully susceptibilities is a valuable and useful prerequisite to identify hazardous areas and to develop effective measures to cope with and eventually prevent soil loss due to gully erosion processes. In this study we show that terrain analysis and stochastic modelling are powerful tools for the spatial prediction of gully erosion susceptibilities. The topographic indices derived from high resolution DEM allow to characterize the topographic constraints for the development of gully erosion. Different authors showed

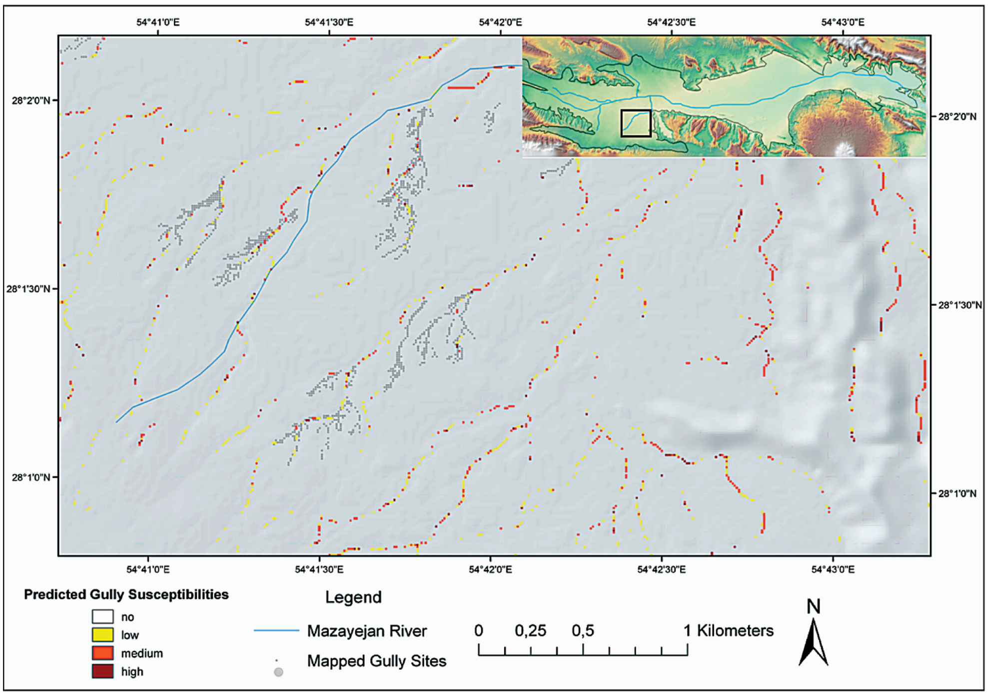

FIG. 5 - Predicted gully erosion susceptibilities in Mazayejan plain.

FIG. 6 - Photo of Gully head cut sections in Southwest of Mazayejan plain.

that the location of gullies is strongly associated with topography, and especially with the upslope contributing area and slope degree: e.g. Koco (2006) analysed old permanent gullies in the Bardejov basin in Slovenia, or Poesen & *alii* (2003) studied gullies in the Belgian Loess Belt.

In Iran Nazari Samani & *alii* (2010) illustrates the importance of topographic indices such as contribution area, slope or curvatures for gully erosion in Hableh Rood Basin. However, most studies conducted on gully erosion in Iran analyze single gullies in terms of morphology and stages of gully development (Nazari Samani & *alii*, 2009; Ahmadi & *alii*, 2007; Sadeghi & Noormohamadi, 2011; Shahrivar & *alii*, 2012) but there are no studies that stochastically predict the spatial distribution of gully susceptibilities. Beside the prediction of the areas susceptible to gully erosion, the model provides also information on the most important environmental layers triggering gully erosion processes in the Mazayejan plain. As expected, the most important topographic indices like curvatures, slope and catchment area depict concave morphologies and medium sized contributing areas. The latter ones produce enough runoff that concentrates (concave curvatures) and at a certain point become turbulent and start eroding the substrates. In our study area we found a threshold in the contributing (or upslope catchment area) of about 10 ha for the location of the gull head cut points. Thus higher susceptibilities in the upper parts of the drainage network generally indicate the point where the runoff becomes turbulent under the given climatic conditions and hence often head cuts are formed. This was also revealed by the field work and mapping campaign conducted in the Mazayejan plain. Moreover, the very good model performance with AUC values of 0.95 for training and 0,94 for the test data set suggests that gully erosion in the Mazayejan plain seem to be only dependent on the topography. This means that land use and vegetation as well as substrates are very homogeneous. This is confirmed by fieldwork showing a very homogeneous distribution of surface texture. Moreover, the land use is also not varying very much. The Mazayejan plain is mainly characterized by range land and rain fed agriculture.

According to the proposed methodology we were able to analyse the spatial distribution of gully susceptibilities especially in areas with lacking ground data. Following our methodology we identified and spatially predict gully susceptibilities using GE images and DEM derived information as well as a mechanical statistics approach. With the obtained results a proper management of susceptible area is feasible since we know the triggering mechanisms and the spatial distribution of susceptible areas.

REFERENCES

AHMADI H. (2004) - *Iranian Model of Desertification Potential Assessment,* Faculty of Natural Resources, University of Tehran.

AHMADI H., ABRISHAM E. & EKHTESASI M.R. (2005) - *Evaluation and mapping of desertification condition in Fakhr Abad region with the ICD and MICD models*. Biban (Desert Journal) Journal, 10 (1-1) 37.

AHMADI H., MOHAMMADI A., GHODOUSI J. & SALAJEGHEH A. (2007) - *Testing the four models for prediction of gully head advancement (case study: Hableh Rood basin - Iran).* Biaban 12, 61-68.

ANGILERI E.S. (2012) - *Water erosion prediction by stochastic and empirical models in the Mediterranean: A case study in Northern Sicily (Italy)*. Ph.D thesis, Department of Geography Eberhard Karls Universität Tübingen, Germany.

AVNI Y. (2005) - *Gully incision as a key factor in desertification in an arid environment, the Negev highlands, Israel.* Catena, 63, 185-220.

BAYRAMÜN I., DENGÜZ O., BAPKAN O. & PARLAK M. (2003) - *Soil Erosion Risk Assessment With ICONA Model; Case Study: Beypazary area.* Turkish Journal of Agriculture and Forestry, 27, 105-116.

CAPRA A. & SCICOLONE B. (2002) - *Ephemeral gully erosion in a wheat-cultivated area in Sicily (Italy)*. Biosystems Engineering, 83 (1), 119-126.

CONFORTI M., AUCELLI P.P.C., ROBUSTELLI G. & SCARCIGLIA F. (2010) - *Geomorphology and GIS analysis for mapping gully erosion susceptibility in the Turbolo stream catchment (Northern Calabria, Italy).* Natural Hazards 56, 881-898.

CONRAD O. (2006) - *SAGA. Entwurf, Funktionsumfang und Anwendung eines Systems für Automatisierte Geowissenschaftliche Analysen*. Ph.D. Thesis, University of Göttingen, Germany.

DIKAU R. (1988) - *Entwurf einer geomorphographisch-analytischen Systematik von Reliefeinheiten*. Heidelberger Geographische Bausteine, 5, 1-45.

EHIOROBO J.O. & AUDU H.A.P. (2012) - *Monitoring of Gully Erosion in an Urban Area Using Geoinformation Technology*. Journal of Emerging Trends in Engineering and Applied Sciences (JETEAS), 3 (2), 270-275.

ELITH J., GRAHAM C.H., ANDERSON R.P., DUDIK M., FERRIER S., GUISAN A., HIJMANS R.J., HUETTMANN F., LEATHWICK J.R., LEHMANN A., LI J., LOHMANN L.G., LOISELLE B.A., MANION G., MORITZ C., NAKAMURA M., NAKAZAWA Y., OVERTON J.M., PETERSON A.T., PHILLIPS S.J., RICHARDSON K., SCACHETTI-PEREIRA R., SCHAPIRE R.E., SOBERON J., WILLIAMS S., WISZ M.S. & ZIMMERMANN N.E. (2006) - *Novel methods improve prediction of species' distributions from occurrence data*. Ecography, 29, 129-151.

FAO-UNEP (1984) - *Provisional methodology for assessment and mapping of desertification*. Food and Agriculture Organization of the United, Rome, p. 73.

FAULKNER H., ALEXANDER R. & WILSON B.R. (2003) - *Changes to the dispersive characteristics of soils along an evolutionary slope sequence in the Vera badlands, southeast Spain: implications for site stabilisation.* Catena, 50, 243-254.

FIELDING A.H. & BELL J.F. (1997) - *A review of methods for the assessment of predictionerrors in conservation presence/ absence models.* Environmental Conservation, 24, 38-49.

FLÜGEL W., MÄRKER M., MORETTI S., RODOLFI G. & SIDORCHUK A. (2003) - *Integrating geographical information systems, remote sensing, ground truthing and modeling approaches for regional erosion classification of semi-arid catchments in South Africa*. Hydrological Processes, 17 (5), 929-942.

FOZONI L. (2007) - *Qunatitative Assessment of Present Status of Desertification Using GIS and RS to Develop a Regional Model.* Msc thesis, Zabol University, Iran.

GOMEZ B., BANBURY K., MARDEN M., TRUSTRUM N.A., PEACOCK D.H. & HOSKIN P.J. (2003) - *Gully erosion and sediment production, Te Weraroa Stream, New Zealand*. Water Resources Research, 39 (7), 1187.

GUTIÉRREZ Á.G., SCHNABEL S. & FELICÍSIMO Á.M. (2009a) - *Modelling the occurrence of gullies in rangelands of southwest Spain*. Earth Surface Processes and Landforms, 34, 1894-1902.

GUTIÉRREZ Á.G., SCHNABEL S. & LAVADO CONTADOR J.F. (2009b) - *Using and comparing two nonparametric methods (CART and MARS) to model the potential distribution of gullies*. Ecological Modelling, 220, 3630-3637.

HENGL T., GRUBER S. & SHRESTHA D.P. (2003) - *Digital terrain analysis in ILWIS: lecture notes and user guide. Enschede*. Netherlands: International Institute for Geo-information Science and Earth Observation (ITC).

HENGL T. & REUTER I.H. (2009) - *Geomorphometry. Concepts, Software, Applications,. Developments*. In: Soil Science, 33, Amsterdam, Oxford, 765 pp. (a cura di).

HOSMER D.W. & LEMESHOW S. (2000) - *Applied Logistic Regression*, 2nd ed. Wiley, NewYork, 392 pp.

HOWARD A.M., BERNARDES S., NIBBELINK N., BIONDID L., PRESOTTO A., FRAGASZY D.M. & MADDEN M. (2012) - *A maximum entropy model of the bearded capuchin monkey habitat incorporating topography and spectral unmixing analysis*. ISPRS Annals of the Photogrammetry, Remote Sensing and Spatial Information Sciences, I-2.XXII ISPRS Congress, Melbourne, Australia.

HUGHES A.O. & PROSSER I.P. (2012) - *Gully erosion prediction across a large region: Murray-Darling Basin, Australia*. Soil Research, 50 (4), 267-277.

HUTCHINSON M.F. (1991) - *The application of thin plate splines to continent-wide data assimilation*. In: J.D. Jasper (ed.), «Data Assimilation Systems». BMRC Res. Rep. No. 27, Bureau of Meteorology, Melbourne, 104-113.

IRANIAN CARTOGRAPHIC CENTER (1994) - Topography maps 1:25000.

~~IRANIAN OF NATURAL~~ RESOURCES CENTER (2006) - *The report of physiography of Mazayjan plain in Fars province*. Department of Natural Resources of Fars Province, Iran.

ISAIE H. & SOUFI M. (2007) - *Classification of Gully Erosion Based on Morphoclimatic and Soil Characteristics in the Northeast of Iran, Golestan province.* http://tucson.ars.ag.gov/isco/isco15/pdf/Isaie%20H_Classification%20of%20Gully%20Erosion.pdf

JOHANSEN K., TAIHEIB S., TINDALL D. & PHINN S. (2012) - *Object-based monitoring of gully extent and volume in north Austrlia using LiDAR data*. Proceedings of the 4th GEOBIA, May 7-9, 2012 - Rio de Janeiro, Brazil, p. 168.

KHEIR R., WILSON J. & DENG Y. (2007) - *Use of terrain variables for mapping gully erosion susceptibility in Lebanon*. Earth Surface Processes and Landforms, 32, 1770-1782.

KHOSRAVI H. (2005) - *Application of MEDALUS model in desertification of Kashan.* M.Sc thesis, University of Tehran, pp. 160.

KOCO Š. (2006) - *Modeling the inception of gully erosion around town of Bardejov using geographic information systems*. Katedra geografie a regionálneho rozvoja, M.sc thesis, Slovenia.

KÖTHE R. & LEHMEIER F. (1993) - *SAGA - Ein Programmsystem zur Automatischen Relief-Analyse.* Zeitschrift für Angewandte Geographie, 4/1993, 11-21.

KUMAR S. & STOHLGREN T. (2009) - *Maxent modeling for predicting suitable habitat for threatened and endangered tree Canacomyricamonticola in New Caledonia*, Journal of Ecology and Natural Environment, 1 (4), 094-098.

LASEMI Y. (2001) - *Facies, depositional environments and sequence stratigraphy of Upper Precambrian and Paleozoic rocks of the deposits.* Iranian Geological Organisation Publications.

MÄRKER M. (2001) - *Assessment of gully erosion process dynamics for water resources management in a semiarid catchment of Swaziland (Southern Africa).* Erosion Prédiction in Ungauged Basins: Integrating Methods and Techniques (Proceedings of symposium HS01 held during IUGG2003 al Sapporo, July 2003), AHS Publ. no. 279.

MÄRKER M. & HEYDARI GURAN S. (2009) - *Application of data mining technologies to predict Paleolithic site locations in the Zagros Mountains of Iran.* Computer Applications to Archaeology 2009, Williamsburg, Virginia, USA, March 22-26.

MÄRKER M., PELACANI S. & SCHRÖDER B. (2012) - *A functional entity approach to predict soil erosion processes in a small Plio-Pleistocene Mediterranean catchment in Northern Chianti, Italy*. Geomorphology, 125 (4), 530-540.

MASOUDI M. & ZAKERINEJAD R. (2010) - *Hazard assessment of desertification using MEDALUS model in Mazayjan plain, Fars province, Iran*. Ecology, Environment and Conservation Journal*,* 16 (Issue 3), 425-430.

MCINNES J., VIGIAK O. & ROBERTS A.M. (2011) - *Using Google Earth to map gully extent in the West Gippsland region (Victoria, Australia)*. 19th International Congress on Modeling and Simulation, Perth, Australia, 12-16 December.

MONTGOMERY D.R. & DIETRICH W.E. (1994) - *A physically based model for the topographic control on shallow landsliding*. Water Resources Research, 30, 1153-1171.

NAZARI SAMANI A., AHMADI H., JAFARI M. & BOGGS G. (2009) - *Geomorphic threshold conditions for gully erosion in Southwestern Iran (Boushehr-Samal watershed)*. Earth Sciences, 35, 180-189.

NAZARI SAMANI A., AHMADI H., MOHAMMADI A., GHODDOUSI J., SALAJEGHEH A., BOGGS B. & PISHYAR R. (2010) - *Factors Controlling Gully Advancement and Models Evaluation (Hableh Rood Basin, Iran)*. Water Resource Management, 24, 1531-1549.

NEKOOEIMEHR M. & EMAMI N. (2007) - *Determination of the most important morphological characteristics of gullies In morpho-climatic classification of gullied regions (Chaharmahal and Bakhtiary province)*. Pajouhesh & Sazandegi, 77, 84-92.

NIKEGBAL M. & FARAJZADEH M. (2007) - *Evaluation of MEDALUS Model for Desertification Hazard Zonation Using GIS; Study Area: Iyzad Khast Plain, Iran*. Biological Sciences, 10 (16), 2622-2630.

NYSSEN J., POESEN J., MOEYERSONS J., DECKERS J., MITIKU H. & LANG A. (2004) - *Human Impact on theenvironment in the Ethiopian and Eritrean highlands- a State of the Art*. Earth Science Reviews, 64 (3-4), 273-320.

OLAYA V. & CONRAD O. (2008) - *Geomorphometry in SAGA*. Hengl T., Reuter H.I. (Eds.), *Geomorphometry: Concepts, Software, Applications.* Elsevier, Amsterdam, 293-308.

PALLARIS K. (2000) - *Terrain modelling for erosion risk assesment in the Cabuyal river catchment: comparison of results with farmer perceptions.* Advances in Environmental Monitoring and Modelling, 1 (1), 149-177.

PEASLEY B. & TAYLOR S. (2009) - MER - *Soil and land resource condition in NSW: water erosion - monitor and evaluate gully erosion.* NSW DECC, Sydney.

PHILLIPS S.J., ANDERSON R.P. & SCHAPIRE R.E. (2006) - *Maximum entropy modeling of species geographic distributions. Ecological Modelling,* 190, 231-259.

PHILLIPS S.J., DUDIK M. & SCHAPIRE R.E. (2004) - *A maximum entropy approach to species distribution modeling. Proceedings of the 21st International Conference on Machine Learning*. ACM Press, New York, 655-662.

PLANCHON O. & DARBOUX F. (2001) - *A fast, simple and versatile algorithm to fill thedepressions of digital elevation models.* Catena, 46Ž 2001.159-176.

POESEN J., NACHTERGAELE J., VERSTRAETEN G. & VALENTIN C. (2003) - *Gully erosion and environmental change:importance and research needs*, Catena, 50, 91-133.

POESEN J.W. (1996) - *Contribution of gully erosion to sediment production on cultivated lands and rangelands, Yield*. Global and Regional Perspectives (Proceedings of the Exeter Symposium July 1996). IAHS Publ., 236.

POTERE D. (2008) - *Horizontal positional accuracy of Google earth's high resolution imagery archive*. Sensors, 8, 7973-7981.

ROSSITER D.G. (2012) - *Technical Note: Co-kriging with the gstat packageof the R environment for statistical computing*. University of Twente, Faculty of Geo-Information Science & Earth Observation (ITC), http://www.itc.nl/~rossiter/teach/R/R_ck.pdf.

SADEGHI S.H. & NOORMOHAMADI F. (2011) - *Gullies' allometric models in Dareshahr region, Ilam province, Iran.* Whatershed Management Research, 85.

SEPEHR A., HASSANLI A.M., EKHTESASI M.R. & JAMALI J.B. (2007) - *Erosion probability maps: Quantitative assessment of desertification in south of Iran using MEDALUS method*. Journal of Environmental Monitoring and Assessment, 134, 1-3, 243-254.

SHAHRIVAR A., TEHBCONSUNG C., JUSOP S., ABDUL RAHIM A. & SOUFI M. (2012) - *Roles of SAR and EC in Gully Erosion Development (A Case Study of Kohgiloye va Boyerahmad Province, Iran).* Journal of Research in Agricultural Science, 8 (1), 1-12.

SHRUTHI R.B.V., KERLE N. & JETTEN V. (2011) - *Object-based gully feature extraction using high spatialresolution imagery*. Geomorphology, 134, 260-268.

SIDORCHUK A., MÄRKER M., MORETTI S. & RODOLFI G. (2003) - *Gully erosion modelling and landscape response in the Mbuluzi River catchment of Swaziland.* Catena, 50, 507-525.

SOLIEMANPOUR S.M., SOUFI M. & AHMADI H. (2010) - *A Study on the Topographic Threshold and Effective Factorson Sediment Production and Gully Development in Neyriz, Fars Province*. Journal of Range and Watershed Management, Iranian Journal of Natural Resources, 63 (1), 41-53.

SOUFI M. (2004)- *Morpho-climatic classification of gullies in Fars province, Southwest of Iran*. ISCO (2004) - 13th International Soil Conservation Organisation Conference, Brisbane, July 2004, Conserving Soil and Water for Society: Sharing Solutions.

SOUFI M. (2008) - *The Impact of land use and Soil Characteristics on Gully Formation in an Arid Ecosystem, Southwest of I.R. Iran*. Soil and Water Conservation, Climate Change and Environmental Sensitivity, 15th ISCO Congress, Budapest.

SURIYAPRASIT M. (2008) - *Digital terrain analysis and image processing for assessing erosion prone areas*. M.Sc thesis, International Institute for Geo-Information Science and Earth Observation, Netherland.

SWEETS J.A. (1988) - *Measuring the accuracy of diagnostic systems*. Science, 240, 1285-1293.

TORKASHVAND A.M. (2008) - *Investigation of some methodologies for gully erosion mapping*. Journal of Applied Sciences, 8 (13), 2435-2441.

VALENTIN C., POESEN J. & LI Y. (2005) - *Gully erosion: Impacts, factors and control*. Catena, 63, 132-153.

VANDEKERCKHOVE L., MUYS B., POESEN J., DE WEERDT B. & COPPÉ N. (2001) - *A method for dendrochronological assessment of medium-term gully erosion rates*. Catena, 45, 123-161.

VÁZQUEZ SELEM L. & ZINCK J.A. (1994) - *Modelling gully distribution on volcanic terrains in the Huasca area*, *Central Mexico*. ITC Journal, 3, 238-251.

VIGIAK O., NEWHAM L.T.H., WHITFORD J., MELLAND A & BORSELLI L. (2009) - *Comparison of landscape approaches to define spatial patterns of hillslope-scale sediment delivery ratio*. 18th World IMACS / MODSIM Congress, Cairns, Australia.

VORPAHL P., ELSENBEER H., MÄRKER M. & SCHRÖDER B. (2012) - *How can statistical models help to determine driving factors of landslides*. Ecological Modelling, 239, 27-39.

WILSON J.P. & GALLANT J.C. (2000) - *Digital terrain analysis.* In: Wilson J.P. & Gallant J.C. (Eds.), «Terrain Analysis: Principles and Applications», J. Wiley, New York, 1-27.

ZEVENBERGEN L.W. & THORNE C.R. (1987) - *Quantitative Analysis of Land Surface Topography*. Earth Surface Processes and Landforms, 12, 47-56.

(Ms received 1 June 2013; accepted 15 January 2014)

Paper B

An integrated assessment of soil erosion dynamics with special emphasis on gully erosion in the Mazayjan basin, southwestern Iran

Current status: published, Natural Hazards, 79(1): 25-50

Nat Hazards (2015) 79:S25–S50
DOI 10.1007/s11069-015-1700-3

ORIGINAL PAPER

An integrated assessment of soil erosion dynamics with special emphasis on gully erosion in the Mazayjan basin, southwestern Iran

Reza Zakerinejad[1,2] · **Michael Maerker**[1,3]

Received: 31 August 2014 / Accepted: 11 March 2015 / Published online: 1 May 2015

Abstract Soil erosion by water is a significant problem in arid and semi-arid areas of large parts of Iran. Water erosion is one of the most effective phenomena that leads to decreasing soil productivity and pollution of water resources; especially, in the Mazayjan watershed in the southwest of Fars Province gully erosion contributes to the sediment dynamics in a significant way. Consequently, the intention of this research is to identify the different types of soil erosion processes acting in the area and to assess the process dynamics in an integrative way. Therefore, we applied GIS and satellite image analysis techniques to derive input information for the numeric models. For sheet and rill erosion the Unit Stream Power-based Erosion Deposition Model (USPED) was utilized. The spatial distribution of gully erosion was assessed using a statistical approach, which used three variables (stream power index, slope, and flow accumulation) to predict the spatial distribution of gullies in the study area. The eroded gully volumes were estimated for a 7-year period by fieldwork and Google Earth high-resolution images. Finally the gully retreat rates were integrated into the USPED model. The results show that the integration of the SPI approach to quantify gully erosion with the USPED model is a suitable method to qualitatively and quantitatively assess water erosion processes. The application of GIS and stochastic model approaches to spatialize the USPED model input yields valuable results for the prediction of soil erosion in the Mazayjan catchment. The results of this research help to develop an appropriate management of soil and water resources in the southwestern parts of Iran.

✉ Michael Maerker
mmaerker@unifi.it; michael.maerker@geographie.uni-tuebingen.de

Reza Zakerinejad
reza.zakerinejad@student.uni-tuebingen.de

[1] Institute of Geography, Eberhard-Karls-University of Tübingen, Rümelinstraβe 19–23, 72070 Tübingen, Germany

[2] Faculty of Desert Studies, Semnan University, Semnan, Iran

[3] Dipartimento Scienze della Terra, Università degli studi di Firenze, Piazzale delle Cascine 4, 50144 Florence, Italy

Keywords Soil erosion · Gully erosion · GIS · Data mining · Stream power index (SPI) · USPED

1 Introduction

Soil erosion is a severe problem, especially in semi-arid and sub-humid, low- and mid-latitude areas (Lal 2001). In particular, water erosion is one of the most important factors in land degradation in large parts of Iran destroying fertile soils and agricultural land. Nearly 35 Mha of the Iranian territory is affected by different types of water erosion (FAO 1994), e.g., rill, sheet, and gully erosion.

Water erosion is a major problem because of its socioeconomic impact and the reduction in the agriculture productivity by soil loss, leaching of organic matter, and soil nutrients as well as by reducing water availability and water retention (Morgan 1995; Kirkby 2001; Poesen et al. 1996). Quantitative estimates of soil erosion by water are a key component of land-use management plans, which are designed to protect and recover soils (Bonilla et al. 2010). Additionally, the severity and spatial distribution of soil erosion are important factors to soil conservation planning and watershed management (Kumar and Nair 2006; Popp et al. 2000).

The impact of soil erosion and related sediments decreases dramatically water quality and reservoir capacity (Tangestani 2006; Kefi et al. 2011); especially, gully erosion is an important sediment source (see Poesen et al. 1996; Valentin et al. 2005; Sidorchuk et al. 2003) and hence a major threat for agricultural areas. Large parts of the southern Fars Province in Iran are affected by these soil erosion and degradation processes. The latter are related to population growth and related effects such as overgrazing, expanding agricultural land, and deforestation.

In the last decades several models were applied to assess soil erosion phenomena in Iran in a quantitative and qualitative way. Empirical models such as the Erosion Potential Method (EPM, Flanagan and Nearing 1995; Bagherzadeh and Mansouri Daneshvar 2010; Barmaki et al. 2011; Bozorgzadeh and Kaman 2012; Tangestani and Moore 2001), the Modified Pacific Southwest Interagency Committee Model (MPSIAC, Pacific Southwest Interagency Committee 1968; Ahmadi 1995; Ilanloo 2012; Mahmoodabadi and Refahi 2005; Meamarian and Esmaeilzadeh 2003; Najm et al. 2011), or the most commonly used Universal Soil Loss Equation (USLE, Wischmeier and Smith 1978; Bagherzadeh 2012; Najmoddini 2003) and its reviewed version (RUSLE, Renard et al. 1997; Arekhi et al. 2012; Asadi et al. 2011; Eisazadeh et al. 2012; Roshani et al. 2013; Vaezi and Sadeghi 2011) were applied in Iran. Moreover, numerical physically based methods, such as WEPP (Water Erosion Prediction Project, Ahmadi et al. 2011; Cochrane and Flanagan 2003; Landi et al. 2011; Nearing et al. 1989), ANSWERS (Beasley et al. 1980), or EUROSEM (European Soil Erosion Model, Morgan et al. 1998), require very detailed input data (Rusco et al. 2008), which for the southwestern parts of Iran are hardly to achieve. However, to the knowledge of the authors so far soil erosion processes were not assessed in an integrative way including gully erosion in Iran. Even though recently some models using stochastic approaches to assess gully erosion were tested elsewhere (Conoscenti et al. 2014, 2013; Zakerinejad and Märker 2014), a quantitative assessment of gully erosion phenomena do not exist on meso-scale catchments in Iran.

The Mazayjan watershed, Zarindasht, Iran, is a highly susceptible area for soil erosion and desertification because of its specific environmental and socioeconomic settings. The area is characterized by susceptible litho/pedological units, an arid climate with sporadic but intense precipitation events, as well as deforestation processes. Overgrazing and improper cultivation are additional causes of degradation and a common phenomenon in the study area. In recent years especially range land was converted to cultivated areas, even though range land generally shows a low potential to agriculture land, thus causing strong degradation and abandonment of land after a few years. Moreover, as stated by Masoudi and Zakerinejad (2010) the amount of livestock is more than two times higher than the grazing capacity. Finally, future climate change effects with predicted higher precipitation amounts may increase land degradation and soil erosion processes (Alcamo et al. 2007). Consequently, water erosion is a severe problem in this area and causes the migration of many inhabitants in recent years. Particularly, gully erosion processes and related forms and features are very common in this region. Hence, this study is aimed at identifying and quantifying the major erosion process dynamics including gully erosion. Therefore, we applied an integrated approach combining the empirical–conceptual USPED model (Mitasova et al. 1996) and the SPI index together with data mining, remote sensing, and GIS methods.

2 Study area

The Mazayjan study area (Fig. 1) is located in the Zagros Mountains of Fars Province around 32 km southwest of Zarindasht city, southwest of Iran (54°34′ to 54°44′E and 27°59′ to 28°5′N).

The landforms of the Zagros Mountains in southwest Iran reflect recent fault tectonics (Dehbozorgi et al. 2010) stretching from northwest to southwest of Iran. The study area covers ca. 966 km^2 and is drained by the Mazayjan River toward the east. The elevation ranges from 671 m to a maximum altitude of 1969 m. The average elevation of the area is 1063 m. Mean annual precipitation is around 243 mm showing a high inter-annual variability with very dry summer months (June–October) followed by short periods of heavy rainfall from December till March coming along with severe erosion and flooding events. The precipitation intensity is 23.5 and 56.1 mm h^{-1}, for a 2- and 25-year return period, respectively. In this arid environment, the hottest month is August and the coldest is February, with mean monthly maximum and minimum temperatures of 31 and 18 °C, respectively. Land use is dominated (Tab. 1) by barren land (52,782 ha), poor land (40,127 ha) and very poor range land (1758 ha), as well as agricultural areas (1168 ha), and marsh land (531 ha); especially, the barren land is characterized by very scarce vegetation of shrub and grass type and mainly concentrated in the more humid drainage lines of the pediments (see Fig. 2). Thus, vegetation might also influence the development of micro-rills. However, due to the scale of the study these processes are not taken into account.

The Mazayjan watershed is dominated by a syncline structure covered by substrates and sediments of Quaternary alluvial deposits. These deposits are eroded and transported from the mountains toward the plain in the central part of the basin. The lower Mazayjan catchment is characterized by large pediments with rills and gullies, especially located in areas with fluvio-eolian Quaternary deposits. Generally, the Mazayjan watershed is built up by conglomerates of the Plio-Pleistocence Bakhtiyari formation, Aghajari marls, Mishan

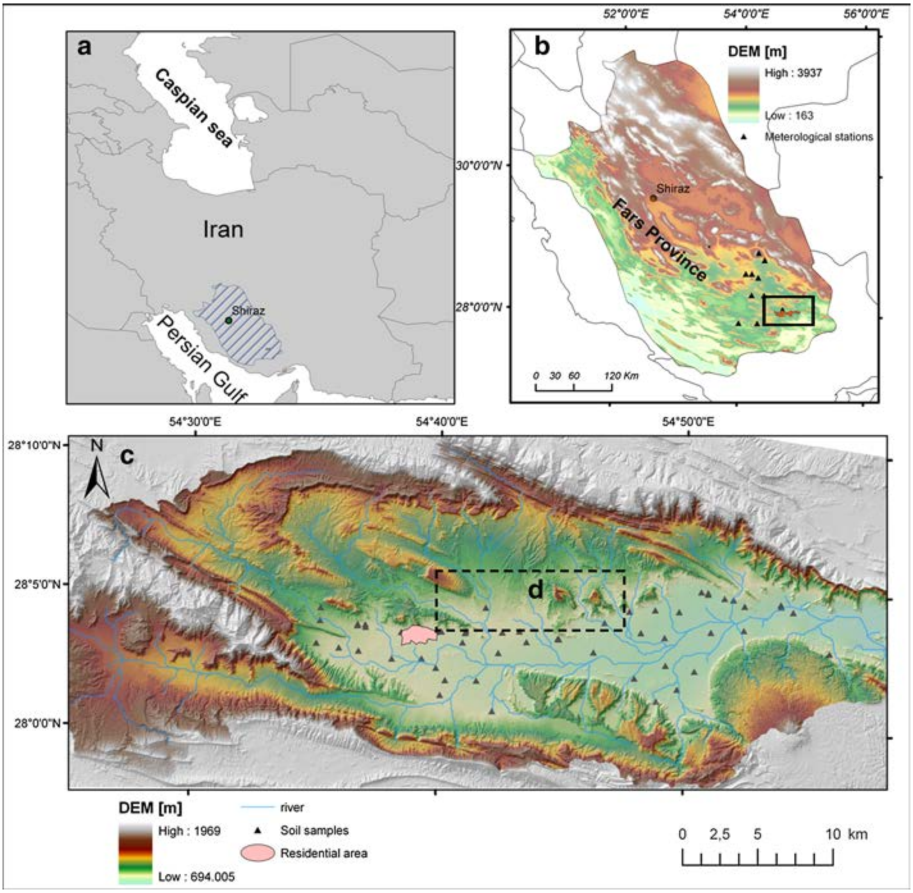

Fig. 1 Study area: Fars Province in Southern Iran (**a**). Mazayjan watershed and the locations of soil samples (**c**) and meteorological stations used for R-factor calculation (**b**). Enlarged area shown in Figs. 5, 13, and 14 (*d*)

Fig. 2 Pediment area with very poor vegetation

carbonates, and Gachsaran Anhydrite, Marl, and salt formations. The chemical properties of these deposits favor water erosion and affect also the quality of ground water. The soils of the study area are mainly Aridisols and Entisols according to soil taxonomy, and the soil moisture and temperature regimes are Aridic and Hyper Thermic. Generally the soils are not covered by stone pavements. Only in the immediate vicinity of drainage systems a higher skeleton content at the surface can be observed.

Agriculture production and animal husbandry are the main incomes in this area. The dominant agricultural products of the area are wheat, cotton, and barely. However, due to low and further decreasing productivity of soils, after some years the fields are abandoned and thus prone to erosion processes. In recent years, groundwater level decreased because of droughts and overexploitation of wells, especially for irrigation purposes.

The study area is affected by different types of water (rill, inter-rill, gully erosion) and wind erosion, especially in the eastern parts of the watershed. A major problem in this area is the large salt diaper in the southeast of the study area heavily affecting the water quality. According to the dry climate and shortage of water, the poor vegetation is sparsely distributed and also overgrazing is considered as an important cause of land degradation in this area.

3 Materials and methods

In this study the Unit Stream Power Erosion Deposition Model (USPED, Mitasova et al. 1996) was used to assess the spatial distribution of erosion and deposition processes. The parameters of this model are similar to the RUSLE model except of the topography factor that is computed by combining slope, aspect, flow direction, and flow accumulation. The USPED model predicts the spatial distribution of erosion in a steady overland flow with uniform rainfall excess conditions (Mitasova et al.1996; Mitas and Mitasova 1998; Mitasova and Mitas 2001).

The USPED model is based on the assumption that soil erosion depends on the detachment capacity and the sediment transport capacity of surface runoff. However, the USPED models do not consider the sediment yields from gullies, stream banks, and stream bed erosion (Grove and Rackham 2001). In the USPED model erosion and deposition (ED) are computed as the change in sediment flow in the direction of flow (Leh et al. 2011):

$$\mathrm{ED} = \mathrm{d}(T\cos a)/\mathrm{d}x + \mathrm{d}(T\sin a)/\mathrm{d}y \tag{1}$$

where a is the aspect of the terrain surface, dx, dy is the grid resolution, and T is the sediment flow at transport capacity. ED can be positive, indicating soil deposition, or negative, indicating soil erosion. Transport capacity is expressed as;

$$T = RKCPA^{m}(\sin b)^{n} \tag{2}$$

where R is a rainfall–runoff erosivity factor, K is a soil erodibility factor, C is a cover management factor, P is a support practice factor, b is the slope, A is the upslope contributing area, and m and n are constants. For prevailing rill erosion $m = 1.6$, $n = 1.3$, while for prevailing sheet erosion, $m = n = 1$. The USPED model was applied using Arc map 10, SAGA 2.1.0 (System for Automated Geoscientific Analysis, Conrad 2007), and ENVI 3.4 software following Mitas and Mitasova (1998).

3.1 USPED parameters

3.1.1 Rainfall erosivity factor (R)

The annual rainfall erosivity (R-factor, Renard et al. 1997) is defined as the integral measure of the amount and intensities of individual rain storms over the year that cause soil erosion (Wischmeier and Smith 1978; Mitasova et al. 1996). The R-factor in RUSLE and USPED models is calculated from the rainfall pattern or from the long-term continuous 30-min rainfall intensity (Karami et al. 2012) according to Eq. 3. The Erosivity Index (EI30), for each storm, is calculated as product of rainfall intensity of a maximum 30-min precipitation and the kinetic energy, as following:

$$R = \frac{1}{N}\sum_{1}^{N} EI_{30} \tag{3}$$

R, erosivity factor in the observed years (MJ/mm ha h years); E, total storm kinetic energy (MJ ha^{-1}); I_{30}, intensity of the maximum 30-min rainfall intensity (mm h^{-1}); N, number of observed years (Table 1).

However, the calculation of the R-factor is often difficult due to a lack of high-resolution time series (Wordofa 2011). For these reasons in many studies the annual and monthly data were used to estimate R-factor (Elsenbeer et al. 1993; Renard and Freimund 1994; Maerker et al. 2008; Karami et al. 2012).

In this study the monthly perception (January–December) was provided by the Iranian Meteorological Service for the period 1985–2006 for eight climatic stations placed around the study area (Fig. 1). Table 2 shows the climate stations that we used for the R-factor calculation. Before using the data sets, they were preprocessed to omit errors. We filled data gaps using regression relations between data of complete and incomplete stations.

To calculate the R-Factor for example the Fournier's index (Arnoldus 1980; Yuksel et al. 2008) was widely applied using mean annual perception and monthly perception according to (Eq. 4, Hu et al. 2000).

$$F = \frac{1}{N}\sum_{j=1}^{N}\left(\sum_{i=1}^{12}\frac{p_i}{p}\right) \tag{4}$$

p_{i}, monthly rainfall depth (mm); p, mean annual rain fall depth (mm) for rainfall stations in the same period.

However, since most of Iranian watersheds (Moussavi et al. 2012), especially in the Fars Province, are lacking sufficient high-resolution rainfall data, we tested several methods to calculate the R-factor based on monthly and annually precipitation. The calculated values finally were validated with iso-erodent maps for Iran (Sadeghi et al. 2011). Table 3 shows

Table 1 Land use/land cover (LULC) of Mazayjan watershed

LULC	Area (ha)	Area (%)
Poor range land	40,127	41.54
Very poor range land	1758	1.82
Agricultural crop	1168	1.21
Barren land	52,782	54.86
Residential area	212	0.22
Marsh land	531	0.55

Table 2 Calculated R-factor values of the rainfall stations for meteorological stations

Station	Longitude (decimal degree)	Latitude (decimal degree)	Elevation (m)	Mean annual rainfall (mm)
Darb ghale	54.23	28.55	1430	344.0
Ghozan	54.27	28.49	1300	347.6
Hajiabad	54.25	28.22	1060	248.3
Brak	53.09	28.39	870	354.0
Farag	55.12	28.22	890	213.5
Khasoe	54.23	28.33	1070	241.5
Layzgan	54.58	28.41	2000	492.9
Larstan	54.19	27.38	860	270.3
Avaz	54.00	27.46	860	236.1

Table 3 Commonly applied equations to estimate erosivity factor in study area

Equation	Parameters	Author(s)	CV	SD	R^2
$R = 0.524\left(\sum_{i=1}^{12}\frac{p_{ij}^2}{p_j}\right)^{159}$	p_{ij} total precipitation (mm) of the generic month i of the year j. P_j total precipitation (mm) of the year j	Ferro et al. (1991)	0.45	448.80	0.84
$Y = 50.0427X - 47.683$	X = maximum daily precipitation (mm)	Sadeghifard et al. (2004)	0.30	172.10	0.75
$R = 0.0483\ P_a^{1.61}$ $P_a \leq 850$ mm $R = 587.8 - 1.249\ Pa + 0.004105\ P_a^2$ $P_a > 850$	Pa denotes annual rainfall amount (mm).	Renard and Freimund (1994)	0.51	241.70	0.81
$R = 0.264\text{MFI}^{1.50}$	Modified Fournier	Renard and Freimund (1994)	0.43	90.50	0.31
$R = (0.07397 \times F\ 1.847)/17.2$ $F < 55$ $R = ((95.77 - (0.681 \times F)) + (0.477 \times F^2)))/17.2$ $F \geq 55$	F; Fournier index	Renard and Freimund (1994)	0.39	768.23	0.48

the utilized equations as well as a comparative statistics with R^2, coefficient of variation (CV), and standard deviation (SD). Subsequently, we calculated the R-factor for all stations and generated R-factor layers for the whole area using a spatial regression between R-factor and elevation as shown in Fig. 2 (Arekhi et al. 2012; Asadi et al. 2011; Arekhi and Niazi 2010).

3.1.2 Crop and management factor (C)

The C-factor represents the effects of (1) plants above the soil surface, (2) the below-ground biomass, (3) residuals of crops on the surface, and (4) special effects of former

Table 4 C-factor values used in the USPED model

LULC	C-factor	Reference
Poor range land	0.25	Feiznia and Ahzan (2004)
Very poor range land	0.33	Feiznia and Ahzan (2004)
Agricultural crop	0.43	Adediji et al. (2010)
Barren land	0.60	BCEOM (1998)
Residential area	0.00001	Adediji et al. (2010)
Marsh land	0.01	BCEOM (1998)

Table 5 Accuracy of land use/land cover (LULC) from Landsat image 2006 in Mazayjan watershed

Land use	Users accuracy	Producers accuracy	Kappa coefficient
Poor range land	0.79	0.73	0.62
Very poor range land	0.79	0.81	0.74
Agricultural area	0.89	0.86	0.84
Barren land	0.82	0.79	0.74
Marsh land	0.93	0.94	0.91
Overall accuracy	0.88		

agriculture residues on soil erosion (Maerker et al. 2008; Wang et al. 2003). In other words the C-factor indicates how vegetation and land-use management affect soil erosion. The C-factor is often estimated as a function of land use and land cover (LULC) (Maerker et al. 2008; Pelacani et al. 2008; Terranova et al. 2009; Renard et al. 1997; Yuksel et al. 2007). For different land-use/land-cover classes C-factor values can be attributed based on existing published studies. The C-factor can also be derived using vegetation indices based on satellite image analysis (Kouli et al. 2009). Table 4 shows the land-use classes and the attributed C-factor values we assigned (Adediji et al. 2010; BCEOM 1998; Feiznia and Ahzan 2004). The land-use/land-cover classification was derived using a Landsat ETM images from March 2006 and a maximum likelihood classification implemented in ENVI 3.4. Subsequently, a majority filter was applied on the classified data in order to reduce noise and artifact pixels. The final land-use/land-cover map was validated in the field. Error matrices and Kappa coefficient were calculated as shown in Table 5. The C-factor values vary from 0 to 1 (nondimensional), reflecting the effect of cropping and land cover to protect soil from rainfall and runoff erosion. Values tending to 0 reduce soil loss.

3.1.3 Soil erodibility factor (K)

The erodibility of a soil is characterized by inherent soil resistance to both detachment and transport, by raindrop impact and surface flow processes (Bryan 2000; Lal 2001; Onori et al. 2006). The soil erodibility factor or K-factor (in t h MJ^{-1} mm^{-1}) accounts for the influence of soil properties on soil loss during storm events on upland areas (Onori et al. 2006). The soil erodibility factor is usually derived using nomographs and/or formulae and is determined by soil texture, soil organic content, soil structure, and infiltration capacity (Wischmeier and Smith 1978). In this study, the K-factor was estimated according to Renard et al. (1997):

$$K = 7.594\left\{0.0034 + 0.0405\exp\left(\left(-\frac{1}{2}\cdot\frac{\log D_g + 1.659}{0.7101}\right)^2\right)\right\} \quad (5)$$

K, soil erodibility factor (t ha^{-1} MJ^{-1} mm^{-1}); Dg, geometric mean particle diameter (mm); f_i, primary particle size fraction; m_i = arithmetic mean of the particle size limits of that size.

To calculate the mean particle diameter, we used the percentage of clay, silt, and loam (Tables 6, 7, 8).

In this research 52 soil samples (Fig. 1) were collected and analyzed for soil texture using a standard analytical method (Gee and Bauder 1986). Soil samples were selected using a catena-based sampling design (Conacher and Dalrymple 1977). Soil texture and organic matter (OM) prevalently affect the soil water content and hence the amount of runoff (Saxton and Rawls. 2006). Moreover also electric conductivity (EC) and sodium absorption rates (SAR) are analyzed. High EC and SAR values facilitate soil erosion and favor especially piping processes (Faulkner et al. 2004).

3.1.3.1 Spatial Prediction of K-factor using stochastic modeling The spatial distribution of K-factor was estimated using a stochastic gradient boosting technique (TreeNet, Salford Systems) (Elith et al. 2008; Friedman 1999). Predictor variables are based on terrain parameters and landsat image spectral bands. TreeNet has several advantages since it is resistant to over-training and outliers (Friedman 2002). Since topography controls both hydrological and soil processes (Amundsen et al. 1994; Sariyildiz et al. 2005; Seibert et al. 2007), the topography data can be utilized to predict soil types or soil properties (Behrens et al. 2005). In this model, different topographic indices (Tab. 6) were extracted from a DEM with 5-m resolution. Laboratory-estimated K-factor values are used as the dependent variable.

The DEM is based on 19 stereo aerial photographs from 1994 of 1:20.000 scale provided by the Iranian Cartographic Centre. With the software AGISOFT we generated the

Table 6 Topographic indices used for environmental predictors in TreeNet model

Topographic indices	Method
Watershed sub bins	Olaya and Conrad (2009)
Wetness index	Olaya and Conrad (2009)
Stream power	Olaya and Conrad (2009)
Slope	Zevenberg and Thorn (1987)
LS-factor	Olaya and Conrad (2009)
Profile curvature	Olaya and Conrad (2009)
Plan curvature	Zevenberg and Thorn (1987)
Catchment area	Olaya and Conrad (2009)
Curvature classification	Dikau (1989)
Curvature	Zevenberg and Thorn (1987)
Convergence index	Köthe and Lehmeier (1993)
Channel network base level	Olaya and Conrad (2009)
Channel network	Olaya and Conrad (2009)
Aspect	Zevenbergen and Thorne (1987)
Altitude above channel network	Olaya and Conrad (2009)
Elevation	Preprocessed in ArcGIS9.2

Table 7 Frequency ratio values of gully areas and soil erosion/deposition classes in study area

Soli Erosion/ Deposition	Area (ha)	Erosion and deposition areas (%) (P)	Gully erosion points*	Gully erosion points % (G)	Frequency ratio G/P
Very high erosion	33,113.07	32.26	1020	4.33	0.12
High erosion	4893.74	7.06	1000	4.24	0.83
Medium erosion	7363.81	7.62	2000	8.49	1.11
Low erosion	6190.18	6.40	1890	8.03	1.25
Very low erosion	11,898.44	10.31	3450	14.66	1.19
Stable	11,898.44	3.77	6380	27.11	7.18
Very low deposition	3645.74	7.75	2440	10.36	1.80
Low deposition	5562.88	2.33	1500	6.37	2.72
Medium deposition	2617.74	2.70	1750	7.43	2.74
High deposition	1668.31	1.72	1020	4.33	2.51
Very high deposition	17,422.24	18.02	1080	4.58	0.25

* Each point corresponds to one pixel or 25 m^2 gully areas (5*5 m^2)

Table 8 Categories of soil loss in Mazayjan watershed

Erosion/Deposition (categories)	Erosion/Deposition (t ha^{-1} $year^{-1}$)	Area (ha)	Total area (%)
Very high erosion	<-30	27,241.2	28.2
High erosion	−20 to −30	8887.2	9.2
Medium erosion	−10 to −20	5989.2	6.2
Low erosion	−5 to −10	3284.4	3.4
Very low erosion	−1 to −5	5699.4	5.9
Stable	−0.1 to 0.1	5989.2	6.2
Very low deposition	0.1 to 5	5119.8	5.3
Low deposition	5–10	2898	3.0
Medium deposition	10–20	3477.6	3.6
High deposition	20–30	9466.8	9.8
Very high deposition	>30	18,547.2	19.2

DEM using 60 ground control points (GCP) taken in the field with a DGPS. The DEM was georeferenced using an UTM projection. The DEM was preprocessed with low-pass filtering (3*3 filter) to extract artifacts and errors such as local noise and terraces. Thereafter, it was hydrologically corrected to eliminate sinks using the algorithm proposed by Planchon and Darboux (2001). Finally, the spatial relations between dependent and independent variables revealed by the TreeNet model are used to predict the spatial distribution of the K-factor (Fig. 3).

To evaluate the performance of the TreeNet model the data were randomly divided into training (80 %) and a test data subset (20 %). The model results were evaluated using the receiver operating curve characteristics (ROC) for training and test data. The ROC integral values range between 0 and 1. A value near to 1 indicates high model accuracy, and values of 0.5 show a random model. According to Hosmer and Lemeshow (2000) ROC integral or area under curve (AUC) values exceeding 0.7/0.8/0.9 indicate acceptable/excellent/outstanding predictions.

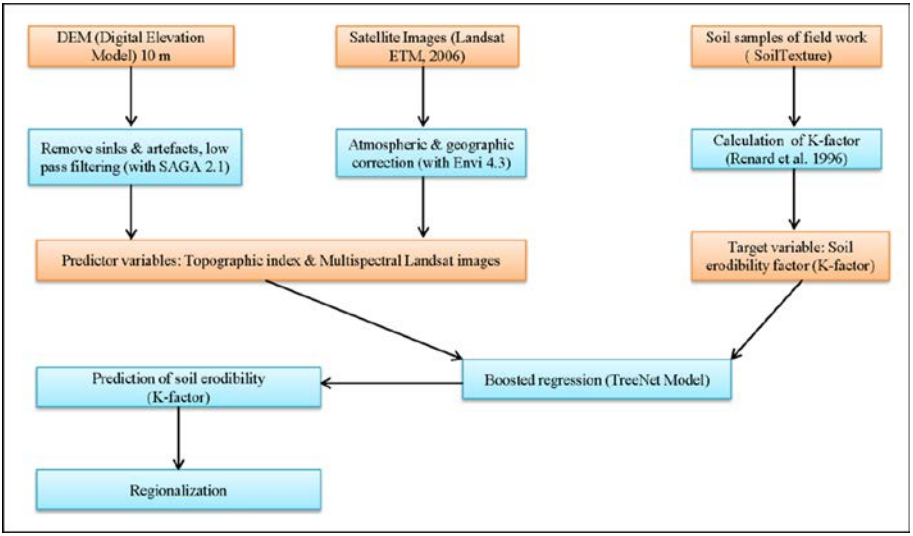

Fig. 3 Flowchart of the applied methodology for the prediction of K-factor used in the USPED model

3.1.4 Support practice factor (P)

The support practice (P) is related to management practices such as contouring and terracing to reduce the soil erosion. In other words, the P-factor describes the impact of management practices on average annual of soil erosion (Arekhi et al. 2012).

The values range between 0 and 1, and for areas with no support practice, the P-factor value is set to 1 (Simms et al. 2003). According to our survey in the study area we have identified no practice management to be considered, and thus, we assumed a P-factor value of 1 for the entire study area.

3.2 Gully erosion assessment using a steam power index (SPI) threshold

Gully erosion is a very intensive type of water erosion in southwestern Iran. As already mentioned the USPED model can only assess rill and inter-rill or sheet erosion processes. However, gully erosion affects large parts of the study area. In order to assess this deep linear gully erosion features we applied a stream power index (SPI)-based approach with a flow accumulation threshold. The SPI indicates the erosive power of flowing water over a specific area (Tagil and Jenness 2008; Kakembo et al. 2009; Moore and Wilson, 1992) and thus describes the potential energy to entrain sediments (Shruthi et al. 2011). The SPI (Moore and Wilson 1992) as one of the secondary terrains attributes (Wilson and Gallant 2000) is calculated as follows:

$$\mathrm{SPI} = \ln(A_s * \tan\beta) \qquad (6)$$

where A_s is specific catchment area and β is slope in degree.

The SPI values highlighted distinct preferential topographic areas for gully formation (Kakembo et al. 2009). This index has been calculated from the DEM with 5-m resolution based on the 1994 stereo aerial photographs 1:20.000 scale provided by the Iranian Cartographic Centre. Consequently, the DEM was generated before we mapped the gully

Fig. 4 Gully erosion features after a precipitation event

features. Actually, in many studies the relations between slope and flow accumulation were utilized to estimate the thresholds of gully initiation (see, e.g., Kheir et al. 2007; Tagil and Jenness 2008; Wilson and Gallant 2000). To calibrate the SPI approach we identified threshold values for SPI around existing gully heads. Therefore, we used high-resolution satellite images from Google Earth (GE). The available GE images for the Mazayjan watershed are built on Spot images with a 2.5-meter resolution. We identified 49 gully head locations based on field survey and using the available GE images. However, the absence or scarcity of vegetation facilitates the mapping procedure (Figs. 2, 4).

To extract a SPI threshold value for gully erosion we overlay the gully headcut areas with the SPI raster map (Fig. 5). Although there are different thresholds for gully erosion initiation, e.g., due to land use, soil character, and hydraulic conductivity, the study area is very homogenous, and hence, the main controlling factor is the topography. In the study

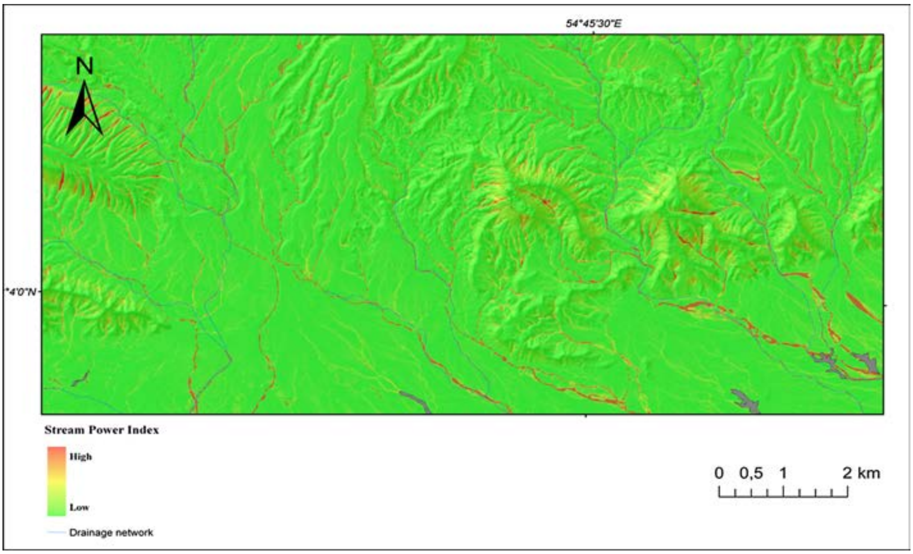

Fig. 5 Stream Power Index for the zoomed area in *dark gray*: gully areas (enlarged area (*d*) shown in Fig. 1)

area 12 gullies out of 49 were selected to determine the rate and expansion for a 7-year period. GE provides SPOT images from 2003 to 2009. Based on these images, the expansion of head cuts was estimated by digitizing the gully area for the two time steps. During a field survey in 2013 we measure the gully depth and growth areas in order to validate the GE image analysis. According to the satellite images, aerial photos from 1996, and field survey the gully features are mainly located in the flat and low sloping areas. Therefore, we limit our SPI approach to these areas using a low flow accumulation threshold of 100 ha and a maximum slope of 35°. We converted the eroded gully volumes to tons per hectare using a soil bulk density value of 1.23 g/cm^3 (Kompani-Zare et al. 2011). To get the yearly gully erosion rates we divided the value by the duration of our observation period (7 years). We integrate the gully erosion estimated for the single spatial units into the USPED model by adding the amount of sediments eroded by gullies to the sediment flow at sediment transport capacity.

4 Results and discussions

4.1 USPED–factors

According to the USPED model algorithm the input data (R, K, C, P and topographic factor) were multiplied with the Raster Calculator in ArcGIS 10.0 to get the erosion/deposition rates in t ha^{-1} yr^{-1} for each grid cell.

According to Table 3, the best equation to calculate the R-factor is the one developed by Sadeghifard et al. (2004) for the arid climate in south of Iran. Consequently, we applied this equation to estimate the erosivity factor for the Mazayjan watershed. Since the relationship between elevation and average annual precipitation shows a high correlation ($R^2 = 0.89$), we used elevation to regionalize the R-factor for the Mazayjan watershed ($R^2 = 0.75$) (Fig. 6). The obtained values (Fig. 7) range from 212.6 to 424.6 MJ mm/ha year^{-1}. The average values for the Mazayjan watershed amount to 265.2 MJ mm/ha year^{-1}. The spatial distribution of R-factor values for the Mazayjan watershed is presented in Fig. 7. In particular, high precipitation values occur along the ridges of this basin.

According to the soil laboratory analysis soil texture is dominated by silt loam and sandy loam and thus is highly susceptible to soil erosion. The amount of organic matter in all samples was <2 %. Soil organic matter reduces the erodibility of soil. In many arid and semiarid areas soil organic matter is low due to scarce vegetation, and hence, soil is more susceptible to erosion. Particularly in the southwest of Iran, due to arid climate and lack of

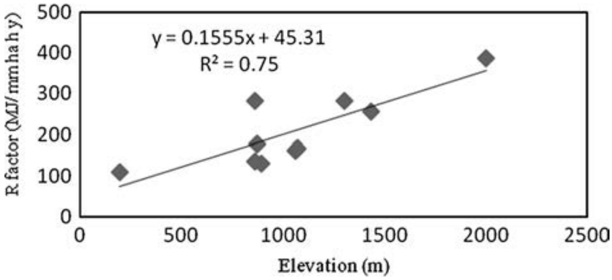

Fig. 6 Relationship between R-factor and elevation

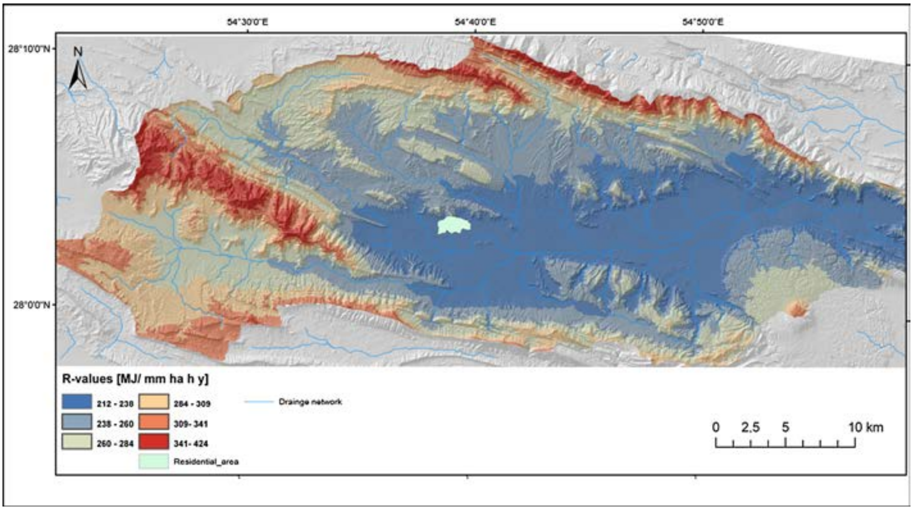

Fig. 7 R-factor layer of Mazayjan watershed

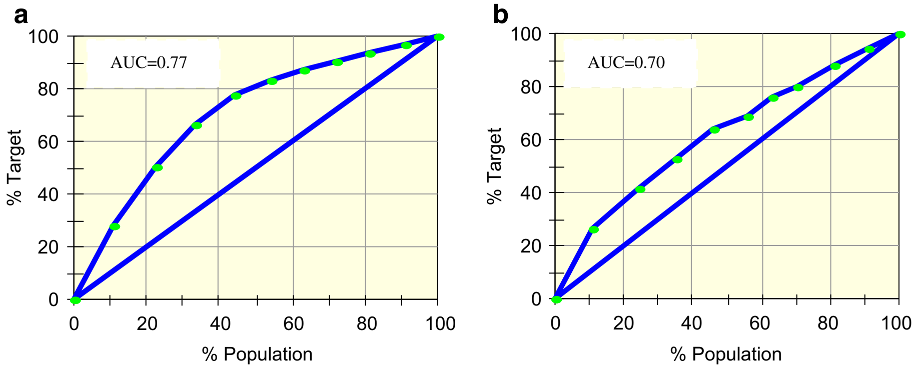

Fig. 8 ROC diagram and AUC values for K-factor. *Left*: train data set; *right*: test data set

organic matter wind erosion affects large areas. Moreover, the laboratory analysis shows that the EC and SAR values of soil samples indicate high sodium contents that amplify gully erosion and the degradation of rangeland (Shahrivar et al. 2012; Masoudi et al. 2006). The stochastic modeling of the K-factor values based on the soil samples (dependent variable) and on terrain parameters and Landsat spectral bands (independent variables) was validated internally using the ROC integral (area under curve, AUC) for training and testing data. According to Hosmer and Lemeshow (2000) the K-factor model shows an acceptable performance with AUC integrals of 0.77 and 0.70 for training and testing data set, respectively (Fig. 8). Figure 9 shows the variable importance. The most important factors are slope and vertical distance to channel network. Finally we applied the TreeNet model to predict the spatial distribution of the K-factor as shown in Fig. 10. High K-factor values are related to the plain areas with flat slope (<2 %) and to the vicinity of the channel network in the central part of watershed.

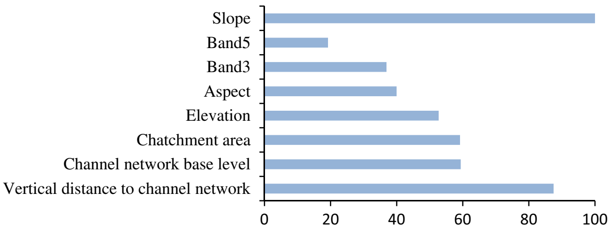

Fig. 9 Variable importance obtained by the boosted regression tree model for soil erodibility (values in %)

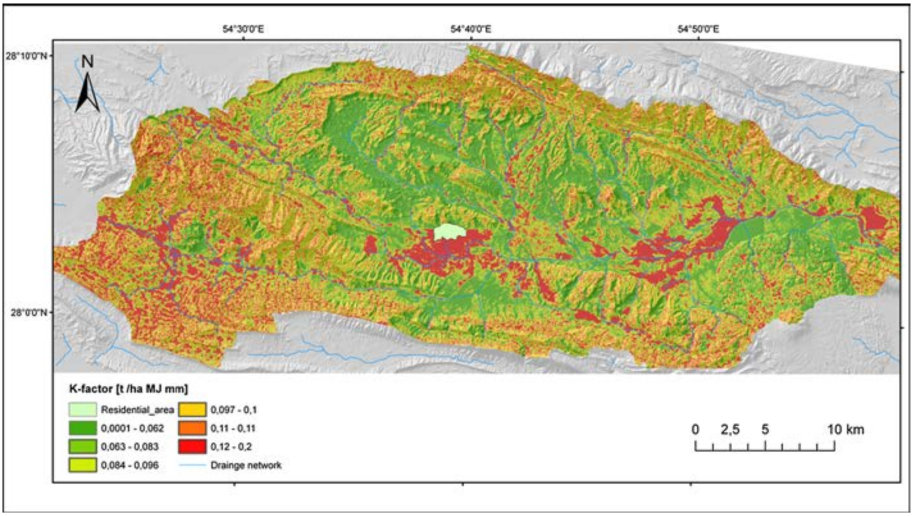

Fig. 10 K-factor layer of Mazayjan watershed

Soil erodibility values vary from 0.11 t ha MJ^{-1} mm^{-1} in the northern and northeastern part of the study area with more sandy loam and sandy clay soils, to 0.32 t ha MJ^{-1} mm^{-1} in the southwestern and southeastern part of the area with silty loam soils. The total mean is 0.11 t ha MJ^{-1} mm^{-1} with a standard deviation of 0.02 t ha MJ^{-1} mm^{-1}. According to the K-factor map low K-factor values coincide with the Asmari-Jahrom (AS-Ja) and the Tarbur formation that are relatively resistant to water erosion (Feiznia 2000). The high values of K-factor are more related to Quaternary formations and alluvial deposition.

We derived C-factor values using the land-use map. The classification result based on Landsat images was validated using field data. In this research some accuracy estimating indexes are shown, such as overall accuracy, user's accuracy, producer's accuracy and kappa coefficient (Table 5). Accuracy analysis was completed by means of a confusion or error matrix. This method relates the numbers of classified pixel in the assigned classification to the ground truth data (Congalton and Green 1999). In addition, the Kappa coefficient accuracy for all classes was higher than 0.60. Finally, this index is used to calculate the classification. High values of the Kappa coefficient indicate higher reliability of the classification results. The overall accuracy of the supervised classification of LULC is 88 %. According to Table 4 C-factor values were attributed to the singles LULC classes. Values range from 0 to 1 with bare rocks and no vegetation having values of 1. In the Mazayjan watershed the vegetation is poor due to the arid climate and over grazing;

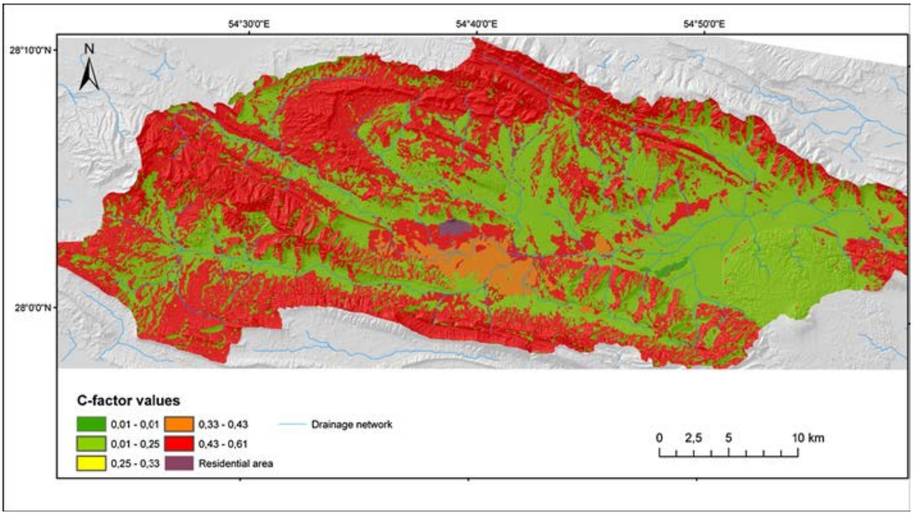

Fig. 11 C-factor layer of Mazayjan watershed

especially, the southwest of the study area is characterized by no vegetation at all or scarce shrubs. The major LULC in this area is poor and very poor vegetation with C-factor values of 0.23. The rest of the study area is covered with agriculture land use having C-factor values of 0.43. Figure 11 shows the maximum amount of C-factor values coinciding with barren areas in ridge positions in the north and southwest of the watershed, whereas the lowest values are related to the areas with scarce vegetation. The artificial and rural area was masked in the C-factor map. The mean C-factor value is 0.15 with a standard deviation of 0.12.

4.2 Distribution of Gully erosion processes

In this study the gully head cut locations were identified using GE image interpretation. We set up a regression model between headcut location and SPI values using a set of 12 mapped gully headcut locations. Subsequently, the gully erosion rates were estimated by mapping the growth rates of the 12 gullies over a 7-year time period. As already pointed out by other studies there is a strong relationship between catchment area and slope and turbulent concentrated runoff forming longitudinal deep incisions (Kakembo et al. 2009; Nazari Samani et al. 2009; Poesen et al. 1996; Vandekerckhove et al. 2001). As illustrated in Fig. 12 the regression between the volume of soil losses for each gully location and SPI values shows a very good fit ($R^2 = 0.84$). Consequently, we can use a threshold value of SPI to identify potential gully initiation points. Extreme high values of SPI are related to the stream network in the flat areas.

In the study area gully erosion threads the agricultural land and infrastructures like roads. The SPI threshold characterizing gully erosion ranges between 100 and 1700 in different parts of this catchment. SPI values higher than 1700 indicate stream network, while values of less than 100 display areas not affected by gullying. In fact using this threshold, we are also able to compare potential and actual gully erosion (Kakembo et al. 2009). Figure 5 shows that the susceptible zones are prevalently in the low sloping and

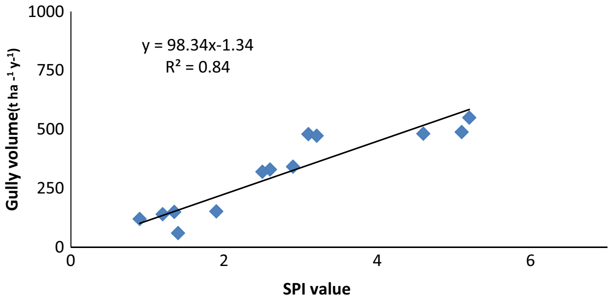

Fig. 12 Relationship between SPI values and gullies volumes for 2003–2009 [t ha^{-1} year^{-1}]

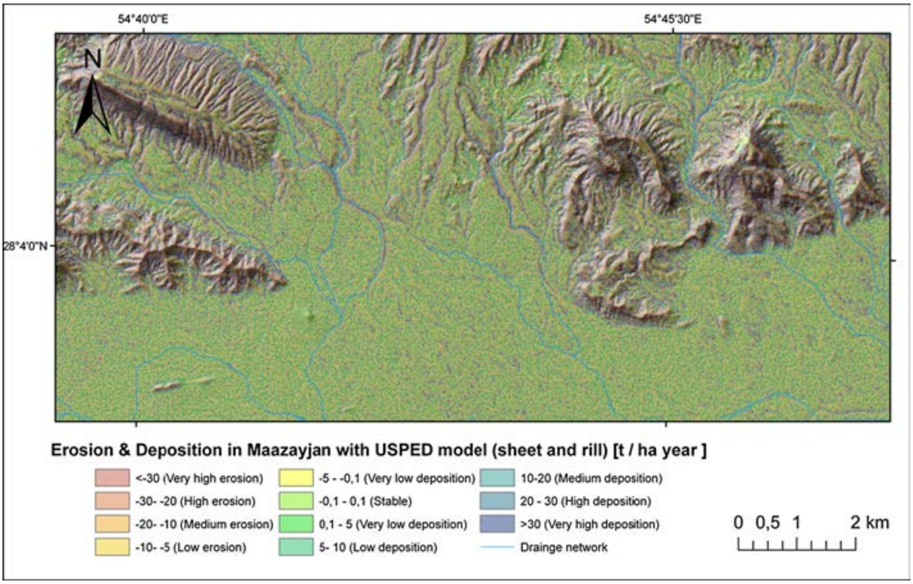

Fig. 13 Predicted soil erosion and deposition for the Mazayjan [t ha^{-1} year^{-1}] derived with the USPED model for enlarged area (*d*) shown in Fig. 1)

pediment areas. However, the USPED model simulates for these areas low soil loss or instead deposition (Fig. 13).

4.3 Comparison of the USPED model and the gully erosion approach

We compared the model results of the USPED erosion/deposition values with the gully sample points creating a Frequency ratio. As illustrated in Figs. 13 and 14, the gully features are frequent in bare soil in pediment and glacis areas. However, the steeper areas around the Mazayjan plain show no predominant gully erosion phenomena due to shallow soils and small specific catchment areas. Table 7 shows the frequency ratio for gully points and the respective soil categories. According to this table the frequency ratio for two classes of very high erosion and deposition is 0.12 and 0.25, respectively, while the low and very low erosion are higher than 1. The frequency ratio clearly demonstrates that gully

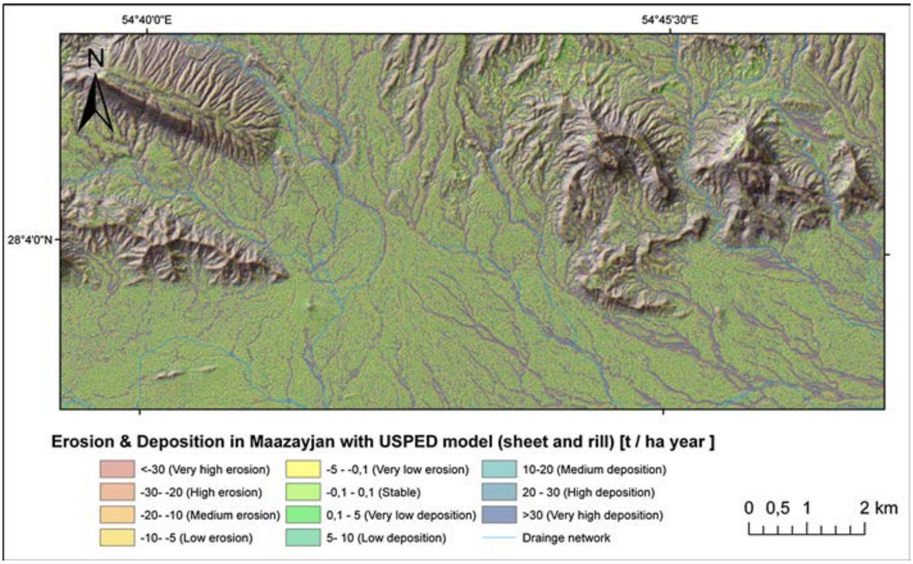

Fig. 14 Spatial distribution of soil erosion and deposition in the Mazayjan watershed [t ha^{-1} $year^{-1}$], based on the integrated USPED/SPI approach for the enlarged area (*d*) as shown in Fig. 1

erosion is completely underestimated by the USPED model. This was already documented for RULSE-type models (Biesemans et al. 2000; Le Roux et al. 2008).

4.4 Integrated assessment of erosion processes in the Mazayjan basin

In order to get the total amount of soil eroded, transported, and deposited by sheet (rill/inter-rill erosion) and gully erosion processes we utilized the USPED model adding the volumetric contribution of the deep linear gully erosion processes estimated with the SPI approach as layer in the calculation of the transport capacity.

According to field work and aerial photo interpretation gullies generated by overland flow occur in abandoned land, rangeland and agricultural areas.

4.5 Soil erosion/deposition potentials

According to Fig. 13 and Table 7 more than 50 % of the area is affected by high to very high erosion and deposition process intensities. The stable areas and low erosion and deposition zones cover about 21 % of the area. However, some of the mapped and predicted gully processes are located in the stable and low intensity soil erosion classes. The extreme values are characterized by steep slopes in ridge positions in the northern and western parts of the basin.

Figure 14 shows the final map combining the USPED (for rill and sheet) with the SPI and flow accumulation approaches (for gully erosion) for the entire study area. This map shows that the flat areas are highly susceptible to gully erosion, while the USPED model shows low sheet erosion susceptibility for these areas (Fig. 13). In other words large parts of the flat areas are very prone to gully erosion.

Table 8 illustrates the soil erosion and deposition values classified in 11 classes for the integrated model as follows: Stable areas range between −0.1 and 0.1 t/ha year, values <−0.1 t/ha year characterize erosion, and values with more than 0.1 t/ha year describe deposition/sedimentation processes (De Rosa 2005). Consequently, areas with a higher soil loss rate with respect to the tolerable one of 10 t/ha year (see, e.g., Ahmadi 1995; Pradhan et al. 2012; Le Roux et al. 2008) fall into the moderate and high soil loss classes.

According to the combined final map of erosion deposition processes modeled with USPED and including the gully erosion processes derived by SPI (Fig. 14) round about 17.5 % of area is stable or characterized by very low erosion or deposition classes. Very high erosion values cover 28.2 % of the area, whereas 19.2 % of the area is related to deposition processes. The spatial variation of erosion/deposition processes show more intensive processes in the north, northwest, and east part of the study area that are generally associated with the steeper relief of the mountain ranges (Table 9). Area with high deposition is mainly located in the central part and along the drainage networks because of low transport capacities. However, the plain areas are characterized by high SPI values due to large specific catchment areas and hence are more susceptible to gully erosion. Areas of low erosion and deposition tend to coincide with flat areas showing low soil erodibility and better vegetation cover.

The integrated USPED/SPI approach shows that more than 43 % of the area is affected by soil erosion with more than 10 t ha^{-1} $year^{-1}$. Moreover, the average value of erosion with 37.6 t ha^{-1} year is higher than the annual average of soil erosion (33 t ha^{-1} $year^{-1}$) for Iran (Hoseini and Gorbani, 2005; Omidvar 2010). Furthermore, the average predicted soil loss rate for the study area is four times higher than the mean global soil loss (Omidvar, 2010). However, the integrative soil erosion maps (Fig. 14) show similar values reported by other studies using the PASAC and EPM model in southwest of Iran (Nikeghbal and Rafati 2009; Tangestani 2006).

Table 9 Error matrix showing predicted erosion and observed erosion on pixel basis

Classes	Slight and low erosion [no. of pixel]	Moderate erosion [no. of pixel]	Severe and very severe erosion [no. of pixel]	Row total	Omission error*	Commission error**
Stable, low, and very low erosion/deposition classes	34	14	5	53	35.84 %	16.98 %
Moderate erosion/deposition classes	5	32	10	47	34.42 %	29.78 %
High and very high erosion/deposition classes	4	6	41	51	19.60 %	29.40 %
Overall Accuracy	0.70	–	–	–	–	–

Predicted erosion intensity is compared with values based on field survey and qualitative IMDPA model; Masoudi and Zakerinejad (2011)

* Omission error: Sample points for each pixel that has not been correctly classified and has been

Omitted from the category for each class

** Commission error: Sample points that have been inaccurately commissioned into a different category

The Mazayjan basin area is characterized by surrounding high mountain ranges with steep slopes and thus shows intensive erosion processes. In fact steeper slopes increase runoff velocity, detachment, and transport of sediments (Kefi et al. 2011; Wordofa 2011). Therefore, in the affected areas priority should be given to increase vegetation cover to decrease runoff velocities and protect soils. The deposition areas mainly concentrate close to or along the stream networks. These areas are characterized by high erodibilities of the substrates and turbulent runoff with the consequent evolution of gully networks.

4.6 Validation of the integrated USPED/SPI approach

The validation of soil loss predictions with numerical models is often difficult due to a lack of measured data to compare to (Gobin et al. 2004; Tangestani 2006). In some research the USLE-based erosion models are validated using landslide initiation points (Pradhan et al. 2012), ephemeral gully headcut locations (Suriyaprasit 2008), or simple field survey or qualitative models (Tangestani 2006; Kefi et al. 2011); especially, the assessment of soil loss through ground survey particularly in areas with complex terrain or restricted accessibility due to property rights is limited (Jianping et al. 2012).

The accuracy of numerous empirical soil modeling studies is difficult to validate in many basins of Iran due to the lack of gauging stations (Safamanesh 2004). Therefore, in this research the validation of the final integrated soil erosion/deposition map was performed using a combined approach based on aerial photos interpretation, field survey, and satellite image interpretation utilizing freely available high-resolution satellite images from GE. Additionally, we compared also to a qualitative model applied in the area (Masoudi and Zakerinejad 2011).

In this study we validate the soil loss of the prediction model with the field observation map of water erosion (see Masoudi and Zakerinejad 2011). The validation is illustrated as error matrix (Table 9). The error matrix contains a simple pixel-to-pixel comparison between predicted and observed soil loss. The error matrix in Table 9 shows omission, commission error, and overall accuracy for each class. According to this table the omission error is higher for the stable and low soil erosion classes than for severe and very severe soil erosion classes. The overall accuracy of the water erosion prediction map compared to the field observations is 77 %. Generally, the result of this validation procedure shows a high accuracy of the estimated soil loss by our integrated model. However, especially in flat parts of the study area the DEM is characterized by some noise and artifacts that affected the USPED modeling and also the SPI calculation. However, the validation procedure shows that our approach gives a proper picture of the spatial distribution of sheet erosion, gullying, and deposition processes. Moreover, also the process intensities are simulated adequately as shown in (Fig. 14).

5 Conclusions

During recent years, the role of water erosion as one of the land degradation factors in arid and semi-arid areas of large parts of Iran has increased (Ahmadi 2006; Hoseini and Gorbani 2005; Masoudi et al. 2006). In our study we applied a combined approach using the USPED model, the SPI, and a flow accumulation index in the southwest of Iran to characterize areal rill/inter-rill (sheet) erosion processes, gully erosion processes, and deposition processes. To the knowledge of the authors, this is the first attempt integrating different erosion processes and deposition dynamics in Iran.

The parameters utilized in this integrated model consist of (1) the erosivity factor (R-factor) calculated from monthly rain fall data, (2) the erodibility factor (K-factor) derived by data mining techniques, (3) the land-use factor (C-factor) delineated from Landsat ETM land-use classification, (4) the topography factor derived from a DEM with 10-m resolution, and finally (5) the SPI and flow accumulation to identify gullied areas. The results of this research show the spatial distribution of soil erosion and deposition processes. Thus, the integrated model is a useful tool to indentify susceptible areas for erosion and deposition processes. Hence, the obtained results consent a better land management and land-use planning in order to control soil loss.

In many previous studies in Iran qualitative models like IMDPA or MPSIAC were used for the assessment of water erosion processes as one important indicator of desertification (Ahmadi 2006; Masoudi et al. 2006; Masoudi and Zakerinejad 2010). Consequently, the proposed methodology provides spatially distributed information about process intensities and thus outperforms the qualitative models, especially in regard to land-use planning purposes. The application of a threshold value of SPI together with an estimate of gully volume using GE images is a simple but powerful tool to predict gully locations and gully erosion intensities.

In the study area soil loss is concentrated especially in the abandoned agricultural areas. The protection of bare soil to reduce soil loss should be ensured by appropriate cultivations (Lesschen et al. 2007). According to the results a large part of severe erosion occurs in the steep areas in the north and northwest of the study area. Main gully erosion activity is concentrating in the low sloping pediment and alluvial areas. Agricultural cultivations may change the land cover, leading to poorer vegetation cover or bare land, especially after harvest and thus increase erosion processes and land degradation. Also overgrazing even though not directly considered in the modeling procedure, but via the C-factor, and improper cultivation are two main causes of degradation processes in southwest of Iran and especially in Fars Province. In fact socioeconomic factors have an important role on land degradation and soil loss in this area; therefore, it is suggested to assess these factors in more detail maybe with questionnaires about land-use practices and livestock farming on farmers level.

Acknowledgments The authors would like to thank the Iranian Ministry of Science and Technology for providing the fellowship of Mr. Zakerinejad. Moreover, we would like to thank the Heidelberg Academy of Sciences and Humanities for field work and travel funding and the Department of Geography at University of Tübingen, Germany for hosting the research activities and providing laboratory and computer facilities. Finally we would like to thank also the Marie Curie EU-IRSES project entitled FLUMEN for support and assistance. The authors also express their gratitude to the Haseb Karaji Company in Iran, for providing the aerial photos and climate data for this research.

References

Adediji A, Tukur AM, Adepoju KA (2010) Assessment of Revised Universal Soil Loss Equation (RUSLE) in Katsina Area, Katsina State of Nigeria using remote sensing (RS) and geographic information system (GIS). Iran J Energy Environ 1(3):255–264

Ahmadi H (1995) Applied geomorphology. Tehran University Publication, Iran, p 613 (in Persian)

Ahmadi H (2006) Iranian model of desertification potential assessment in (East of Esfahan). Faculty of Natural Resources University of Tehran (in Persian)

Ahmadi H, Taheri S, Feiznia S, Azarnivand H (2011) Runoff and sediment yield modeling using WEPP in a semi-arid environment (Case study: Orazan Watershed). Desert 16(2011):5–12

Alcamo J, Flörke M, Märker M (2007) Future long-term changes in global water resources driven by socio-economic and climatic changes. Hydrol Sci J 52(2):247–275

Amundsen R, Harden JW, Singer MJ (1994) Factors of soil formation: a fiftieth anniversary perspective. Soil Sci Soc Am J, Special publication, 33

Arekhi S, Niazi Y (2010) Investigating application of GIS and RS to estimate soil erosion and sediment yield using RUSLE (Case study: upper part of Ilam Dam Watershed, Iran). J Water Soil Conserv 17(2):1–27 (in Persian)

Arekhi S, Darvishi Bolourani A, Shabani A, Fathizad H, Ahamdyasbchin S (2012) Mapping soil erosion and sediment yield susceptibility using RUSLE, remote sensing and GIS (Case study: Cham Gardalan Watershed, Iran). Adv Environ Biol 6(1):109–124

Arnoldus HMJ (1980) An approximation of the rainfall factor in the universal soil loss equation. In: De Boodt M, Gabriels D (eds) Assessment of erosion. Wiley, Chichester, pp 127–132

Asadi H, Vazifehdoost M, Moussavi A, Honarmand M (2011) Assessment and mapping of soil erosion hazard in Navrood watershed using revised universal soil loss equation (RUSLE), geographic information system (GIS) and remote sensing (RS). http://www.glrw.ir/fa/upload/f04641c2/306ef144.pdf

Bagherzadeh A (2012) Estimation of soil losses by USLE model using GIS at Mashhad plain, Northeast of Iran. Arab J Geosci 7(1):211–220

Bagherzadeh A, Mansouri Daneshvar M (2010) Estimating and mapping sediment production at Kardeh watershed by using GIS. The 1st International Applied Geological Congress, Department of Geology, Islamic Azad University, Mashad Branch, Iran

Barmaki M, Pazira E, Hedayat N (2011) Investigation of relationships among the environmental factors and water erosion changes using EPM model and GIS. Int Res J Appl Basic Sci 3(5):945–949

BCEOM (1998) Abay River Basin Integrated Development Master Plan, Main Report. Ministry of Water Resources, Addis Ababa

Beasley DB, Huggins LF, Monke EJ (1980) ANSWERS: a model for watershed planning. Trans ASCE 23:938–944

Behrens T, Föster H, Scholten T, Steinrücken U, Spies E, Goldschmitt M (2005) Digital soil mapping using artificial neural networks. J Plant Nutr Soil Sci 168:21–33

Biesemans J, Van Meirvenne M, Gabriels D (2000) Extending the RUSLE with the Monte Carlo error propagation technique to predict long-term average off-site sediment accumulation. J Soil Water Conserv 55:35–42

Bonilla CA, Reyes JL, Magri A (2010) Water erosion prediction using the revised universal soil loss equation (RUSLE) in a GIS framework, Central Chile. Chil J Agric Res 70(1):159–169

Bozorgzadeh E, Kaman N (2012) A geographic information system (GIS)-based modified erosion potential method (EPM) model for evaluation of sediment production. J Geol Min Res 4(6):130–141

Bryan RB (2000) The concept of soil erodibility and some problems of assessment and application. Catena 16:393–412

Cochrane TA, Flanagan DC (2003) WEPP watershed modeling with DEM's and GIS: the representative hill slope profile method. Trans Am Soc Agric Eng 46(4):1041–1049

Conacher AJ, Dalrymple JB (1977) The nine-unit land surface model: an approach to pedo-geomorphic research. Geoderma 18:1–154

Congalton RG, Green K (1999) Assessing the accuracy of remote sensing data: principle and practises. CRC Press Inc, Denvers 173p

Conoscenti C, Angileri S, Cappadonia C, Rotigliano E, Agnesi V, Märker M (2013) Gully erosion susceptibility assessment by means of GIS-based logistic regression: a case of Sicily (Italy). Geomorphology. In Press. doi:10.1016/j.geomorph.2013.08.021

Conoscenti C, Agnesi V, Angileri S, Cappadonia C, Rotigliano E, Märker M (2014) A GIS-based approach for gully erosion susceptibility modelling: a test in Sicily, Italy. Environ Earth Sci 70(3):1179–1195

Conrad O (2007) SAGA—Entwurf, Funktionsumfang und Anwendung eines Systems für Automatisierte Geowissenschaftliche Analysen. Dissertation, University of Göttingen

De Rosa P (2005) Analisi e confronti di modelli di erosione del suolo e tra-sporto di sedimenti tramite l'uso di sistemi G.I.S. Degree Thesis, Universitá degli studi di Perugia, Italia

Dehbozorgi M, Pourkermani M, Arian M, Matkan AA, Motamedi H, Hosseiniasl A (2010) Quantitative analysis of relative tectonic activity in the Sarvestan area, central Zagros, Iran. Geomorphology 121(3–4):329–341

Dikau R (1989) The application of a digital relief model to landform analysis in geomorphology. In: Raper J (ed) Three dimensional application in Geographic Information Systems. London, pp 51–77
Eisazadeh L, Amani RS, Pazira E, Homaee M, Sokouti R (2012) Comparison of empirical models to estimate soil erosion and sediment yield in micro catchments. Int J Agric Res Rev 2(3):303–307
Elith J, Leathwick JR, Hastie T (2008) A working guide to boosted regression trees. J Anim Ecol 77:802–813
Elsenbeer H, Cassel DK, Tinner W (1993) Daily rainfall erosivity model for western Amazonian. J Soil Water Conserv 48:439–444
FAO (1994) Land degradation in South Asia: its severity causes and effects upon the people. FAO, UNDP and UNEP report, Rome
Faulkner H, Alexander R, Teeuw R, Zukowskyj P (2004) Variations in soil dispersivity across a gully head displaying shallow sub-surface pipes, and the role of shallow pipes in rill initiation. Earth Surf Process Land 29:1143–1160
Feiznia S (2000) Rock resistance against corrosion in different climates in Iran. Nat Resour J 47:95–116 Iran (in Persian)
Feiznia S, Ahzan K (2004) Determining soil erodibility of Damavand basin with USLE model. Sediment Sediment Rock J 4:13–29 (in Persian)
Ferro V, Giordano G, Iovino M (1991) Isoerosivity and erosion risk map for Sicily. Hydrol Sci J 36:549–564
Flanagan DC, Nearing MA (1995) USDA water erosion prediction project: hillslope profile and watershed model documentation. NSERL Report No. 10. USDA-ARS National Soil Erosion Research Laboratory, West Lafayette
Friedman JH (1999) Stochastic gradient boosting. Technical Report. Department of Statistics, Stanford University, USA. http://www.salford-systems.com/treenet.html
Friedman JH (2002) Stochastic gradient boosting. Comput Stat Data Anal 38:367–378
Gee GW, Bauder JW (1986) Particle-size analysis. In Burt R (ed) Soil survey field and laboratory methods manual; report no 51: 53–54, US Department of Agriculture, Lincoln, Nebraska
Gobin A, Jones R, Kirkby M, Campling P, Govers G, Kosmas C, Gentile AR (2004) Indicators for pan-European assessment and monitoring of soil erosion by water. Environ Sci Policy 7(1):25–38
Grove AT, Rackham O (2001) The nature of Mediterranean Europe: an ecological history. Yale University Press, New Haven
Hoseini S, Gorbani M (2005) Economics of soil erosion. Ferdowsi University of Mashhad Press, Mashhad (in Persian)
Hosmer DW, Lemeshow S (2000) Applied logistic regression. Wiley series in Probability and Statistics
Hu Q, Clark JG, Jung P, Lee B (2000) Rainfall erosivity in the Republic of Korea. J Soil Water Conserv 55(2):115–120
Ilanloo M (2012) Estimation of soil erosion rates using MPSIAC models (Case Study Gamasiab basin). Int J Agric Crop Sci 16:1154–1158
Jianping G, Niu T, Rahimy P, Wang F, Zhao H, Zhang J (2012) Assessment of soil erosion susceptibility using empirical modeling. J Acta Meteorol Sin 27(1):98–109
Kakembo V, Xanga WW, Rowntree K (2009) Topographic thresholds in gully development on the hillslopes of communal areas in Ngqushwa Local Municipality, Eastern Cape, South Africa. Geomorphology 110(3–4):188–194
Karami A, Homaee M, Neyshabouri MR, AfzalInia S, Basirat S (2012) Large scale evaluation of single storm and short/long term erosivity index models. Turk J Agric For 36:207–216
Kefi M, Yoshino K, Setiawan Y, Zayani K, Boufaroua M (2011) Assessment of the effects of vegetation on soil erosion risk by water: a case of study of the Batta watershed in Tunisia. Environ Earth Sci 64(3):707–719
Kheir R, Wilson J, Deng Y (2007) Use of terrain variables for mapping gully erosion susceptibility in Lebanon. Earth Surf Process Land 32:1770–1782
Kirkby M (2001) Modelling the interactions between soil surface properties and water erosion. Catena 46:89–102
Kompani-Zare M, Soufi M, Hamzehzarghani H, Dehghani M (2011) The effect of some watershed, soil characteristics and morphometric factors on the relationship between the gully volume and length in Fars Province, Iran. Catena 86(3):150–159
Köthe R, Lehmeier F (1993) SARA - Ein Programmsystem zur Automatischen Relief-Analyse. Z. f. Angewandte Geographie, 4/93:11-21; Cologne, Germany
Kouli M, Soupios P, Vallianatos F (2009) Soil erosion prediction using the revised universal soil loss equation (RUSLE) in a GIS framework, Chania, Northwestern Crete, Greece. Environ Geol 57:483–497

Kumar BM, Nair PKR (2006) Tropical homegardens: a time-tested example of sustainable agroforestry. Springer Science, Dordrecht 380p

Lal R (2001) Soil degradation by erosion. Land Degrad Dev 12:519–539

Landi A, Barzegar AR, Sayadi J, Khademalrasoul A (2011) Assessment of soil loss using WEPP model and geographical information system. J Spat Hydrol 11(1):40–51

Le Roux JJ, Morgenthal TL, Malherbe J, Pretorius DJ, Sumner PD (2008) Water erosion prediction at a national scale for South Africa. Water SA 34, http://www.wrc.org.za. (last view 30.01.2015)

Leh M, Bajwa S, Chaubey I (2011) Impact of land use change on erosion risk: an integrated remote sensing, geographic information system and modeling methodology. Land Degrad Dev 24:409–421. doi:10.1002/ldr.1137

Lesschen JP, Kok K, Verburg PH, Cammeraat LH (2007) Identification of vulnerable areas for gully erosion under different scenarios of land abandonment in Southeast Spain. Catena 71:110–121

Maerker M, Angeli L, Bottai L, Costantini R, Ferrari R, Innocenti L, Siciliano G (2008) Assessment of land degradation susceptibility by scenario analysis: a case study in Southern Tuscany, Italy. Geomorphology 93:120–129

Mahmoodabadi M, Refahi HG (2005) Sediment yield assessment using MPSIAC model in GIS framework. Tehran University, Tehran

Masoudi M, Zakerinejad R (2010) Hazard assessment of desertification using MEDALUS model in Mazayjan plain, Fars province, Iran. Ecol Environ Conserv 16(3):425–430

Masoudi M, Zakerinejad R (2011) A new model for assessment of erosion using desertification model of IMDPA in Mazayjan plain, Fars province, Iran. Ecol Environ Conserv 17(3):489–594

Masoudi M, Patwardhan AM, Gore SD (2006) Risk assessment of water erosion for the Qareh Aghaj subbasin, southern Iran. Stoch Env Res Risk Assess 21:15–24

Meamarian H, Esmaeilzadeh H (2003) The Sediment yield potential estimation of Kashmar watershed (Iran) using MPSIAC model in the GIS framework. http://www.gisdevelopment.net/application/2003. (last view 30.01.2015)

Mitas L, Mitasova H (1998) Distributed soil erosion simulation for effective erosion prevention. Water Resour Res 34:505–516

Mitasova H, Mitas L (2001) Multiscale soil erosion simulations for landuse management. In: Harmon R, Doe W (eds) Landscape erosion and landscape evolution modeling. Kluwer Academic/Plenum Publishers, Dordrecht, pp 321–347

Mitasova H, Hofierka J, Zlocha M, Iverson LR (1996) Modelling topographic potential for erosion and deposition using GIS. Int J Geogr Inf Syst 10:629–641

Moore D, Wilson JP (1992) Length-slope factors for the revised universal soil loss equation: simplified method of estimation. J Soil Water Conserv 47:423–428

Morgan RPC (1995) Soil erosion and conservation. 2nd edn. Longman, London, 198 pp

Morgan RPC, Quinton JN, Smith RE, Govers G, Poesen JWA, Auerswald K, Chisci G, Torri D, Styczen ME (1998) The European Soil Erosion Model (EUROSEM): a dynamic approach for predicting sediment transport from fields and small catchments. Earth Surf Process Land 23:527–544

Moussavi E, Nikkami D, Mahdian MH, Pazir A (2012) Investigating rainfall erosivity indices in arid and semi arid climates of Iran. Turk J Agric For 36:365–378

Najm Z, Keyhani N, Rezaei K, Naeimi Nezamabad A, Vaziri H (2011) Sediment yield and soil erosion assessment by using an empirical model of MPSIAC for Afjeh & Lavarak sub-watersheds, Iran. Earth Sci J 2(1):14–22

Najmoddini N (2003) Assessment of erosion and sediment yield process using RS and GIS. M.Sc. Thesis, International institute for Geo-Information science and earth observation (ITC), the Netherlands, 63p

Nazari Samani A, Ahmadi H, Jafari M, Boggs G (2009) Geomorphic threshold conditions for gully erosion in Southwestern Iran (Boushehr-Samal watershed). Earth Sci 35:180–189

Nearing MA, Foster GR, Lane LJ, Finkner SC (1989) A process-based soil erosion model for USDA-water erosion prediction project. Trans ASAE 32(5):1587–1593

Nikeghbal M, Rafati S (2009) A GIS-based assessment of the relationships between erosion and desertification in a semi-arid climate: Zarindasht district, Fars province, national geo informatics, Tehran, Iran

Olaya V, Conrad O (2009) Geomorphometry in SAGA. In: Hengl T, Reuter HI (eds) Geomorphometry concpets, software, applications. Developments in soil science, vol 33. Elsevier, UK, pp 293–308

Omidvar K (2010) Introduction to soil conservation and watershed, 2nd edn. Yazd University Press, Yazd (in Persian)

Onori F, Bonis PD, Grauso S (2006) Soil erosion prediction at the basin scale using the revised universal soil loss equation (RUSLE) in a catchment of Sicily (Southern Italy). Environ Geol 50:1129–1140

Pacific Southwest Interagency Committee (1968) Report of the water management subcommittee on factors affecting sediment yield in the pacific southwest area and selection and evaluation of measures for reduction of erosion and sediment yield. ASCE, 98, Report No. HY12

Pelacani S, Märker M, Rodolfi G (2008) Simulation of soil erosion and deposition in a changing land use: a modelling approach to implement the support practice factor. Geomorphology 99:329–340

Planchon O, Darboux F (2001) A fast, simple and versatile algorithm to fill the depressions of digital elevation models. Catena 46:159–176

Poesen JW, Vandaele K, Van Wesemael B (1996) Contribution of gully erosion to sediment production on cultivated lands and rangelands. In: Walling DE, Webb BW (eds) Erosion and Sediment Yield: Global and Regional Perspectives (Proceedings of the Exeter Symposium, July 1996) IAHS Publication, 236: 251–266

Popp JH, Hyatt DE, Hoag D (2000) Modeling environmental condition with indices: a case study of sustainability and soil resources. Ecol Model 130(1–3):131–143

Pradhan B, Chaudhari A, Adinarayana J, Buchroithner M (2012) Soil erosion assessment and its correlation with landslide events using remote sensing data and GIS: a case study at Penang Island, Malaysia. Environ Monit Assess 184(2):715–727

Renard KG, Freimund JR (1994) Using monthly precipitation data to estimate the R-factor in the revised USLE. J Hydrol. 157:287–306, European Commission Joint Research Centre Institute for Environment and Sustainability

Renard KG, Foster G.R, Weesies GA, McCool DK, Yoder DC (1997) Prediction soil erosion by water: a guide to conservation planning with the revised universal soil loss equation. Agricultural Handbook 703. US Department of Agriculture p. 404

Roshani MR, Rangavar A, Javadi MR, Ziyaee A (2013) A new mathematical model for estimation of soil Erosion. Int Res J Appl Basic Sci 5(4):491–497

Rusco E, Montanarella L, Bosco C (2008) Soil erosion: a main threats to the soils in Europe. In: Tóth G, Montanarella L, Rusco E (eds) Threats to soil quality in Europe. No. EUR 23438 EN in EUR—scientific and technical research series. Office for official publications of the European Communities: 37–45. Google Scholar: 16771305971362909763

Sadeghi SHR, Moatamednia M, Behzadfar M (2011) Spatial and temporal variation in the rainfall erosivity factor in Iran. J Agric Sci Technol 13:451–464

Sadeghifard D, Jabari E, Ghayasian H (2004) Rainfall erosivity zonation in Iran, the first national conference on civil engineering, Sharif University of Technology, Iran. CIVILICA online journal: http://www.civilica.com/Paper-NCCE01-226_2417394703.html, 1–8. (in Persian) (last view 30.01.2015)

Safamanesh R (2004) Validation of the MPSIAC Model for sediment yield prediction in Zargeh watershed, Iran. MSc Thesis, University Putra Malaysia

Sariyildiz T, Anderson JM, Kucuk M (2005) Effects of tree species and topography on soil chemistry, litter quality, and decomposition in Northeast Turkey. Soil Biol Biochem 37(9):1695–1706

Saxton KE, Rawls WJ (2006) Soil water characteristic estimates by texture and organic matter for hydrologic solutions. Soil Sci Soc Am J 70:1569–1578

Seibert J, Stendahl J, Sorensen R (2007) Topographical influences on soil properties in boreal forests. Geoderma 141:139–148

Shahrivar A, Tehbconsung C, Jusop S, Abdul Rahim A, Soufi M (2012) Roles of SAR and EC in Gully Erosion Development (A Case Study of Kohgiloye va Boyerahmad Province, Iran). J Res Agric Sci 8(1):1–12

Shruthi RBV, Kerle N, Jetten V (2011) Object-based gully feature extraction using high spatialresolution imagery. Geomorphology 134:260–268

Sidorchuk A, Märker M, Moretti S, Rodolfi G (2003) Gully erosion modelling and landscape response in the Mbuluzi River catchment of Swaziland. Catena 50:507–525

Simms AD, Woodroffe CD, Jones BG (2003) Application of RUSLE for erosion management in a coastal catchment, southern NSW. International Congress on Modelling and Simulation 2, Social and Economic Systems for Resource Management Solutions, Townsville, Queensland, 678–683

Suriyaprasit M (2008) Digital terrain analysis and image processing for assessing erosion prone areas. PhD Thesis, International institute for geo-information science and earth observation, The Netherlands

Tagil S, Jenness J (2008) GIS-based automated landform classification and topographic, landcover and geologic attributes of landforms around the Yazoren Polje, Turkey. J Appl Sci 8:910–921

Tangestani M (2006) Comparison of EPM and PSIAC models in GIS for erosion and sediment yield assessment in a semi-arid environment: Afzar Catchment, Fars Province, Iran. J Asian Earth Sci 27:585–597

Tangestani MH, Moore F (2001) Comparison of three principal component analysis techniques to porphyry copper alteration mapping, A case study, Meiduk area, Kerman, Iran. Can J Remote Sens 27(2): 176–182

Terranova O, Antronico L, Coscarelli R, Iaquinta P (2009) Soil erosion risk scenarios in the Mediterranean environment using RUSLE and GIS: an application model for Calabria (Southern Italy). Geomorphology 112:228–245

Vaezi AR, Sadeghi SHR (2011) Evaluating the RUSLE model and developing an empirical equation for estimating soil erodibility factor in a semi-arid region. Span J Agric Res 9(3):912–923

Valentin C, Poesen J, Yong L (2005) Gully erosion: impacts, factors and control. Catena 63:132–153

Vandekerckhove L, Muys B, Poesen J, De Weerdt B, Coppé N (2001) A method for dendrochronological assessment of medium-term gully erosion rates. Catena 45:123–161

Wang G, Gertner G, Fang S, Anderson AB (2003) Mapping multiple variables for predicting soil loss by geostatistical methods with TM image sand a slope map. Photogramm Eng Remote Sens 69:889–898

Wilson JP, Gallant JC (2000) Terrain analysis: principles and applications. Wiley, New York, 520 pp

Wischmeier WH, Smith SS (1978) Predicting rainfall-erosion losses: a guide to conservation planning. Agriculture Handbook No. 537. US Department of Agriculture, Washington, DC

Wordofa G (2011) Soil erosion modeling using GIS and RUSLE on the Eurojoki watershed Finland. Bachelor's thesis, Tampere University, Finland

Yuksel A, Akay A, Reis E, Mand Gundogan R (2007) Using the WEPP model to predict sediment yield in a sample watershed in Kahramanmaras region. Int Congr River Basin Manag 2:11–22

Yuksel A, Gundogan R, Akay AE (2008) Using the remote sensing and GIS technology for erosion risk mapping of Kartalkaya dam watershed in Kahramanmaras, Turkey. Sensors 8:4851–4865

Zakerinejad R, Märker M (2014) Prediction of Gully erosion susceptibilities using detailed terrain analysis and maximum entropy modeling: a case study in the Mazayejan Plain, Southwest Iran. Geogr Fis Din Quat 37(1):67–76

Zevenbergen LW, Thorne CR (1987) Quantitative analysis of land surface topography. Earth Surf Process Landf 12(1):47–56

Paper C

Morphotectonic analysis of the Zagros Mountains using high resolution DEM to assess gully erosion processes: A case study in the Fars province, Southwest of Iran.

Current status: accepted for publication, International Geoinformatics Research and Development Journal (IGRDJ).

Morphotectonic analysis of the Zagros Mountains using high resolution DEM to assess gully erosion processes: A case study in the Fars province, Southwest of Iran

Zakerinejad R [1,2], Hochschild V[1], Rahimi M[2], Maerker M[3,4]

[1] Department of physical geography, University of Tübingen, Rümelinstr. 19-23, 72070 Tübingen, Germany

[2] Faculty of Desert Studies, Semnan University, Semnan, Iran

[3] Heidelberg Academy of Sciences and Humanities, Rümelinstr. 19-23, 72070 Tübingen, Germany

[4] Department of Earth Sciences, University of Florence, Via La Pira 4, 50121 Florence, Italy

Abstract

Tectonic activities in the Zagros Mountain significantly contributed to the formation of the existing drainage systems and hence, to landscape evolution in the Fars province in the Southwestern Iran. Soil erosion and severe gullying recently affect large parts of the southwestern parts of the country. Neotectonics (Upper Quaternary) in form of earthquakes and associated uplifting, fracturing and faulting are still active in large parts of the Zagros range. In this paper we focus especially on the assessment of the vulnerability of geologic formations to gullying induced by the effects of neotectonic processes. Recent tectonics cause disturbances on the ground surface that propagate through the hydrological system triggering also gullying. This research investigates the morphotectonics of the Mazayjan basin, which is part of the Zagros Mountains in the Southwest of Iran, using terrain and stream profile analysis. To the knowledge of the authors the mechanics of stream networks and erosional process related to neo-tectonics are still poorly studied in the Zagros Mountains. The tectonic features extracted from a geological map and validated with filed survey in the study area. An investigation on the location of gully features like head cuts and stream profile knickpoints reveals that the highly sensitive areas to gullying are related to areas with uplifting and faulting. In this study we utilized the TecDEM software to identify knickpoints showing that the abrupt change in the river profiles are located in the central part (Alluvial deposition) of the catchment. Hence, the location of knickpoints indicates tectonic activity in turn changing the drainage network in the longitudinal profile. We illustrate that severe gully erosion is strongly related to these tectonic processes, especially in the Southwest of the Mazayjan catchment.

Keywords: Morphotectonic analysis, TecDEM, Zagros Mountain, GIS, Gully erosion

1. Introduction

The Zagros Mountain (ZM) belt extends about 1500 km from the Taurus Mountain southeast of Turkey, through southwestern Iran, stretching till the strait of Harmoz [6]. The Zagros morphogenesis is the morphotectonic expression of the Alpine-Himalayan subduction cycle and hence, the collision of the Arabian and Iranian plates [51]. The landscapes in these areas result from the complex combination of the effects of active tectonics like faulting and erosional as well as depositional processes. The main structural architecture of the Zagros is defined by the so called Zagros fold belt, which attains an average elevation of over 3000 m a.s.l. [11, 51].

The morphogenesis of the ZM took place during the last 4-5 Ma with the opening of the Red Sea [16] and related uplift processes in turn followed by soil erosion, transport and deposition processes and the resulting forms and features. However, analysis of satellite images implies the prevalence of North-South striking faults in the ZM [11, 22]. The strong connection between slope morphology and erosion rates was revealed by geomorphologists already in the late 18th century [18, 37]. Especially tectonic geomorphology explores the balance of erosion and uplift [54]. However, only few researches have presented quantitative data related to the assessment of such relations over spatial and temporal scales relevant to the evolution of tectonically active landscapes [37] and only little research was carried out concerning the role of neotectonics on gully formation in general but especially in southern Iran.

In the Zagros belt the main factors influencing soil erosion processes include geology, tectonics, climate, topography and land cover. Active tectonics in these areas is involved in the formation of landforms and drainage networks. Climatic factors influence the weathering processes and the water availability for erosion and sediment transport [64]. Actually, the tectonic activity in this area seems to have an important role in the evolution and intensity of soil erosion processes.

Digital Elevation Models (DEMs) are especially useful to analyze active regional tectonics from topography [9, 71]. Nevertheless, some parts of the study area have already been studied in terms of the general distribution of soil erosion processes using DEMs [34, 73].

Gully erosion is a very intensive form of soil erosion affecting soil fertility, degrading agricultural areas and rangelands and also threatens infrastructures such as roads. Moreover, soil erosion processes cause also the migration of the inhabitants of the affected areas. This type of erosion represents an important sediment source and is an indicator of environmental change [32, 48, 58]. Many researchers have shown that gully formation and expansion is related to climatic change, topographic factors, anthropogenic and hydrogeotechnical characteristics [13, 19, 74]. In some studies active tectonics were identified as the main factor of the geologic formation and expansion of gully systems [17, 41]. Still, to the knowledge of the authors there are no studies on the effects of tectonic activities on the process of drainage network evolution in southern Iran. Hence, morphotectonic analysis and also studies assessing the role of tectonics on gully erosion processes are lacking. Thus, this study aims at investigating the effects of neotectonics on gully erosion processes and dynamics.

Reliable estimates of fault slip-rates are keys to understand the distribution of gully erosion events and changing drainage morphology in active mountain ranges [14, 15]. Consequently, the specific objectives of this study are threefold in terms of:

i) an evaluation of the role of tectonics on drainage systems.

ii) an assessment of different DEM resolutions (30 m, 10 m, and 5 m) utilized for the stream network and geomorphotectonic analysis.

iii) an evaluation of the role of active tectonics on the spatial distribution of gully erosion derived satellite images and aerial photos of the study area.

2. Study area

The study area is part of the Zagros folded zone and is situated in the Southwest of the Fars province, Iran. Different tectonic phases and neotectonic activities are intensively affecting this area. The region shows a complicated structure with numerous active tectonics and deformation processes causing several large and intensive earthquakes in recent years. The Zagros fold is a zone of active convergence between the Arabian and Eurasian plates [46, 51]. Hence, the landforms of the ZM reflect recent fault tectonics [11] stretching from the

Northwest to the Southwest of the Iran. The Southwestern parts of the Zagros belt are subject to active faulting and are about 100 km wider than the northwestern part of this fold belt [5].

In the Fars province, there are several right lateral faults that expand North–South following the overall trend of the Zagros fault-and-fold belt [5]. Regional uplift represented by geo-flexures indicates that the Zagros fold rose at a minimum rate of 1 mm/yr since the early Pliocene [16]. Our study area, the Mazayjan (MZJ) basin , is located in the Fars province around 32 km southwest of Zarindasht city, Southwest of Iran (54° 34' to 54° 44' E and 27° 59' to 28° 5' N; Fig 1).

The study area covers ca 900 km² and is drained by the MZJ seasonal River that is the main ephemeral river flowing from the West to the East of the basin.

The elevation is ranging from 671 m to a maximum altitude of 1969 m a.s.l.. The study area is characterized by large alluvial fans in the southeastern part of the catchment. Moreover, a large Precambrian salt dome dominates the landscape in the southwest and southeast of the basin. According to the geology the largest part of the landscape is relatively young showing active geomorphic features. The field survey in 2013/14 and an aerial photo interpretation indicates immature topography in large part of this basin characterized by dynamic soil erosion and deposition processes. The geology of the study area (Iranian National Survey Mapping; 1:25000) is mostly belonging to Quaternary depositions (Qt) in the plain areas of the central and northern parts. In the Southwest of the catchment the Bakhtiari formation (Bk) mainly consisting of Pliocene-Conglomerates is dominating the morphology. The Asmari (As) formation with predominant limestone layers prevails in the western and northern parts of the catchment. Upper Cretaceous succession was described in the Fars province as Tarbur Formation by Wynd [72] which is composed by rudist limestone [2]. It occurs in a narrow strip in the West of the study area. The Gachsaran Formation (Gs) is composed of chalky-gypsiferous limestones to dolomites intersected by horizons of marls and nodular to crystalline gypsum. The Gs formation is divided into Champeh (Cpm) and Mole (Mlm) members. These areas are more stable compared to the Agha-Jari formation (Aj). The latter formation is composed of sandstone especially in the north of the catchment. Moreover, the Ghachsaran (Grm) and the Guri (Grm)-Formations show riff sandstone morphologies whereas the Hormoz formation (Salt plug) is characterized by salt domes and is widespread in the catchment (Fig1).

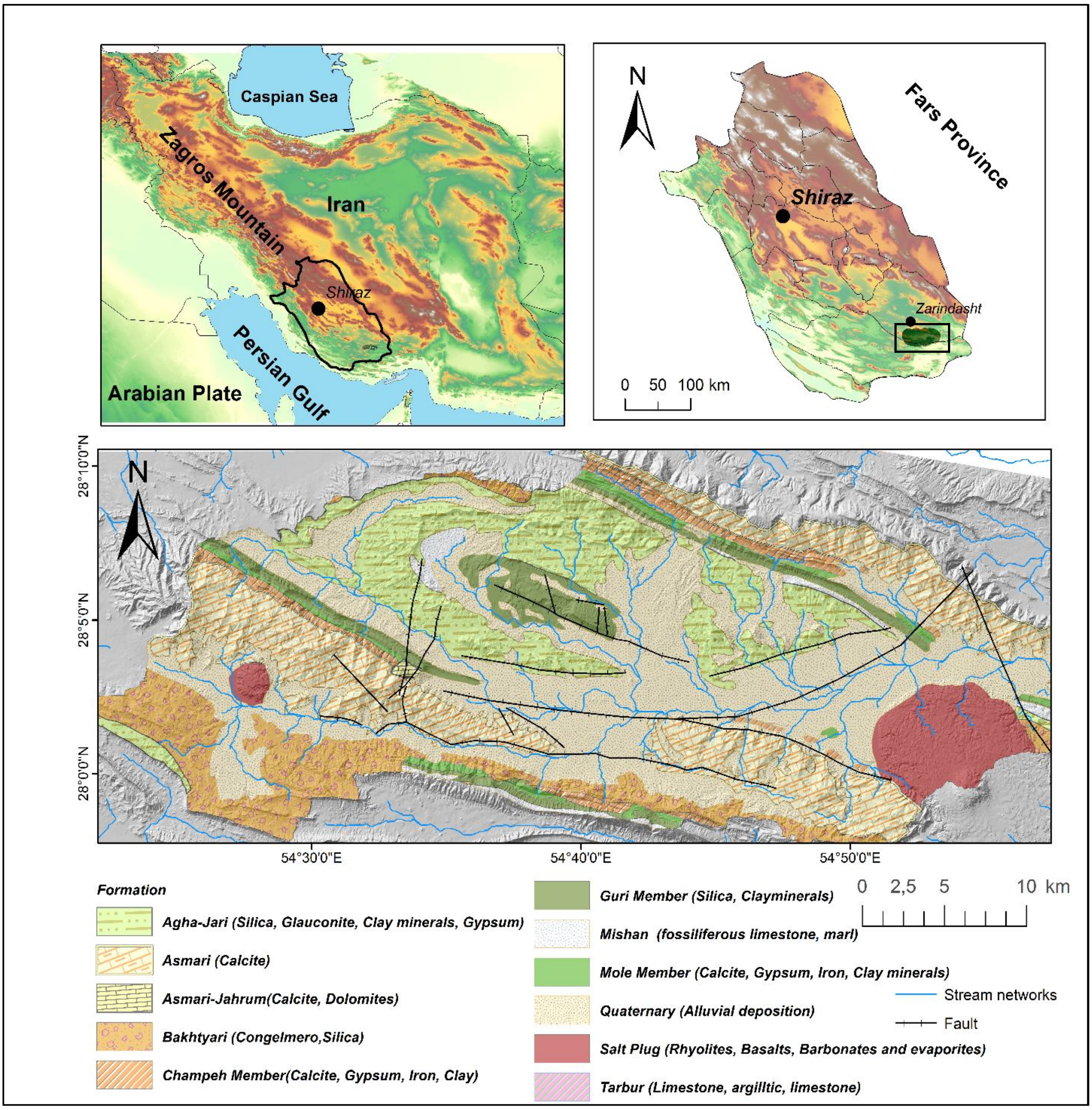

Fig. 1: Study area: Geological settings of the MZJ catchment based on the geological map (1:25.000)

3. Materials and methods

In this study the analysis of neotectonics is mainly based on digital elevation models (DEM). DEMs constitute an important spatial information source for different branches of earth sciences [56]. DEMs are useful tools to analyse landscapes, thus, representing an active field of research in geomorphological applications [25] DEMs can also be assessed to reveal active regional tectonics from topography [9, 71].

The preprocessing of a DEM for the extraction of topography parameters like slope, aspect and curvature etc. is fundamental to guarantee a certain DEM quality to conduct the neotectonic analysis. DEM preprocessing eliminates artifact and blunders or gross errors and also reduces noise due to acquisition techniques or data fusion problems [67, 70]. In the following the data preprocessing and DEM analysis utilized are described in detail. Moreover, we conducted also fieldwork and aerial photo interpretation (API) to calibrate and validate the DEM assessment.

3.1 DEM sources

Digital terrain analysis (DTA) is a process to describe the terrain in a quantitative form. DEM derivatives are grouped in morphometric parameters describing; terrain units in terms of hydrological processes, climatic processes, geological settings and geomorphological processes [23, 36]. In fact a digital elevation model consists of finite points that collectively describe a topographic surface [57; http://www.tecdem.org]. The quality of a DEM is very important as it directly affects the quality of spatial modeling [23, 33]. In this study three different DEM sources and resolutions were used:

1) The Advanced Space borne Thermal Emission and Reflection Radiometer (ASTER) DEM with 30 m resolution, also known as ASTER GDEM.
2) A contour line based DEM (10 m resolution) generated from the official topographic map (Iranian survey map organization 2006; 1:25.000 scale) using the Spatial Analyst tools (Topo to raster function) in Arc map 10.2.
3) A stereo aerial photograph based DEM with 5 m resolution. The DEM was generated using Agisoft PhotoScan software (Agisoft) and scanned 1:20.000 scale aerial photographs. This software is an advanced image-based 3D modeling solution aimed at creating high quality 3D content from images or aerial photos.

3.1.1 DEM generation from stereo aerial photographs

To generate the high resolution DEM we utilized stereo aerial photographs at 1:20.000 scale (Iranian National Survey Mapping) having 60 % overlap. We processed the images with Agisoft PhotoScan software (http://www.agisoft.com). Agisoft PhotoScan is commercial software capable to generate completely automated alignments and 3D contents from overlapping. To calibrate and validate the model we collected ground control points (GCPs) from satellite images of Google Earth. In this study the aerial photos coverage consists of 19 photos and 42 ground control points from satellite images based on SPOT 5 data–with 2.5 m ground resolution.

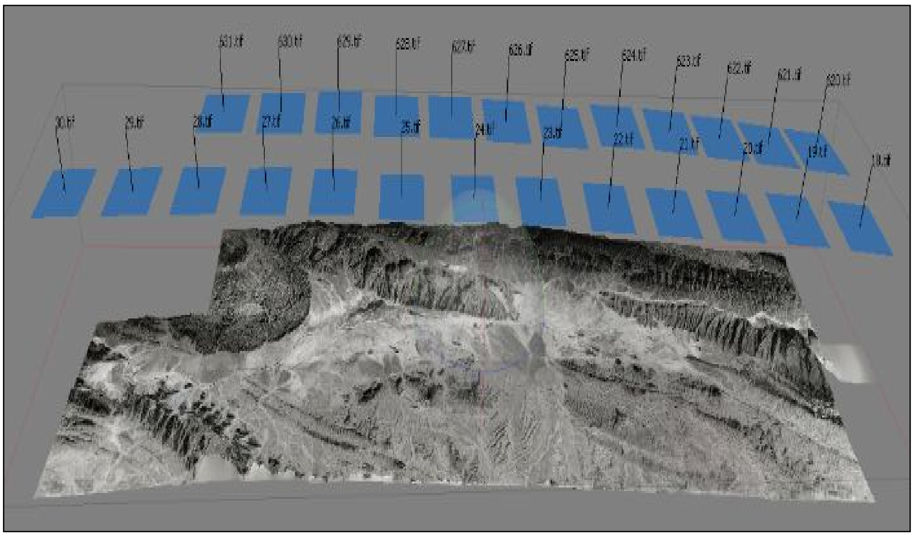

Fig. 2: DEM of the study area derived with Structure from Motion Technology and stereo aerial photographs

3.2 Geomorphometric analysis

Morphometry is described as the quantitative measurement of a landscape shape allowing the comparison of landforms [26, 52] Especially, geomorphometric indices permit a proper assessment of fluvial systems in different regions of the world and in a variety of tectonic settings [4, 27]. Actually, morphotectonics describe the interface of geomorphology and tectonics or in other words the study of landforms indicating recent tectonic movements [20]. Hence, anomalies in landform distribution, stream direction, the form of channels and stream profiles can be detected [7, 20]. In fact in many parts of Zagros a change in stream direction or in slope gradient may be induced by by an ongoing tectonic activity [46, 49]
The latter plays an important role on the severity and intensity of soil erosion and deposition processes [45]. There are different methods to evaluate the role of tectonics and lithology on topography and drainage systems e.g. by stream longitudinal profiles or the analysis of basin asymmetry and basin hypsometry. In fact, drainage networks or rivers are very sensitive to tectonic activity, especially to uplift and tilting [65]. Consequently, there are distinct relationships between topography, shape and denudation rates [28]. The active faults may change the pattern of drainage networks. This can be assessed by field observations or with

using satellite or aerial photos. The delineated indices are useful tools for assessing the catchment evolution and also to detect contemporary tectonics in the catchment.
For the extraction of these indices we used TecDEM (http://www.tecdem.org), a toolbox implemented in MATLAB [55, 57].

3.2.1 Asymmetry factor (AF)

Drainage basin tilting is significant to evaluate the basin asymmetry, which is an important indicator of tectonic activities at the scale of a drainage basin [3, 26]. AF values under the effects of active tectonics or strong lithologic control are significantly greater or smaller than 50 [26]. AF values close to 50 shows little or no tilting perpendicular to the direction of the trunk channel. AF is defined as:

$$AF = 100\ (A_r / A_t) \qquad \text{Equation (1)}$$

Where, A_r is the area of the basin to the right of the trunk stream while facing downstream and A_t is the total area of the drainage basin. In this study we used the asymmetry classification according to Equation 2 following [44]:

$$AF = |100 \times (A_r / A_t) - 50\ | \qquad \text{Equation (2)}$$

The AF is divided into four classes: AF< 5 (symmetric basins), AF= 5–10 (gently asymmetric basins), AF= 10– 15 (moderately asymmetric basins), and AF>15 (strongly asymmetric basins).

3.2.2 Basin Hypsometry Analysis

Hypsometric analysis is useful to understand the geomorphometric stage of a river basin and to assess factors forcing the basin evolution [35] and is an index that is independent of the basin area [25]. The basin hypsometry represents the relative surface of a watershed below or above a given elevation [43].

This index reflects the interaction between tectonics, soil erosion, climatic conditions and lithology of a basin [24, 68]. The area under the hypsometric curve (Hypsometric integral) (HI) [35] indicates the erosion process dynamics in a watershed [59]. Actually, the shape of the hypsometry curve shows the evolutionary stage of a basin. As illustrated in Figure 3 the curves with convex shape are related to young basin morphologies while basins with concave curved shapes are more mature basins [1, 35, 62]

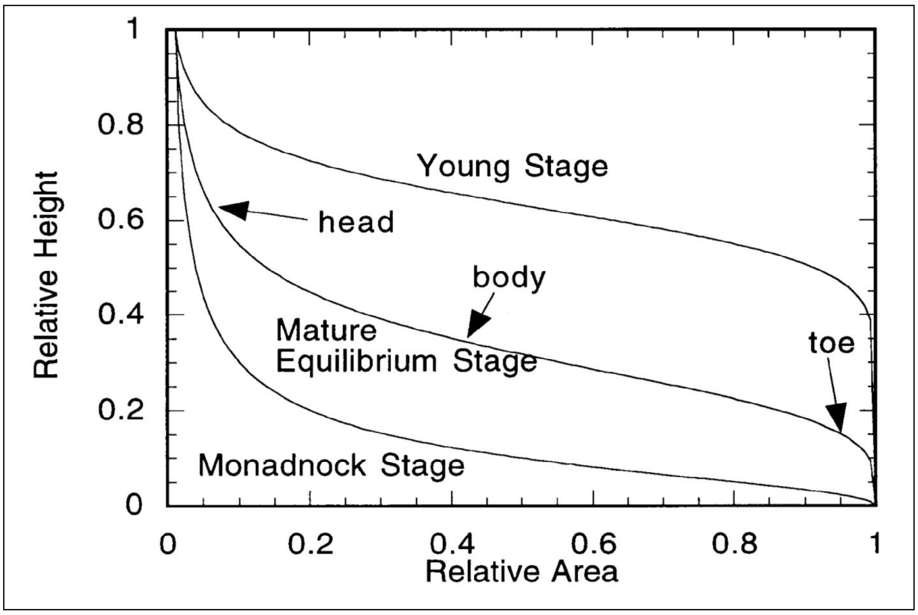

Fig. 3: Three types of hypsometric curves – young, mature and old stages – showing toe, head and body [after 62].

The MZJ basin as part of the ZM is expected to have a quite young morphology characterized by high erosion rates due to general uplift processes. In this study a simple and more common equation for the HI among the different methods [3, 26, 59] has been used according to Equation 3

Hypsometric Integral (HI): $Elev_{mean} - Elev_{min} / Elev_{max} - Elev_{min}$ Equation (3)

Where, HI is the elevation–relief ratio equivalent; $Elev_{mean}$ is the average elevation of the catchment; $Elev_{min}$ and $Elev_{max}$ are the minimum and maximum elevations within the catchment and the average elevation is gained from 50 points of elevation taken randomly taken from the DEM [3].

The hypsometry and the HI are used in classical conceptual geomorphometric models of landscape evolution as follows: i) for HI above 0.60 the area is considered young; ii) for HI ranging between 0.35 - 0.60 the area is in a steady state balance or mature phase and iii) HI below 0.35 characterizes a Monadnock phase in landscape evolution [35, 57, 62]. The HI does not have a direct relation with relative active tectonics [3]. In this study the hypsometric curves for each of the 8 sub-catchments were extracted and the stream order after Strahler [62] was determined (Fig. 5). We utilized the 4^{th} order streams extracted from the DEM, which are corresponding to Strahler orders 3 and 4 in the topography map. 4^{th} order streams are a compromise between the too dense lower order network and too big higher stream orders. Figure 3 shows the different stages of river evolution according to the concavity and the convexity index.

The skew and kurtosis values are used to compare the erosion phases in the different parts of the study area. Skew represents the asymmetry of the normal distribution in respect to the mean. The skew is 0, when the variable distribution is symmetrical. A positively skewed distribution has scores clustered to the left, with the tail extending to the right. A negatively skewed distribution has scores clustered to the right, with the tail extending to the left. A positive value of the skewed distribution indicates an arithmetic mean elevation above the median value while the negative skewness shows a higher value of median than mean.Positive kurtosis is indicated by a peak while negative values are characterized by a flat distribution. Both skewness and kurtosis are 0 in a normal distribution. Kurtosis values are used as a measure of flatness of the distribution. Heavier tailed distributions have larger kurtosis measures. The normal distribution has a kurtosis of 3 (peakness > 3 or flatness < 3) [43]. The hypsometric skewness demonstrates the amount of headward erosion in the upper reach of a basin and a large value of kurtosis signifies erosion on both upper and lower reaches of a basin [21, 31].

3.2.3 Stream longitudinal profiles analysis

For this process the DEMs with 30 m (ASTER GDEM), 10 m (extracted from topography map) and 5 m (extracted from aerial photos) were used. Stream longitudinal profiles are useful tools to evaluate the change of stream topography. These profiles show the elevation over the downstream distance [50]. In this study we calculated with TecDEM the longitudinal profiles or channel slopes and the related catchment areas from the DEMs. Moreover, we determined the concavity (θ) and the steepness indices (*ks*). The relation between steepness and concavity index is expressed by Eq. 4:

$S = k_s A^{-\theta}$ Equation (4)

Where S is channel slope, A is the upstream drainage area, θ is the concavity and *ks* is the steepness. Stream longitudinal profiles of 8 channels in the MZJ basin were extracted by TecDEM. For this analysis, the DEM was hydrologically corrected to eliminating sinks using the algorithm proposed by Planchon and Darboux (2001) [47]. In the next step the DEMs were imported to the TecDEM toolbox running with MATLAB 2012. We generated the stream network and the tectonic process following Shahzad & Gloaguen [57] [see also: 17, 57].

The concavity of the longitudinal profile of rivers is a general landscape feature [60]. The local slope of a river is mainly depending on its discharge, width and substrates grain size distribution [12]. Some studies show that θ is relatively sensitive to tectonics or climate conditions, and that k_s is correlating with the rate of rock uplift [61; 69]. For this analysis the longitudinal profiles and catchment areas were generated from the three DEMs (30 m, 10 m and 5m resolution).

In the last step we use a semi-automatic approach in TecDEM to identify the knickpoints along the longitudinal profiles of the 8 selected tributaries extracted from the DEM. The TecDEM automatically calculates the concavity and steepness factor for each of the detected knickpoints. Knickpoints reflect different environments and processes along the stream or river network and are often caused by previous erosion or variances in lithology or tectonic activity. The rate of knickpoint migration is often used as an alternative measure for the required time to return to a new balance after tectonic changes [30] with the related erosion transport and deposition processes [54] Although the rate of knickpoint migration is depending on the lithology and the climate generally knickpoint migration rates vary between 0.001 and 0.1 m y^{-1} [e.g. 66].

3.3 The role of active tectonics on gully erosion

Gully erosion is one of the dominant types of water erosion primarily in arid and semi- arid areas in large parts of Iran, but especially in the southwest of Iran [38, 63, 73]. Gully erosion is an important source of sediments that are effectively conducted to the channel network. Gully systems destroy vast agricultural areas in southwestern Iran. Particularly in the MZJ basin gully erosion processes are the predominant type of water erosion especially in the plain areas in the south and southwest of the catchment [74]. Although there are a lot of factors driving gully erosion such as land use change, climate change, high soil erodibility and specific topographic conditions, the role of tectonics, even though an obvious driver in the geomorphology of the ZM, have widely been neglected. In the MZJ basin uplift processes may be responsible for the changing base levels of the mayor tributaries. Hence, we assessed the spatial distribution of gully erosion features in relation to uplift and fault processes especially in the alluvial flat areas of the basin. The spatial distribution of gully systems in the MZJ basin was mapped according to SPOT 5 satellite data with 2.5 m resolution, aerial geomorphometric (1.20.000; Iranian National Survey Mapping 2006) and a field survey in 2013/14. Finally, we overlay the spatial distribution of gully locations with the results of the tectonic analysis in terms of knickpoint locations and potential fault lines to reveal spatial correlations.

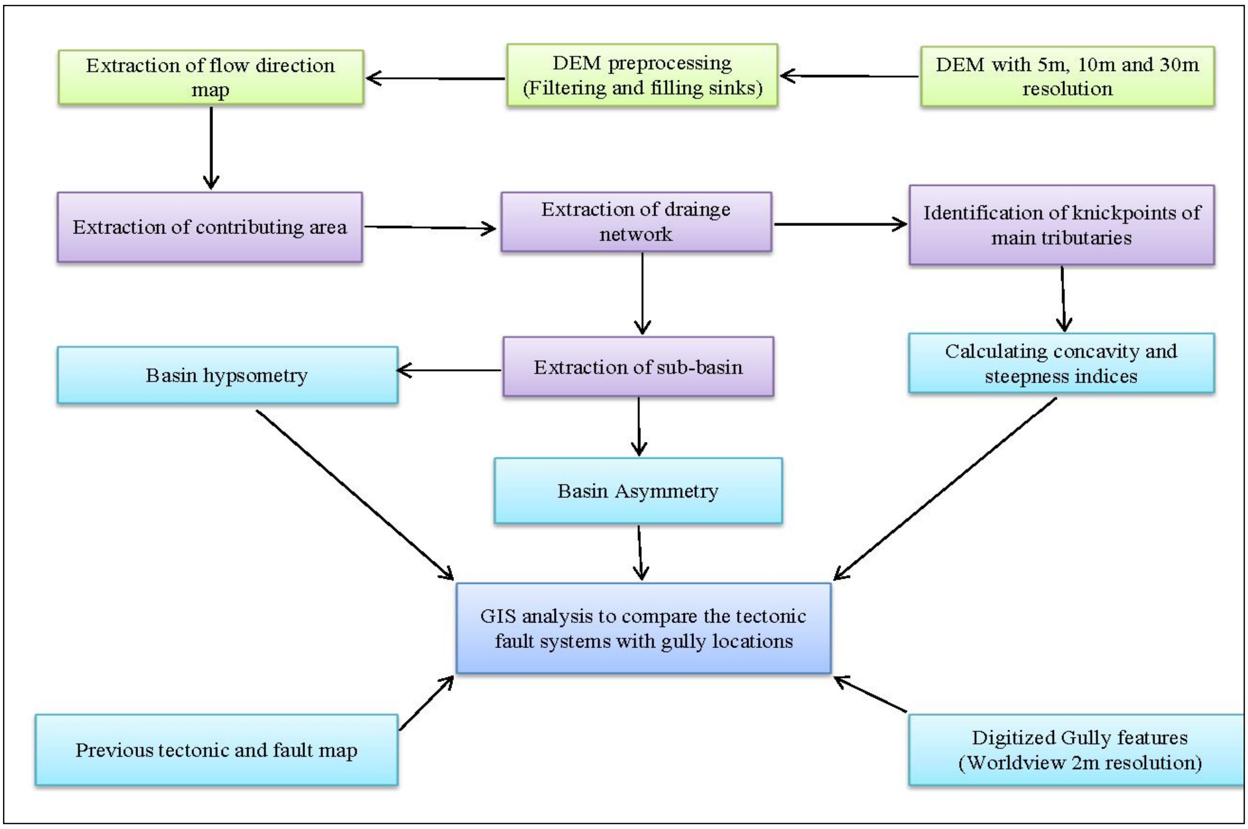

Fig. 4: Flow chart showing the applied analysis steps to assess the relation between tectonics and gully erosion processes

12

4. Results

We calculated the basin asymmetry for the eight 4th order subcatchments and one 5th order catchment as shown in Figure 5. The calculated AF values indicate a moderate to strong asymmetry of the subbasin as shown in Table 1 and Figure 5. The values of *AF* vary from 10.34 for the 5th order basin (subbasin 9) over 10.43 a moderately or gently asymmetric 4th order basin in the Northeast (subbasins 8) to 19.60 indicating a strong asymmetry in the West (subbasin 1). Strong asymmetries are also reported for subcatchments 5, 6 and 7. Consequently, strong tectonic activity can be supposed especially in the Southern and western parts of the catchment. The basin asymmetries also yield information about the prevailing direction of tilting. As shown in Figure 5 the tilting directions point towards the south in the Western, central and southern parts and into northern directions in the East and central western parts of the of the study area. This is in line with the geological surveys conducted in the area and reported in the geological maps.

Tab. 1: Asymmetry factor (AF) of sub-basin in the study area

Basin No.	Area(ha)	AF	Class of AF
1	20.54	19.6	strongly asymmetric
2	31.26	11.90	moderately asymmetric
3	21.09	10.91	moderately asymmetric
4	23.93	12.50	moderately asymmetric
5	26.54	18.01	strongly asymmetric
6	19.49	15.46	strongly asymmetric
7	53.7	17.96	strongly asymmetric
8	18.2	10.43	moderately asymmetric
9	49.10	10.34	moderately asymmetric

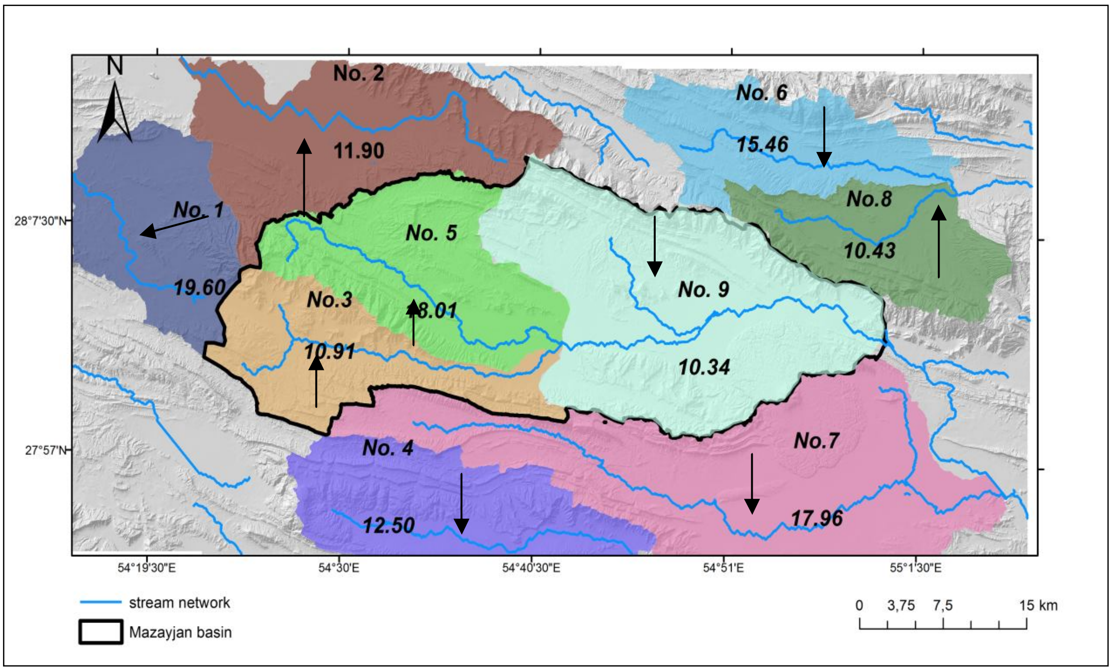

Fig. 5: Tilt direction according to the basin asymmetry analysis for 4th/5th order streams and the related asymmetry factors. Black outline indicates the MZJ catchment used for specific stream longitudinal profile analysis.

Apart of the basin asymmetry, we calculated also the basin hypsometric indices as illustrated in Table 2 and Figure 6. The HI for the south and south western parts of the catchment is almost 0.60 indicating an active phase of soil erosion while in the North the values are lower than 0.30 pointing to a Monadnock phase in landscape evolution (see Tab. 2). In this study the skewness varied from 0.47 to 2.48 while the kurtosis varied from 3.00 to 12.32. The higher values are related to the sub-catchments in the South and southwestern parts of the study area while the low values occur in the northern parts. However, kurtosis and skewness indicate subcatchments with prevailing erosion processes in both upper and lower parts of the subcatchments. Figure 6 and Table 2 show the hypsometric indices for all sub-catchments indicating a general differentiation between North, South and Southwest of the catchment. For example in the basin No. 3, in the Southwest of the study area, the hypsometric graph shows a convex shape (young stage) while the sub-basin No. 6 and 8 in the North and West of this catchment shows a concave shape (mature stage). The kurtosis values indicate generally strong erosion process dynamics in all sub-catchments but especially in sub-catchment 1 and 7. Values of the skewness index are ranging between 0.61 and 2.48. This parameter shows positive value in the entire study area. The highest value of this index is shown for the sub-catchments 1 and 7 and the lowest value for the sub-catchment 2 (Fig. 6 and Tab. 2). In other words the value of this index show high tectonic activity especially in the Southern and southwestern parts of the study area.

Tab. 2: Hypsometric parameters for the sub-catchments of the study area (4th order catchments)

Basin No.	Hi	Skewness	Kurtosis	Profile shape
1	0.59	2.32	10.58	Convex
2	0.12	0.99	3.00	Concave
3	0.05	1.39	4.77	Concave
4	0.59	0.61	3.51	Convex
5	0.59	0.61	3.51	Convex
6	0.66	1.29	5.36	Concave
7	0.78	2.48	12.32	Convex
8	0.16	0.94	3.45	Concave

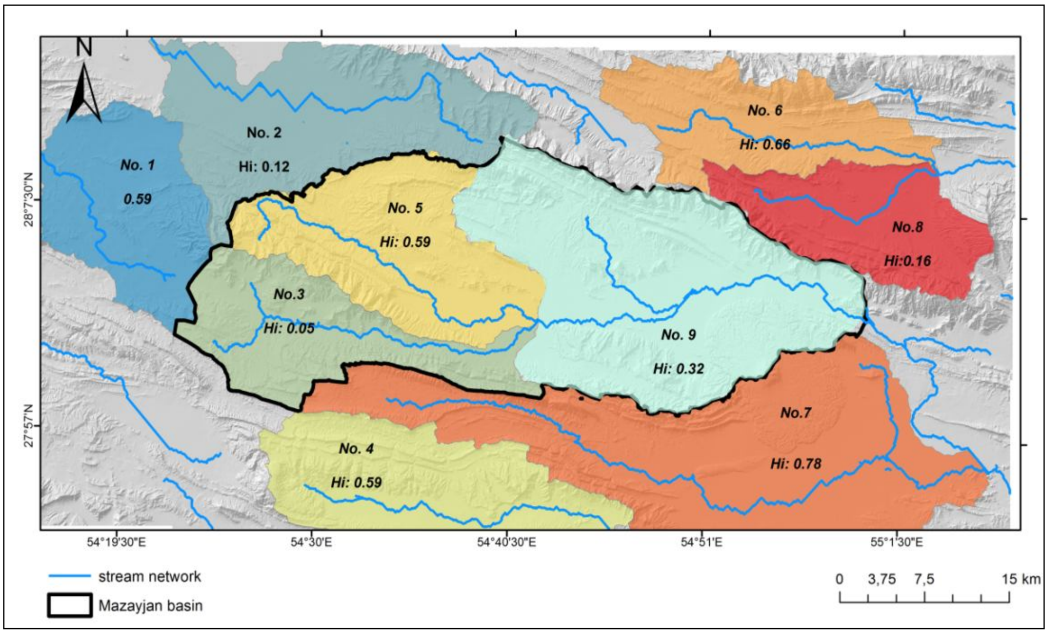

Fig. 6: Hypsometry index (HI) for the eight 4th order basins and one 5th order basin (No.9). Black outline is indicating the MZbasin used for the detailed analysis stream longitudnal profiles

The hypsometric curves of the eight 4th order basin, illustrated in Figure 7, indicate juvenile evolutionary stages of the basins No 1, No. 5 and No. 7. The basins of tributaries No. 2, No. 4 and No. 6 are seem to be in stage between juvenile and mature (see Fig 7). Tributaries No. 3 and No. 8 show a mature to Monadnock stage of evolution.

15

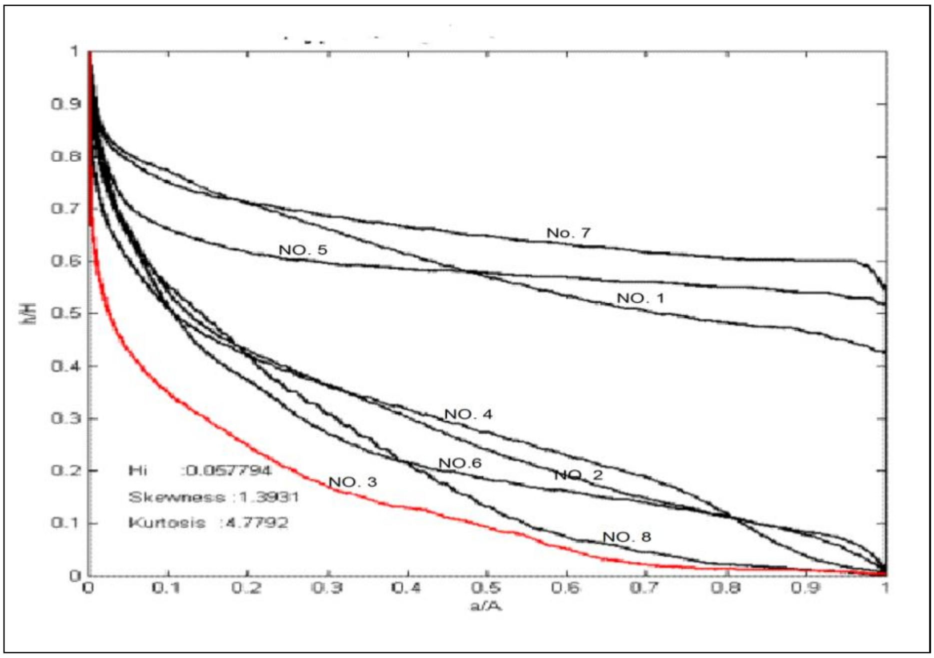

Fig. 7: Hypsometric curves for the 4th order catchments (H = maximum elevation difference of the basin; h = height of a given point in the basin; A = total area of the basin; a = surface area within basin above h).

However, especially the juvenile 4th order subcatchment No. 5 is related to the occurrence of gully systems that are further spreading into the 5th order catchment No.9. Hence, in the following we concentrate especially on these high dynamic young subcatchments No. 9 and No. 5. We analyze the longitudinal profiles in detail and particularly assess the knickpoints along these longitudinal profiles.

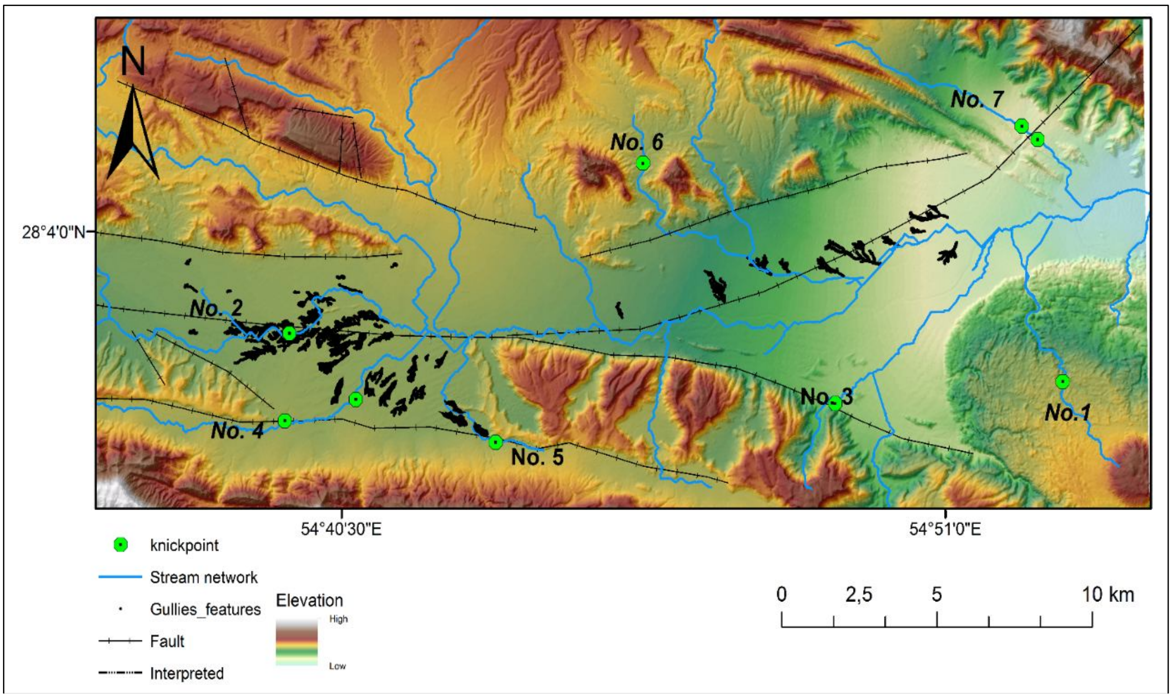

Fig. 8: Analyzed 4th order streams (No. I-VII) and the related knickpoints (green dots). Black lines illustrate fault systems. Black dots show the existing gully systems.

Even though, there are many other parameters like topography and soil characteristics triggering gully erosion processes in the MZJ basin [34, 74] it seems that there is a close relation to the fault systems and hence tectonic processes especially in the west and southwest of the Mazayjan basin. In order to assess this relation we investigate in detail the longitudinal profiles of seven tributaries within the MZJ catchment as illustrated in Figure 8. Particularly we focus on the tributaries draining the gully areas. The investigated tributaries are reported with roman numbers in Figure 8.

Figure 8 shows the location of the digitized gully systems and the fault locations derived from the geological map. According to the field survey, aerial photography and satellite images, the MZJ basin is heavily affected by gully erosion especially in the South, southwest and in some part of the Northern study area. However, Figure 8 reveals that gully erosion features are located in the direct vicinity of the fault lines and mainly within the lower parts of the MZJ catchment in alluvial Quaternary deposits.

Longitudinal profiles of the 7 tributaries of the MZJ catchment were extracted with concavity and steepness indices (Fig 9/10). The concavity and steepness indices for each segment of the profiles are illustrated in log area - log slope plots. In this study we utilized a normalized steepness (θ = 0.45) as suggested by Schoenbohm et al. (2004) [53] to compare the concavity indices.

However, the analysis showed that the DEM with 10 m resolution from the topographical map (1:25000) and the 30 m ASTER GDEM do not have a proper quality due to artifacts and errors and hence, tectonic processes cannot be assessed adequately. Especially, the flat valley bottom areas are not represented well with these DEMs due to terrace effects (contour line interpolation) or noise (ASTER GDEM). Consequently, the extraction of stream profiles and knickpoints was only conducted with the 5m stereo-aerial photography based DEM. Fig. 9 is showing the effects of the low quality DEMs on the longitudinal profile analysis.

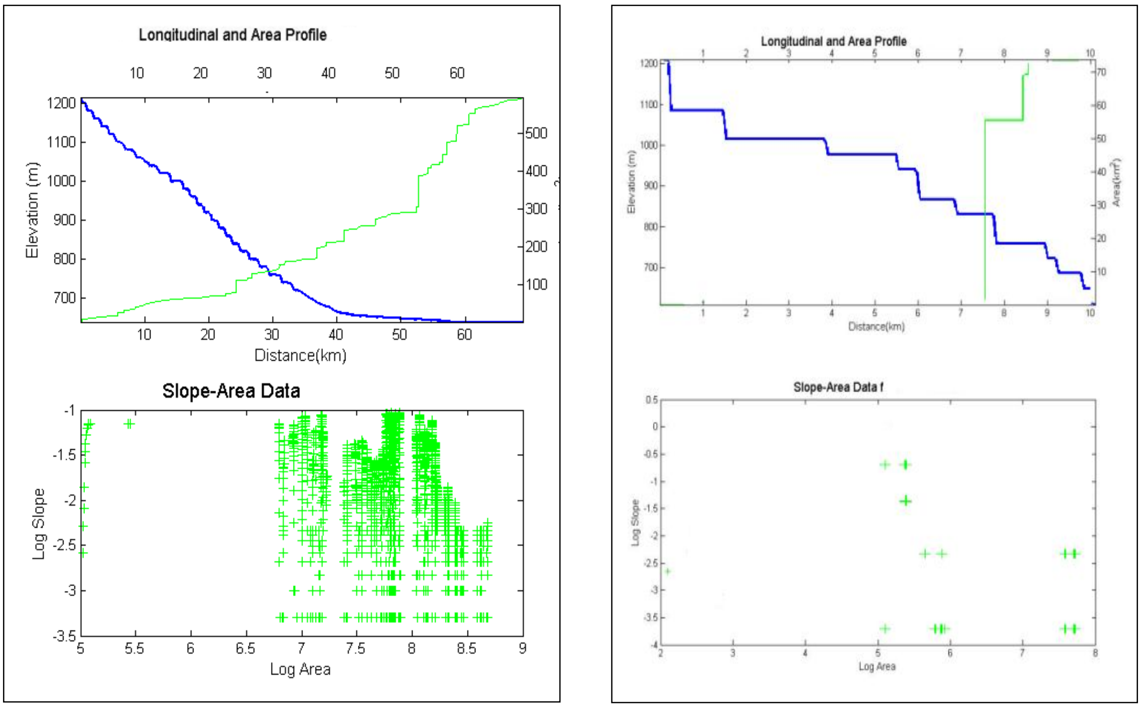

Fig 9: Example of the low quality DEM effects on the stream profile analysis (Left: 30m ASTER GDEM Right: 10m topographic map based DEM; upper part: Longitudinal profile and cumulative catchment area, Bottom: Log area- log slope data),

Figure 10 shows different profiles and knickpoints position for the 7 selected tributaries in the MZJ catchment study area. According to these diagrams we identified different trends of concavity and convexity in elevation- distance profile (top) as well as the concave trends in the log area - log slope graph (bottom). According to Figure 10 for example in longitudinal profile No. III there is a concave and convex trend. The convex section starts around 3.5 km below the initiation of the stream. Therefore, we compared this profile with the tectonic map of the study area showing uplift in this section. Since the geology and tectonics are very important as indicator for the knickpoint location and migration. The geological map (1:

25.000) was overlapped to reveal if knickpoints are related to changes in the lithology or related to faulting effects. Generally, the geologic map indicates homogenous alluvial sediments in the plain areas predominantly characterized by gully erosion features. Figure 8 reveals that knickpoints are identified for all seven profiles. Profiles Nos. IV and VII are characterized by two knickpoints. The knickpoints of the profile II and IV are directly related to gully areas. Moreover, the geological map shows that these areas are quite homogeneous and belonging to alluvial deposits. Hence knickpoints seem to be influenced by tectonics and not by lithology. The other catchments also show knickpoints related to fault lines such as III, V and VII but these are not clearly related to gully systems and characterized by other formations. Profile No. I and VI show no clear connection to fault lines. However, the knickpoints are closely related to fault lines and hence it seems that the knickpoints did not retreat much except profile No II where a head ward movement seem to be very likely.

Tab. 3 Steepness and concavity

Stream No.	Concavity (θ)	Steepness (k_s)
I	0.42	14.75
II	0.69	18.16
III	1.18	22.77
IV	2.52	13.83
V	1.10	7.64
VI	3.01	32.09
VII	0.41	27.31
Mean	1.48±0.40	18.207±1. 8

Table 3 shows the concavity (θ) and steepness indices for the selected stream profiles. Generally, concavity is relatively sensitive to tectonics or climate conditions, and steepness (k_s) is correlating with the rate of rock uplift (61; 69). Since the climate throughout the MZJ catchment is quite homogeneous the concavity index mainly points to tectonic activity. The highest concavity values are 3.01 for stream profile No.VI and 2.52 for stream profile No VI. Both catchments are characterized by gully systems in the lower parts and two mayor fault lines, while the lowest concavity values are reported with 0.42 for stream profile No. I draining the salt dome and 0.41 for catchment No VII draining the northeastern parts of the MZJ basin.

The highest values for the steepness index are 32.09 at profile No V and 7.64 respectively for profile No. VI (Tab. 3). The steepness is higher than 14 in all profiles except profile No V. According to these result most drainage systems in the MZJ catchment indicate high uplift rates. However, the high steepness and concavity values in the South, Southwest and central part of the MZJ basin point to higher tectonic deformations in this part of the study area. While the Eastern tributaries Nos. I and VII show less tectonic influence.

Since the climatic conditions are almost similar throughout the MZJ catchment the differences can be attributed to lithological or tectonic factors.

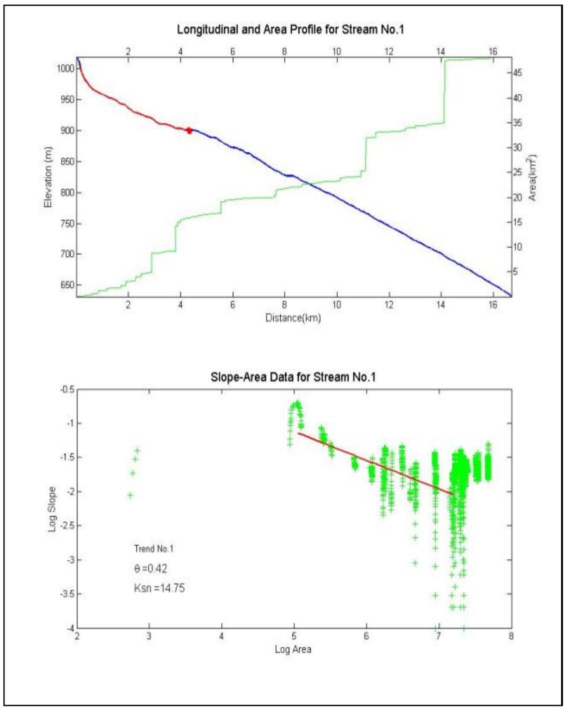

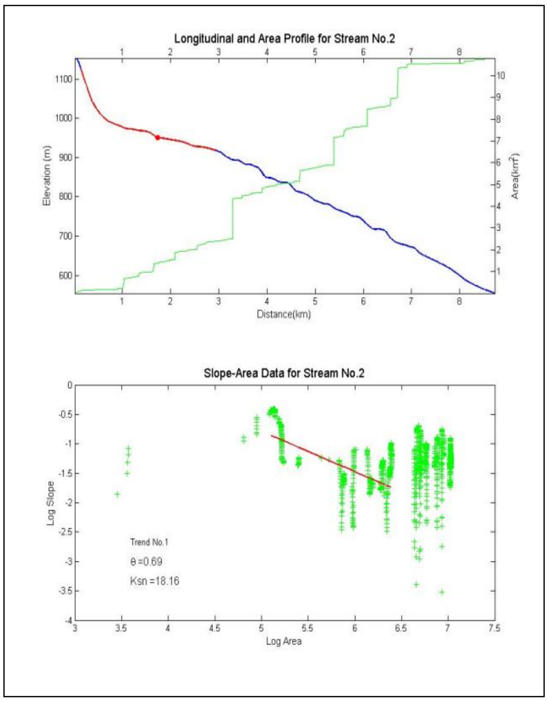

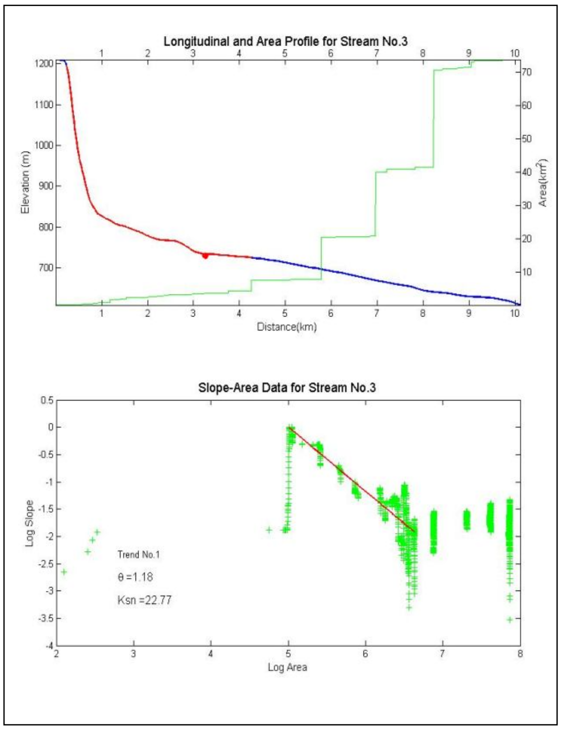

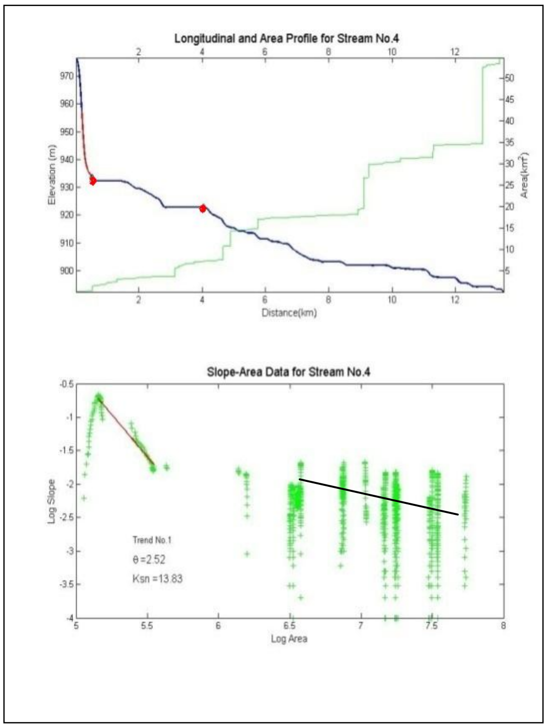

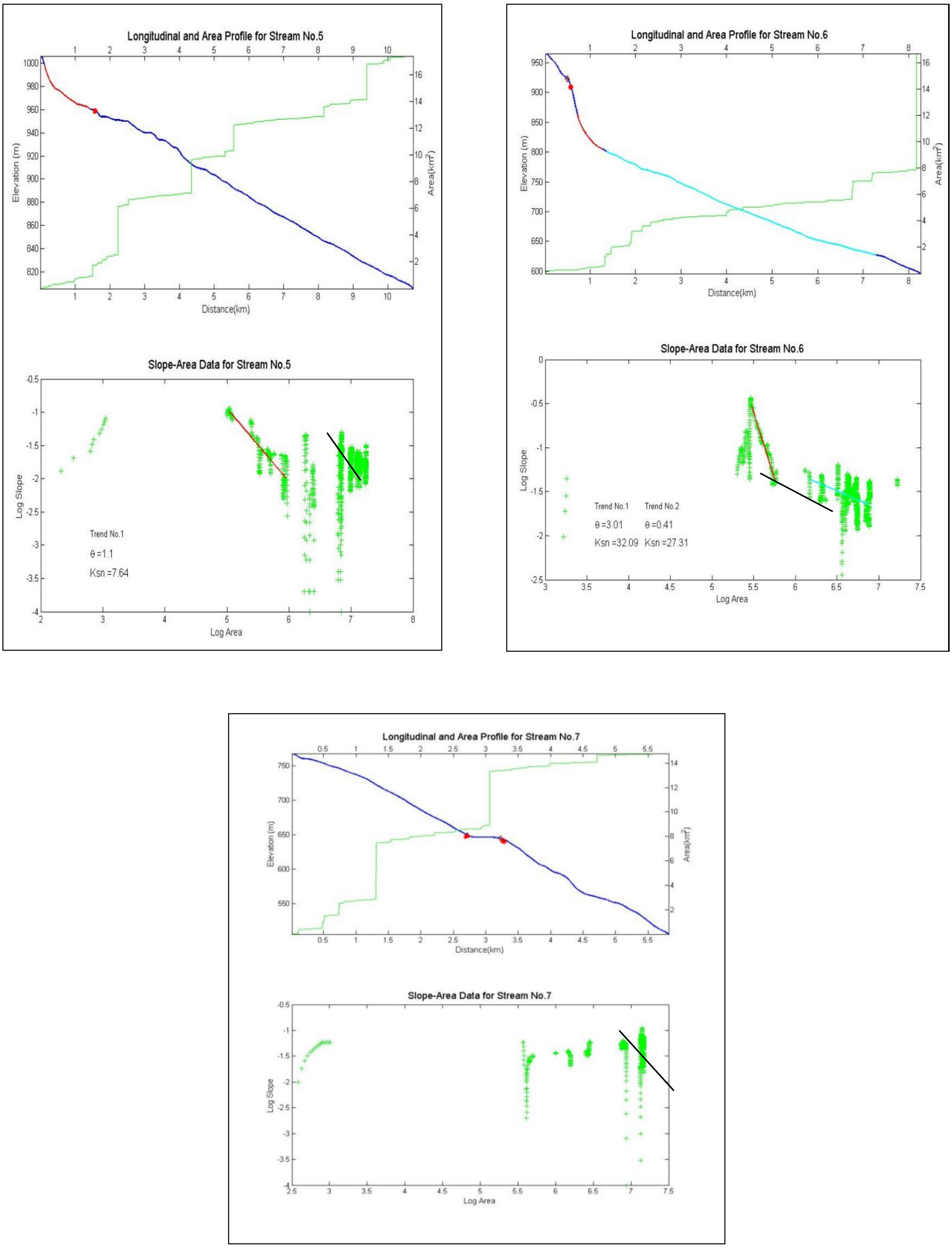

Fig. 10: Stream profile analysis (Top: Longitudinal profile and cumulative catchment area, Bottom: Log area-log slope data) and knick points as red points.

5. Discussion

In this investigation we tested different DEMs in order to assess the morphotectonics of the MZJ catchment. We have shown that DEMs with errors and artefacts or low spatial resolution like the ASTER GDEM or the one created from the 1: 25000 scale contour lines are not suitable for our analysis. Especially in the low land areas these DEMs are not sensitive enough to get proper results to prove tectonic activities related to small changes in elevation. Particularly the ASER GDEM showed a lot of noise and terrace effects on the entire selected tributaries streams. It seems that the artefacts are due to interpolation errors and/ or the sensing techniques. Especially the optical sensors like ASTER produce noise effects due to the fact that the vegetation like bushed and shrubs are included in the DEM. Hence, we utilized in the further analysis only the highest resolution DEM with 5 m based on aerial photographs. Even though it is also based on optical data the spatial resolution is higher and hence vegetation effects are more restricted and thus, less influencing.

The analysis of basin asymmetry and hypsometry that was performed on a wider area of the ZM around the MZJ basin illustrates the prevailing direction of tilting. As shown in Figure 5 the tilting directions point towards the South in the Western, central and southern parts and into northern directions in the East and central western parts of the of the study area. This is in line with the geological surveys conducted in the area and reported in the geological maps and hence reveal the high tectonic activity in the entire area. The basin hypsometry analysis indicate an active phase of soil erosion especially in the South and South western parts of the catchment while in the north the values point to a Monadnock phase in landscape evolution. The kurtosis values specify generally strong erosion process dynamics in all sub-catchments but especially in sub-catchment 1 and 7. Generally kurtosis and skewness indicate high tectonic activity especially in the southern and southwestern parts of the larger Zagros Mountain study area.

However, having a look at the smaller 4th order tributaries of the MZJ basin, mainly consisting of catchments No 5 and 9, it was shown that the active and dynamic process in the MZJ basin have affected the stream network and also the sub-catchment areas. Especially we reveal the role of active tectonics on the spatial distribution of gully systems for longitudinal profiles No II and IV. Comparing the fault lines and gullies location in the catchment it was shown that more knickpoints are approximately near to fault lines in the Southwest and North-east of the catchment. Since the climatic conditions do not changed much and also the geology of the valley bottom areas are quite homogeneous it seems that the tectonic processes control the watershed dynamic in terms of knickpoint development and migration. The convexity and concavity of the hypsometric curves can be used as a powerful tool for the assessment of the erosional phase of each sub-catchment. With the steepness and concavity index we identified areas with high erosion dynamics. The hypsometry curve index seems to be a useful tool to determine active tectonic dynamics especially in the West and South of the study area.

Tectonic activities may be driver or amplifier of processes like land sliding, and gully erosion [8, 10]. Although many researchers around the world and specifically in Iran have focused on the role of anthropogenic and climatic effects on soil erosion and especially gully erosion [6, 34, 38, 39, 40] there are only a few or no investigations revealing the role of tectonics as a driver for gully erosion. In recent years especially soil erosion processes are intensified due to various reasons causing severe problems for inhabitants coming along with serious damages to agriculture and range land particularly in the South and Southwest of Iran. As we show, the erosion processes may also be amplified by the high tectonic activity in these areas. Since knickpoint migrations seem to be very slow the activities can be considered as neotectonic origin.

6. Conclusions

In this study a morphotectonic analysis of the MZJ basin in southwestern Iran was carried out using a high resolution DEM (5 m) based on stereo aerial photography. The lower resolution DEMs such as ASTER GDEM (30 m) and the one based on the topographic map 1:25.000 (10m) do not show a proper quality to perform small scale tectonic analysis. Consequently, the best results of the morphotectonic analysis were achieved by the 5m stereo aerial photograph DEM. The analysis was finally carried out based on automated tools and software like TecDEM, Agisoft and GIS analysis.

The obtained results on the basin asymmetry and hypsometry, the morphology of the stream longitudinal profiles and the field survey suggest that active tectonics is an important factor for gully evolution. Fault lines and knickpoints are clearly related to areas with high gully density. Especially the lower alluvial flood plains seem to be affected as shown for the profile No II and IV. However, due to the fact that these areas are characterized by very small elevation differences only the highest DEM resolution of 5m was able to detect these features.

Our study illustrates that there is a clear spatial correlation between tectonic activity in terms of fault lines and knickpoints and gully erosion features. As we show, the erosion processes may also be also amplified by the high tectonic activity in these areas. Since knickpoints migrations seem to be very slow the activities can be considered as neotectonic origin.

References

[1] Ahnert, F., Einführung in die Geomorphologie, Stuttgart (1996).

[2] Afghah, M., Yaghmour S., Biostratigraphy Study of Tarbur Formation (Upper Cretaceous) in Tang-E Kushk and East of Sarvestan (SW of Iran). Journal of Earth Science, 25, 263–274 (2014).

[3] Alipoor, R., Poorkermani, M., Zare M., Hamdouni, R.E., Active tectonic assessment around Rudbar Lorestan dam site, High Zagros Belt (SW of Iran). Geomorphology 128, 1–14 (2011).

[4] Azor, A., Keller, E.A., Yeats, R.S., Geomorphic indicators of active fold growth: South Mountain-Oak Ridge anticline, Ventura basin, southern California. Geological Society of America Bulletin, 114(6), 745-753 (2002).

[5] Bachmanov, DM., Trifonov, VG., Hessami, KhT., Kozhurin, AI., Ivanova, TP., Rogozhin et al., Active faults in the Zagros and central Iran. Tectonophy, 380 (3-4), 221-241 (2004).

[6] Berberian, M., & King, G C P., Toward a Palaeogeography and Tectonic Evolution of Iran. Can. Jour. Earth Sci., 18 (1981).

[7] Burbank, D., Anderson, R., 2009. Tectonic Geomorphology,Wiley (2009).

[8] Burke, K., Dessauvagie, T. E., Whiteman, A., Opening of the Gulf of Guinea and geological history of the Benue depression and Niger Delta. Nature, Phys. Sci. 233, 51-55 (1971).

[9] Codilean, A.T., Bishop P., & Hoey, T.B., 2006. Surface process models and the links between tectonics and topography. Progress in Physical Geography, 30(3), 307-333 (2006).

[10] Costa, J. E., & Baker, V. R.,. Surficial geology, building with the Earth. New York, John Wiley and Sons, 498 (1981).

[11] Dehbozorgi, M., Pourkermani, M., Arian M., Matkan, A., Motamedi, H., Hosseiniasl, A., Quantitative analysis of relative tectonic activity in the Sarvestan area, central Zagros, Iran. Geomorphology, 121, 329-341 (2010).

[12] Devauchelle, O., Petroff, A., Lobkovsky, A. E., Rothman D. H., Longitudinal profile of channels cut by springs. J. Fluid Mech, 667, 38–47 (2011).

[13] Egboka, B. C., Nwankwor, G. I., Hydrogeological and geotechnical parameters as agents for gully-type erosion in the Rain-Forest Belt of Nigeria, J. African Earth Sci. 3, 417-25 (1985).

[14] Egboka, BCE., Nwakwor ,GI., Orajaka, IP ., Implications of palæo- and neotectonics in gully erosion-prone areas of southeastern nigeria. Natural Hazards, 3(3), 219-231 (1990).

[15] Ezezika, O., Adetona, O., Resolving the gully erosion problem in Southeastern Nigeria: Innovation through public awareness and community-based approaches. Journal of Soil Science and Environmental Management, 2(10), 286-291 (2011).

[16] Falcon, N L. An outline of the geology of the Iranian Makran. Geogr. Jour, 140 (2), 284-291 (1974).

[17] Flores E., Quénéhervé G., Bachofer F., Shahzad, F., Maerker M., Morphotectonic Interpretation of the Makuyuni Catchment in Northern Tanzania using DEM and SAR Data. Geomorphology, 248, 427–439 (2015).
[18] Gilbert, G.K., Report on the Geology of the Henry Mountains (INTRO ONLY) US Geographical and Geological Survey of the Rocky Mountain Region, Department of the Interior, 1-17(1877).
[19] Grove, A. T., Soil erosion and population problems in South-east Nigeria. Geogr. J. 117, 191-306 (1951).
[20] Goudie, A., Encyclopedia of Geomorphology. Taylor & Francis (2013).
[21] Harlin, J. M., Geology and geomorphology of the southern plains research watershed. Okla, Geol. Notes, 42, 168-178 (1982).
[22] Hessami, K., Nilforoushan F., Talbot C J., Active deformation within the Zagros Mountains deduced from GPS measurements. Journal of the Geological Society, London, 163, 143–148 (2006)
[23] Hengl, T., David G., Rossiter, T., Supervised landform classifi- cation to enhance and replace photo-interpretation in semidetailed soil survey. Soil Sci Soc Am J, 67, 1810–182 (2003).
[24] Huang, X.J., Niemann, J.D., Modelling the potential impacts of ground water hydrology on long-term drainage basin evolution. Earth Surface Processes and Landforms, 31, 1802–1823 (2006).
[25] Jayappa, K. S., Markose, V.J., Nagaraju, M., Identification of geomorphic signatures of neotectonic activity using DEM in the precambrian terrain of western Ghats, India, International Archives of the Photogrammetry, Remote Sensing and Spatial Information Sciences, Melbourne, Australia. Int. Arch. Photogramm, Remote Sens, Spatial Inf. Sci, 215-220 (2012).
[26] Keller, EA., Pinter, N., Active Tectonics: Earthquakes, Uplift and Landscape. Prentice Hall, New Jersey, 362 (2002).
[27] Kirby, E., & Whipple, K., Quantifying differential rock-uplift rates via stream profile analysis. Geology, 29(5), 415-418 (2001).
[28] Kirby, E., Whipple, K. X., Expression of active tectonics in erosional landscapes. J. Struct. Geol. 44, 54–75 (2012).
[29] Kothyari, G., Pant, P. D., Luirei, K., Landslides and Neotectonic Activities in the Main Boundary Thrust (MBT) Zone: Southeastern Kumaun, Uttarakhand. Journal Geological Society of India, 80, 101-110 (2012).
[30] Loget, N., Van Den Driessche, J., Wave train model for knickpoint migration, Geomorphology 106, 376–382 (2009).
[31] Luo, W., Quantifying groundwater-sapping landforms with a hypsometric technique. Journal of Geophysical Research: Planets, 105(E1), 1685-1694 (2000).
[32] Maaoui, M.A., Felfoul, M.S., Boussema, M.R., Snane, M.H., Sediment yield from irregularly shaped gullies located on the Fortuna lithologic formation in semi-arid area of Tunisia. Catena, 93, 97–104 (2012)
[33] Maerker M., Quénéhervé G., Bachofer F., Mori, S., A simple DEM assessment procedure for gully system analysis in the Lake Manyara area, northern Tanzania. Nat Hazards, 79(1), 235-253 (2015).
[34] Masoudi, M., & Zakerinejad, R., Hazard assessment of desertification using MEDALUS model in Mazayjan plain, Fars province, Iran. Ecology, Environment and Conservation Journal, 16 (3), 425-430 (2010).
[35] Markose, V., & Jayapp, K.S., Hypsometric analysis of Kali River Basin, Karnataka, India, using geographic information system. Geocarto International, 26 (7), 553–568 (2011).
[36] Miliaresis, G., Extraction of Bajadas from digital elevation models and satellite imagery. Comput. Geosci, 27, 1157-1167 (2001).

[37] Montgomery, D.R., Brandon, M., Topographic controls on erosion rates in tectonically active mountain ranges. Earth and Planetary Science Letters 201, 481-489 (2002).
[38] Nazari, S.A., Ahmadi H., Mohammadi, A., Ghoddousi, J., Salajegheh, A., Boggs., et al., Factors Controlling Gully Advancement and Models Evaluation (Hableh Rood Basin, Iran). WaterResource Management, 24, 1531-1549 (2011).
[39] Nwajide, S.C., Hoque, M., Gullying processes in south-eastern Nigeria. The Nigerian Field Journal. 44(2), 64-74 (1979).
[40] Ofomata, G. E. K., Soil erosion in the Enugu Region of Nigeria, African Soils 9, 289-319. (1965).
[41] Okereke, C. N., Onu N.N., Akaolisa, C.Z., Ikoro, D.O., Ibeneme, S.I., Ubechu, B., et al., Mapping Gully Erosion Using Remote Sensing Technique: A Case Study of Okigwe Area, Southeastern Nigeria, International Journal of Engineering Research and Applications. 2(3), 1955-1967 (2012).
[43] Pérez-Peña, J.V., Azañón, J.M., Azor, A., An ArcGIS extension to calculate hypsometric curves and their statistical moments. Applications to drainage basin analysis in SE Spain. Computers & Geosciences, 35(6), 1214-1223 (2009).
[45] Pérez-Peña, J.V., Azor, A., Azañón, J.M., Keller, E. A., Active tectonics in the Sierra Nevada (Betic Cordillera, SE Spain): Insights from geomorphic indexes and drainage pattern analysis. Geomorphology 119: 74–87 (2010).
[44] Pelletier, J., Rasmussen, C., Geomorphically based predictive mapping of soil thickness in upland watersheds, Water Resour. Res., 45, W09417, doi:10.1029/2008WR007319 (2009).
[46] Pirasteh S., Pradhan B., Rizvi S. M., Tectonic process analysis in Zagros Mountain with the aid of drainage networks and topography maps dated 1950–2001 in GIS. Arab J Geosci, 4(1-2), 171-180 (2009).
[47] Planchon, O., Darboux, F., A fast, simple and versatile algorithm to fill the depressions of digital elevation models, Catena 46Ž2001, 159–176 (2001).
[48] Poesen, J., Nachtergaele J., Verstraeten, G., Valentin, C., Gully erosion and environmental change: Importance and research needs. Catena, 50, 91–133 (2003).
[49] Pradhan, B., Singh, RP., Buchroithner, MF., Estimation of stress and its use in evaluation of landslide Prone Regions using remote sensing data. Adv Space Res 37, 698–709 (2006).
[50] Rãdoane doane, M., Nicolae, Rãdoane., Dan, Dumitriu., Geomorphological evolution of longitudinal river profilesin the Carpathians. Geomorphology 50, 293–306 (2003).
[51] Rangzan, K., Iqbaluddin., Morpho-Tectonic Study of Zagros Structural Belt of SW Iran Using Remote Sensing Techniques. Journal of the Indian Society of Remote Sensing, 23(4), 211-224 (1995).
[52] Ruszkiczay-Rudiger, Z., Fodor, L., Horváth, E., Telbisz, T., Discrimination of fluvial, eolian and neotectonic features in a low hilly landscape: A DEM-based morphotectonic analysis in the Central Pannonian Basin, Hungary: Geomorphology, 104, 203-217 (2009).
[53] Schoenbohm, L.M., Whipple, K.X., Burchfiel, B.C., Chen, L., Geomorphic constraints on surface uplift, exhumation, and plateau growth in the Red River region, Yunnan Province, China. Geological Society of America Bulletin, 116 (7-8), 895-909 (2004).
[54] Selander, J.A., Processes of knickpoint propagation and bedrock incision in the Oregon Coast Range. University of Oregon, B.S. thesis, Eugene, Oregon (2004).

[55] Shahzad, F., Gloaguen, R., TecDEM: A MATLAB based toolbox for tectonic geomorphology, Part 1: Drainage network pre-processing and stream profile analysis. Computers & Geosciences, 37(2), 250-260(2011a).
[56] Sharma, A., Tiwari K. N., Bhadoria, P. B. S., Determining the optimum cell size of digital elevation model for hydrologic application, J. Earth Syst. Sci. 120(4), 573–582 (2011).
[57] Shahzad F., Gloaguen, R., TecDEM: A MATLAB based toolbox for tectonic geomorphology, Part 2: Surface dynamics and basin analysis. Computers & Geosciences, 37(2), 261-271 (2011b).
[58] Sidorchuk, A., Maerker, M., Moretti, S., Rodolfi G., Gully erosion modelling and landscape response in the Mbuluzi River catchment of Swaziland. Catena, 50, 507-525 (2002).
[59] Singh, O., Sarangi A., Sharma, M.C., Hypsometric integral estimation methodsand its relevance on erosion status of North-Western lesser Himalayan watersheds. Water Resource Management, 22, 1545–1560 (2008)
[60] Sinha, S. K. & Parker, G., Causes of concavity in longitudinal profiles of rivers. Water Resources Research 32 (5), 1417-1428 (1996).
[61] Snyder, N.P., Whipple, K.X., Tucker, G.E., Merritts D.J., Landscape response to tectonic forcing: Digital elevation model analysis of stream profiles in the Mendocino triple junction region, northern California. Geological Society of America Bulletin, 112, no. 8, 1250-1263 (2000).
[62] Strahler, A.N., Hypsometric (area-altitude) analysis of erosional topography. Bulletin of Geological Society of America, 63, 1117–1142 (1957).
[63] Soufi, M., The Impact of land use and Soil Characteristics on Gully Formation in an Arid Ecosystem, Southwest of I.R. Iran. Soil and Water Conservation, Climate Change and Environmental Sensitivity, 15th ISCO Congress, Budapest (2008).
[64] Tiercelin, J., Rift-basin sedimentation: responses to climate, tectonism and volcanism. Examples of the East African Rift. Journal of African Earth Sciences (and the Middle East), 10(1–2), 283-305 (1990)
[65] Toudeshki, V. H., & Arian, M., Morphotectonic Analysis in the Ghezel Ozan River Basin, NW Iran. Journal of Geography and Geology, 3(1), 1-21 (2011).
[66] Van Heijst M.W.I.M., Postma, G., Fluvial response to sea-level changes: a quantitative analogue, experimental approach. Basin Research, 13, 269-292. (2001).
[67] Vorpahl, P., Elsenbeer, H., Maerker, M., Schroeder, B., How can statistical models help to determine driving factors of landslides. Ecological Modelling, 239, 27-39 (2012).
[68] Weissel, J.K., Pratson, L.F., Malinverno, A., The length-scaling properties of topography. Journal of Geophysical Research, 99, 13997–14012 (1994).
[69] Whipple, KX., Tucker, GE., Dynamics of the stream power river incision model: implications for height limits of mountain ranges, landscape response timescales and research needs. Journal of Geophysical Research, 104, 661–17 674 (1999).
[70] Wilson, J.P., Gallant, J.C., Digital terrain analysis. In: Wilson J.P. & Gallant J.C. (Eds.), Terrain Analysis: Principles and Applications, J. Wiley, New York, 1-27 (2000).
[71] Wobus, C., Whipple, K.X., Kirby, E., Snyder, N., Johnson, J., et al., Tectonics from topography: Procedures, promise, and pitfalls. Geological Society of America Special Papers, 398, 55-74 (2006).
[72] Wynd, J. G., Biofacies of Iranian Oil Consortium Agreement Area. IOOC Report No. 1082, Tehran (unpublished) (1965).

[73] Zakerinejad, R., Maerker, M., An integrated assessment of soil erosion dynamics with special emphasis on gully erosion in the Mazayjan basin, southwestern Iran. Natural hazards. DOI: 10.1007/s11069-015-1700-3 (2015).
[74] Zakerinejad R., Maerker M., Prediction of gully erosion susceptibilities using detailed terrain analysis and maximum entropy modeling: a case study in the Mazayejan plain, southwest Iran. Geogr Fis Dinam Quat 37(1), 67–76 (2014).

Paper D

Assessment of gully erosion using multispectral remote sensing, GIS and stochastic modelling in the Southwest of the Zagros Mountains- Iran.

Current status: in review, Natural Hazards journal.

Assessment of gully erosion using multispectral remote sensing, GIS and stochastic modeling in the Southwest of the Zagros Mountains- Iran

Reza Zakerinejad[1,2,*], Adel Omarn[1,4] Volker Hochschild[1], Michael Maerker[1,3]

[1] Department of Physical Geography, University of Tübingen, Rümelinstr. 19-23, 72070Tübingen, Germany;

[2] Faculty of Desert Studies, Semnan University, Semnan, Iran

[3] Department of Earth Sciences, University of Florence, Via La Pira 4, 50121 Florence, Italy

[4] Department of Science and Mathematical Engineering, Faculty of Petroleum and Mining Engineering, Suez University, Egypt.

* Author to whom correspondence should be addressed; E-Mail: reza.zakerinejad@unibund.uni-tuebingen.de; Tel.: +4915252041457

Abstract: Soil erosion in arid and semi-arid areas in Iran is a major environmental threat. Soil erosion in form of gullies is very common especially in the South and Southwest of Iran. According to previous research in the area the influence of lithology, vegetation density, climate change as well as land use and land cover change are effective drivers for soil loss in general and gully erosion in particular. The overall objective of this research is to assess the relation between substrates, lithology and gully spatial distribution in the Mazayejan (MZJ) basin in southwest of Iran as a part of the Zagros Mountains (ZM). In this study, data was collected by field survey, aerial photo interpretation, and ASTER (Advanced Space borne Thermal Emission and Reflection Radiometer) multispectral image analysis. The spatial gully susceptibility modeling was performed with a GIS-based statistical mechanics model (Maxent) taking into account the factors most likely influencing the spatial distribution of gully erosion like proper bands ratios from the ASTER images. The results show that the multispectral analysis of the ASTER data yield valuable results in terms of mineral differentiation in the Zagros Mountain area and hence, can be utilized as a useful tool for lithological mapping. Using a statistical mechanics approach we assessed the relation between existing gully locations and the combinations of predictor variables consisting in topographic indices and ASTER band rations. The spatial prediction show that gullies have a high probability in areas with high amounts of salt, gypsum and marl especially in the plain part of the study area. The model performance showed a very high accuracy

both for train and test data. The spatial prediction shows a concentration of gully erosion in the areas of eolic sediments on top of alluvial substrates.

Keywords: Gully erosion, ASTER data, GIS, lithology

1. Introduction

Gully erosion is one of the most serious types of soil erosion and land degradation in agriculture and range land especially in the south and southwest of Iran (Wasson et al., 2002; Masoudi & Zakerinejad 2010; Shahrivar et al., 2012; Zakerinejad & Maerker 2014). This type of water erosion is aggravated by climate and socioeconomic changes. The diversity and the impact of various factors driving the formation and development of gully erosion show a high variety and thus the understanding of the most important drivers on gully initiation and further extent is an important need for land use management and soil erosion protection.

Many researchers studied the factors and mechanism that are affecting gully events and process in many parts of the world especially in arid and semi-arid areas (Ghodosi 2006; Kheir et al. 2007; Sharivar 2009; Samani et al. 2010; Zakerinejad & Maerker 2015). This type of water erosion usually is caused by several factors acting at the same time or sequentially to degrade the soil in susceptible regions. Especially areas with low vegetation and a high amount of silty soils are affected. Most gullies occur in not consolidated materials such as colluvial or alluvial, deeply weathered substrates (Conoscenti et al. 2008; Frankl et al. 2012) or eolic deposits like loess formations. Moreover, soils prone to piping and tunneling such as dispersive soils (Shahrivar et al. 2012; Valentin et al. 2005, Faulkner et al. 2003) often show gully erosion features.

Some factors such as erodibility of geological formations, terrain parameters (egg. SPI, flow accumulation, transport capacity), Neo-tectonic effects and land use/ land cover changes, as well as climate change, are considered the main drivers for gulling in many arid and semi-arid areas but in particularly in large parts of Iran (Onwuemesi 1990; Obiefuna & Adamu 2011; Zakerinejad & Marker 2014; Zakerinejad & Maerker 2015). In this area gully erosion is more developed in the pediment and flat areas and low angled slopes because they receive high volumes of runoff from upslope and often they are digging into already deposited unconsolidated material (Ahmadi 2007).

Moreover, chemical aspects such as critical values of Na^+ have negative impacts on aggregate stability. Hence, high amounts of the Sodium Absorption Ratio (SAR), electric conductivity (EC) influence gully erosion processes especially in soils of arid and semi-arid environments in Iran (Kemper & Koch 1966; Servati 2008; Shahrivar et al. 2012).

However, a comprehensive study of the role of lithologic and substrate thresholds influencing gully initiation are important to understand the spatial distribution of gully features. In this study, we will focus on the influence of the lithology and surface- substrate on gully erosion in the MZJ catchment in the southwest of Iran using a stochastic modeling approach taking into account ASTER spectral bands and band ratios as proxies for the lithological conditions. However, the role of the lithology on gullying, can only be assessed with a detailed lithological map representing an essential background information for land use planner and hence, a proper management of the susceptible area.

Available geological and lithological maps were generated by the Iranian National Petroleum Organization (INPO) with a scale of 1:100.000 in 1954 and were mainly developed to identify different formations containing oil resources (Samani et al., 2009). These maps are generated with large scales and thus, not very accurate in the details in many part of Iran. Nevertheless, there has not been generated a more detailed geological map since then. Therefore, we utilized remote sensing data to get detailed information about the lithology and especially more precise information for the gully erosion assessment. In this study we used ASTER spectral bands to derive detailed information on the litho-geological settings as many applications in arid and semi-arid area have shown (Omran et al. 2012; Matar & Bamousa 2013).

The study area conditions represent a good starting point to examine the suitability of different ASTER band ratios to map each rock unit. ASTER data are frequently used to assist in geologic mapping (see: Omran et al. 2012; Wynn et al. 2011; Matar & Bamousa 2013 & Bachofer et al. 2015). Consequently, the present study aims at proposing suitable ASTER band ratios appropriate to differentiate between different rock units in order to evaluate the correlations between gully locations and mineral contents. A further objective of the study is to estimate the potential areas for gully erosion processes, forms and features in relation to the lithology and mineral components using a statistical mechanics model that allows for a spatial prediction of the gully erosion susceptibility in the entire Mazayjan (MZJ) catchment.

2. Study Area

The study area is located in the MZJ catchment of Fars province, Southwestern Iran (54°34' to 54°44'E and 27°59' to 28°5'N; Figure 1). The area is located in the Zagros Mountains (ZM) close to Zarindasht city. The ZM belt extends for 1500 km from the Torus mountain southeast

Turkey, through southwest Iran, ending near the strait of Harmoz at the mouth of Persian Gulf.

This area is characterized by an arid climate with almost 230 mm average annual precipitation and a mean annual temperature of 16.5°C. However, field survey reveals that pediment and alluvial areas mapped as Quaternary deposits in the central part of the catchment, based on the 1:25,000 geological maps show significant more mapped gully systems. These gully systems in turn provide high amounts of sediments, which are transported into river systems or deposited in reservoirs and check dams within the catchment. The study area is characterized by very scarce vegetation. Lowest elevation is 690 m and the highest peaks of the ZM of the study area are 1969m. Most of the gully features occur on the pediment areas with low slope and alluvial sediments (Zakerinejad & Maerker 2014).

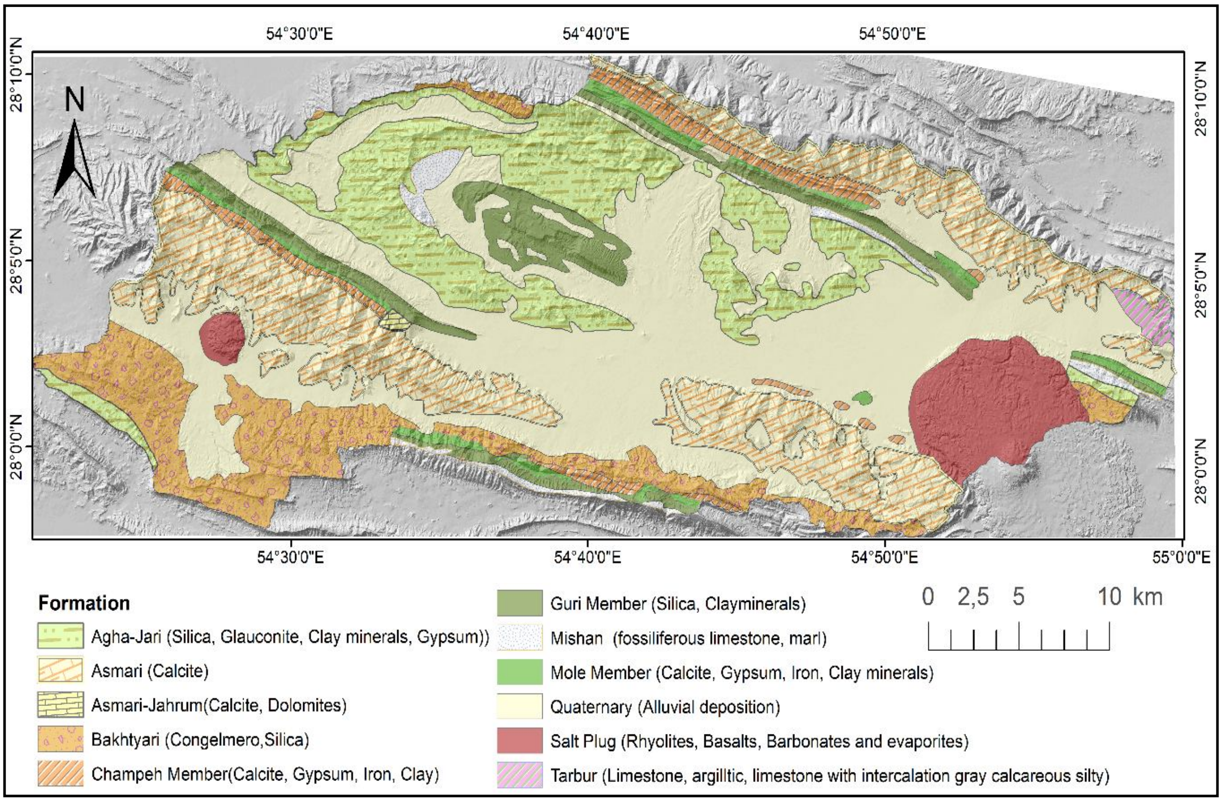

Figure 1 Study area: MZJ catchment and its lithological map (1:25.000)

3.1.Satellite Data

The multispectral Advanced Space borne Thermal Emission and Reflection Radiometer (ASTER) or ASTER sensor is a joined collaboration between NASA and Japan’s Ministry of Economy. The sensor carried by the TERRA satellite launched in December 1999 1999 (Fujisada 1995; Matar & Bamousa 2013) has 14 bands that covers a vast spectral range, with three bands in the Visible and one band in the Near Infra-Red with 15 m resolution (VNIR) and six bands in the Short Wave Infrared with 30 m resolution (SWIR) as well as four Thermal Infra-Red (TIR) bands with 90 m resolution (Fujisada 1995). The ASTER data of our study area was acquired on 28- 02-2006. Each scene covers about 60 km × 60 km. In general, the Short Wave Infrared bands were used for the discrimination of minerals or rock types (Yamaguchi et al., 1998). Firstly, the acquired data with compacted bands were separated and then processed conducting radiometric and geometric corrections (Bachofer et al. 2015). The scene used in this research is an ASTL1B–14 bands–from 2007. The data was projected in UTM zone 40 (WGS 84) and orthorectified using a DEM. The scene covers an area of 60 by 60 km (3600km^2) and hence covers the MZJ completely. The proposed procedure for mineral enhancement of the study area using ASTER data mainly relies on the SWIR bands 4, 5, 6, 7, 8 and 9. The spectral ranges of the 30 m resolution SWIR bands are: 1.600–1.700 μm (band 4), 2.145–2.185 μm (band 5), 2.185–2.225 μm (band 6), 2.235–2.285 μm (band 7), 2.295–2.365 μm (band 8) and 2.36–2.43 μm (band 9).

3.2. Lithologyof the Mazayjan River catchment

The geology of Harmoz is discussed by many authors such as Hull and Warman (1970), Gill and Ala (1972), Falcon (1974), Kashfi (1980), Bahroudi and Koyi (2004), Edgell (1996) and Bosak et al. (1998). The study area includes many rock types which can be subdivided according to their age into Precambrian rocks and Phanerozoic rocks. In this chapter the geology of the basin is summarized in respect to the occurring rock types and it's forming minerals.

Lithologically, the study area is subdivided into two main rocks units (Figure 1). The first unit consists in Precambrian rocks which are covered by the salt plugs or glacier salts with an area about 109 km^2. The plug is composed mostly of brownish gray to purple gray, sometimes pale red, purple or reddish brown siltstones. The past reductive environment helped to form minerals like pyrite. The Halite commonly occurs at plug margins. Crystalline gypsum occurs most often in brecciated forms with fragments of shales, light-colored limestones and grayish brown siltstones. Dark gypsum with organic admixture and local intercalations of iron compounds are common. Mineralogical, the slat plugs are covered by weathered minerals such as clay minerals, ferriginated minerals and some relicts from gypsum and halite at the distal part of the dome features.

The second rock units represent the Phanerozoic rocks which are mainly sedimentary rocks that are formed from Cretaceous to Quaternary age with a total area of ca. 1300 km^2. The main lithological formations from Phanerozoic rocks are outcropping with predominant occurrence in the study area; the oldest rocks represent Oligocene to Lower Miocene age named as Asmari Formation. It covered about 200 $km^2$of the study area. They consist of dolomitic, in places even of dolostones and sandstones at the basal parts while the upper parts are composed of limestone that differentiated from nummuliticgrain stones to fine-grained pack stones. The Gachsaran Formation range from Lower Miocene to Pliocene. This formation is composed of the evaporitic Guri Member, the carbonate Champeh Member and the clastic-evaporitic Mol Member. Mishan Formation rocks (Lower to Middle Miocene) consists of bedded limestones, often chalky with an argillaceous admixture at the basal parts, while the upper parts are composed of mostly green marls, in places slightly gypsiferous with silty sandstone, sandy mudstone and sandstone inter beds.

The Upper Miocene to Pliocene rocks represents the Agha-Jari Formation. These rocks consist of an alternation of sandstones, mudstones to shales and sandy siltstones. The youngest formation represents the Bakhtyari Formation (Upper Pliocene to Pleistocene). This formation consists of pebble to boulder conglomerate with subordinate cross-bedded sandstones and sandy siltstones. Quaternary deposits have a large areal distribution of about 470 km^2. Quaternary sediments are represented mostly by complex alluvial systems which formed by coarse-grained - boulder conglomerates to gravels, often cross bedded with minor sandy interbeds. There are a higher proportion of soft shales to marls, gypsum and anhydrite where the weathered materials are derived from Miocene- Pliocene rocks. These sediments are enriched with gypsum, clay minerals (Kaolinite) and salt minerals (halite).

3.3. Rock differentiation using remotely sensed data

The analysis depends mainly on the discrimination between the existing rocks types using their mineralogical composition as illustrated in the processing workflow (Figure 2). The highly concentrated minerals within the rocks types are used to discriminate them. Band rationing has been widely used for lithological mapping due to its proven ability to produce distinct differences corresponding to the occurrence of the minerals given by certain band ratios. The majority of fractional values are between zero and two or three. Thus for visibility reasons the ratios are often rescaled to produce ratio images with higher contrast. Which band ratio is particularly suitable for enhancing a certain rock type or mineral depends on the dominance of the mineral in the reflected data. Spectral signatures give useful hints to decide about the bands used for rationing. Combinations of three band ratio images can be visualized as color composites. Features or minerals show up in distinct colors in these stacked ratio images. The question concerning which band ratios or band ratio stackings enhances the visibility of a particular rock type is analyzed and discussed extensively in the next section.

The selected minerals are chosen based on the previous mineralogical studies of this area and field visits. We decided to use the calcite mineral to distinguish Oligocene–Lower Miocene carbonate rocks (Asmari and Gachsaran formations), Hematite and Pyrite minerals to characterize Precambrian rocks (Salt Plug) and Glauconite, Gypsum and Kaolinite to discriminate between Upper Miocene to Pliocene rock sandstone rocks (Agha-Jahri formation) and Middle Miocene rock (Mischan formation). The selected band ratios depend on their ability to identify the spatial signature of minerals characterizing the rock unit. The reflectance spectra of minerals are well known and catalogued, e.g. USGS Digital Spectral Library (Clark et al., 2007). The fact that rocks are a complex mixture of materials limits the direct utilization of these spectra in remote sensing analysis. The use of the spectra is further reduces by the fairly broad band width and the low number of spectral bands of ASTER. The challenge for the Remote Sensing approach is to analyze the reflectance of the mineral mix recorded by the ASTER bands (Omran et al. 2012).

To increase the degree of automation within the mapping process we employed image classification methods. An unsupervised classification is used to show the different sedimentary classes in stacked layers even though the results are not always optimal. However, applying this classification in specific cases where no data or only inaccurate data are available it might be a very useful procedure to identify different lithology components. Actually, due to a lack of ground truth information in the study area we applied an unsupervised classification to get a first idea of the spatial distribution of the lithological units. Moreover, there are similarities of the mineral compositions between different rock formation as Agha-Jahri sandstone formation and Bakhtyari conglomerate formation making it difficult to distinguish between them. Therefore, the analysis of the study area includes six sedimentary rock units. Namely: these are the Asmari, Agha-Jahri, Mischan, Gachsaran formations, Slat Plugs and quaternary rocks. Spectral indices derived from the ASTER VNIR and SWIR bands could help to figure out different mineral compositions and also to emphasize the spectral differences of target objects (Bachofer et al. 2015). In this study a band ratio stacking with the following ratios 4/9–4/6–9/8 is used for differentiation between the six sedimentary rock units. For a better understanding of this stacking the band ratio images are discussed in the context of the spectral signature of the dominant minerals. In consequence, the band ratios with SWIR bands have been used for the prediction of the susceptible area to gullying according to the respective lithology information (Figure 2).

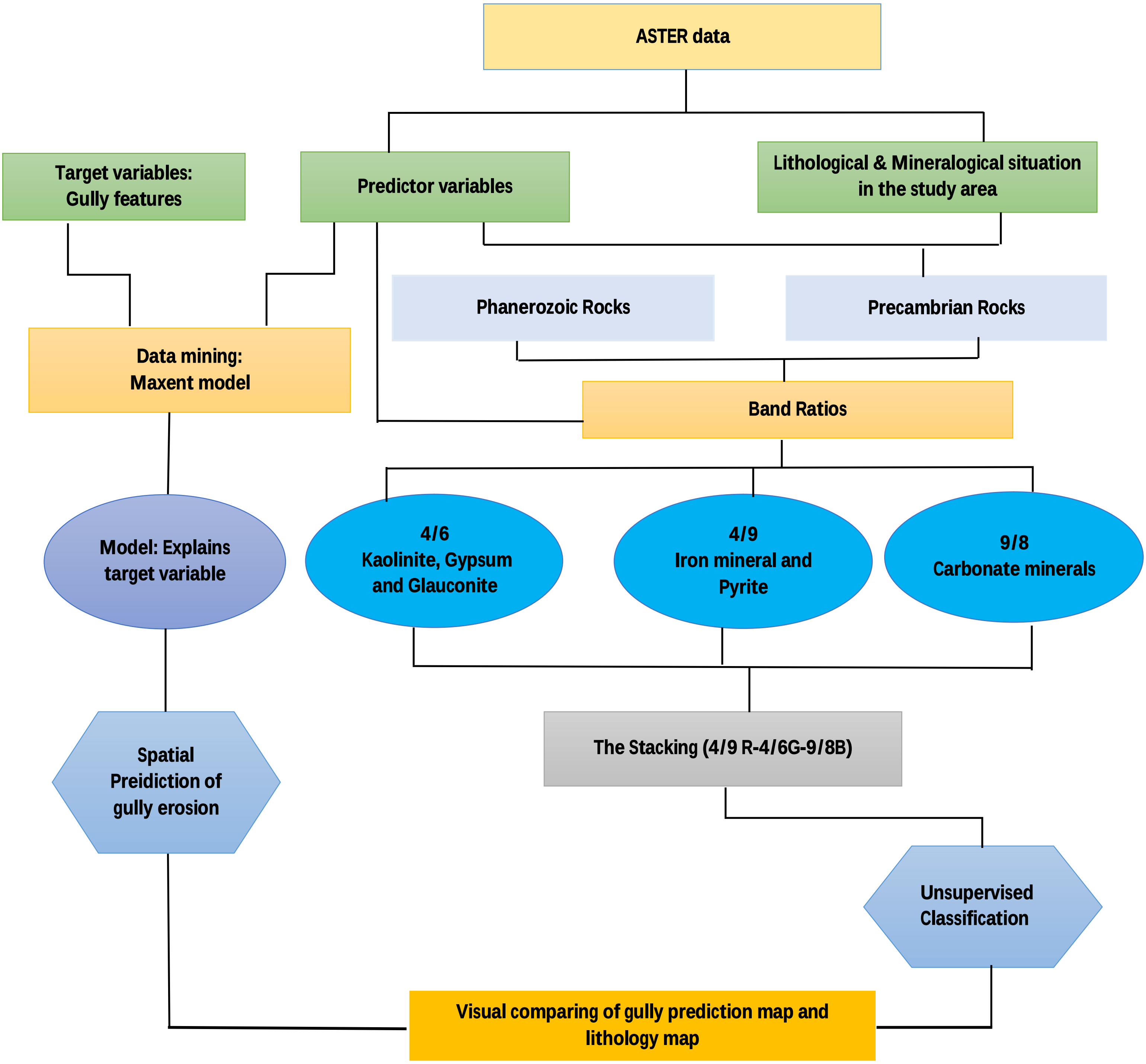

Figure 2 Flow chart of the applied methodology

3.4. Stochastic modeling of gully erosion

In this investigation the Maximum entropy model or short Maxent Model (MEM) (Phillips et al., 2006) was applied to predict the spatial distribution of gully susceptibilities and to reveal the most influencing triggering factors. Generally, data mining techniques are powerful and useful methods to identify susceptible areas prone to gully erosion using different environmental layers. Here we use version 3.3.3k (http://www.cs.princeton.edu/~schapire/maxent/) to assess the environmental relations responsible for the spatial distribution of gully erosion features. The model requires presence only data and a set of environmental variables that are spatially continuously distributed (Zakerinejad & Maerker 2014). In this case the probability distribution of gullies are estimated using the presence of gully features and environmental predictor variables (continuous or categorical) that are delineated form ASTER spectral information (single bands and ASTER band ratios). MEM was successfully applied in environmental studies dealing with presence only data (Elith et al. 2006; Howard 2012; Vorpahl et al. 2012; Hosseini et al. 2013; Zakerinejad & Maerker 2014). In recent studies the method was used to predict the spatial distribution of soil erodibility, landslides and gullies using terrain parameters as independent variables (; Maerker et al. 2014; Zakerinejad & Maerker 2015; Mahamane 2015).

Essentially, in this study the MEM approach was used to classify gully erosion processes and also to define the relationship between spatial data sets of driving factors (independent variable) such as lithology/ substrate proxies and gully features (dependent variable). We selected the six spectral bands of the SWIR system and band ratios of SWIR (Figure 2) as the most important input features for the analysis. Finally, MEM yield also information on the impact of each predicator variable for the final model. Moreover, we analysed partial dependency plots as univariate response curves for each continuous predictor variable as a basis for interpreting the effect of predictors.MEM was trained and tested using a sample of 80% and 20% of localities (cases) respectively showing gully erosion phenomena. The gully features samples were collected from the aerial photos (2003), Google earth GE image (SPOT, 5m) and field survey at different locations of the study area in 2012.

3.5. Environment layers (independent variables)

For this study we set the ASTER SWIR bands (4–9) and band ratios (4/6; 4/9; 9/8) as environment layers (predictor variables) in the MEM approach (see also 45). The layers were post processed and transformed into ascii raster data with the same spatial reference (WGS84, Zone 40) and resolution (30 m) using SAGA 2.0.3 software.

3.6. Model Validation

It has been evaluate the performance of the model using the receiver operator characteristic (ROC) curve for training and test data. Values near to 1 indicate that the model prediction is perfect, while values near or below 0.5 indicate random prediction (Phillips & alii 2004). In an ROC curve the true positive rate (sensitivity) is plotted over the false positive rate (1-specificity) for all possible cut-off points (Swets et al. 2000).According to Hosmer and Lemeshow (Hosmer), AUC values exceeding 0.7/0.8/0.9 indicate acceptable/excellent/outstanding predictions. The contribution of the most important variables for the model is illustrated in the variable importance graph. Moreover, a Jackknife graph is exploring the variables which had the greatest contribution to the generation of the distribution model and its importance when used alone (Phillips et al. 2006; Elith et al. 2011). Finally we also show the most important variables plotted as susceptibility/probability over the variable parameter range. Hence, identifying the relevant parts of the specific spectra contributing mainly to the model.

4. Results andDiscussion

In the following, It will discuss the results obtained from the different analysis. First we highlight the results of the assessment of the geological map to derive the proper band ratios able to describe the lithological units characterized by a specific mineral composition. Subsequently, the obtained band ratios describing the lithological units are used in an unsupervised classification to get a better spatial resolution of the geological units. Finally we describe the results of the MEM approach utilized for the assessment of the relations between gully locations and spectral band or band ratios.

4.1. Spectral band ratios and related Lithology

Based on the geological map the following band ratios were attributed to specific lithological units. The first ratio of bands 4/6 (Figure 3) describes best the Agha-Jahri formation appearing in dark color due to high concentration of Glauconite mineral (Bosak et al. 1998), whereas the presence of Gypsum and Kaolinite minerals in the Mischan formation produce a grey to light grey color (Figure 3). Gypsum deposits at the distal part of the Salt plug zone are also discriminated. The evaporation of sea water resulted in the most important deposits of rock gypsum of the world. Band ratio 4/9 characterize especially, Precambrian rocks because of their high contents in pyrite and iron minerals (Hematite) (Bosak et al. 1998). The rock unit appears darker than other rocks (Figure 4). Band ratio 9/8 identifies carbonate rocks with brighter color (white color) than other rock types. The rocks units (Asmari, Gachsaran Formation) are shown with white to light grey color in the scene, indicating their high carbonate content whereas weathered minerals like Gypsum and kaolinite occur with dark grey to black color especially in alluvial deposits (Black color) (Figure 5).

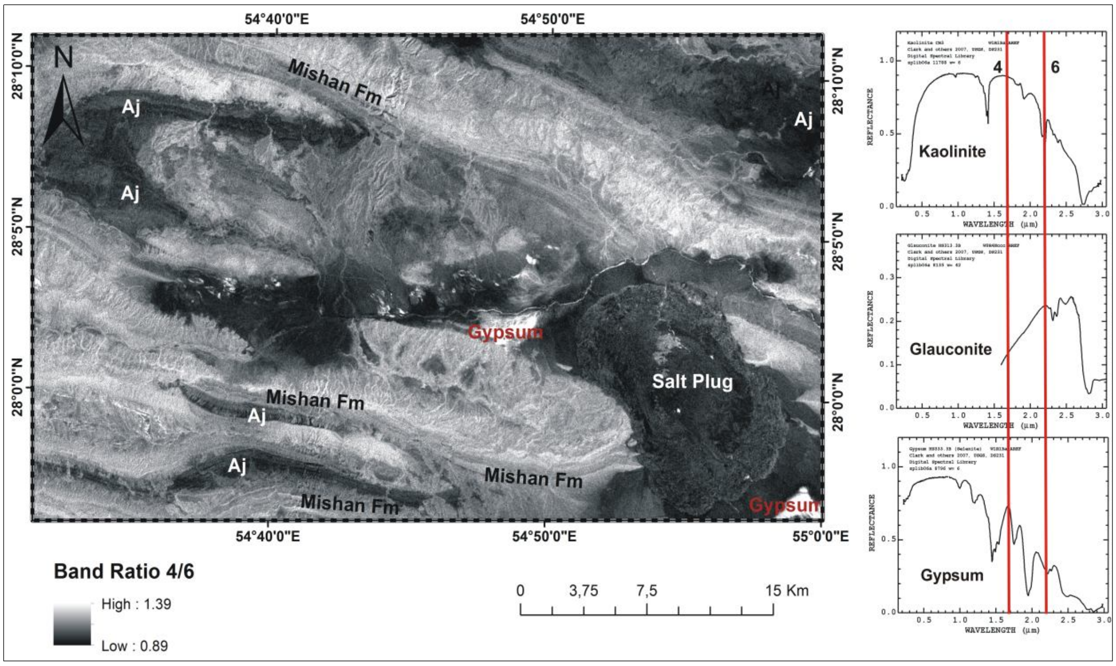

Figure 3 Ratio of Band 4 / Band 6 of the MZJ catchment.

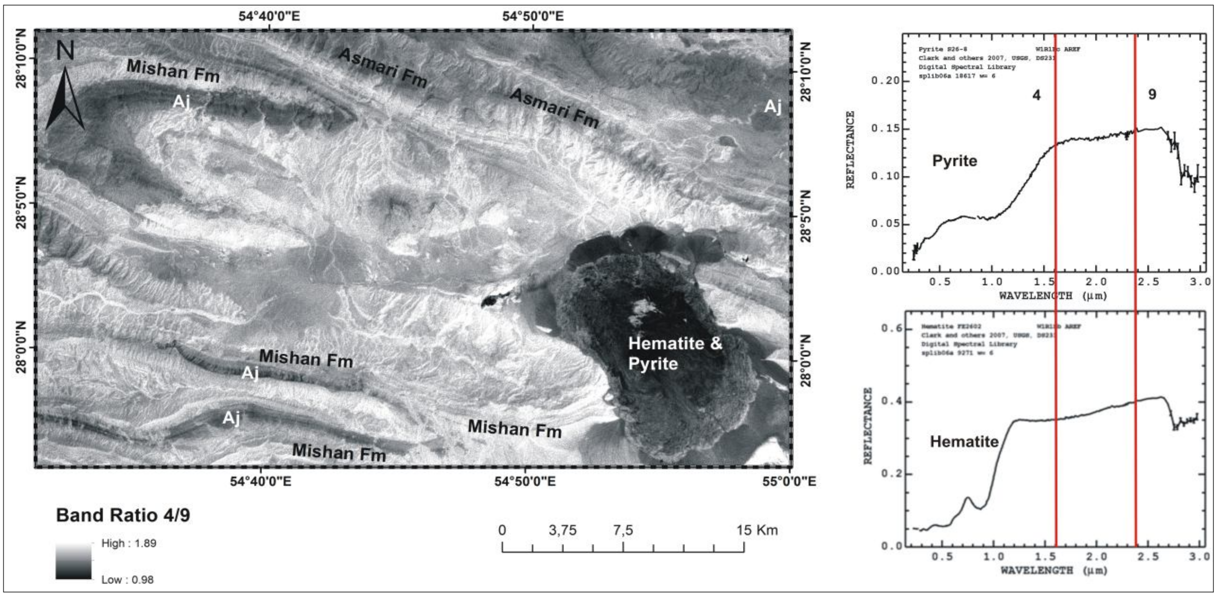

Figure 4 Ratio of Band 4 / 9 of the MZJ catchment.

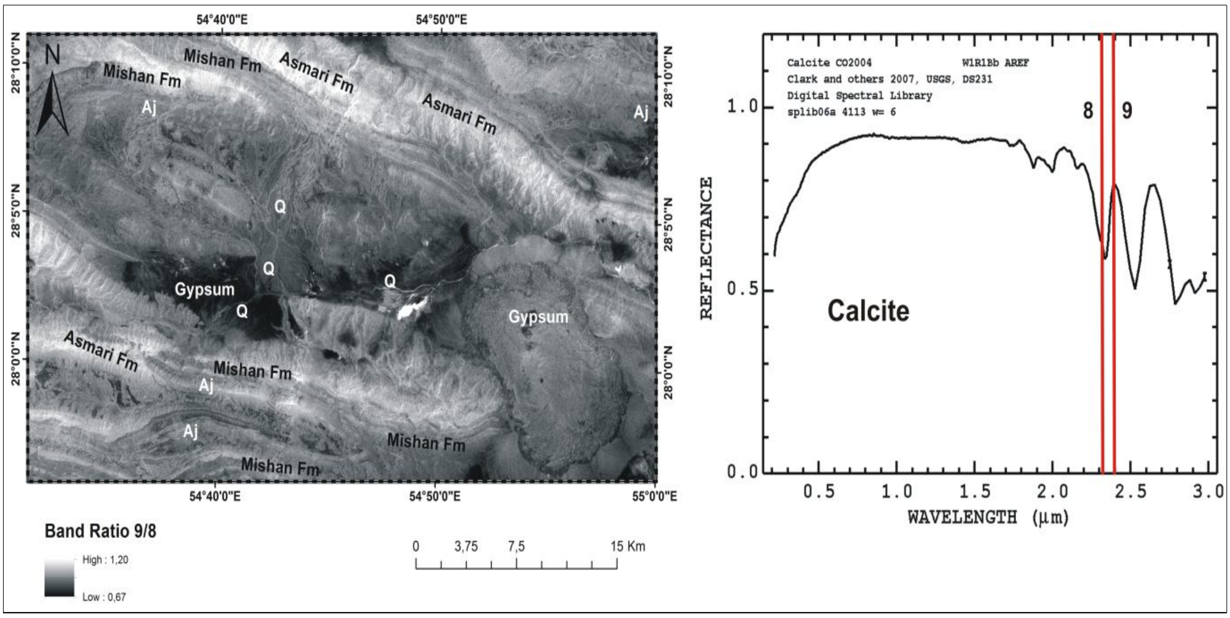

Figure 5 Ratio of Band 9 /8 of the MZJ catchment.

4.2. Unsupervised classification of lithological units

In experiments with different band ratio stackings, it was found that the color composite (4/9 R–4/6 G and 9/8 B) reveals subtle differences between Asmari, Agha-Jahri, Mischan formations and Slat Plug with Quaternary rocks (Figure 6). Furthermore, it was shown that the Asmari Formation appears in pale blue colors, Agha-JahriFormation in dark blue to purple color, Mischan Formation in dark yellow, Gachsaran Formation in white color, Precambrian rock appears as blue to greenish blue colors and quaternary deposits in brown to dark brown color. The unsupervised classification is used as a first approximation of the lithological units using the stacking layer as shown in figure (Figure 7). The results of this classification cannot differentiate between the Precambrian rock and the Upper Miocene to Pliocene rocks (Agha-Jahri Formation) with red color. Additionally the Mischan Formation is not represented well in this layer with pale blue and yellow color , it seems because of the spatial distribution of this formation as very narrow strip in the north east and southwest of study area beside of Gachsaran Formation (Mol member), additionally the similarity of the mineral components between both of them.

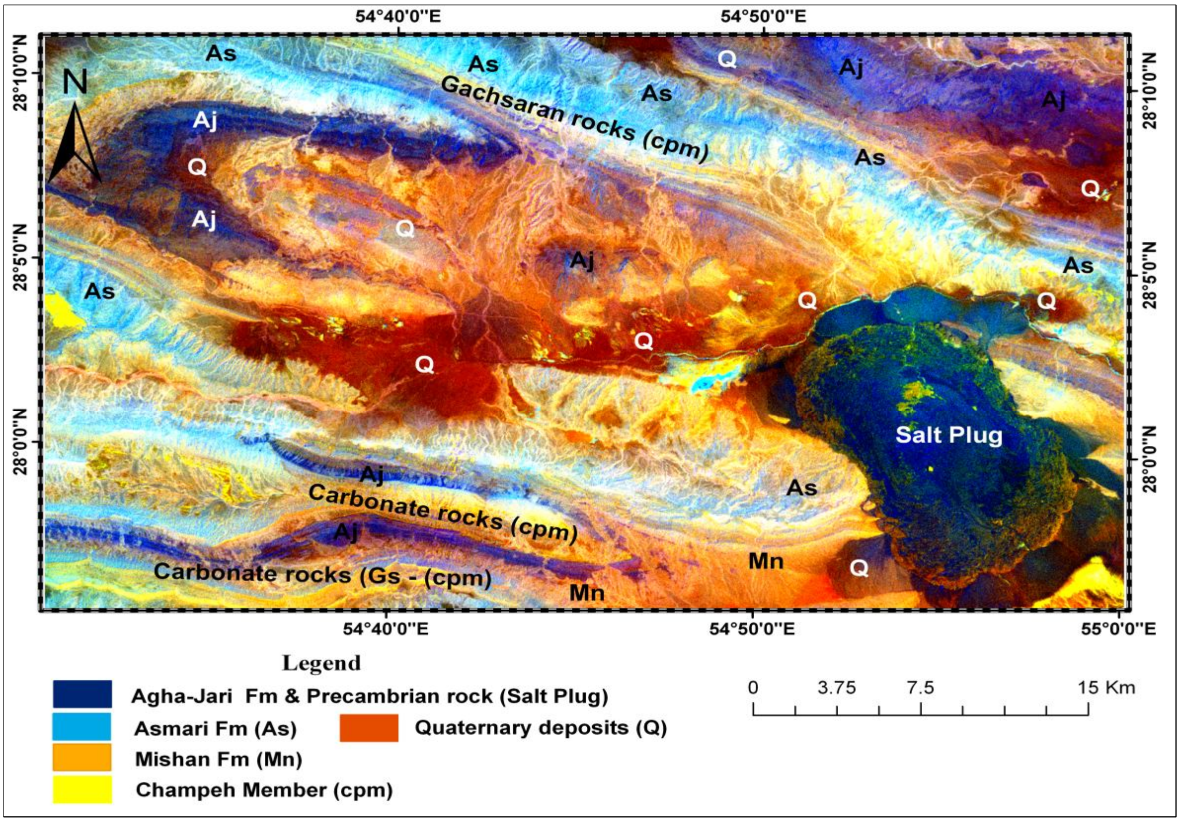

Figure 6 Stacking (4/9, 4/6, 9/8)–RGB of the MZJ catchment.

Nevertheless, this classification has been distinguished the Asmari Formation with Dark blue color and the alluvial sediments (Quaternary deposits) into two classes (red and green). The reddish units are more related to the gypsum and kaolinite minerals which are represented the main minerals components in the Agha-Jahri and Precambrian rocks. While the green color belongs to the areas with low amounts of salt and gypsum deposition especially at the flat area regarding to field work observations. Comparing field data from the gully locations and the result of this map show that many gullies features were found in susceptible lithologies with high kaolinite, gypsum and salt concentrations. These components were mostly related to the

Agha-Jahri formation and Salt Plugs Precambrian rocks (Figure 7). However, a proper supervised classification was not possible due to a lack of field survey and the low quality of available geology maps.

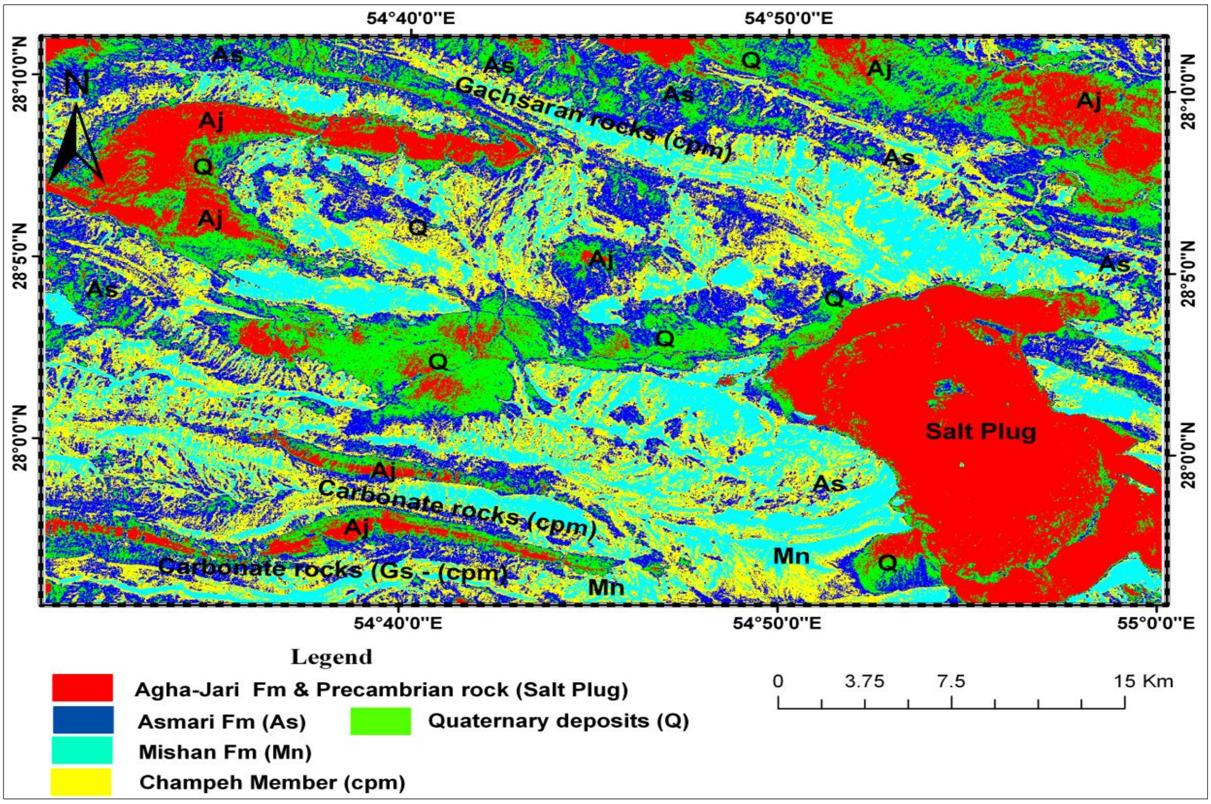

Figure 7 Unsupervised classification of the MZJ catchment.

4.3. Maxent modeling

In this research the Maxent model was selected to assess the relation between gully locations and ASTER spectral bands and/or band ratios. Moreover the generated model was used to predict the susceptible areas for gully erosion in the MZJ catchment. The model predicts spatially distributed probabilities or susceptibilities to gully erosion processes according to the lithology of the study area (Figure 8). Although, gully processes and resulting forms and features are affected by many different factors such as topography, climate condition, tectonics, *etc.* (Kheir et al., 2007; Sharivar 2009; Zakerinejad & Maerker 2014) in this study we focused on the role of the lithology to reveal its effects on this type of water erosion. Moreover, climate and vegetation are almost homogenous for the whole study area. Since the modeling approach (Maxent) handles presence only data just the digitized locations of existing gully features are needed as dependent or target variable.

To evaluate the performance of the applied model and its predictions, we divided the data randomly into training and a test subset, hence creating quasi-independent data for model testing (Fielding & Bell, 1997). In this research the model was applied to a 20% test data set selected randomly from the entire data set of gully points. The remaining 80% of the data were used as train dataset. Model results were evaluated using the ROC curves both for train and test data. According to Figure 9 the AUC values for train and test data are 0.97 and 0.96 respectively, indicating an outstanding model performance (Hosmer & Lemeshow 2000) with a high low sensitivity (true positive rate) and specificity (false positive rate). The most important variables indicating gully erosion are shown in Table 1. The variables with the highest contribution to the model are the band ratio 9/8 followed by band ratio 4/6 and band 7. To get a proper insight into the variables mainly influencing the model results we performed a Jackknife test shown in Figure 10.According to that figure we can identify the relevance of the band ratios and single bands for the modeled gully susceptibility. According to this results the band ratios 9/8 & 4/ 6 are the most effective in the prediction of gully susceptibility area. The important role of the band ratio 9/8 can be explained by the high content of silica material in alluvial deposits illustrated by dark grey to black color (Figure 4).

Moreover, we analysed partial dependency plots as univariate response curves by calculating non-parametric loess regressions from predicted values for single continuous predictor variable as a basis for interpreting the effect of predictors. Figures 11 show the response curves for the important variables (band ratio 9/8, band ratio 4/6 and band 7). According to this figure, the band ratio 9/8 graph, varying from 0.80 to 1.10, therefore the amount more than these two thresholds are the most important range for the prediction of susceptible area, and also the values between 0.90 and 0.97 have more effective on the predicted model while in the band 7 the values more than 200 are more effective on the predicted model.

Table 1 Thevariables important.

Spectral Bands or Band Ratios	Percent Contribution	Permutation Importance
Band 9/8	54.6	46.4
Band 4/6	17.8	1.8
Band 7	14.4	2.4
Band 8	5.2	6.8
Band 4/9	4.6	14.6
Band 9	1.9	6.6
Band 4	1	3.8
Band 5	0.4	1.8
Band 6	0.2	15.8

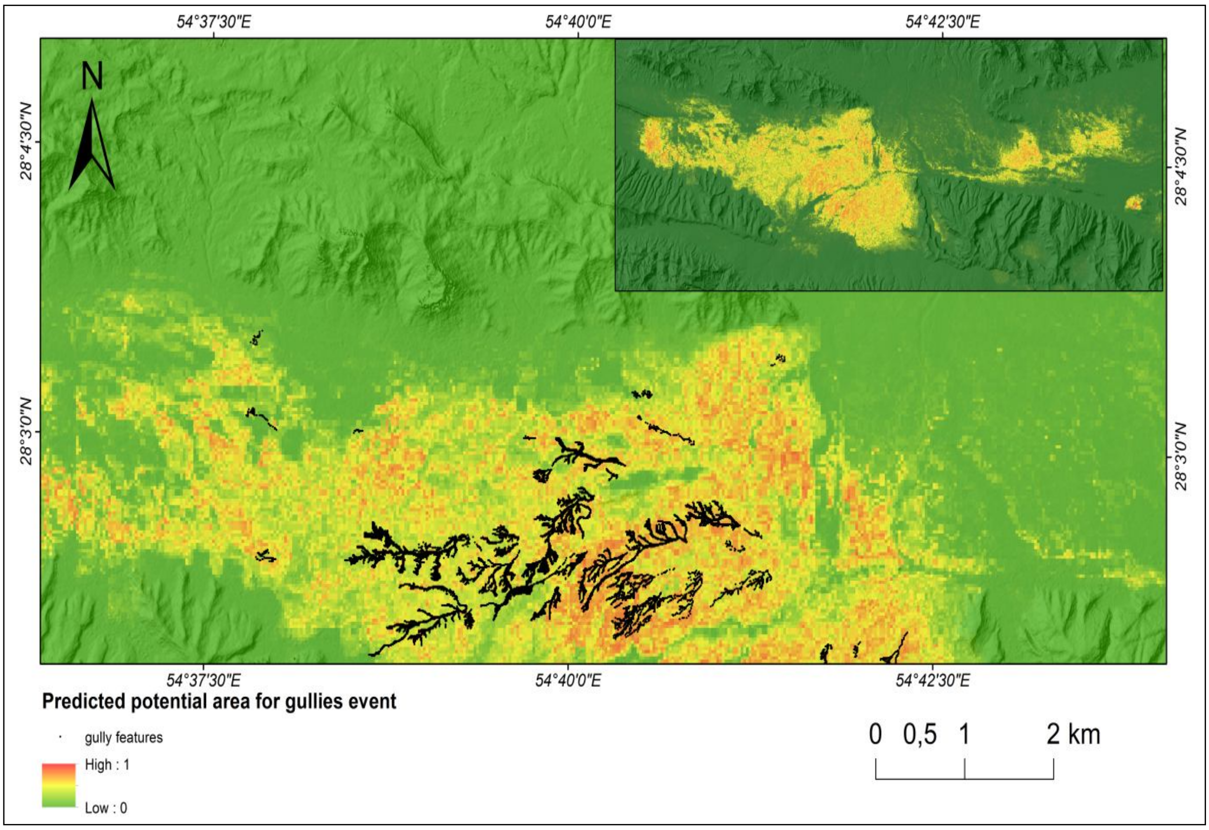

Figure 8 Predicted gully erosion susceptibilities in the MZJ basin.

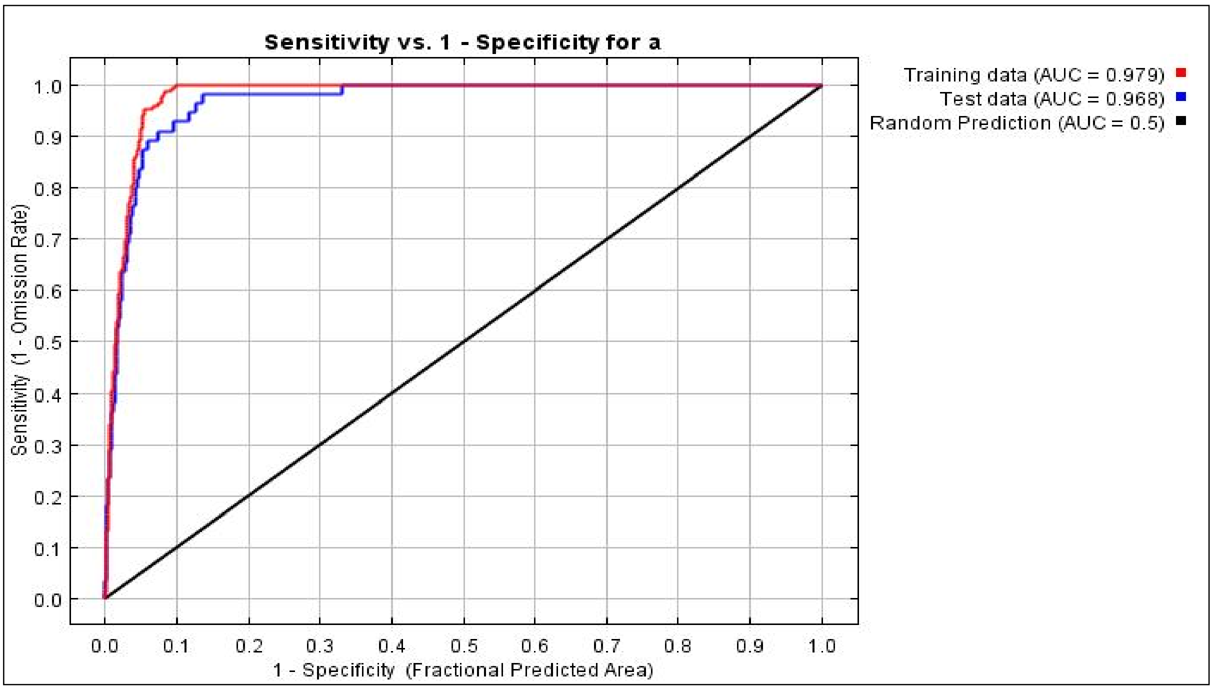

Figure 9 Area under ROC curve for validation of gully suitability model.

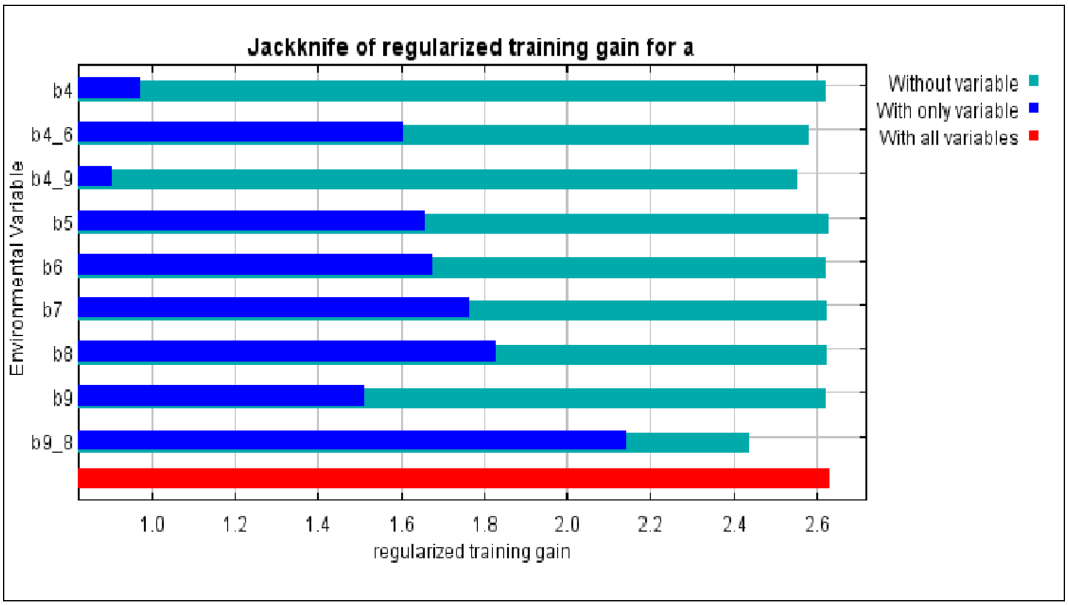

Figure 10. The Jackknife test for evaluating the relative importance of environmental factors for prediction of susceptible area for gully event.

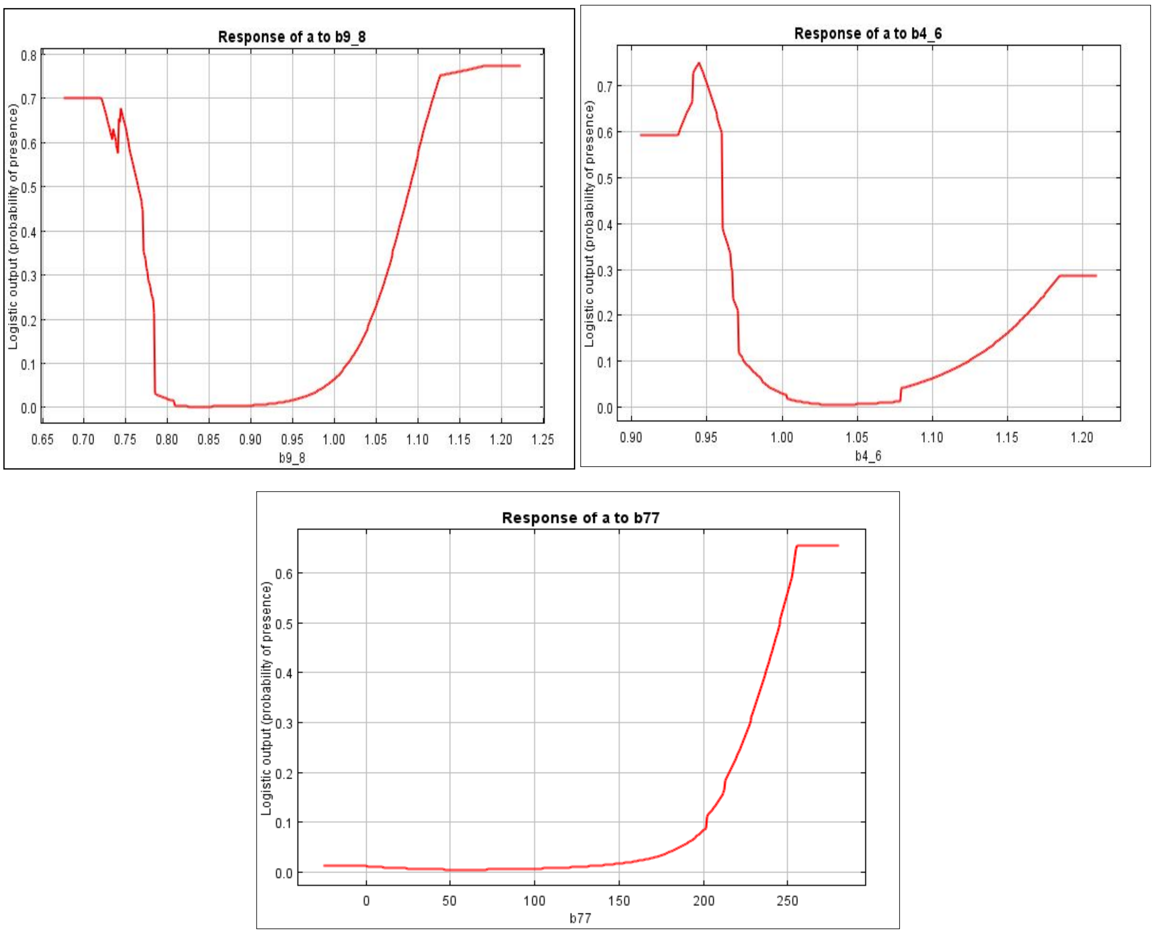

Figure 11. Responses curves of the most important predictor's important variable (Bands7, 8 and band 9/8, 4/6 ratio) in the study area.

4.4. Prediction of gully erosion susceptibilities

In the following it will be discussed the spatial prediction of Gully sites using the MEM approach. Figure 8 illustrates the spatial distribution of gully susceptibilities according to the lithology represented by different spectral bands and/or band ratios. Generally, it is shown that the mountainous areas are less susceptible to gully erosion processes which are mainly concentrating in the alluvial and colluvial parts of the catchment and hence, gullies especially occur in the plain areas in the West and East of the catchment (Figures7 and 8). The locations of gullies highly correlate with the red signature especially in the plain/ alluvial areas also revealed by GE image interpretation and a field survey conducted in March 2012 (Figures 13). According to the predicted probabilities the most susceptible areas for gullying are in the southwestern, western and in the eastern parts of the study area. These areas are characterized by alluvial Quaternary sediments. Moreover, in these areas high amounts of salt, marl and gypsum are found and thus, they are more susceptible to concentrated water erosion processes. Particularly, EC and SAR values of soil samples of the susceptible part of the area are very high indicating high Sodium contents amplifying gully erosion as shown by various authors in the past (Faulkner & *alii* 2003; Masoudi & Zakerinejad 2010; Shahrivar & *alii* 2012). According to many authors gully erosion in alluvial plains is the major land degradation process especially in arid and semi-arid area (Pickup 1991; Pringle et al. 2006).

5. Conclusion

In this study we assessed the relation between lithology represented by different spectral bands and band ratios of the ASTER multispectral sensor and gully locations mapped in the field and by GE image interpretation. Therefore, first the ASTER multispectral bands and band ratios that describe specific lithology characterized by particular mineral compositions using the existing geological map has been identified. With the mineral differentiation analysis, different rock types like sedimentary rocks and Quaternary deposits in the ZM have been distinguished.

Furthermore It was used the identified bands and band ratios with an unsupervised classification method in order to get a higher detailed geological differentiation of the area. As shown especially the flat alluvial and colluvial parts are distinguished in a much higher detail and hence already reveals a specific relation between gully sites and lithologic characteristics given by spectral band combinations. In the last step we assessed these relations using a MEM approach developing a model that showed a strong influence of the band ratios 9/8 and 4/6 as well as band 7 with the gully locations. This spectral information indicates high salt and sodium contents and hence high SAR and EC values making the substrates particularly prone to gully erosion. The MEM model shows an outstanding performance for train and test data and hence can be considered as robust prediction tool. Furthermore, a map showing the spatial distribution of susceptible areas for gully erosion was derived that is matching well with the mapped gullies by GE image interpretation and field survey.

The result showed that there was matching between the locations of predicated gully area from Maxent model and the result from mineral differentiation analysis using ASTER data, mostly of gully features were located on the alluvial deposition with the loosely consolidated and highly kaolinite, Gypsum and salt minerals content.

In fact the prevention of gully erosion is much easier and low cost than controlling it that with having the predicted map it's easier to identify the prone area for more protect of soil loss. Therefore the prevention processes should be taken for all land management especially in the prone area in this part of ZM in Iran. By considering the mineral differentiation analysis using ASTER data, terrain parameters, the climate condition and the other related parameters with using of data mining, it should be to identify the degree of susceptibility area to gully erosion and inconsequence carry out any preventive program. Regarding to the lack of data in this study for supervised classification, it should here recommend that for future research, an extensive field survey to collect the ground data supervised classification of the lithology map is an essential needed.

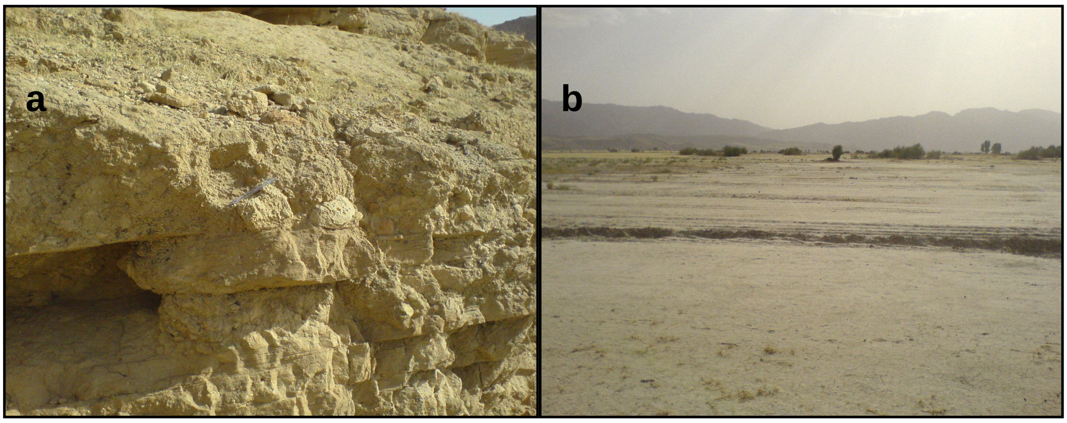

Figure 12. Sedimentary structures in Aghajari sandstones (**a**) and the Quaternary deposition in south (**b**) of the MZJ.

Acknowledgments

The authors would like to thank the Iranian Ministry of Science and Technology for providing the fellowship of Mr. Zakerinejad to study Ph.D. abroad.

References

Ahmadi H (2007) Applied Geomorphology (water erosion), Tehran University (in Persian)

Abrams M (2000) The Advanced Space borne Thermal Emission and Reflection Radiometer (ASTER): data products for the high spatial resolution imager on NASA's Terra platform. International Journal of Remote Sensing 21: 847–859.

Bachofer F, Quénéhervé G, Hochschild, V, Maerker M (2015) Multisensoral Topsoil Mapping in the Semiarid Lake Manyara Region, Northern Tanzania. Remote Sens. 7, 9563–9586.

Bosak P, Jaro J, Spudil J, Sulovsky P, Václavek V (1998) Salt Plugs in the Eastern Zagros, Iran: Results of Regional Geological Reconnaissance. GeoLines7: 1–174.

Bahroudi A, Koyi H. A (2004) Tectono-sedimentary framework of the Gachsaran Formation in the Zagros foreland basin. Marine and Petroleum Geology, 21: 1295–1310.

Clark R.L, Swayze G.A, Wise R, Livo K.E, Hoefen T, Kokaly R.F et al. (2007) USGS Digital Spectral Library U.S. Geological Survey.

Conoscenti C, Di Maggio C, Rotigliano E (2008) Soil erosion susceptibility assessment and validation using a geostatistical multivariate approach: a test in Southern Sicily. Natural Hazards, 46; 287–305.

Edgell H.S (1996) Salt tectonism in the Persian Gulf Basin, inG. I. Alsop, D. Blundell, and I. Davison, eds., Salt Tectonics.Geological Society Special Publication100: 129–151.

Elith J, Graham C.H., Anderson R.P., Dudik M., Ferrier S., Guisan A., Hijmans R.J., et al. (2006) Novel methods improve prediction of species, distributions from occurrence data. Ecography 29: 129–151.

Falcon N.L (1974) Southern Iran: Zagros Mountains, In: A. Spencer, ed., Mesozoic-Cenozoic Orogenic Belts. Data for Orogenic Studies, Geological Society of London, Special Publication 4: 199–211.

Faulkner H, Alexander R, Wilson B.R (2003) Changes to the dispersive characteristics of soils along an evolutionary slope sequence in the Vera badlands, southeast Spain: implications for site stabilisation. Catena, 50: 243–254.

Frankl A, Poesen J, Deckers J, Haile M, Nyssen J (2012) Gully head retreat rates in the semi-arid highlands of Northern Ethiopia, Geomorphology, 173: 185–195.

Faulkner H, Alexander R, Wilson B.R (2003) Changes to the dispersive characteristics of soils along an evolutionary slope sequence in the Vera badlands, southeast Spain: implications for site stabilisation. Catena, 50: 243–254.

Feiznia S *(*2000) Rock resistance against corrosion in different climates in Iran. *Nat Resour J*, 47, 95–116 (in Persian).

Fujisada H (1995) Design and performance of ASTER instrument: Proceedings of the International Society for Optical Engineering 2583:16−25.

Gill W.D, Ala M.A (1992) Sedimentology of Gachsaran Formation (Lower Fars Series), southwest Iran. Amer. Assoc. Petrol. Geol. Bull**,** 56: 1965–1974.

Ghodosi J (2006) The effects of soil physico-chemical characteristics on gully erosion initiation. 3rd Erosion and Sediment National Conference Soil Conservation and Watershed Management, 282–289.

Hull C.E, Warma H. R (1970) Asmari Oil Fields of Iran, in M. T. Halbouty, ed., Geology of Giant Petroleum Fields, American Association Petroleum Geologists, Memoir, *14*: 428–437.

Hosseini S.Z, Kappas M, Zare Chahouki, M A, Gerold G, Erasmi S, RafieiEmam A (2013) Modelling potential habitats for Artemisia sieberi and Artemisia aucheri in Poshtkouh area, central Iran using the maximum entropy model and geostatistics. Ecological Informatics, 18: 61−68.

Howard A.M, Bernardes S, Nibbelink N, Biondid L, Presotto A, Fragaszy D.M. Madden M.A (2012) Maximum entropy model of the Bearded Capuchin monkey habitat incorporating topography and spectral un mixing analysis ISPRS Annals of the Photogrammetry, Remote Sensing and Spatial Information Sciences, I-2

Hosmer D.W, Lemeshow S. (2000) Applied Logistic Regression, 2nd ed. *Wiley,* New York 392 pp.

Kashfi M.S (1980) Stratigraphy and Environmental Sedimentology of Lower Fars Group (Miocene), South-Southwest Iran: American Assiociaton of Petroleum Geologists Bulletin 64: 2095–2107.

Kemper W.D., E.J. Koch (1966) Aggregate stability of soils from western USA and Canada. USDA Technical Bulletin No.1355, US Government Printing Office, Washington, DC.

Kheir R, Wilson J, Deng Y (2007) Use of terrain variables for mapping gully erosion susceptibility in Lebanon. Earth Surf Process Land32, 1770–1782.

Masoudi M, Zakerinejad R (2011) A new model for assessment of erosion using desertification model of IMDPA in Mazayjan plain, Fars province, Iran. Ecol Environ Conserv, 17(3): 489–594.

Masoudi M, Zakerinejad R (2010) Hazard assessment of desertification using MEDALUS model inMazayjan plain, Fars province, Iran. Ecol Environ Conserv 16 (3): 425–430.

Masoudi M., Patwardhan AM, GoreSD (2006) Risk assessment of water erosion for the QarehAghajsubbasin, southern Iran. Stoch Env Res Risk Assess, 21: 15–24.

Matar S.S, Bamousa A.O (2013) Integration of the ASTER thermal infra-red bands imageries with geological map of Jabal Al Hasir area, Asir Terrane, the Arabian Shield. Journal of Taibah University for Science, *7*: 1–7.

Mahamane M (2015) Assessing soil erosion risk in the Tillabery landscape, Niger, *African* Journal of Environmental Science and Technology, 9 (3): 176–191.

Samani-Nazari A, Ahmadi H, Jafari M, Boggs G (2009) Geomorphic threshold conditions for gully erosionin Southwestern Iran (Boushehr-Samal watershed). Earth Sci, 35: 180–189.

Omran A, Hahn M, Hochschild V, El Rayes A, Geriesh M (2012) Lithological Mapping of Dahab Basin, South Sinai, Egypt, using ASTER Data. PFG. Schweizerbrat Science Publishers, 711–726.

Ogbonna J.U, Alozie M, Nkemdirim V, Eze M.U (2011) GIS Analysis for Mapping Gully Erosion impacts on the Geo-formation of the Old Imo State, Nigeria. ABSU Journal of Environment, Science and Technology1: 48–61.

Phillips S.J, Anderson R.P. Schapire R.E (2006) Maximum Entropy Modeling of species geographic distributions. Ecological Modelling190: 231–259.

Pringle H.J, Watson I. W, Tinley K.L (2006) Landscape improvement, or ongoing degradation - reconciling apparent contradictions from the arid rangelands of Western Australia. Landscape Ecology 21: 1267–1279.

Pickup G (1991) Event frequency and landscape stability on the floodplain systems of arid Central Australia. Quaternary Science Reviews, 10: 463–473.

Servati M.R, Ghoddosi J, Dadkhah M (2008) Factor effecting initiation and advancement of gully erosion in loesses. Pejouhesh and Sazandegi, 20–33 (in Persian).

Shahrivar A, Tehbconsung C, Jusop S, Abdul Rahim A, Soufi M (2012) Roles of SAR and EC in GullyErosion Development (A Case Study of Kohgiloyeva Boyerahmad Province, Iran). J Res AgricSci, 8: 1–12.

Swets J.A, Dawes R.M, Monahan J (2000) Better decisions through science. Scientific American 283: 82–87.

Valentin C, Poesen, J., Yong Li (2005) Gully erosion: impacts, factors and control. Catena, 63:132–153.

Vorpahl P, Elsenbeer H, Maerker M, Schröder B (2012) How can statistical models help to determine driving factors of landslides? Ecological Modelling, 239: 27- 39.

Wasson R.J, Caitcheon G, Murray A.S, McCulloch M, Quade J (2000) Sourcing sediment using multiple tracers in the catchment of Lake Argyle, northwestern Australia. Env. Manag, 29: 634–646.

Yamaguchi Y, Kahle AB, Tsu H, Kawakami T, Pniel M (1998) Overview of advanced space borne thermal emission and reflection radiometer (ASTER). IEEE Trans Geosci Remote Sens, 36: 1062–1071.

Zakerinejad R, Maerker M (2014) Prediction of Gully erosion susceptibilities using detailed terrain analysisand maximum entropy modeling: a case study in the Mazayejan Plain, Southwest Iran. GeogrFis DinQuat, 37: 67–76.

Zakerinejad R, MaerkerM (2015) An integrated assessment of soil erosion dynamics with special emphasis on gully erosion in the Mazayjan basin, Southwestern Iran. Natural hazards journal, 79: S25-S50.